ENG.20030520.0003

OCRWM	DESIGN CALCULATION OR ANALYSIS COVER SHEET	1. QA: QA 2. Page 1

3. System	4. Document Identifier
Engineered Barrier System	000-00C-EBS0-00300-000-00B

5. Title

Structural Calculations of Waste Package Exposed to Vibratory Ground Motion

6. Group

Analyses and Component Design

7. Document Status Designation

☒ Preliminary ☐ Final ☐ Cancelled

8. Notes/Comments

An interdisciplinary review was completed on 16 May 2003.

An impact review was completed on 15 May 2003.

This Document Has Been Superseded By 000-00C-WIS0-01400-000-00A

Attachments	Total Number of Pages
List of attachments is presented in Section 8.	

RECORD OF REVISIONS

9. No.	10. Reason For Revision	11. Total # of Pgs.	12. Last Pg. #	13. Originator (Print/Sign/Date)	14. Checker (Print/Sign/Date)	15. QER (Print/Sign/Date)	16. Approved/Accepted (Print/Sign)	17. Date
00A	Initial issue	216	IX-15	Sreten Mastilovic	Valerie de la Brosse	Daniel J. Tunney	Michael J. Anderson	04/08/03
00B	Three approximate calculations for annual frequency of occurrence of 1e-5 per year are added as Attachment XI. NOTE: Document pages affected by this revision are: 9, 14, 15, 80, 82 through 113, and XI-1 through XI-4. Compact disc #3 of Attachment X is also affected by this revision. The changes in Table 8-1 referring to compact discs #1 and #2 (pages 83 through 112) are only editorial changes as indicated in the second note at the end of the table.	220	XI-4	Sreten Mastilovic [signature] 21 May 2003	Valerie de la Brosse [signature] May 21, 03	Daniel J. Tunney [signature] 5/21/2003	Michael J. Anderson [signature]	5/21/03

Enclosure 4

CONTENTS

ENG.20040217.0008

OCRWM	DESIGN CALCULATION OR ANALYSIS COVER SHEET	1. QA: QA 2. Page 1

3. System Waste Isolation System	4. Document Identifier 000-00C-WIS0-01400-000-00A

5. Title

Structural Calculations of Waste Package Exposed to Vibratory Ground Motion

6. Group

Waste Package and Components/Structural

7. Document Status Designation

☒ Preliminary ☐ Final ☐ Cancelled

8. Notes/Comments

The review of this document was completed on 03 February 2004.

This document is a revision and supersedes the document of the same title identified by document identifier (DI) 000-00C-EBS0-00300-000-00B.

Attachments have not been affected by this revision. Consequently, they are anticipated to be moved from the check copy (00Aa) to the initial issue of this document (00A). The only exception is the third compact disc of Attachment X, which is expanded by addition of the files corresponding to the simulation of the seismic event with annual frequency of occurrence (annual exceedance frequency) of 1e-4 per year.

Document pages affected by this revision are: 1 through 4, 8 through 16, 29, 34, 46, 50, 54, 60, 61, 68, 71 through 85, 88, 89, 119, and 120. Compact disc #3 of Attachment X is also affected by this revision.

Prior to the DI change the revision history was as follows:

00A: Initial Issue

00B: Three approximate calculations for annual frequency of occurrence of 1e-5 per year are added as Attachment XI. NOTE: Document pages affected by this revision are: 9, 14, 15, 80, 82 through 113, and XI-1 through XI-4. Compact disc #3 of Attachment X is also affected by this revision. The changes in Table 8-1 referring to compact discs #1 and #2 (pages 83 through 112) are only editorial changes as indicated in the second note at the end of the table.

Attachments	Total Number of Pages
List of attachments is presented in Section 8.	

RECORD OF REVISIONS

9. No.	10. Reason For Revision	11. Total # of Pgs.	12. Last Pg. #	13. Originator (Print/Sign/Date)	14. Checker (Print/Sign/Date)	15. QER (Print/Sign/Date)	16. Approved/Accepted (Print/Sign)	17. Date
00A	See Block 8	216	IX-15	Sreten Mastilovic	Valerie de la Brosse	Daniel J. Tunney	Michael J. Anderson	04/08/03
00B	See Block 8	220	XI-4	Sreten Mastilovic	Valerie de la Brosse	Daniel J. Tunney	Michael J. Anderson	11/12/03
00A	One calculation for annual frequency of occurrence of 1e-4 per year is added as Section 6.4. (Consequently, the former Section 6.4 is now designated as Section 6.5.) Also, the technical error in calculation of the damaged area for realization 7 at 10-7 per year, described in CAP Condition Report Number 1133, is corrected (Tables 6.2.2-7, 6.2.2-16 and 6.2.4-2). References are updated.	227	XI-4	Sreten Mastilovic 05 FEB 2004	Daniel McKenzie IV 5 FEB 2004	Daniel J. Tunney 2-5-2004	Michael J. Anderson	2/5/04

CONTENTS

FIGURES

TABLES

1. PURPOSE

The objective of this calculation is to determine the residual stress distribution in the outer shell (OS) of a waste package (WP) exposed to vibratory ground motion, and to estimate the area of the WP OS for which the residual stress exceeds certain limits. The WP OS area for which the residual 1st principal stress exceeds certain limits will be, for brevity, referred to as "the damaged area" throughout this document. The stress limit (damage threshold) is defined as a fraction of the yield strength of the OS material, Alloy 22 [SB-575 N06022], at given temperature. Two, lower and upper, stress limits used throughout this document are respectively defined as 80 percent and 90 percent of yield strength of Alloy 22 (see Assumption 3.22) at temperature of 150 $^{\circ}C$ (except for the simulations presented in Attachments V and VIII when 200 $^{\circ}C$ is used). The maximum stress intensity is also presented for all calculations since it can be used to estimate whether or not the WP OS is safe from immediate breach.

A set of 15 calculations is performed at two different annual frequencies of occurrence (annual exceedance frequency): $1\cdot10^{-6}$ *per year* $(1/yr)$ and $1\cdot10^{-7}\ 1/yr$. One calculation is also performed per each of the following two annual frequencies of occurrence: $1\cdot10^{-4}\ 1/yr$ and $5\cdot10^{-4}\ 1/yr$. Additionally, three simulations are performed using approximate time histories for annual frequency of occurrence of $1\cdot10^{-5}\ 1/yr$. (These approximate time histories are created by scaling the three acceleration components of the selected $1\cdot10^{-6}\ 1/yr$ ground motions [see Attachment XI].) The WP used to perform these simulations is the 21-PWR (Pressurized Water Reactor) WP.

The scope of this document is limited to: 1) reporting the calculation results in terms of maximum stress intensity in the course of transient simulation, 2) reporting the calculation results in terms of residual 1st principal stress plot (see Section 2 for details), and 3) estimating the damaged area. All these results are evaluated in the WP OS.

This calculation is intended for use in support of the Total System Performance Assessment–License Application seismicity modeling. This calculation is associated with the WP design and was performed by Waste Package Design. AP-3.12Q, *Design Calculations and Analyses* (Ref. 1) is used to perform the calculation and develop the document. The 21-PWR WP is classified as a Safety Category item (Ref. 5, p. A-3). Therefore, this calculation is subject to the requirements of *Quality Assurance Requirements and Description* (Ref. 4).

The design of the 21-PWR WP used in this calculation is that defined in Reference 24; exceptions are the gap between the inner shell and the OS (for which a value of 4 *mm* was used [Ref. 25, Section 8.1.8]), and the OS thickness (for which a value of 18 *mm* was assumed [Assumption 3.21]). The sketch in Attachment I provides additional information not included in Reference 24. Design of the emplacement pallet (pallet, for brevity, throughout the document) used in this calculation is that defined in Reference 22; the sketch in Attachment II provides additional information not included in Reference 22 (see also Assumption 3.17). Finally, design of the interlocking drip shield (DS) used in this calculation is provided in Attachment III. All obtained results are valid for these designs only.

2. METHOD

The finite element (FE) mesh is created by using the commercially available ANSYS V5.6.2 FE code (Software Tracking Number [STN] 10364-5.6.2-01, Ref. 6). The FE calculation was then performed by using the commercially available LS-DYNA V960.1106 (STN 10300-960.1106-00, Ref. 7) FE code. One calculation for annual frequency of occurrence of $1 \cdot 10^{-4}\ 1/yr$ was performed by using the commercially available LS-DYNA V970.3858 (STN 10300-970.3858 D SMP-00, Ref. 39) finite element code.

The results of these calculations were provided in terms of residual 1st principal stress plot in the WP OS. Subsequent analysis of residual 1st principal stress plot was performed to identify the damaged area. It is important to acknowledge the conservatism of the criterion used to define the damaged area (conservatism unrelated to the choice of the residual stress-threshold distribution). Namely, the failure criterion implies (see Section 1 and Assumption 3.22) that if a region on (either inner or outer) surface of WP OS exceeds the residual stress threshold the area "fails" (i.e., it is considered damaged) regardless of the residual stress distribution across the thickness of the region. Finally, the maximum stress intensity was presented to make an assessment regarding the safety of the WP OS from immediate breach.

3. ASSUMPTIONS

In the course of developing this document, the following assumptions are made regarding the structural calculation.

3.1 Some of the temperature-dependent material properties (specifically: density, Poisson's ratio, and elongation) are not available for Alloy 22, SA-240 S31600 (316 stainless steel [SS]), and SB-265 R52400 (Titanium Grade 7 [Ti-7]) except at room temperature (RT) ($20\ ^{\circ}C$). The RT density and RT Poisson's ratio are assumed for these materials. The impact of using RT density and RT Poisson's ratio is anticipated to be small. The rationale for this assumption is twofold: first, the said mechanical properties of the materials used do not change significantly at the temperature of interest in this calculation; and second, the material properties in question do not have dominant impact on the calculation results. This assumption is used in Section 5.1 and corresponds to paragraph 5.2.8.6 of Reference 8.

3.2 The temperature-dependent material properties are not available for TSw2 (Topopah Spring Welded-Lithophysal Poor) rock except at RT. The corresponding RT material properties are assumed for this material. The impact of using RT material properties is anticipated to be small. The rationale for this assumption is that the material properties of the rock do not have an impact on the calculation results. This assumption is used in Section 5.1 and corresponds to paragraph 5.2.16.1 of Reference 8.

3.3 Some of the rate-dependent material properties are not available for Alloy 22, 316 SS and Ti-7 at any strain rate. The material properties obtained under the static loading conditions are assumed for these materials. (Note that the following discussion is, for all practical purposes, relevant exclusively for Alloy 22 since all parts made of 316 SS and Ti-7 are represented as rigid in the FE representation [see Section 5.2].) The impact of using material properties obtained under static loading conditions is anticipated to be small. The rationale for this assumption is that the mechanical properties of subject materials (most importantly, Alloy 22) do not significantly change at the peak strain rates that occur during the earthquake simulation. The maximum plastic-strain rates in the WP OS observed in this calculation are of the order of $1\,s^{-1}$ (as indicated by maximum slopes of the effective-plastic-strain time histories), but this may not be a sufficiently accurate estimate due to the relatively coarse result-output frequency ($0.025\,s$) that is necessarily used in the lengthy seismic calculations. More reliable estimate of the peak strain rate, presented in Reference 27 (Section 3), is $50\,s^{-1}$; this strain rate is obtained for impact speed of $20\,m/s$ (see Ref. 27, Fig. 1), which is bounding for all impacts encountered in the course of vibratory ground motions in this document. As elaborated in Reference 27 (Section 3) no significant strain-rate sensitivity is observed at this strain-rate level. Furthermore, the end impacts (WP-WP interactions) addressed in Reference 27 are the dominant contributors to the cumulative damaged area in almost all realizations presented in this document (see Tables 6.1.4-2 and 6.2.4-2). This assumption is used in Section 5.1 and corresponds to paragraph 5.2.5 in Reference 8.

3.4 The Poisson's ratio of Alloy 22 is not available in literature. The Poisson's ratio of Alloy 625 (SB-443 N06625) is assumed for Alloy 22. The impact of this assumption is anticipated to be negligible. The rationale for this assumption is that the chemical compositions of Alloy 22 and Alloy 625 are similar (see Ref. 9 and Ref. 10 [p. 143], respectively). This assumption is used in Section 5.1 and corresponds to paragraph 5.2.8.2 of Reference 8.

3.5 The modulus of elasticity and Poisson's ratio of the TSw2 are characterized by significant scatter of data (see Ref. 28, Tables 3 and 4, respectively). For the purpose of the present calculation, modulus of elasticity is assumed to be 33 *GPa*, and Poisson's ratio 0.21. The rationale for this assumption is that these values agree well with typical values of said properties for most rocks of interest (see Ref. 28, Tables 3 and 4). This assumption is used in Section 5.1 and corresponds to paragraph 5.2.16.3 of Reference 8.

3.6 The density of the TSw2 is assumed to be $2370\,kg/m^3$. The rationale for this assumption is that this value agrees well with all Topopah Spring Welded rocks and is not exceeded by any of other rocks presented in Reference 23 (Table 2). It should be noted that this assumption has no effect on the calculation results since density of the rock affects only masses of the essentially rigid invert and the rigid drift walls. This assumption is used in Section 5.1 and corresponds to paragraph 5.2.16.4 of Reference 8.

3.7 The exact geometry of the loaded internals is simplified for the purpose of this calculation. The WP inner shell (including the inner shell lids) and its internals (including the spent nuclear fuel [SNF]) are represented by a thick-wall cylinder of uniform thickness and circular cross section, made from 316 SS (see Section 5.2). The thickness of this cylinder is determined based on the cumulative mass of these components. The rationale for this assumption is that the inner shell internal structure and the SNF affect the results of this calculation predominantly through the mass and overall dimensions. This assumption is used in Section 5.2.

3.8 The uniform strain (strain corresponding to tensile strength on the stress-strain curve) of Alloy 22 is not available in literature. Therefore, it is conservatively assumed that the uniform strain is 90 percent of the elongation. The rationale for this assumption is the character of stress-strain curve for Alloy 22 (see Ref. 15). This assumption is used in Section 5.1.2 and corresponds to paragraph 5.2.6.3 of Reference 8.

3.9 The uniform strain of 316 SS is not available in literature. Therefore, it is conservatively assumed that the uniform strain is 90 percent of the elongation. The rationale for this assumption is the character of stress-strain curve for 316 SS (see Ref. 16 [p. 304]). This assumption is used in Section 5.1.2 and corresponds to paragraph 5.2.6.3 of Reference 8.

3.10 The change of minimum elongation with increase of temperature for 316 SS is not available in literature. Therefore, the magnitude of this change at 150 $°C$ and 200 $°C$ is assumed to be –23 percent and –25 percent, respectively, based on the relative change of typical elongation for 316 SS available in Reference 14 (p. 8) (see Section 5.1.2 for details). The rationale for this conservative assumption is that the relative change of typical elongation should be bounding for the relative change of minimum elongation. This assumption is used in Sections 5.1 and 5.1.2 and corresponds to paragraph 5.2.8.7 of Reference 8.

3.11 The friction coefficients for metal-to-metal contact and metal-to-rock contact are considered random parameters in this calculation. The range of values for both of these friction coefficients is 0.2 to 0.8. The rationale for this assumption follows:

Reference 26 (Table 3.2.1, p. 3-26) provides coefficients of static and sliding friction for various metals and other materials. However, coefficients of friction for the materials used in this calculation are not specifically mentioned in this handbook. The potential for long-term corrosion to modify the sliding friction must also be considered in defining the friction coefficient. In this situation, the appropriate coefficients of friction for the repository components have high uncertainty. It is thus appropriate to pick a distribution of values for the coefficients of friction that encompass a range of materials and a range of mechanical responses from little or no sliding between components to substantial sliding between components.

A distribution of values for the friction coefficient between 0.2 and 0.8 will achieve these goals (see Section 6.1 and Ref. 35, Table I-4). First, this distribution is broad enough to encompass typical values of the dry sliding friction coefficients for a wide variety of metals and other materials (Reference 26, Table 3.2.1, p. 3-26). The appropriateness of this range is independently confirmed by seismic analyses for spent fuel storage racks (Ref. 32). This distribution is also broad enough to represent a range of mechanical response for the WP, pallet, and DS. A friction coefficient near 0.2 maximizes sliding of the WP on the pallet, of the pallet on the invert, and of the DS on the invert. Similarly, a friction coefficient near 0.8 minimizes sliding among the various components.

This assumption is used in Section 5.2.

3.12 The variation of functional friction coefficient between the static and dynamic value as a function of relative velocity of the surfaces in contact is not available in literature for the materials used in this calculation (see Section 5.2). Therefore, the effect of relative velocity of the surfaces in contact is neglected in these calculations by assuming that the functional friction coefficient and static friction coefficient are both equal to the dynamic friction coefficient. The impact of this assumption on results presented in this document is anticipated to be negligible. The rationale for this conservative assumption is that it provides the bounding set of results by minimizing the friction coefficient within the given FE-analysis framework. This assumption is used in Section 5.2 and corresponds to paragraph 5.2.14.2 of Reference 8.

3.13 The FE representation of DS is simplified in this analysis (see Section 5.2 for details), and density of Ti-7 is accordingly modified to account for the simplified DS representation. The impact of this assumption on results presented in this document is anticipated to be negligible. The rationale for this assumption is that it enables capturing the essential kinematics of freestanding components in the drift, while reducing the computer execution time. This assumption is used in Section 5.2.

3.14 The interaction between the WP and the longitudinal boundaries (representing the neighboring WPs) is, for the purpose of the calculation of the damaged area, assumed to be adequately described by a sequence of impacts of the WP on an essentially unyielding surface (Ref. 27). The rationale for this notably conservative assumption is that the initial longitudinal distance between the neighboring WPs is only $0.1\ m$ (Ref. 33, Table 2). In the course of the strong vibratory ground motions considered in this study, it is conceivable - if not very likely - that the motion of the WP-pallet assemblies would results in the local pile-up of the assemblies along the drift. Consequently, it may happen that the WP colliding with the neighboring WP cannot slide off but resists the impact as if it is fixed to the ground. This assumption is used in Section 5.2.

3.15 The interaction between the WP and DS (i.e., the lateral or side impacts) is not taken into account for the calculation of the total OS damaged area. The impact of this assumption on results presented in this document is anticipated to be negligible. The rationale for this assumption is twofold. First, the WP is by an order of magnitude heavier than the DS (see Attachments I and III); consequently, the impact between the WP and DS would result in the DS being simply pushed around by the WP without significant deformation of the WP OS. Second, the interaction between WP and DS (similarly to the longitudinal interaction [end impacts]) takes place by the way of the trunnion collar sleeves. Since the longitudinal interactions are much more frequent, and the WP is much stiffer "target" than the DS, it is not likely (see Ref. 27, Tables 4 through 8, for impact angles) that the side impacts would damage an area that is not already damaged by the end impacts. This assumption is used in Sections 6.1.3 and 6.2.3, and Attachment VIII.

3.16 All interactions between the WP and the longitudinal boundaries (representing the neighboring WPs) with impact velocities less than 1 m/s are not taken into account for the calculation of the OS damaged area. The impact of this assumption on results presented in this document is negligible. The rationale for this assumption is that Reference 27 (Tables 4 through 8) indicates that the damaged area for impact velocity of 1 m/s is either zero or negligible compared to the other evaluated impact velocities. This assumption is used in Section 6.1.2 and Attachment XI.

3.17 The longitudinal pallet tubes (Tube 1 in Attachment II) are, for the purpose of this calculation, assumed to be made of Alloy 22. This assumption has a significant impact on the calculation results. The rationale for this assumption is that due to the long-term corrosion it is impossible to take structural credit for these tubes as long as they are made of 316 SS. Thus, unless this design change is made, the pallet is going to fail due to an unacceptable performance (i.e., it would fail to support the WP as intended). This assumption is used in Sections 1, 5.1, and 5.2.

3.18 The damaged area of the OS due to the WP-pallet interaction is evaluated only on one WP end, in the finely meshed OS region (see Section 5.2 for details). The total damaged area due to the WP-pallet interaction is obtained by assuming that the damaged areas on the two WP ends are the same (i.e., by multiplying by two the damaged area evaluated on one side). The rationale for this assumption is that the number and intensity of impacts on the two ends should be statistically similar. This assumption is used in Sections 6.1.1 and 6.5.2.

3.19 The WP is assumed to be symmetric about its mid-plane. Both WP ends are represented based on the bottom-end configuration (see Attachment I and Reference 24). This simplification has no effect on the results, as obtained in this calculation. The rationale for this assumption is that it simplifies FE representation, without affecting the calculation results. This assumption is used in Section 5.2.

3.20 The temperature of the WP is assumed to be 150 °C for temperature-dependent material properties. The rationale for this assumption is that this temperature is conservative for most of the regulatory period for high-temperature operating modes (97 percent of the regulatory period [see Reference 21, Figure 6-3]) and strictly conservative for low-temperature operating modes. This assumption is used in Section 5.1 and Attachment V.

3.21 The thickness of the WP OS is reduced by 2 mm. The rationale for this assumption is that the thickness reduction of 2 mm over the regulatory period of 10,000 years is conservative (Reference 3, Sheet 1 in accordance with Reference 40, Section 6.3.4). This assumption is used in Sections 1 and 5.2.

3.22 The distribution of the residual stress threshold is assumed to be uniform with a lower bound of 80 percent of the yield strength of Alloy 22 and an upper bound of 90 percent of the yield strength of Alloy 22. The basis for this assumption is the data provided in Reference 36. This assumption is used in Sections 1 and 2.

4. USE OF COMPUTER SOFTWARE

One of the FE analysis computer codes used for this calculation is ANSYS V5.6.2, which is obtained from Software Configuration Management in accordance with appropriate procedure (Ref. 2), and is identified by STN 10364-5.6.2-01 (Ref. 6). ANSYS V5.6.2 is a qualified commercially available FE code and is appropriate for application performed in this calculation. The calculations using ANSYS V5.6.2 software were executed on four Hewlett-Packard (HP) 9000 series UNIX workstations (Operating System HP-UX 11.00) identified with the YMP (Yucca Mountain Project) property tag numbers 151324, 151325, 151664, and 151665, located in Las Vegas, Nevada. The development of FE mesh by ANSYS is fully within the range of the validation performed for ANSYS V5.6.2 code. Access to the code is granted by the Software Configuration Management in accordance with the appropriate procedures.

The input files (identified by .inp file extension) and output files (identified by .out file extension) for ANSYS V5.6.2 are listed in Section 8, and provided in Attachment X.

A qualified FE analysis computer code used for this calculation is Livermore Software Technology Corporation (LSTC) LS-DYNA V960.1106 (Ref. 7). LS-DYNA V960.1106 was obtained from Software Configuration Management in accordance with the appropriate procedure (Ref. 2) and is identified by STN 10300-960.1106-00. Double-precision version of LS-DYNA V960.1106 is appropriate for its intended use. The LS-DYNA V960.1106 evaluation performed for this calculation is fully within the range of the validation performed for the LS-DYNA V960.1106 code. The calculations were executed on eight HP 9000 series UNIX workstations (Operating System HP-UX 11.00) identified with the YMP property tag numbers 151324, 151325, 150688, 150689, 150690, 151691, 151664, and 151665 located in Las Vegas, Nevada. Access to LS-DYNA V960.1106 was granted by the Software Configuration Management in accordance with the appropriate procedures.

The second qualified FE analysis computer code used for $1 \cdot 10^{-4}\ 1/yr$ calculation is LSTC LS-DYNA V970.3858 (Ref. 39). LS-DYNA V970.3858 was obtained from Software Configuration Management in accordance with the appropriate procedure (Ref. 2) and is identified by STN 10300-970.3858 D SMP-00. Double-precision version of LS-DYNA V970.3858 is appropriate for its intended use. The LS-DYNA V970.3858 evaluation performed for this calculation is fully within the range of the validation performed for the LS-DYNA V970.3858 code. The calculations using LS-DYNA V970.3858 were executed on the HP Itanium2 (IA64) series UNIX workstations (Operating System HP-UX 11.22), identified with YMP tag number 501711, located in Las Vegas, Nevada. Access to LS-DYNA V970.3858 was granted by the Software Configuration Management in accordance with the appropriate procedures.

The input files (identified by .k, .dat, and .inc file extensions) and output files (d3hsp, d3plot, and messag) for LS-DYNA V960.1106 and LS-DYNA V970.3858 are listed in Section 8, and provided in Attachment X. (LS-DYNA V960.1106 output files rcforc and glstat are provided for realizations number 1 [at annual frequency of occurrence $1 \cdot 10^{-6}\ 1/yr$ and $1 \cdot 10^{-7}\ 1/yr$] for illustration.)

As identified in Section 6, LSPOST V2.0 and LS-PREPOST V1.0 (LSTC) are postprocessors used for visual display and graphical representation of results that are exempt of the requirements defined in Reference 2 (Section 2.1.2). Note that LS-PREPOST V1.0 is used only for postprocessing results of the $1 \cdot 10^{-4}$ $1/yr$ calculation.

5. CALCULATION

5.1 MATERIAL PROPERTIES

Material properties used in these calculations are listed in this section. The material properties are evaluated for two different WP OS temperatures experienced in the repository emplacement drift: 150 $^{\circ}C$ (Assumption 3.20) and 200 $^{\circ}C$. The latter is selected as a reasonable upper bound for high-temperature operating modes (according to Ref. 21 [Fig. 6-3] temperature of 200 $^{\circ}C$ is conservative for more than 99 percent of the regulatory period) to study the effect of ambient temperature on calculation results. Some of the temperature-dependent and rate-dependent material properties are not available for Alloy 22, 316 SS, Ti-7, and TSw2 rock. Therefore, RT density and RT Poisson's ratio are used for Alloy 22, 316 SS, and Ti-7 (see Assumption 3.1). The change of minimum elongation for 316 SS is estimated based on the relative change of typical elongation available in vendor catalogue (Assumption 3.10). The RT material properties are used for TSw2 rock (Assumption 3.2). Finally, the material properties obtained under the static loading conditions are used for all materials in this calculation (Assumption 3.3).

SB-575 N06022 (Alloy 22) (OS, OS lids, upper and lower trunnion collar sleeves, and pallet [see Assumption 3.17]) (Note: All properties of Alloy 22 are obtained from Reference 9. But while the density, Poisson's ratio, and modulus of elasticity are uniquely defined therein, the elongation and strengths are available in more than one table. The latter properties are, for the purpose of this calculation, obtained from Table "*Plate,* $\frac{1}{4}-\frac{3}{4}$ *in.* $(6.4-19.1\ mm)$ *thick*"):

Density = 8690 kg/m^3 (at RT) (Ref. 9)

Yield strength = 338 MPa (at 200 $^{\circ}F$ = 93 $^{\circ}C$) (Ref. 9)
Yield strength = 283 MPa (at 400 $^{\circ}F$ = 204 $^{\circ}C$) (Ref. 9)

Tensile strength = 738 MPa (at 200 $^{\circ}F$ = 93 $^{\circ}C$) (Ref. 9)
Tensile strength = 676 MPa (at 400 $^{\circ}F$ = 204 $^{\circ}C$) (Ref. 9)

Elongation = 0.65 (at 200 $^{\circ}F$ = 93 $^{\circ}C$) (Ref. 9)
Elongation = 0.66 (at 400 $^{\circ}F$ = 204 $^{\circ}C$) (Ref. 9)

Poisson's ratio = 0.278 (at RT) (Ref. 9; see Assumption 3.4)

Modulus of elasticity = 203 GPa (at 93 $^{\circ}C$) (Ref. 9)
Modulus of elasticity = 196 GPa (at 204 $^{\circ}C$) (Ref. 9)

SA-240 S31600 (316 SS) (Inner shell and inner shell lids):

Density = 7980 kg/m^3 (at RT) (Ref. 11, Table X1.1, p. 7)

Yield strength = 161 MPa (23.4 ksi) (at 300 $°F$ = 149 $°C$) (Ref. 12, Sec. II, Part D, Subpart 1, Table Y-1)
Yield strength = 148 MPa (21.4 ksi) (at 400 $°F$ = 204 $°C$) (Ref. 12, Sec. II, Part D, Subpart 1, Table Y-1)

Tensile strength = 503 MPa (72.9 ksi) (at 300 $°F$ = 149 $°C$) (Ref. 12, Sec. II, Part D, Subpart 1, Table U)
Tensile strength = 496 MPa (71.9 ksi) (at 400 $°F$ = 204 $°C$) (Ref. 12, Sec. II, Part D, Subpart 1, Table U)

Elongation = 0.40 (at RT) (Ref. 12, Sec. II, Part A, SA-240, Table 2)

Poisson's ratio = 0.298 (at RT) (Ref. 10, Figure 15, p. 755)

Modulus of elasticity = 186 GPa ($27.0 \cdot 10^6$ psi) (at 300 $°F$ = 149 $°C$) (Ref. 12, Sec. II, Part D, Subpart 2, Table TM-1)
Modulus of elasticity = 183 GPa ($26.5 \cdot 10^6$ psi) (at 400 $°F$ = 204 $°C$) (Ref. 12, Sec. II, Part D, Subpart 2, Table TM-1)

SB-265 R52400 (Titanium Grade 7 [Ti-7]) (DS) (Note: Poisson's ratio and moduli of elasticity of Ti-7 are obtained from Reference 19; both properties are uniquely defined in Section "Mechanical Properties"):

Poisson's ratio = 0.32 (at RT)

Modulus of elasticity = 101 GPa (at 149 $°C$)
Modulus of elasticity = 97 GPa (at 204 $°C$)

TSw2 Rock:

Density = 2370 kg/m^3 (at RT) (Assumption 3.6)

Poisson's ratio = 0.21 (at RT) (Assumption 3.5)

Modulus of elasticity = 33.0 GPa (at RT) (Assumption 3.5)

5.1.1 Calculations for Elevated-Temperature Material Properties

The structural calculations are performed at two different WP OS temperatures: $150\ ^{\circ}C$ and $200\ ^{\circ}C$. The material properties at these two temperatures are obtained by linear interpolation of corresponding material properties presented in Section 5.1, by using the formula:

$$p = p(T) = p_l + \left(\frac{T - T_l}{T_u - T_l}\right)\cdot(p_u - p_l)$$

Subscripts u and l denote the bounding values of generic material property p at the corresponding bounding temperatures.

The following parameters are used in the subsequent calculations:

$s_y \approx \sigma_y$ = yield strength
s_u = engineering tensile strength
el = elongation
E = modulus of elasticity

These material properties are obtained from Section 5.1.

In the case of Alloy 22, the material properties at $150\ ^{\circ}C$ are:

$$\sigma_y \approx s_y = 338 + [(150-93)\cdot(283-338)]/(204-93) = 310 MPa$$
$$s_u = 738 + [(150-93)\cdot(676-738)]/(204-93) = 706 MPa$$
$$el = 0.65 + [(150-93)\cdot(0.66-0.65)]/(204-93) = 0.66$$
$$E = 203 + [(150-93)\cdot(196-203)]/(204-93) = 199 GPa$$

For the temperature of $200\ ^{\circ}C$, the material properties of Alloy 22 are:

$$\sigma_y \approx s_y = 338 + [(200-93)\cdot(283-338)]/(204-93) = 285 MPa$$
$$s_u = 738 + [(200-93)\cdot(676-738)]/(204-93) = 678 MPa$$
$$el = 0.65 + [(200-93)\cdot(0.66-0.65)]/(204-93) = 0.66$$
$$E = 203 + [(200-93)\cdot(196-203)]/(204-93) = 196 GPa$$

Similarly, for 316 SS at $150\ ^{\circ}C$:

$$\sigma_y \approx s_y = 161 + [(150-149)\cdot(148-161)]/(204-149) = 161 MPa$$
$$s_u = 503 + [(150-149)\cdot(496-503)]/(204-149) = 503 MPa$$
$$E = 186 + [(150-149)\cdot(183-186)]/(204-149) = 186 GPa$$

While at $200\,^{\circ}C$:

$$\sigma_y \approx s_y = 161 + [(200-149)\cdot(148-161)]/(204-149) = 149\,MPa$$
$$s_u = 503 + [(200-149)\cdot(496-503)]/(204-149) = 497\,MPa$$
$$E = 186 + [(200-149)\cdot(183-186)]/(204-149) = 183\,GPa$$

Finally, for Ti-7:

$$E = 101 + [(150-149)\cdot(97-101)]/(204-149) = 101\,GPa \quad (150\,^{\circ}C)$$
$$E = 101 + [(200-149)\cdot(97-101)]/(204-149) = 97\,GPa \quad (200\,^{\circ}C)$$

5.1.2 Calculations for True Measures of Ductility

The material properties in Section 5.1 refer to engineering stress and strain definitions: $s = P/A_0$ and $e = L/L_0 - 1$ (see Ref. 13, Chapter 9), where P stands for the force applied during a static tensile test, L is the length of the deformed specimen, and L_0 and A_0 are the original length and cross-sectional area of the specimen, respectively. The engineering stress-strain curve does not give a true indication of the deformation characteristics of a material during plastic deformation since it is based entirely on the original dimensions of the specimen. In addition, ductile metal that is pulled in tension becomes unstable and necks down during the course of the test. Hence, LS-DYNA V960.1106 FE code requires input in terms of true stress and strain definitions: $\sigma = P/A$ and $\varepsilon = \ln(L/L_0)$ (see Ref. 13, Chapter 9).

The relationships between the true stress and strain definitions and the engineering stress and strain definitions, $\sigma = s\cdot(1+e)$ and $\varepsilon = \ln(1+e)$, can be readily derived based on constancy of volume ($A_0 \cdot L_0 = A \cdot L$) and strain homogeneity during plastic deformation (see Ref. 13, Chapter 9). These expressions are applicable only in the hardening region of the stress-strain curve that is limited by the onset of necking.

The following parameters are added in the subsequent calculations:

σ_u = true tensile strength
$e_y \approx \varepsilon_y$ = strain corresponding to yield strength
e_u = engineering strain corresponding to tensile strength (engineering uniform strain)
ε_u = true strain corresponding to tensile strength (true uniform strain)

In absence of data on the uniform strain in available literature, the uniform strain needs to be estimated based on the character of stress-strain curves and elongation (strain corresponding to rupture of the tensile specimen).

Furthermore, the change of minimum elongation with increase of temperature for 316 SS is not available in literature. Therefore, for 316 SS the magnitude of this change at the two temperatures of interest in this calculation ($150\,^{\circ}C$ and $200\,^{\circ}C$) is estimated based on the change of typical elongation for said material (Assumption 3.10). Reference 14 (p. 8) suggests that the elongation decreases by 21 percent for an increase of temperature from RT to 93 $^{\circ}C$, and by 25 percent for an increase of temperature from RT to 204 $^{\circ}C$. Hence, the decrease of elongation corresponding to an increase of temperature from RT to 150 $^{\circ}C$ is 23 percent, while the decrease of elongation corresponding to an increase of temperature from RT to 200 $^{\circ}C$ is 25 percent. Consequently, the true measures of ductility and tangent moduli have to take into account the variability of elongation due to change of temperature.

The stress-strain curves for Alloy 22 and 316 SS do not manifest three-stage (elastic-hardening-softening) deformation character (see Assumptions 3.8 and 3.9). Therefore, the elongation reduced by 10 percent (to take into account the specimen-failure part of the stress-strain curve) is assumed for uniform strain for both materials.

In the case of Alloy 22

$$e_u = 0.9 \cdot el = 0.9 \cdot 0.66 = 0.59 \text{ (at 150 } ^{\circ}C\text{)}$$
$$e_u = 0.9 \cdot el = 0.9 \cdot 0.66 = 0.59 \text{ (at 200 } ^{\circ}C\text{)}$$

The true measures of ductility at 150 $^{\circ}C$ are

$$\varepsilon_u = \ln(1+e_u) = \ln(1+0.59) = 0.46$$
$$\sigma_u = s_u \cdot (1+e_u) = 706 \cdot (1+0.59) = 1120\,MPa$$

while at 200 $^{\circ}C$

$$\varepsilon_u = \ln(1+e_u) = \ln(1+0.59) = 0.46$$
$$\sigma_u = s_u \cdot (1+e_u) = 678 \cdot (1+0.59) = 1080\,MPa$$

Therefore, the true tensile strength of Alloy 22 at 150 $^{\circ}C$ and 200 $^{\circ}C$ is, respectively, 1120 MPa and 1080 MPa.

For 316 SS

$$e_u = (1-0.23) \cdot (0.9 \cdot el) = (1-0.23) \cdot (0.9 \cdot 0.40) = 0.28 \text{ (at 150 } ^{\circ}C\text{)}$$
$$e_u = (1-0.25) \cdot (0.9 \cdot el) = (1-0.25) \cdot (0.9 \cdot 0.40) = 0.27 \text{ (at 200 } ^{\circ}C\text{)}$$

Therefore, the true uniform strain and true tensile strength at 150 $^{\circ}C$ are

$\varepsilon_u = \ln(1+e_u) = \ln(1+0.28) = 0.25$
$\sigma_u = s_u \cdot (1+e_u) = 503 \cdot (1+0.28) = 644\,MPa$

while at 200 $°C$

$\varepsilon_u = \ln(1+e_u) = \ln(1+0.27) = 0.24$
$\sigma_u = s_u \cdot (1+e_u) = 497 \cdot (1+0.27) = 631\,MPa$

Hence, the true tensile strength of 316 SS at 150 $°C$ and 250 $°C$ is, respectively, 644 MPa and 631 MPa.

5.1.3 Calculations for Tangent Moduli

As previously discussed, the results of this simulation are required to include elastic and plastic deformations for Alloy 22 and 316 SS. When the materials are driven into the plastic range, the slope of the stress-strain curve continuously changes. A ductile failure is preceded by a protracted regime of hardening and substantial accumulation of inelastic strains. Thus, a simplification for stress-strain curve is needed to incorporate plasticity into the FE analysis. A standard approximation commonly used in engineering is to use a straight line that connects the yield point and the tensile strength point of the material. The parameters used in the subsequent calculations in addition to those defined in Section 5.1.2 are modulus of elasticity (E) and tangent (hardening) modulus (E_1). The tangent modulus represents the slope of the stress-strain curve in the plastic region.

In the case of Alloy 22, the tangent modulus is:

$E_1 = (\sigma_u - \sigma_y)/(\varepsilon_u - \sigma_y/E) = (1.12 - 0.310)/(0.46 - 0.310/199) = 1.77\ GPa$ (see Sections 5.1, 5.1.1, and 5.1.2) (at 150 $°C$)
$E_1 = (\sigma_u - \sigma_y)/(\varepsilon_u - \sigma_y/E) = (1.08 - 0.285)/(0.46 - 0.285/196) = 1.73\ GPa$ (see Sections 5.1, 5.1.1, and 5.1.2) (at 200 $°C$)

Similarly, for 316 SS:

$E_1 = (\sigma_u - \sigma_y)/(\varepsilon_u - \sigma_y/E) = (0.644 - 0.161)/(0.25 - 0.161/186) = 1.94\ GPa$ (see Sections 5.1, 5.1.1, and 5.1.2) (at 150 $°C$)
$E_1 = (\sigma_u - \sigma_y)/(\varepsilon_u - \sigma_y/E) = (0.631 - 0.149)/(0.24 - 0.149/183) = 2.02\ GPa$ (see Sections 5.1, 5.1.1, and 5.1.2) (at 200 $°C$)

5.2 FINITE ELEMENT REPRESENTATION

Three-dimensional FE representation, used for the vibratory ground-motion simulations, is presented in Figure 1. A corresponding cut-away view (portions of various parts are removed to offer a more revealing outlook) is presented in Figure 2. As seen in these figures, the FE representation consists of the WP mounted on the pallet, the DS, the invert surface, and the lateral and longitudinal boundaries. The longitudinal boundary represents the neighboring WP/pallet assembly (Assumption 3.14), while the lateral boundary represents the repository emplacement drift. The FE representation is developed in ANSYS V5.6.2, by using the dimensions provided in References 22 and 24; and Attachments I, II, and III (see Assumption 3.17).

According to Reference 33 (Table 2) the average WP skirt-to-skirt spacing is $0.1\,m$. Thus, the distance between the WP (specifically, the trunnion collar sleeve [i.e., skirt]) and the longitudinal boundary (representing the neighboring WP-pallet assembly) in all FE representations developed for the purpose of this calculation is $0.1\,m$.

Three components of the ground-motion acceleration time history are simultaneously applied on the platform representing the invert surface. The invert surface is essentially unyielding (elastic). (This is just a formal LS-DYNA requirement; the same acceleration time history applied to all platform nodes result in zero deformation by definition.)

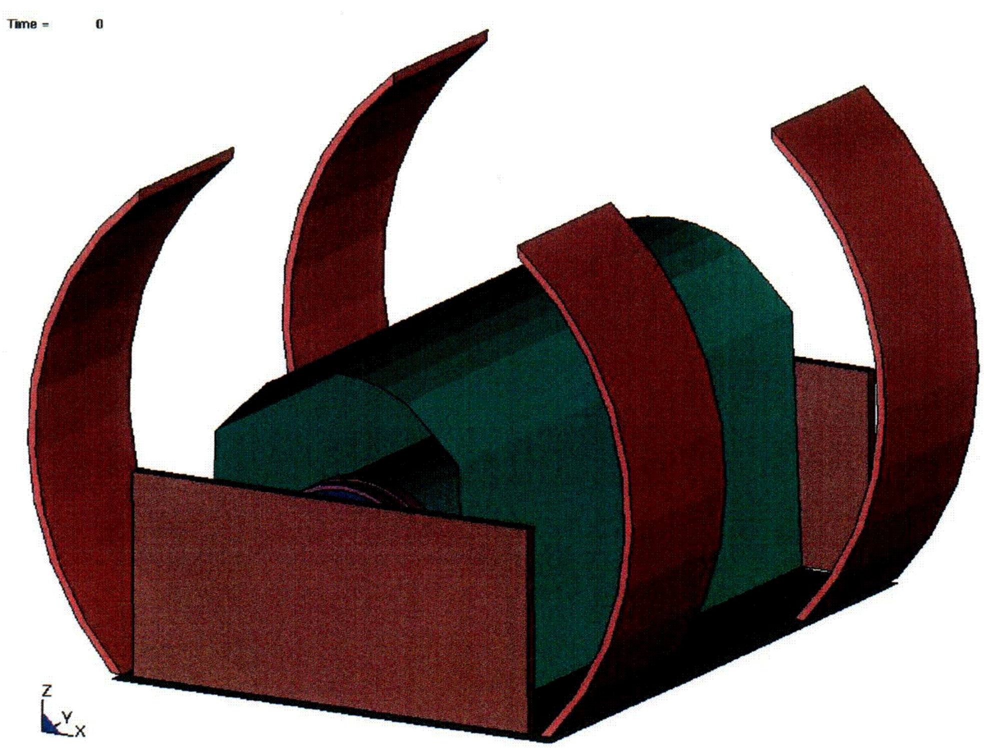

Figure 1. Setup for WP Vibratory Simulations at $1 \cdot 10^{-6}\ 1/yr$ Annual Frequency of Occurence

C01

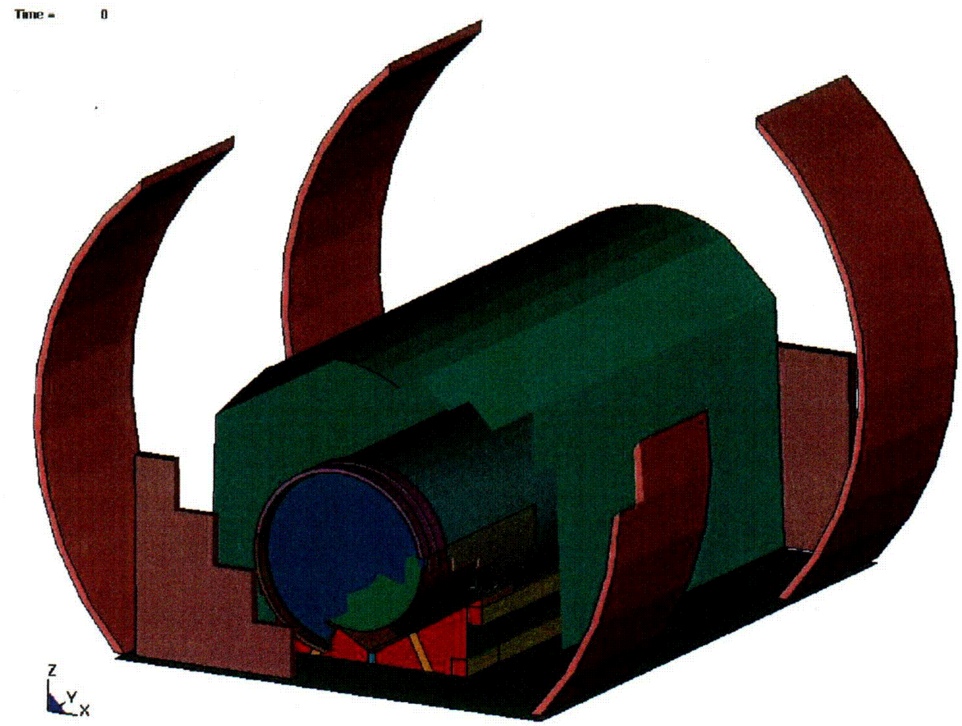

Figure 2. Cut-Away View of Setup for WP Vibratory Simulations

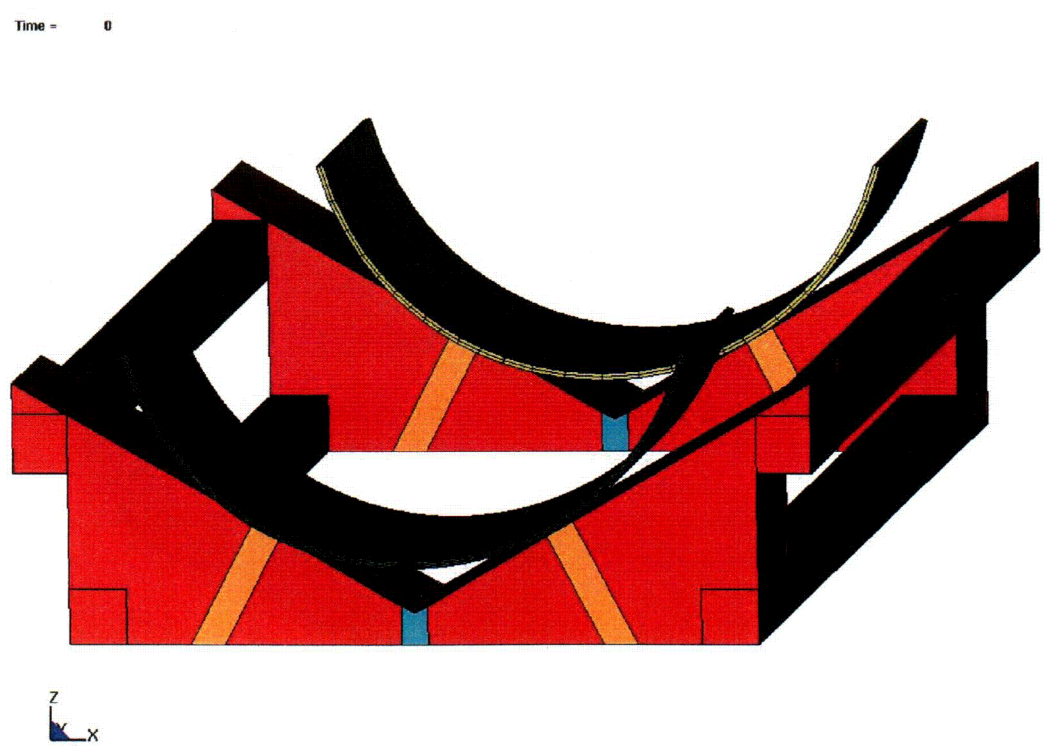

Figure 3. Pallet and Two Regions of WP OS That Can Come in Contact with Pallet

C02

The lateral and longitudinal boundaries are both rigid and fixed to the platform in such a way that their motion is completely synchronous. Externally applied momentum is transferred to all freestanding (unanchored) objects solely by the way of friction and impact.

The WP is represented as symmetric throughout this calculation (Assumption 3.19). Thus, both WP ends are represented based on the bottom-end configuration (see Attachment I and Reference 24). The details of the WP top end (such as, for example, the extended OS lid and closure lid) are ignored and their mass is taken into account by increasing thickness of the OS lid.

For the simulation of the WP/pallet assembly exposed to vibratory ground motion, the thickness of the WP OS is reduced by 2 *mm* (from 20 *mm* to 18 *mm*; see Assumption 3.21). It needs to be emphasized, though, that the objective of this calculation is not to rigorously evaluate the OS-thickness reduction due to corrosion or the corrosion-acceleration effects. A depth of corroded layer of 2 *mm* is, therefore, a conservatism within the stated objective of this calculation (see Section 1).

The WP OS, the trunnion collar sleeve, and the boundary walls are represented by 8-node solid (brick) elements. The part of the OS that can come in contact with the pallet (see Figs. 3 and 7; also designated by F and C in Fig. 4), is of the most importance in this calculation. The FE representation of this region of the OS is finely meshed on one side of the WP (F in Fig. 4), with four layers of brick elements across the OS thickness and relatively dense in-plane mesh. The corresponding OS region on the other side (C in Fig. 4) is more coarsely meshed with only two layers of brick elements across the thickness (see Figs. 3 and 4). These two parts of the WP OS are represented as elastoplastic (linear kinematic hardening).

All results reported in this document are presented for the part of the OS designated by F in Figure 4. The part of the OS designated by C (Fig. 4), although coarsely meshed compared to F, is still relatively finely meshed compared to the remaining part of the OS (P and R in Fig. 4), in order to ensure proper WP-pallet interaction and, consequently, the WP rigid-body motion. In a way, the main purpose of the WP OS parts P and R is to provide appropriate boundary conditions for the WP OS parts F and C. The main difference between parts of the OS designated as P and R is that P is represented as elastoplastic (linear kinematic hardening) while R is rigid. The WP components (excluding inner shell and inner shell lids) represented as rigid bodies are presented in Figures 5 and 7b. These components are also called "rigid Alloy 22 components" throughout this document.

It cannot be overemphasized that the region F is especially important since the stress state, and consequently the damaged area, are evaluated for that region only. Two regions of the OS that can get in contact with pallet (F and C) are connected to the remaining part of the OS (P and R) by tied-interface contacts (Refs. 17 [Section 23.9] and 18 [p. 6.29]).

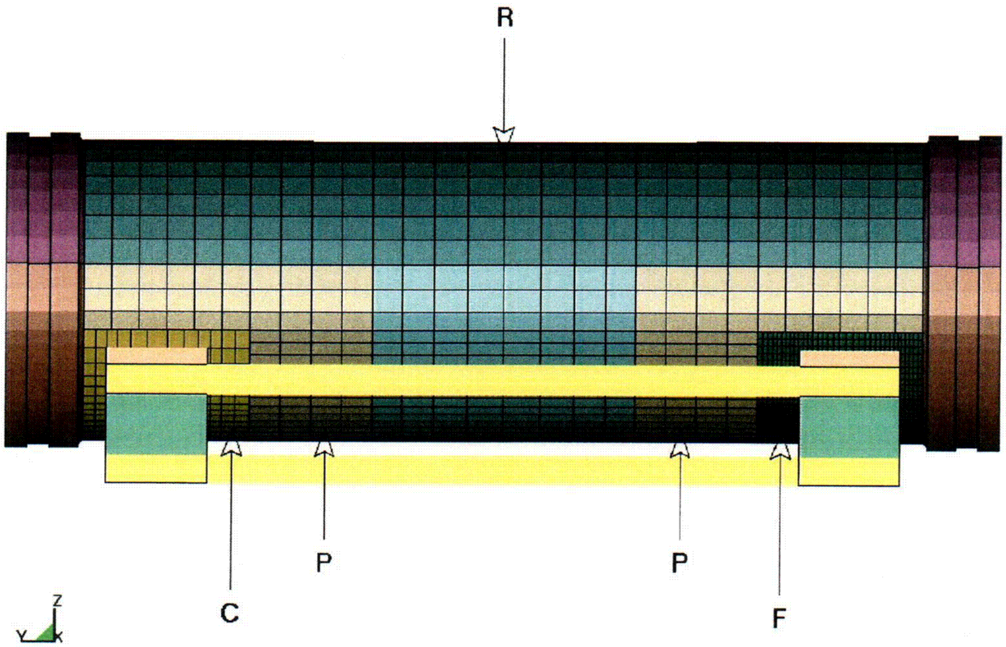

Figure 4. WP OS Regions (Side View)

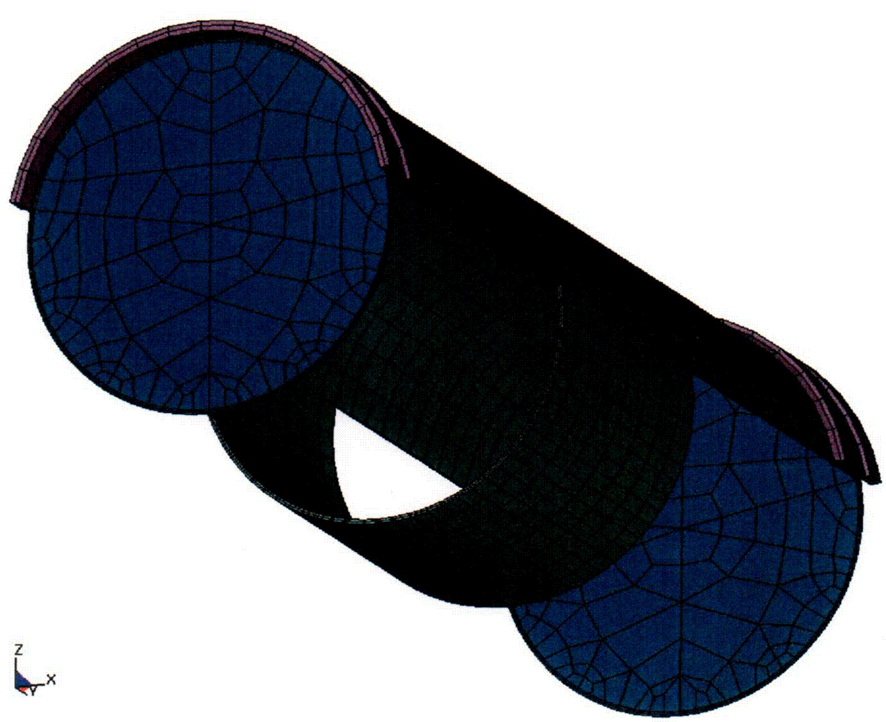

Figure 5. Parts of WP Represented as Rigid Bodies (Inner Shell and Inner Shell Lids Excluded)

The WP inner shell and its lid, pallet, and DS are represented by shell elements. The shell elements are adequate for representation of said components since their dominant mode of deformation is local bending. Additionally, the stress states in the inner shell, pallet, and DS are of secondary importance in this analysis that is focused on the WP OS. In order to reduce the computer execution time while preserving all the features relevant for the solution, the inner shell and inner shell lids, and DS are represented as rigid bodies (see Attachment VI).

The pallet is represented as elastoplastic but it is very coarsely meshed (see Fig. 6). The coarse mesh of the pallet – necessitated by the computer-execution-time considerations – results in an artificial increase of the pallet stiffness. In other words, the pallet is not as flexible as in reality and some of the cushioning effect of the pallet on the WP is, therefore, lost. The ultimate consequences of the coarse pallet mesh are increase in the relative motion between the WP and pallet, and increase of stress in the WP. Both of these effects are conservative from the viewpoint of the results of this analysis. Nonetheless, for the set of calculations performed for the annual frequency of occurrence of $10^{-7}\ 1/yr$ the pallet mesh is refined (see Fig. 6b) to prevent excessive relative motion and ensure more realistic results. This change is necessitated by the much higher intensity of the ground motion at the annual frequency of occurrence of $10^{-7}\ 1/yr$.

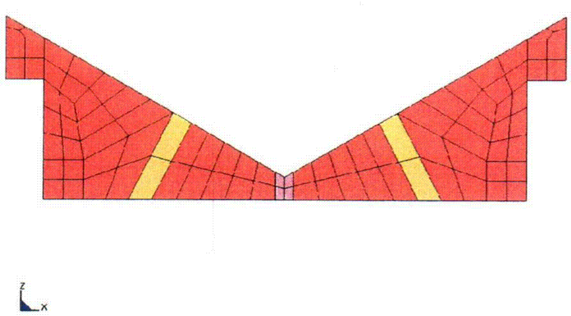

(a)

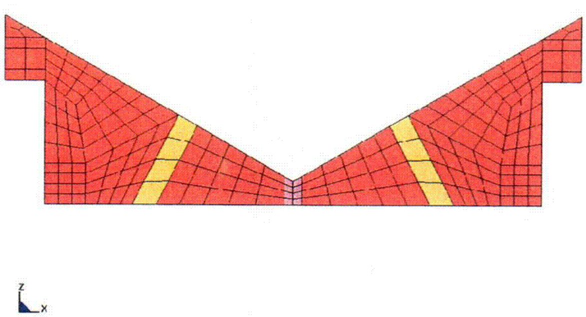

(b)

Figure 6. Front View of Pallet Mesh for: (a) $10^{-6}\ 1/yr$ Calculations, and (b) $10^{-7}\ 1/yr$ Calculations

The structure of the 21-PWRWP is simplified by reducing the structure of the inner shell and all WP internals, including the SNF, to a thick-wall cylinder of circular cross section and uniform density (Assumption 3.7). The outside diameter of the inner shell is kept unchanged. The thickness of the inner shell is determined by using the material properties (including density) of 316 SS, and matching the total mass of the inner shell and internals as presented in Attachment I. The benefit of using this approach is to reduce the computer execution time while preserving all features of the problem relevant to the structural response.

The FE representation of the 21-PWR WP is developed in such a way that the loose-fit gap between the outer and inner shell is maximized to $4\,mm$ (Ref. 25, Section 8.1.8). Consequently, the inner

C04

shell is free to move within the OS. This maximized gap provides a conservatively bounding set of results, as demonstrated in Reference 27 (Attachment II).

The FE representation of DS is simplified in this analysis (Assumption 3.13). All the details of the DS structure are disregarded, and the DS is represented as a rigid shell structure following the contour of the actual DS presented in Attachment III. For the same reason, the DS is considered to be made completely of Ti-7. Density of Ti-7 is accordingly modified to account for the simplified DS representation (i.e., to match the DS mass). These simplifications make it possible to capture the essential kinematics of freestanding components in the drift, while reducing the computer execution time. The impact of this DS-representation on results presented in this document is anticipated to be negligible.

The most notable differences (in addition to the pallet mesh [Fig. 6]) between the two FE representations ($1 \cdot 10^{-7}$ $1/yr$ vs. $1 \cdot 10^{-6}$ $1/yr$) is that the finely-meshed region is fully extended in the circumferential direction, and that the configuration of the rigid OS parts is changed (as illustrated by Figure 7). These modifications are necessitated by much more intense ground motion, causing much more relative (rigid-body) motion between the unanchored repository components. Figures 7(a) and 7(b) (for the FE representation for 10^{-7} $1/yr$ calculations) correspond to Figures 3 and 5 (for the FE representation for 10^{-6} $1/yr$ calculations).

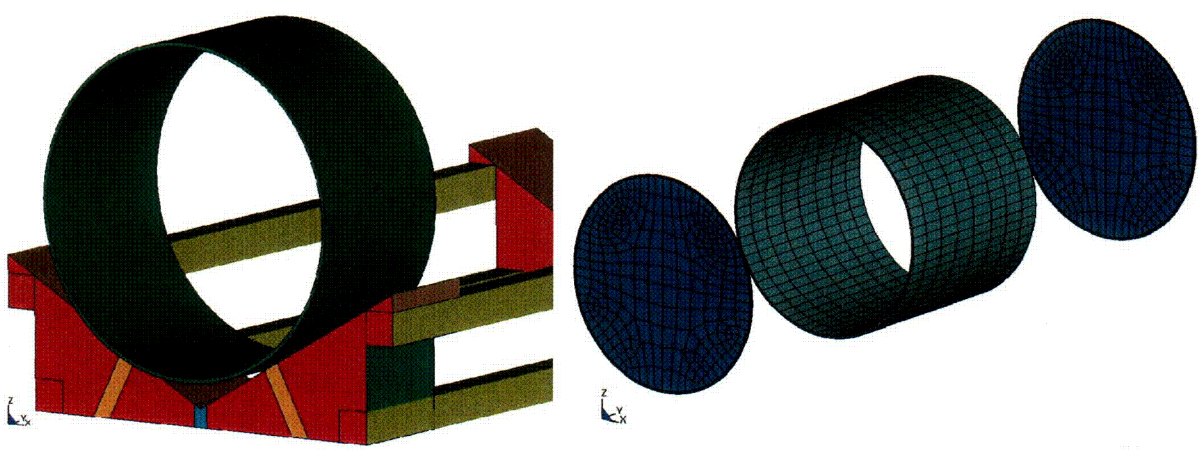

(a) (b)

Figure 7. Modifications in FE Representation for 10^{-7} $1/yr$ Calculations: (a) Extended Finely-Meshed OS Region, and (b) Rigid Parts

The FE representation is then used in LS-DYNA V960.1106 and LS-DYNA V970.3858 to perform a transient dynamic analysis of the WP exposed to vibratory ground motion.

Contacts are specified between: OS and inner shell, OS and pallet, WP (i.e., trunnion collar sleeve) and longitudinal and lateral boundaries, pallet and invert, pallet and longitudinal and lateral boundaries, etc. In absence of more specific data, the dynamic friction coefficients for all contacts are

C05

randomly sampled from a uniform distribution between 0.2 and 0.8 (see Assumption 3.11). One metal-to-metal friction coefficient and one metal-to-rock friction coefficient are sampled for each realization (see Table 6.1-1), and applied to all metal-to-metal and metal-to-rock contacts. In other words, the friction coefficients vary from realization to realization (random sampling) but all metal-to-metal contacts have the same friction coefficient in a specific realization regardless of the contact pair; the same applies to metal-to-rock contacts. Moreover, the functional friction coefficient used by LS-DYNA V960.1106 and LS-DYNA V970.3858 FE codes is defined in terms of static and dynamic friction coefficients, and relative velocity of the surfaces in contact (Ref. 18, p. 6.9). The effect of the relative velocity of the surfaces in contact is introduced by the way of a fitting parameter - exponential decay coefficient. The variation of friction coefficient between the static and dynamic value as a function of relative velocity of the surfaces in contact is not available in literature for the materials used in this calculation. Therefore, it is not possible to objectively evaluate the exponential decay coefficient. Hence, the effect of the relative velocity of the surfaces in contact is neglected in these calculations by assuming that the functional friction coefficient and the static friction coefficient are equal to the dynamic friction coefficient. This approach maximizes the relative motion of the unanchored repository components by minimizing the friction coefficient within the given FE-analysis framework (Assumption 3.12).

The simulation is performed in two steps. First step is the vibratory part. During this computational phase the three components of ground-motion acceleration time history are simultaneously applied to all invert nodes. The stochastic (uncertain) input parameters for 15 simulations of events corresponding to annual frequencies of occurrence $1 \cdot 10^{-6}$ $1/yr$ and $1 \cdot 10^{-7}$ $1/yr$ are listed in Table 6.1-1 (Ref. 35, Table I-4). In the course of this vibratory simulation neither system damping nor contact damping are applied. This, admittedly conservative, approach is used in order to prevent unwanted interference of the damping with the rigid-body motion of unanchored structures that could contaminate results. The second step of the simulation is the post-vibratory relaxation. During this computational phase the motion of the invert nodes is constrained in all three directions, and the only load applied to freestanding objects is the acceleration of gravity. In the course of this phase the system damping is applied globally (to all objects). The goal of this step is to obtain steady-state results (i.e., residual stresses) in a reasonable time, and the purpose of the global system damping is to reduce this time as much as possible (see Section 5.2.2 for details). The specified duration of this post-vibratory relaxation part of simulation is such to allow for the steady-state stresses to establish; most of the time duration of 0.5 s suffices.

The mesh of the FE representation was appropriately generated and refined in the contact regions according to standard engineering practice. Thus, the accuracy and representativeness of the results of this calculation were deemed acceptable (see Section 6.5 and Attachments V through IX for discussion of results). The uncertainties are taken into account by random sampling (from appropriate probability distributions) of the calculation inputs that are inherently stochastic (uncertain) and characterized by a large scatter of data (namely, ground-motion time histories and friction coefficients). The results are suitable for the intended use, but Section 6.5 should be carefully studied prior to use of the results.

5.2.1 Ground-Motion Time History Cutoff

Structural calculations of WP exposed to vibratory ground motion are extremely computationally intense. This is not surprising having in mind the complex FE representation (Section 5.2), the highly nonlinear nature of the problem (large deformation plasticity, friction, impacts, etc.), the small computational time step necessary to ensure convergence ($\approx 1\ \mu s$ or less), and a long duration of the ground-motion time histories ($\approx 30-40\ s$). In order to obtain credible results in a reasonable time, it is necessary to reduce the duration of seismic excitation used in the simulation.

Therefore, the specified termination times of the vibratory part of simulations at the annual frequency of occurrence $1 \cdot 10^{-6}\ 1/yr$ are such to cover the range from 5 percent to 95 percent of the externally applied energy. (For brevity, the minimum time corresponding to 5 percent of energy of ground motion is, in the remainder of this document, called "5%-time". Similarly, the maximum time corresponding to 90 percent and 95 percent of energy of ground motion is called "90%-time" and "95%-time", respectively. Note that all three time instances are determined by taking into account all three components of ground motion.) In few $1 \cdot 10^{-6}\ 1/yr$ cases the termination time is extended beyond this 95%-energy cutoff to examine the effect of the cutoff (i.e., the ending time is larger than the 95%-time). Similarly, in five realizations the starting time is moved slightly below the 5%-time to encompass some pertinent feature of the time history in question (i.e., the starting time is smaller than the 5%-time, see Table 5.2.1-1).

All simulations at the annual frequency of occurrence $1 \cdot 10^{-7}\ 1/yr$ are performed from 5%-time to 90%-time. Thus, the starting time coincides with the 5%-time, while the ending time coincides with the 90%-time.

Table 5.2.1-1 presents the duration of each simulation, and characteristic times used to define the duration. The time in the third column is the starting time of the simulation. (In other words, the starting point of simulation [$t = 0$] corresponds to this time in Reference 29.) The three components of initial velocity, specified in LS-DYNA input file (see as an example Attachment X: 1E-6/RN1/seisWPPc.k, lines 312 through 319), correspond to this time in Reference 29. The starting time, for most realizations, is defined as the 5%-time. The ending time is nominally the 95%-time (see again Ref. 29). The calculated duration of the simulation is then obtained by subtracting the 5%-time from the 95%-time. The duration of the simulation that was actually run is calculated by subtracting the starting time from the ending time.

As previously mentioned, the duration that is actually run during simulation is, in a few cases, different from the computed duration calculated based on the characteristic times. Specifically, the realizations 1, 2, 4, 9, and 12 are extended for a short time after 95%-time for the purpose of examining the damage-evolution trend as a function of time-history cutoff (see Attachment VII). On the other hand, realizations number 3, 8, 13, and 14 are not run up to the 95%-time since – as indicated in Table VII-1 – it was unnecessary from the standpoint of the damage evolution.

Additionally, Table 5.2.1-2 presents the 90%-time and corresponding duration for $1 \cdot 10^{-6}\ 1/yr$ time histories. The values from the fourth column (Duration of Simulation to 90%-Time) represent the time in the simulation (thus, measured from the starting time corresponding to $t = 0$ in the simulation) when the 90 percent of energy is reached for all three components of ground motion. This data is used in Attachment VII (specifically, in Table VII-5) to examining the damage-evolution trend as a function of time-history cutoff.

Table 5.2.1-1 Duration and Characteristic Times Corresponding to 5%-95% Energy Range (Annual Frequency of Occurrence $1 \cdot 10^{-6}$ $1/yr$)

Ground Motion Number	5%-Time (s)	Starting Time (s)	95%-Time (s)	Ending Time (s)	Duration of Simulation (s)		Realization Number
					Calculated	Run	
1	0.85	0.85	7.05	7.05	6.2	6.2	6
2	0.58	0.41	8.13	8.41	7.6	8.0	7
3	1.7	1.5	5.04	5.00	3.4	3.5	15
4	1.3	1.1	15.0	13.9	13.7	12.8	3
5	2.0	2.0	10.3	10.3	8.3	8.3	11
6	2.3	2.3	9.96	11.2	7.7	8.9	12
7	4.0	4.0	11.6	12.9	7.6	8.9	1
8	1.1	1.1	5.99	6.80	4.9	5.7	4
9	0.79	0.6	8.18	7.90	7.4	7.3	10
10	1.6	1.6	10.8	11.9	9.2	10.3	9
11	2.1	2.1	10.3	10.3	8.2	8.2	5
12	1.4	1.4	13.6	12.9	12.2	11.5	13
13	1.9	1.85	17.0	15.4	15.1	13.5	8
14	7.2	7.2	21.5	18.2	14.3	10.9	14
16	3.8	3.8	11.8	12.8	8.0	9.0	2

Finally, Table 5.2.1-3 presents the duration of each simulation and characteristic times used to define the duration for $1 \cdot 10^{-7}$ $1/yr$ (see Reference 30). In this case, as discussed previously, the starting time presented in the second column coincides with the 5%-time (i.e., the starting time is the 5%-time rounded to two significant digits). The most pronounced difference between $1 \cdot 10^{-6}$ $1/yr$ realizations and $1 \cdot 10^{-7}$ $1/yr$ realizations is that the latter are run only up to the maximum of 90 percent energy of ground motion (i.e., the ending time coincides with the 90%-time). The rationale is to reduce the simulation running time without significantly affecting the simulation results. This rationale is based on the results for $1 \cdot 10^{-6}$ $1/yr$ realizations (see Attachment VII), and its appropriateness is confirmed to a large extent by the results of $1 \cdot 10^{-7}$ $1/yr$ realizations (see Section 6.2).

Table 5.2.1-2 Duration and Characteristic Times Corresponding to 5%-90% Energy Range (Annual Frequency of Occurrence $1 \cdot 10^{-6}$ $1/yr$)

Ground Motion Number	Starting Time (s)	90%-Time (s)	Duration of Simulation to 90%-Time (s)	Realization Number
1	0.85	5.21	4.36	6
2	0.41	6.05	5.47	7
3	1.5	3.64	1.94	15
4	1.1	10.2	8.90	3
5	2.0	7.46	5.46	11
6	2.3	9.20	6.90	12
7	4.0	11.1	7.10	1
8	1.1	5.12	4.02	4
9	0.6	6.98	6.19	10
10	1.6	7.66	6.06	9
11	2.1	8.30	6.20	5
12	1.4	12.2	10.8	13
13	1.85	12.7	10.8	8
14	7.2	19.8	12.6	14
16	3.8	9.57	5.77	2

Table 5.2.1-3 Duration and Characteristic Times Corresponding to 5%-90% Energy Range (Annual Frequency of Occurrence $1 \cdot 10^{-7}$ $1/yr$)

Ground Motion Number	Starting Time (s)	Ending Time (s)	Duration of Simulation (s)		Realization Number
			Calculated	Run	
1	1.3	6.5	5.2	5.2	6
2	0.80	5.8	5.0	5.0	7
3	1.75	3.45	1.7	1.7	15
4	1.5	11.8	10.3	10.3	3
5	1.7	9.3	7.6	7.6	11
6	2.4	9.2	6.8	6.8	12
7	3.6	11.4	7.8	7.8	1
8	1.2	5.1	3.9	3.9	4
9	0.70	6.7	6.0	6.0	10
10	1.6	7.2	5.6	5.6	9
11	2.1	8.5	6.4	6.4	5
12	2.0	12.7	10.7	10.7	13
13	1.9	15.2	13.3	13.3	8
14	5.3	21.0	15.7	15.7	14
16	3.4	9.0	5.6	5.6	2

5.2.2 System Damping

In order to obtain steady-state results (i.e., residual stresses) in a reasonable time, it is necessary to apply damping in the course of the post-vibratory relaxation. The system damping is applied globally.

As discussed in Reference 17 (Section 28.2), the most appropriate damping constant for the system is usually the critical damping constant. Therefore,

$$DC = 2 \cdot \omega_{\min} = 2 \cdot 350 = 700\, rad/s$$

Where $\omega_{\min} = 2 \cdot \pi \cdot 56 \approx 350\, rad/s$ is the minimum non-zero frequency of the WP OS (see Attachment X [Modal Analysis/wpp6Bmod.out, line #6517]). This value represents the closest analogue to the natural frequency in the more familiar case of anchored objects. Having in mind that the objects we are dealing with in this study are unanchored, the damping constant is conservatively reduced to $DC = 200\, rad/s$, to avoid over-damping of the system. Furthermore, the parametric study of various damping constants presented in Reference 27 confirms the appropriateness of this choice. The system is obviously not over-damped, and the steady-state results are reached in reasonable time (see Ref. 27, Fig 4, p. 21).

6. RESULTS

Attachment X includes the input files and results files that show execution of the programs occurred correctly. The stress time histories, residual stress distribution plots, impact parameters, and damaged areas have been obtained by using postprocessors LSPOST V2.0 and LS-PREPOST V1.0.

The stress intensity presented in this section is defined as

$$\sigma_D = \sigma_1 - \sigma_3 = 2 \cdot \tau_{max}$$

where σ_1 and σ_3 are maximum principal stress and minimum principal stress, respectively; and τ_{max} is the maximum shear stress (Ref. 12, Sec. III, Div. 1, Art. NB-3000; and Ref. 13, Chapter 3).

Recall that the area of the WP OS where the residual 1st principal stress exceeds certain limits is, for brevity, called "damaged area" throughout this document (see Section 1).

6.1 EVENTS WITH ANNUAL FREQUENCY OF OCCURRENCE $1 \cdot 10^{-6}$ $1/yr$

The stochastic (uncertain) input parameters for 15 simulations of events corresponding to annual frequency of occurrence $1 \cdot 10^{-6}$ $1/yr$ are listed in Table 6.1-1 (see Ref. 35, Table I-4). (The same simulation parameters were subsequently used for annual frequency of occurrence $1 \cdot 10^{-7}$ $1/yr$, as well.) The values of the friction coefficients presented in Table 6.1-1 are, for the purpose of this calculation, presented (and used) with two significant digits. The ground motion (acceleration, velocity, and displacement) time histories are available in Reference 29. The time history cutoff and the simulation duration are discussed in detail in Section 5.2.1 (see Table 5.2.1-1).

Table 6.1-1 Simulation Parameters

Realization Number	Ground Motion Number	Friction Coefficient (-)	
		Metal to metal	Metal to rock
1	7	0.80	0.34
2	16	0.33	0.49
3	4	0.50	0.62
4	8	0.60	0.22
5	11	0.20	0.24
6	1	0.27	0.69
7	2	0.71	0.60
8	13	0.56	0.54
9	10	0.55	0.36
10	9	0.36	0.41
11	5	0.42	0.67
12	6	0.65	0.73
13	12	0.75	0.31
14	14	0.29	0.45
15	3	0.46	0.78

6.1.1 Interaction between Waste Package and Pallet

The damaged area due to the WP-pallet interaction is evaluated only on one WP end, specifically in the finely-meshed region (see Figures 3 and 4, and corresponding discussion in Section 5.2). The total damaged area due to the WP-pallet interaction is then obtained by multiplying by two the measured damaged area on one side (see Assumption 3.18).

Throughout this document the damaged area is also presented as a fraction of the total OS area (including the OS lids). For this purpose the area of the WP OS is calculated based on the WP dimensions presented in Reference 24 and Attachment I. Specifically, the outer diameter of the OS is $D_{OS} = 1.564\ m$, the total length of the WP is $L = 5.165\ m$. The distance from the WP bottom end to the OS flat bottom lid is $d = 0.1\ m$; the distance from WP top end to the extended lid base is the same. Hence, the OS length is $L_{OS} = L - 2 \cdot d = 5.165 - 2 \cdot 0.1 = 4.965\ m$. Thus, the area of the intact WP OS (including the OS lids) is

$$A_{OS} = L_{OS} \cdot D_{OS} \cdot \pi + 2 \cdot \left(D_{OS}^2 \cdot \pi\right)/4 = 4.965 \cdot 1.564 \cdot \pi + 2 \cdot \left(1.564^2 \cdot \pi\right)/4 = 28.2\ m^2$$

This area of the OS ($28.2\ m^2$) is used henceforth throughout this document.

Table 6.1.1-1 presents the damaged area resulting from the WP-pallet interaction during the vibratory ground motion. The damaged area is evaluated based on the residual 1st principal stress plot (see Section 1) by using postprocessor LSPOST V2.

Table 6.1.1-1 Damaged Area from WP-Pallet Interaction at $1 \cdot 10^{-6}\ 1/yr$

Realization Number	Ground Motion Number	Damaged Area (m^2; % of total OS area)	
		80% Yield Strength	90% Yield Strength
1	7	0.0029; 0.010%	0.0014; 0.0050%
2	16	0; 0	0; 0
3	4	0.0050; 0.018%	0; 0
4	8	0.030; 0.11%	0.0064; 0.023%
5	11	0.0015; 0.0053%	0; 0
6	1	0.025; 0.089%	0.0028; 0.0099%
7	2	0.017; 0.060%	0; 0
8	13	0; 0	0; 0
9	10	0.0035; 0.012%	0; 0
10	9	0; 0	0; 0
11	5	0.012; 0.043%	0.0037; 0.013%
12	6	0.0039; 0.014%	0; 0
13	12	0; 0	0; 0
14	14	0.010; 0.035%	0.0043; 0.015%
15	3	0.0078; 0.028%	0.0015; 0.0053%

According to results presented in Table 6.1.1-1 the damage due to the WP-pallet interaction is relatively small, especially for the upper stress limit.

6.1.2 Interaction between Waste Package and Waste Package (Longitudinal Boundary)

This section presents the damaged area of the WP OS resulting from the impacts in longitudinal direction. This damaged area is, thus, attributed to the WP-WP interaction (end impacts) during the vibratory ground motion. It is calculated (by using Reference 27 [Tables 4,5,7, and 8]) based on the speed, location, and angle of the end impacts, estimated from the simulations of the vibratory ground motion.

The end-impact parameters presented in this section are evaluated by using the postprocessor LSPOST V2. The "time" presented in the second column (Tables 6.1.2-1 through 6.1.2-15) is the time of impact, and it can be obtained directly from the postprocessor. The impact speed (the third column) is relative speed between the longitudinal boundary (representing the neighboring WP) and the first WP (i.e., its trunnion collar sleeve) node that first comes in contact with the axial boundary at the time of impact. The impact angle presented in the fourth column defines inclination of the WP with respect to the longitudinal boundary; zero angle corresponding to ideal end impact. The impact location is important for the damage accumulation. The rationale for introducing the impact location is to prevent excessive conservatism by simply adding the damage from individual impacts regardless of their location. The used approach is based on purely geometrical arguments. If two impacts take place sufficiently close to each other their damage may overlap to a certain extent. The extent of damaged area depends on both the impact speed and the impact angle, and is presented in Reference 27. The convention used for evaluation of the impact location – presented in the first column – is illustrated in Figure 8.

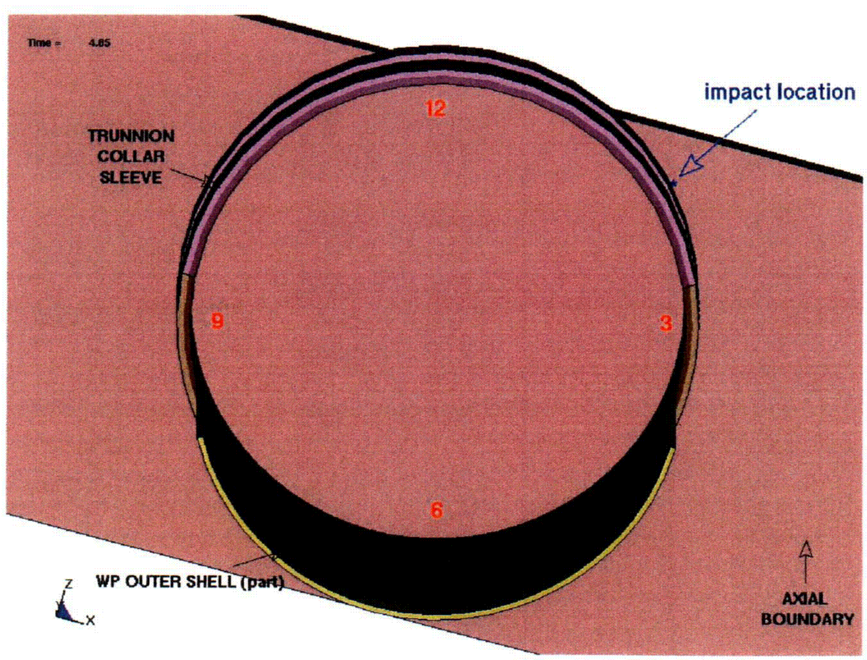

Figure 8. Convention Used for Evaluation of Impact Location

C06

The impact location in circumferential direction is defined with 12 discrete values (i.e., from 1 to 12 with 30^o increments) equidistantly distributed in clockwise direction (see red numbers in Fig. 8). Moreover, an end impact can take place on the WP side corresponding to the finely meshed (as distinguished by designation "F" in Fig. 4) or coarsely meshed ("C") part of the OS. As an example, assuming that the impact between WP and axial boundary takes place on the "coarse side" of the WP OS, the impact location marked by blue asterisk in Figure 8 would be designated as "C 2."

Throughout this analysis, damage contribution of each individual impact, with impact speed exceeding $1\ m/s$ (Assumption 3.16), is taken into account in one of the three ways, depending of the location and the circumferential extent of damage. The damage contribution can be either fully taken into account, or just one-half of it (designated with "$\times 0.5$" in appropriate tables), or it may not be taken into account at all (designated as "NC" for "not counted"). Furthermore, if damage caused by two impacts partially overlap, the larger damage is fully taken into account while the smaller is reduced.

As an example, the damage contribution from the impact at location "C 10" in Table 6.1.2-1 is taken into account as one-half of the corresponding value, since the damage caused by impact at location "C 11" partially overlaps the "C 10" damage according to Reference 27 (Tables 4 and 5). On the other hand, the "C 6" damage in Table 6.1.2-3 is not taken into account at all ("NC") since it is completely overlapped by "C 7" damage.

Table 6.1.2-1 End-Impact Parameters and Damaged Area for Realization Number 1 at $1 \cdot 10^{-6}\ 1/yr$

Impact Location	Time (s)	Speed (m/s)	Angle (degree)	Damaged Area (m2)	
				80% Yield Strength	90% Yield Strength
F 8	6.025	1.3	1.0	0.0089	0.0046
C 10	4.750	1.0	1.5	0.0031X0.5	0.0017X0.5
C 11	4.875	1.5	1.3	0.0122	0.0063
Total				0.023	0.012

The end-impact parameters and corresponding damaged areas (calculated for both the lower and upper damage thresholds) are presented in Tables 6.1.2-1 through 6.1.2-15 for all 15 realizations at $1 \cdot 10^{-6}\ 1/yr$.

Table 6.1.2-2 End-Impact Parameters and Damaged Area for Realization Number 2 at $1 \cdot 10^{-6}\ 1/yr$

Impact Location	Time (s)	Speed (m/s)	Angle (degree)	Damaged Area (m2)	
				80% Yield Strength	90% Yield Strength
F	0.750	1.2	0	0	0
F 8	3.150	1.8	0.5	0.0092X0.5	0.0047X0.5
F 9	5.000	1.5	1.0	0.0127	0.0065
Total				0.017	0.0089

Table 6.1.2-3 End-Impact Parameters and Damaged Area for Realization Number 3 at $1 \cdot 10^{-6}\ 1/yr$

Impact Location	Time (s)	Speed (m/s)	Angle (degree)	Damaged Area (m^2)	
				80% Yield Strength	90% Yield Strength
F 1	6.050	1.3	1.3	0.0086	0.0045
F 6	3.500	3.9	3.4	0.0771	0.0374
F 9	0.675	1.5	1.1	0.0125	0.0064
F 11	3.100	2.4	0.9	0.0296	0.0124
C 4	0.975	1.1	1.6	0.0048	0.0026
C 6	2.625	1.1	1.6	0.0048 NC	0.0026 NC
C 7	3.225	3.6	0.9	0.0588	0.0192
C 8	4.575	1.5	1.6	0.0117 NC	0.0060 NC
C 8	7.350	1.1	1.1	0.0051 NC	0.0027 NC
Total				0.19	0.083

Table 6.1.2-4 End-Impact Parameters and Damaged Area for Realization Number 4 at $1 \cdot 10^{-6}\ 1/yr$

Impact Location	Time (s)	Speed (m/s)	Angle (degree)	Damaged Area (m^2)	
				80% Yield Strength	90% Yield Strength
F 3	2.400	1.9	1.0	0.0202	0.0103
F 9	2.775	2.5	4.1	0.0307	0.0162
C 9	2.650	2.6	2.9	0.0354 NC	0.0166 NC
C 9	2.700	3.5	4.0	0.0650	0.0343
Total				0.12	0.061

It is necessary to make an observation regarding the end impact at $t = 2.700\,s$ presented in Table 6.1.2-4. Studious examination of the kinematics suggests that a strong impact takes place at $t = 2.700\,s$. Unfortunately, the output frequency ($0.025\,s$) is – in this case – not fine enough to capture the impact speed. Thus the impact speed (at this moment only) is obtained by examination of the same realization performed without the rigid Alloy-22 parts (i.e., with all Alloy-22 parts represented as deformable [namely elastoplastic with kinematic hardening]) (see Attachment VI).

Table 6.1.2-5 End-Impact Parameters and Damaged Area for Realization Number 5 at $1 \cdot 10^{-6}\ 1/yr$

Impact Location	Time (s)	Speed (m/s)	Angle (degree)	Damaged Area (m^2)	
				80% Yield Strength	90% Yield Strength
F 2	0.425	1.6	1.2	0.0142 NC	0.0073 NC
F 2	2.025	2.0	1.7	0.0201 NC	0.0102 NC
F 2	2.075	4.2	1.4	0.0836 NC	0.0275 NC
F 3	3.425	1.3	2.9	0.0068 NC	0.0036 NC
F 3	5.025	1.8	3.0	0.0137 NC	0.0070 NC
F 3	5.075	4.4	2.5	0.0947	0.0385
F 3	5.900	1.3	1.0	0.0089 NC	0.0046 NC
F 9	1.325	1.2	1.7	0.0064	0.0034
F 9	2.500	1.0	3.8	0.0022 NC	0.0013 NC

Impact Location	Time (*s*)	Speed (*m/s*)	Angle (*degree*)	Damaged Area (m^2)	
				80% Yield Strength	90% Yield Strength
C 2	3.125	1.2	0.2	0.0014	0.0007
C 3	0.800	1.2	1.7	0.0064X0.5	0.0034X0.5
C 4	1.650	1.7	2.9	0.0125	0.0064
C 9	2.325	2.4	4.7	0.0262	0.0145
C 11	0.200	1.4	0.2	0.0022	0.0011
Total				0.15	0.066

Table 6.1.2-6 End-Impact Parameters and Damaged Area for Realization Number 6 at $1 \cdot 10^{-6}\ 1/yr$

Impact Location	Time (*s*)	Speed (*m/s*)	Angle (*degree*)	Damaged Area (m^2)	
				80% Yield Strength	90% Yield Strength
F 4	1.950	2.5	1.4	0.0344	0.0140
F 4	2.600	2.4	0.5	0.0186 NC	0.0090 NC
F 8	1.525	1.9	1.0	0.0202X0.5	0.0103X0.5
F 9	1.100	2.4	1.5	0.0315	0.0134
F 9	3.025	1.9	1.6	0.0187 NC	0.0095 NC
C 9	3.125	4.0	2.7	0.0692	0.0300
C 9	2.750	2.9	0.9	0.0418 NC	0.0152 NC
Total				0.15	0.063

Table 6.1.2-7 End-Impact Parameters and Damaged Area for Realization Number 7 at $1 \cdot 10^{-6}\ 1/yr$

Impact Location	Time (s)	Speed (m/s)	Angle (degree)	Damaged Area (m2)	
				80% Yield Strength	90% Yield Strength
F 2	2.350	1.4	0.4	0.0043	0.0022
F 9	3.700	2.7	0.5	0.0243	0.0116
F 10	2.925	2.1	2.5	0.0209 NC	0.0103 NC
C	3.150	2.2	0	0.0024	0.0024
C 3	4.150	1.2	0.8	0.0056 NC	0.0029 NC
C 3	4.200	4.5	0.4	0.0538	0.0265
C 8	2.775	2.4	3.0	0.0290	0.0139
Total				0.11	0.057

Table 6.1.2-8 End-Impact Parameters and Damaged Area for Realization Number 8 at $1 \cdot 10^{-6}\ 1/yr$

Impact Location	Time (s)	Speed (m/s)	Angle (degree)	Damaged Area (m2)	
				80% Yield Strength	90% Yield Strength
F 3	4.025	1.5	0.6	0.0076	0.0039
F 5	2.775	1.9	0.1	0.0020	0.0010
F	3.600	1.7	0	0	0
C 3	1.950	1.8	0.5	0.0092	0.0047
C 9	3.400	1.1	0.8	0.0041	0.0022
Total				0.023	0.012

The initial velocity components are not specified properly for realization number 8. Specifically, the three initial velocity components do not correspond to the beginning of the acceleration time history. Consequently, the velocity and displacement time histories are not appropriately specified, and the results from this realization are not included in the tables summarizing results (Tables 6.1.2-16, 6.1.4-1, and 6.1.4-2).

Table 6.1.2-9 End-Impact Parameters and Damaged Area for Realization Number 9 at $1 \cdot 10^{-6}$ $1/yr$

Impact Location	Time (s)	Speed (m/s)	Angle (degree)	Damaged Area (m2)	
				80% Yield Strength	90% Yield Strength
F 3	0.800	1.5	1.7	0.0116	0.0059
F 3	7.075	1.0	2.4	0.0027 NC	0.0016 NC
F 5	2.625	1.7	2.7	0.0129	0.0066
F 8	1.575	2.8	4.5	0.0408	0.0226
F 9	2.250	1.6	5.0	0.0072 NC	0.0038 NC
F 9	2.325	1.1	4.1	0.0021 NC	0.0013 NC
F 10	3.950	1.8	1.4	0.0174	0.0089
C 8	1.375	1.4	2.6	0.0086	0.0045
C 9	1.925	1.7	4.2	0.0098X0.5	0.0051X0.5
C 10	2.450	2.2	3.8	0.0210	0.0107
Total				0.12	0.062

Table 6.1.2-10 End-Impact Parameters and Damaged Area for Realization Number 10 at $1 \cdot 10^{-6}$ $1/yr$

Impact Location	Time (s)	Speed (m/s)	Angle (degree)	Damaged Area (m2)	
				80% Yield Strength	90% Yield Strength
F 3	5.425	1.1	2.7	0.0041	0.0022
C 3	5.050	1.5	0.3	0.0038 NC	0.0020 NC
C 3	5.175	1.6	3.8	0.0094	0.0049
Total				0.014	0.0071

Table 6.1.2-11 End-Impact Parameters and Damaged Area for Realization Number 11 at $1 \cdot 10^{-6}$ $1/yr$

Impact Location	Time (s)	Speed (m/s)	Angle (degree)	Damaged Area (m2)	
				80% Yield Strength	90% Yield Strength
F 6	4.150	1.7	1.5	0.0154	0.0079
F 10	1.275	1.5	0.3	0.0038 NC	0.0020 NC
F 10	2.125	1.6	1.7	0.0133	0.0068
C 3	0.975	1.1	0.5	0.0026	0.0014
C 8	3.400	1.6	1.9	0.0129 NC	0.0066 NC
C 9	2.000	1.7	1.6	0.0152 NC	0.0078 NC
C 9	2.225	2.8	1.3	0.0425	0.0158
Total				0.074	0.032

Table 6.1.2-12 End-Impact Parameters and Damaged Area for Realization Number 12 at $1 \cdot 10^{-6}$ $1/yr$

Impact Location	Time (s)	Speed (m/s)	Angle (degree)	Damaged Area (m2) 80% Yield Strength	Damaged Area (m2) 90% Yield Strength
F 3	6.400	1.1	0.7	0.0036	0.0019
F 8	5.950	3.0	0.4	0.0264	0.0138
F 9	3.575	1.1	0.8	0.0041 NC	0.0022 NC
C 3	1.025	2.2	0.5	0.0148	0.0073
C 4	5.825	2.2	0.2	0.0074X0.5	0.0044X0.5
C 4	6.175	1.0	1.7	0.0030 NC	0.0017 NC
C 9	3.775	2.3	0.8	0.0246	0.0109
Total				0.073	0.036

Table 6.1.2-13 End-Impact Parameters and Damaged Area for Realization Number 13 at $1 \cdot 10^{-6}$ $1/yr$

Impact Location	Time (s)	Speed (m/s)	Angle (degree)	Damaged Area (m2) 80% Yield Strength	Damaged Area (m2) 90% Yield Strength
F 4	2.300	1.9	0.6	0.0121	0.0062
C 3	2.025	1.2	0.5	0.0035 NC	0.0018 NC
C 3	2.450	2.0	3.2	0.0159	0.0081
C 3	7.625	1.1	0.9	0.0047 NC	0.0025 NC
C 9	9.875	1.1	0.7	0.0036	0.0019
Total				0.032	0.016

Table 6.1.2-14 End-Impact Parameters and Damaged Area for Realization Number 14 at $1 \cdot 10^{-6}$ $1/yr$

Impact Location	Time (*s*)	Speed (*m/s*)	Angle (*degree*)	Damaged Area (m^2) 80% Yield Strength	Damaged Area (m^2) 90% Yield Strength
F 2	2.775	1.4	0.2	0.0022	0.0011
F 3	3.925	1.0	0.6	0.0020	0.0011
C 10	4.450	1.2	0.2	0.0014	0.0007
Total				0.0056	0.0029

Table 6.1.2-15 End-Impact Parameters and Damaged Area for Realization Number 15 at $1 \cdot 10^{-6}$ $1/yr$

Impact Location	Time (*s*)	Speed (*m/s*)	Angle (*degree*)	Damaged Area (m^2) 80% Yield Strength	Damaged Area (m^2) 90% Yield Strength
F 8	1.125	2.0	1.7	0.0201	0.0102
Total				0.020	0.010

Table 6.1.2-16 presents a summary of Tables 6.1.2-1 through 6.1.2-15, except for realization number 8 (see above).

Table 6.1.2-16 Damaged Area from End Impacts (WP-WP Interaction) at $1\cdot10^{-6}\ 1/yr$

Realization Number	Ground Motion	Damaged Area (m^2; % of total OS area)	
		80% Yield Strength	90% Yield Strength
1	7	0.023; 0.082%	0.012; 0.043%
2	16	0.017; 0.060%	0.0089; 0.032%
3	4	0.19; 0.67%	0.083; 0.29%
4	8	0.12; 0.43%	0.061; 0.22%
5	11	0.15; 0.53%	0.066; 0.23%
6	1	0.15; 0.53%	0.063; 0.22%
7	2	0.11; 0.39%	0.057; 0.20%
9	10	0.12; 0.43%	0.062; 0.22%
10	9	0.014; 0.050%	0.0071; 0.025%
11	5	0.074; 0.26%	0.032; 0.11%
12	6	0.073; 0.26%	0.036; 0.13%
13	12	0.032; 0.11%	0.016; 0.057%
14	14	0.0056; 0.020%	0.0029; 0.010%
15	3	0.020; 0.071%	0.010; 0.035%

It should be emphasized that although an attempt has been made (by using the damage accumulation technique described at the beginning of this section and used henceforth) to prevent excessive conservatism of the damaged area resulting from end impacts, the estimate is still extremely conservative. This conservatism is unavoidable consequence of the used FE representation. Two sources of conservatism need to be mentioned herein.

First, the damaged area from the WP impacting the longitudinal boundary (representing the neighboring WP) is calculated based on the end impacts on the surface that is not only unyielding but also completely constrained (see Ref. 27). Consequently, almost entire kinetic energy (characterizing a particular impact) is transformed into the deformation of one WP. In reality the part of kinetic energy transferred into deformation energy is not only distributed between the two colliding WPs but is also smaller to begin with since the WPs are free to bounce off upon the impact.

Second, the damage accumulation technique, as described and used herein, is intrinsically unable to capture damage relaxation during the seismic event. In reality the damaged area is not a nondecreasing deformation measure. A region of the OS that exceeded the residual stress threshold at time t_1 can be below that threshold following a "favorable" impact at time t_2 (where $t_2 > t_1$). It is important to recognize that these aspects of the FE representation lead to extremely conservative estimates of the damage area.

6.1.3 Interaction between Waste Package and Drip Shield

The impact velocity between the WP and the DS is presented in this section. It is assumed in this calculation that these lateral impacts do not cause any damage to the WP (see Assumption 3.15).

The interaction between the WP (i.e., trunnion collar sleeves) and the DS occurred only in realizations 4, 7, 9, 11, and 15. In all other realizations there was no impact between the WP and the DS.

The DS motion was not constrained by the drift wall at any time of impact with the WP. In other words, the DS was free to move following all impacts from Table 6.1.3-1 through 6.1.3-5.

Table 6.1.3-1 Lateral-Impact Parameters for Realization Number 4 at $1 \cdot 10^{-6}$ $1/yr$

Impact Location	Time (s)	Speed (*m/s*)	Angle (*degree*)
F 3	2.700	2.9	3.0

Table 6.1.3-2 Lateral-Impact Parameters for Realization Number 7 at $1 \cdot 10^{-6}$ $1/yr$

Impact Location	Time (s)	Speed (*m/s*)	Angle (*degree*)
C 3	2.800	1.2	3.4

Table 6.1.3-3 Lateral-Impact Parameters for Realization Number 9 at $1 \cdot 10^{-6}$ $1/yr$

Impact Location	Time (s)	Speed (*m/s*)	Angle (*degree*)
C 3	1.000	1.3	3.4
F 3	1.575	2.1	4.4
F 3	2.225	2.0	4.8
F 3	2.300	1.2	4.4
F 9	2.600	4.1	0.2

Table 6.1.3-4 Lateral-Impact Parameters for Realization Number 11 at $1 \cdot 10^{-6}$ $1/yr$

Impact Location	Time (s)	Speed (*m/s*)	Angle (*degree*)
C 9	2.500	1.8	4.8

Table 6.1.3-5 Lateral-Impact Parameters for Realization Number 15 at $1 \cdot 10^{-6}$ $1/yr$

Impact Location	Time (s)	Speed (*m/s*)	Angle (*degree*)
F 3	1.125	1.2	1.0

It is obvious from results presented in Tables 6.1.3-1 through 6.1.3-5 that the side impacts between WP and DS are not only rare events in the course of ground motions at $1 \cdot 10^{-6}$ $1/yr$ annual frequency of occurrence but are also characterized by relatively modest impact speed (mostly between 1 m/s and 2 m/s). The impact speeds in this range do not contribute significantly to the total damaged area even when the WP is impacting an unyielding surface (see Ref. 27, Table 4 through Table 8 [Side Impacts]).

6.1.4 Summary of Results for Events with Annual Frequency of Occurrence $1 \cdot 10^{-6}$ $1/yr$

Table 6.1.4-1 presents the maximum peak stress intensity in the WP OS in the course of the vibratory ground motion for 14 realizations. This stress measure can be used to estimate whether or not the structure in question is safe from immediate breach (i.e., fracture, perforation). The stress-intensity time history plots, used to determine the values presented in Table 6.1.4-1, are presented in Attachment IV. These plots are filtered by using Butterworth filter with the cutoff frequency of 1000 *Hz*.

The initial velocity components are not specified properly for realization number 8. Specifically, the three initial velocity components do not correspond to the beginning of the acceleration time history. Consequently, the velocity and displacement time histories are not appropriately specified, and the results from this realization are not included in Tables 6.1.4-1 and 6.1.4-2.

Table 6.1.4-1 Maximum Stress Intensity During Vibratory Ground Motion of Annual Frequency of Occurrence $1 \cdot 10^{-6}$ $1/yr$

Realization Number	Ground Motion Number	Maximum Stress Intensity (MPa)
1	7	354 *(Figure IV-1)*
2	16	341 *(Figure IV-3)*
3	4	352 *(Figure IV-5)*
4	8	360 *(Figure IV-7)*
5	11	356 *(Figure IV-9)*
6	1	358 *(Figure IV-11)*
7	2	359 *(Figure IV-13)*
9	10	353 *(Figure IV17)*
10	9	340 *(Figure IV-19)*
11	5	363 *(Figure IV-21)*
12	6	348 *(Figure IV-23)*
13	12	344 *(Figure IV-25)*
14	14	348 *(Figure IV-27)*
15	3	358 *(Figure IV-29)*

The maximum stress intensities presented in Table 6.1.4-1 do not vary significantly, although the ground motion energy range is extremely wide. A possible explanation is that the pallet, as a thin-walled structure, can offer a limited resistance to the much heavier and stiffer WP. During the more intense WP-pallet interactions, the pallet bulges (see Fig. 9). This flexibility of the pallet provides a cushioning effect for the WP.

In analyzing the maximum stress intensity reached during the vibratory ground motion at $1 \cdot 10^{-6}$ $1/yr$ (Table 6.1.4-1) it is important to keep in mind that the uniaxial tensile strength for Alloy 22 at 150 $°C$ is 1120 MPa (see Section 5.1.2). Thus, all maximum stress intensities presented in Table 6.1.4-1 are less than one-third of the uniaxial tensile strength implying that the immediate breach of the OS appears highly unlikely.

The damaged areas characterizing 14 different realizations at annual frequency of occurrence $1 \cdot 10^{-6}$ $1/yr$ are summarized in Table 6.1.4-2. According to the results presented in that table the cumulative damage area is dominated by the end-impact contribution. In all realizations (with exception of realization number 14) the damaged area due to the WP-pallet interaction is much smaller than the one due to the WP-WP interaction. (It cannot be overemphasized though that the damaged areas due to the WP-WP interaction are conservatively estimated [see Section 6.1.2].)

Table 6.1.4-2 Damaged Area from Vibratory Ground Motion of Annual Frequency of Occurrence $1 \cdot 10^{-6}$ $1/yr$

Realization Number	Ground Motion Number	Damaged Area					
		WP-Pallet Interaction (m^2)		WP-WP Interaction (m^2)		Cumulative (m^2; % of total OS area)	
		80% Yield Strength	90% Yield Strength	80% Yield Strength	90% Yield Strength	80% Yield Strength	90% Yield Strength
1	7	0.0029; 0.010%	0.0014; 0.0050%	0.023; 0.082%	0.012; 0.043%	0.026; 0.092%	0.013; 0.046%
2	16	0; 0	0; 0	0.017; 0.060%	0.0089; 0.032%	0.017; 0.060%	0.0089; 0.032%
3	4	0.0050; 0.018%	0; 0	0.19; 0.67%	0.083; 0.29%	0.20; 0.71%	0.083; 0.29%
4	8	0.030; 0.11%	0.0064; 0.023%	0.12; 0.43%	0.061; 0.22%	0.15; 0.53%	0.067; 0.24%
5	11	0.0015; 0.0053	0; 0	0.15; 0.53%	0.066; 0.23%	0.15; 0.53%	0.066; 0.23%
6	1	0.025; 0.089%	0.0028; 0.0099%	0.15; 0.53%	0.063; 0.22%	0.18; 0.64%	0.066; 0.23%
7	2	0.017; 0.060%	0; 0	0.11; 0.39%	0.057; 0.20%	0.13; 0.46%	0.057; 0.20%
9	10	0.0035; 0.012%	0; 0	0.12; 0.43%	0.062; 0.22%	0.12; 0.43%	0.062; 0.22%
10	9	0; 0	0; 0	0.014; 0.050%	0.0071; 0.025%	0.014; 0.050%	0.0071; 0.025%
11	5	0.012; 0.043%	0.0037; 0.013%	0.074; 0.26%	0.032; 0.11%	0.086; 0.30%	0.036; 0.13%
12	6	0.0039; 0.014%	0; 0	0.073; 0.26%	0.036; 0.13%	0.077; 0.27%	0.036; 0.13%
13	12	0; 0	0; 0	0.032; 0.11%	0.016; 0.057%	0.032; 0.11%	0.016; 0.057%
14	14	0.010; 0.035%	0.0043; 0.015%	0.0056; 0.020%	0.0029; 0.010%	0.016; 0.057%	0.0072; 0.026%
15	3	0.0078; 0.028%	0.0015; 0.0053%	0.020; 0.071%	0.010; 0.035%	0.028; 0.099%	0.012; 0.043%

6.2 EVENTS WITH ANNUAL FREQUENCY OF OCCURRENCE $1 \cdot 10^{-7}$ 1/yr

The stochastic simulation parameters for the simulations of WP exposed to vibratory ground motion at $1 \cdot 10^{-7}\ 1/yr$ annual frequency of occurrence are the same as those for the $1 \cdot 10^{-6}\ 1/yr$ realizations presented in Table 6.1-1.

The ground motions at annual frequency of occurrence of $1 \cdot 10^{-7}\ 1/yr$ are much more intense than their counterparts at $1 \cdot 10^{-6}\ 1/yr$. As an example the maximum peak ground acceleration reached in ground motion number 9 is approximately $34 \cdot g$ ($g = 9.81\ m/s^2$ being acceleration of gravity), while the maximum peak ground velocity in ground motion number 3 is approximately 16 m/s (see Ref. 30). (For comparison, at the annual frequency of occurrence of $1 \cdot 10^{-6}\ 1/yr$ the maximum peak ground acceleration and the maximum peak ground velocity are approximately $10 \cdot g$ and 2.4 m/s, respectively [see Ref. 29].) As a consequence of these high-intensity ground motions the kinematics of the unanchored repository components are characterized by plethora of rigid-body motion and high-speed impacts (see Figs. 25 and 26).

6.2.1 Interaction between Waste Package and Pallet

Table 6.2.1-1 presents the damaged area resulting from the WP-pallet interaction during the vibratory ground motion.

Table 6.2.1-1 Damaged Area from WP-Pallet Interaction at $1 \cdot 10^{-7}\ 1/yr$

Realization Number	Ground Motion Number	Damaged Area (m^2; % of total OS area)	
		80% Yield Strength	90% Yield Strength
1	7	0.20; 0.71%	0.17; 0.60%
3	4	0.096; 0.34%	0.083; 0.29%
4	8	0.12; 0.43%	0.096; 0.34%
5	11	0.093; 0.33%	0.071; 0.25%
6	1	0.046; 0.16%	0.024; 0.085%
7	2	0.038; 0.13%	0.028; 0.099%
8	13	0.095; 0.34%	0.068; 0.24%
9	10	0.0052; 0.018%	0.0035; 0.012%
10	9	0.16; 0.57%	0.14; 0.50%
11	5	0.0016; 0.0057%	0; 0
12	6	0.062; 0.22%	0.041; 0.15%
13	12	0.027; 0.096%	0.018; 0.064%
14	14	0.020; 0.071%	0.016; 0.057%
15	3	0.0045; 0.016%	0; 0

NOTE: Accuracy of the results (damaged area) due to the WP-pallet interaction is doubtful (see discussion in Section 6.5)

Note that results are not available for realization number 2. That realization was one out of four from the $1 \cdot 10^{-7}\ 1/yr$ set for which the simulation was performed by using the FE representation for

$1 \cdot 10^{-6}$ $1/yr$ calculations (compare Figures 3 and 7a, and see discussion in Section 5.2). Unfortunately, this attempt failed for realization number 2 due to the intensity of motion of the WP and pallet. In other words, the finely meshed region of WP OS could not retain appropriate contact with the pallet (see Figure VIII-2 for illustration). Consequently, since the basic premise of the $1 \cdot 10^{-6}$ $1/yr$ FE representation is violated, the results are not representative and are not presented.

6.2.2 Interaction between Waste Package and Waste Package (Longitudinal Boundary)

This section presents the damaged area of the WP OS resulting from the longitudinal (end) impacts. This damaged area is, thus, attributed to the WP-WP interaction during the vibratory ground motion. It is calculated (by using Reference 27 [Tables 4, 5, 7, and 8]) based on the speed, location, and angle of the longitudinal impacts, estimated from the simulations of the vibratory ground motion.

Table 6.2.2-1 End-Impact Parameters and Damaged Area for Realization Number 1 at $1 \cdot 10^{-7}$ $1/yr$

Impact Location	Time (s)	Speed (m/s)	Angle (degree)	Damaged Area (m^2)	
				80% Yield Strength	90% Yield Strength
F 3	4.825	2.0	2.6	0.0176	0.0090
F 7	2.725	1.4	2.7	0.0085	0.0044
F 8	4.025	1.0	7.2	0.0013 NC	0.0010 NC
F 8	7.100	1.2	3.7	0.0047	0.0025
F 9	2.350	1.0	3.9	0.0021	0.0013
C 2	4.900	4.5	5.3	0.1005	0.0556
C 3	5.400	1.8	1.0	0.0183 NC	0.0093 NC
C 7	2.100	1.8	2.1	0.0158	0.0080
C 10	4.525	1.2	6.6	0.0033	0.0020
C 11	6.900	1.3	4.0	0.0056	0.0030
Total				0.16	0.086

Table 6.2.2-2 End-Impact Parameters and Damaged Area for Realization Number 2 at $1 \cdot 10^{-7}$ $1/yr$

Impact Location	Time (s)	Speed (m/s)	Angle (degree)	Damaged Area (m^2)	
				80% Yield Strength	90% Yield Strength
F 2	3.500	1.1	2.8	0.0040X0.5	0.0022X0.5
F 3	4.975	1.9	1.0	0.0202	0.0103
F 9	0.500	1.6	0.3	0.0044	0.0022
F 12	2.300	1.1	1.0	0.0052	0.0027
C 1	1.600	1.4	0.2	0.0022	0.0011
C 3	4.675	1.3	0.6	0.0054	0.0028
C 7	3.725	1.3	1.0	0.0089	0.0046
Total				0.048	0.025

Table 6.2.2-3 End-Impact Parameters and Damaged Area for Realization Number 3 at $1 \cdot 10^{-7}\ 1/yr$

Impact Location	Time (*s*)	Speed (*m/s*)	Angle (*degree*)	Damaged Area (m^2) 80% Yield Strength	Damaged Area (m^2) 90% Yield Strength
F 1	1.225	1.3	1.7	0.0082 NC	0.0042 NC
F 1	2.650	2.4	1.4	0.0317	0.0133
F 4	5.600	3.4	1.3	0.0584	0.0196
F 5	0.925	1.7	2.2	0.0140 NC	0.0071 NC
F 5	2.900	3.7	2.5	0.0688 NC	0.0288 NC
F 7	3.100	4.0	3.6	0.0809	0.0404
F 8	6.600	1.5	0.3	0.0038 NC	0.0019 NC
F 8	8.450	1.7	1.4	0.0156 NC	0.0080 NC
F 9	1.700	2.2	1.7	0.0257X0.5	0.0118X0.5
F 9	4.725	2.2	0.2	0.0074 NC	0.0044 NC
F 9	9.000	1.1	5.0	0.0026 NC	0.0016 NC
F 10	3.975	2.3	3.2	0.0255	0.0125
F 10	10.275	1.7	3.1	0.0121 NC	0.0062 NC
C 2	1.875	2.7	0.8	0.0338 NC	0.0135 NC
C 3	0.375	2.5	2.8	0.0325	0.0151
C 3	3.825	2.5	0.4	0.0176 NC	0.0064 NC
C 3	8.650	2.0	1.3	0.0177 NC	0.0090 NC
C 4	6.750	1.7	5.2	0.0081 NC	0.0043 NC
C 5	6.075	1.5	0.6	0.0076 NC	0.0039 NC
C 6	6.950	1.3	1.9	0.0079 NC	0.0041 NC
C 7	1.350	1.1	1.8	0.0047 NC	0.0025 NC
C 7	2.825	4.7	1.4	0.1064	0.0357
C 7	7.300	1.8	4.8	0.0095 NC	0.0049 NC
C 8	1.525	1.0	1.4	0.0031 NC	0.0017 NC
C 8	5.425	1.4	1.0	0.0108 NC	0.0056 NC
C 8	9.825	1.5	2.4	0.0105 NC	0.0054 NC
C 9	4.125	2.4	2.5	0.0299 NC	0.0137 NC
C 10	2.150	1.3	1.9	0.0079 NC	0.0041 NC
C 10	3.200	2.2	1.5	0.0261 NC	0.0119 NC
C 10	4.100	2.1	2.6	0.0206 NC	0.0098 NC
C 11	2.225	1.2	2.2	0.0060 NC	0.0031 NC
C 11	3.000	3.8	2.4	0.0715	0.0293
C 11	5.900	1.2	4.7	0.0038 NC	0.0021 NC
C 11	6.150	1.8	0.6	0.0110 NC	0.0056 NC
Total				0.42	0.17

Table 6.2.2-4 End-Impact Parameters and Damaged Area for Realization Number 4 at $1 \cdot 10^{-7}\ 1/yr$

Impact Location	Time (*s*)	Speed (*m/s*)	Angle (*degree*)	Damaged Area (m^2) 80% Yield Strength	Damaged Area (m^2) 90% Yield Strength
F 3	2.125	3.0	2.5	0.0478	0.0207
F 5	2.875	1.5	2.4	0.0105	0.0054
F 6	2.925	1.6	3.0	0.0109 NC	0.0056 NC
F 7	3.000	1.4	2.0	0.0095 NC	0.0049 NC
F 7	3.725	2.2	1.3	0.0266	0.0120
F 12	3.325	1.2	7.0	0.0033	0.0020
C 2	1.250	1.2	0.4	0.0028	0.0015

Impact Location	Time (s)	Speed (m/s)	Angle (degree)	Damaged Area (m^2)	
				80% Yield Strength	90% Yield Strength
C 5	2.475	1.9	4.6	0.0110	0.0057
C 5	3.250	1.7	6.1	0.0082 NC	0.0045 NC
C 6	2.575	1.2	3.6	0.0048X0.5	0.0026X0.5
C 8	1.150	1.3	0.2	0.0018	0.0009
Total				0.11	0.050

Table 6.2.2-5 End-Impact Parameters and Damaged Area for Realization Number 5 at $1 \cdot 10^{-7}\ 1/yr$

Impact Location	Time (s)	Speed (m/s)	Angle (degree)	Damaged Area (m^2)	
				80% Yield Strength	90% Yield Strength
F	3.675	1.8	0	0	0
F 1	1.925	2.0	4.1	0.0134	0.0069
F 1	4.850	1.4	1.6	0.0100 NC	0.0052 NC
F 5	1.300	2.7	0.9	0.0369	0.0141
F 6	2.700	1.8	1.7	0.0167 NC	0.0085 NC
F 6	5.000	1.2	0.4	0.0028 NC	0.0015 NC
F 7	3.425	1.4	2.6	0.0086	0.0045
F 10	0.350	2.1	1.6	0.0232	0.0111
F 12	5.900	1.3	3.0	0.0067X0.5	0.0035X0.5
C 2	0.525	1.6	1.3	0.0140	0.0072
C 3	5.375	1.7	0.1	0.0016X0.5	0.0008X0.5
C 4	0.825	1.2	0.7	0.0049 NC	0.0026 NC
C 4	3.950	1.2	1.0	0.0071X0.5	0.0037X0.5
C 5	3.000	1.9	2.4	0.0166	0.0085
C 8	1.650	3.4	0.8	0.0498	0.0180
C 8	2.300	1.5	1.3	0.0122 NC	0.0063 NC
C 11	6.225	1.3	2.0	0.0078	0.0041
C 12	0.100	1.4	0.2	0.0022	0.0011
C 12	3.125	1.4	0.2	0.0022 NC	0.0011 NC
Total				0.18	0.080

Table 6.2.2-6 End-Impact Parameters and Damaged Area for Realization Number 6 at $1 \cdot 10^{-7}\ 1/yr$

Impact Location	Time (s)	Speed (m/s)	Angle (degree)	Damaged Area (m^2)	
				80% Yield Strength	90% Yield Strength
F 2	0.950	4.0	1.7	0.0754 NC	0.0264 NC
F 2	2.325	4.4	1.7	0.0933	0.0328
F 3	3.225	1.3	0.1	0.0009 NC	0.0004 NC
F 6	3.075	2.0	2.0	0.0193	0.0098
F 8	1.775	3.2	2.9	0.0541 NC	0.0246 NC
F 9	1.275	4.4	6.9	0.0863 NC	0.0455 NC
F 9	1.425	1.4	3.3	0.0077 NC	0.0040 NC
F 9	2.125	1.6	1.5	0.0137 NC	0.0070 NC
F 10	0.600	2.9	0.9	0.0418 NC	0.0152 NC
F 10	2.725	5.0	2.0	0.1200	0.0445
C 1	1.575	3.2	1.1	0.0529 NC	0.0176 NC

Impact Location	Time (s)	Speed (*m/s*)	Angle (*degree*)	Damaged Area (m^2)	
				80% Yield Strength	90% Yield Strength
C 1	2.650	4.6	1.9	0.1024 NC	0.0374 NC
C 1	2.875	2.5	1.2	0.0347 NC	0.0139 NC
C 3	2.250	6.4	1.7	0.1572	0.0563
C 6	0.700	3.7	0.7	0.0522X0.5	0.0200X0.5
C 7	4.275	1.3	0.1	0.0009 NC	0.0004 NC
Total				0.42	0.15

Table 6.2.2-7 End-Impact Parameters and Damaged Area for Realization Number 7 at $1 \cdot 10^{-7}$ $1/yr$

Impact Location	Time (s)	Speed (*m/s*)	Angle (*degree*)	Damaged Area (m^2)	
				80% Yield Strength	90% Yield Strength
F	0.325	1.9	0	0	0
F 1	2.400	6.0	8.4	0.1019 NC	0.0466 NC
F 1	4.150	1.8	0.7	0.0128 NC	0.0065 NC
F 2	4.350	2.3	2.2	0.0275X0.5	0.0126X0.5
F 6	1.700	1.5	1.2	0.0124 NC	0.0063 NC
F 7	4.075	3.4	1.3	0.0584	0.0196
F 9	3.250	3.8	3.7	0.0746 NC	0.0378 NC
F 11	2.175	5.4	1.4	0.1382	0.0472
F 12	2.225	3.1	3.2	0.0511 NC	0.0243 NC
C	2.100	2.0	0	0	0
C 3	2.700	3.3	2.5	0.0568	0.0242
C 3	2.900	1.9	3.3	0.0143 NC	0.0073 NC
C 4	2.000	4.0	0.5	0.0489 NC	0.0228 NC
C 4	3.675	1.6	0.3	0.0044 NC	0.0022 NC
C 6	2.325	1.5	8.0	0.0062	0.0038
C 9	3.375	2.3	1.9	0.0280	0.0126
C 10	4.550	2.0	1.5	0.0207 NC	0.0105 NC
C 11	0.900	1.7	1.3	0.0158	0.0081
Total				0.32	0.12

Table 6.2.2-8 End-Impact Parameters and Damaged Area for Realization Number 8 at $1 \cdot 10^{-7}$ $1/yr$

Impact Location	Time (s)	Speed (*m/s*)	Angle (*degree*)	Damaged Area (m^2)	
				80% Yield Strength	90% Yield Strength
F	12.075	1.2	0	0	0
F 1	2.925	1.7	6.2	0.0082X0.5	0.0045X0.5
F 2	1.100	1.2	1.9	0.0063 NC	0.0033X0.5
F 3	7.025	1.9	4.0	0.0125 NC	0.0064 NC
F 3	9.300	2.0	1.5	0.0207	0.0105
F 4	1.975	1.7	2.5	0.0133 NC	0.0068 NC
F 4	1.550	1.7	1.6	0.0152 NC	0.0077 NC
F 4	5.375	2.2	6.2	0.0179 NC	0.0099X0.5
F 6	3.425	2.6	3.2	0.0351 NC	0.0169 NC
F 7	2.675	3.5	2.9	0.0634	0.0286
F 8	9.350	2.1	0.3	0.0423 NC	0.0254 NC

Impact Location	Time (s)	Speed (m/s)	Angle (degree)	Damaged Area (m^2)	
				80% Yield Strength	90% Yield Strength
F 9	11.325	1.0	1.5	0.0031 NC	0.0017 NC
F 10	6.475	1.5	0.6	0.0076 NC	0.0039 NC
F 10	6.775	2.1	1.7	0.0229	0.0110
F 11	4.325	1.6	0.8	0.0117 NC	0.0060 NC
F 12	3.825	2.0	3.2	0.0159	0.0081
F 12	9.900	1.7	0.2	0.0033 NC	0.0017 NC
C 1	2.375	2.0	1.3	0.0213 NC	0.0108 NC
C 2	4.450	1.7	2.5	0.0071 NC	0.0038 NC
C 2	5.225	1.2	3.5	0.0049 NC	0.0026 NC
C 2	5.450	1.2	6.5	0.0033 NC	0.0020 NC
C 2	6.900	2.3	1.6	0.0286	0.0127
C 3	2.275	1.2	0.4	0.0028 NC	0.0015 NC
C 4	2.825	2.2	4.9	0.0185 NC	0.0102 NC
C 4	3.050	3.0	3.2	0.0479	0.0228
C 5	3.075	2.1	3.0	0.0196 NC	0.0098 NC
C 6	4.625	1.2	1.3	0.0068	0.0036
C 8	3.700	3.4	0.6	0.0416 NC	0.0178 NC
C 9	1.850	4.1	1.2	0.0786	0.0243
C 9	9.500	1.6	2.0	0.0127 NC	0.0065 NC
C 10	2.100	2.2	1.4	0.0263 NC	0.0120 NC
C 10	11.725	1.5	1.6	0.0117 NC	0.0060 NC
C 12	3.375	2.3	1.1	0.0296	0.0127
Total				0.32	0.14

Table 6.2.2-9 End-Impact Parameters and Damaged Area for Realization Number 9 at $1 \cdot 10^{-7}\ 1/yr$

Impact Location	Time (s)	Speed (m/s)	Angle (degree)	Damaged Area (m^2)	
				80% Yield Strength	90% Yield Strength
F 1	1.725	1.7	0.3	0.0049	0.0025
F 8	3.425	1.1	1.0	0.0052	0.0027
C 4	1.475	1.2	0.1	0.0007 NC	0.0004 NC
C 4	3.100	1.4	1.3	0.0104	0.0054
C 11	1.900	1.8	3.2	0.0132	0.0068
Total				0.034	0.017

Table 6.2.2-10 End-Impact Parameters and Damaged Area for Realization Number 10 at $1 \cdot 10^{-7}\ 1/yr$

Impact Location	Time (s)	Speed (m/s)	Angle (degree)	Damaged Area (m^2)	
				80% Yield Strength	90% Yield Strength
F 2	1.250	6.5	8.0	0.1079	0.0486
F 4	4.950	2.1	8.0	0.0143 NC	0.0081 NC
F 5	2.450	2.4	1.5	0.0315	0.0134
F 6	0.600	2.5	3.7	0.0312 NC	0.0159 NC
F 12	0.875	3.6	5.8	0.0673	0.0388
F 12	1.675	2.7	6.2	0.0241 NC	0.0132 NC
C 1	1.475	3.8	1.8	0.0701	0.0254

Impact Location	Time (s)	Speed (m/s)	Angle (degree)	Damaged Area (m^2)	
				80% Yield Strength	90% Yield Strength
C 1	5.200	3.7	8.0	0.0626 NC	0.0322 NC
C 4	0.475	1.3	0.1	0.0009 NC	0.0005 NC
C 4	1.300	1.3	8.0	0.0042	0.0026
C 5	0.825	1.8	4.0	0.0114 NC	0.0057 NC
C 5	1.200	2.5	7.1	0.0273	0.0150
C 5	2.200	1.2	4.3	0.0042 NC	0.0023 NC
C 6	0.975	1.0	7.2	0.0013	0.0010
C 11	4.775	2.8	1.8	0.0422X0.5	0.0169X0.5
Total				0.33	0.15

Table 6.2.2-11 End-Impact Parameters and Damaged Area for Realization Number 11 at $1 \cdot 10^{-7}$ $1/yr$

Impact Location	Time (s)	Speed (m/s)	Angle (degree)	Damaged Area (m^2)	
				80% Yield Strength	90% Yield Strength
F 2	4.950	1.7	1.9	0.0146	0.0075
F 4	2.950	1.7	3.7	0.0108 NC	0.0056 NC
F 4	3.325	1.2	0.8	0.0056 NC	0.0029 NC
F 4	3.875	1.5	3.3	0.0090 NC	0.0046 NC
F 4	5.800	1.6	0.9	0.0131NC	0.0067 NC
F 5	2.375	2.7	2.4	0.0389	0.0171
F 8	2.050	1.4	0.8	0.0087 NC	0.0044 NC
F 8	4.350	3.1	1.0	0.0503	0.0167
F 9	6.200	2.0	0.7	0.0155 NC	0.0078 NC
F 9	6.550	1.4	1.0	0.0108 NC	0.0056 NC
F 10	3.550	3.0	3.3	0.0479X0.5	0.0231X0.5
C 1	3.050	1.9	3.7	0.0133	0.0068
C 1	5.550	1.7	3.9	0.0104 NC	0.0054 NC
C 3	4.225	3.2	2.6	0.0539	0.0234
C 3	6.375	1.7	1.0	0.0165 NC	0.0084 NC
C 4	1.850	2.5	0.2	0.0147 NC	0.0084 NC
C 4	4.650	1.1	2.5	0.0042 NC	0.0023 NC
C 7	3.725	4.6	1.0	0.1013	0.0313
C 8	2.250	2.0	1.2	0.0215 NC	0.0109 NC
C 8	2.275	2.7	1.0	0.0401 NC	0.0147 NC
C 8	3.450	2.5	3.3	0.0318 NC	0.0155 NC
C 8	5.150	2.2	1.7	0.0257 NC	0.0118 NC
Total				0.30	0.11

Table 6.2.2-12 End-Impact Parameters and Damaged Area for Realization Number 12 at $1 \cdot 10^{-7}$ $1/yr$

Impact Location	Time (s)	Speed (m/s)	Angle (degree)	Damaged Area (m^2)	
				80% Yield Strength	90% Yield Strength
F	0.275	1.8	0	0	0
F 1	5.775	2.1	4.8	0.0151	0.0081
F 1	6.225	1.5	5.9	0.0063 NC	0.0035 NC
F 2	3.750	1.9	4.2	0.0120 NC	0.0062 NC

Impact Location	Time (*s*)	Speed (*m/s*)	Angle (*degree*)	Damaged Area (m^2)	
				80% Yield Strength	90% Yield Strength
F 2	5.350	1.4	1.4	0.0103 NC	0.0053 NC
F 2	6.750	1.8	3.4	0.0128X0.5	0.0065X0.5
F 10	1.425	1.2	1.3	0.0068	0.0036
F 12	3.450	2.0	0.6	0.0133X0.5	0.0067X0.5
C 3	3.875	1.6	7.2	0.0072	0.0042
C 5	5.600	1.3	5.4	0.0044 NC	0.0025 NC
C 6	1.150	3.5	0.9	0.0563	0.0187
C 6	3.650	2.2	1.5	0.0261 NC	0.0119 NC
C 7	0.875	2.2	1.5	0.0261 NC	0.0119 NC
C 10	5.125	1.1	2.3	0.0043	0.0024
Total				0.10	0.044

Table 6.2.2-13 End-Impact Parameters and Damaged Area for Realization Number 13 at $1 \cdot 10^{-7}\ 1/yr$

Impact Location	Time (*s*)	Speed (*m/s*)	Angle (*degree*)	Damaged Area (m^2)	
				80% Yield Strength	90% Yield Strength
F 1	7.125	1.2	5.1	0.0035X0.5	0.0020X0.5
F 3	1.075	1.5	0.5	0.0064 NC	0.0033 NC
F 3	2.275	2.2	3.1	0.0225 NC	0.0111 NC
F 3	4.950	1.1	2.8	0.0040 NC	0.0022 NC
F 4	1.625	2.4	1.4	0.0317	0.0133
F 11	6.350	1.2	0.8	0.0056X0.5	0.0029X0.5
F 12	9.375	1.7	3.8	0.0106	0.0055
C 2	9.175	1.8	0.2	0.0037	0.0019
C 3	1.900	1.5	3.9	0.0081	0.0042
C 6	2.475	2.2	2.2	0.0246	0.0116
C 6	2.550	1.0	2.9	0.0025 NC	0.0015 NC
C 6	3.950	2.0	1.2	0.0215 NC	0.0109 NC
C 7	3.900	1.6	1.3	0.0140 NC	0.0072 NC
C 9	0.750	1.1	0.2	0.0010 NC	0.0005 NC
C 9	1.300	2.2	0.7	0.0198 NC	0.0093 NC
C 9	1.350	1.4	0.6	0.0065 NC	0.0033 NC
C 9	2.975	2.4	0.8	0.0269	0.0115
C 12	10.325	1.4	0.5	0.0054	0.0028
Total				0.12	0.053

Table 6.2.2-14 End-Impact Parameters and Damaged Area for Realization Number 14 at $1 \cdot 10^{-7}\ 1/yr$

Impact Location	Time (*s*)	Speed (*m/s*)	Angle (*degree*)	Damaged Area (m^2)	
				80% Yield Strength	90% Yield Strength
F 1	7.150	1.3	2.1	0.0077	0.0040
Total				0.0077	0.0040

Table 6.2.2-15 End-Impact Parameters and Damaged Area for Realization Number 15 at $1 \cdot 10^{-7}$ $1/yr$

Impact Location	Time (s)	Speed (m/s)	Angle (degree)	Damaged Area (m^2)	
				80% Yield Strength	90% Yield Strength
F 4	1.075	4.3	3.3	0.0921	0.0426
F 4	0.850	1.5	0.6	0.0076 NC	0.0039 NC
F 7	0.750	1.5	7.2	0.0062	0.0036
F 7	1.225	1.1	10.0	0.0018 NC	0.0014 NC
F 11	0.025	2.8	0.1	0.0130	0.0103
C 3	0.150	3.5	0.4	0.0352	0.0185
C 4	0.500	2.2	0.6	0.0173 NC	0.0083 NC
C 6*	1.400	8.6	5.2	0.0332	0.0133
C 9	0.925	4.1	2.7	0.0825	0.0353
C 11	0.600	1.6	0.8	0.0117 NC	0.0060 NC
C 11	1.200	2.4	7.8	0.0235X0.5	0.0128X0.5
C 12	0.325	1.6	1.9	0.0129	0.0066
Total				0.29	0.14

* NOTE: Trunnion collar sleeve impacts the invert not the axial boundary

Table 6.2.2-16 presents a summary of Tables 6.2.2-1 through 6.2.2-15.

Table 6.2.2-16 Damaged Area from End Impacts (WP-WP Interaction) at $1 \cdot 10^{-7}$ $1/yr$

Realization Number	Ground Motion	Damaged Area (m^2; % of total OS area)	
		80% Yield Strength	90% Yield Strength
1	7	0.16; 0.57%	0.086; 0.30%
2	16	0.048; 0.17%	0.025; 0.089%
3	4	0.42; 1.49%	0.17; 0.60%
4	8	0.11; 0.39%	0.050; 0.18%
5	11	0.18; 0.64%	0.080; 0.28%
6	1	0.42; 1.49%	0.15; 0.53%
7	2	0.32; 1.13%	0.12; 0.43%
8	13	0.32; 1.13%	0.14; 0.50%
9	10	0.034; 0.12%	0.017; 0.060%
10	9	0.33; 1.17%	0.15; 0.53%
11	5	0.30; 1.06%	0.11; 0.39%
12	6	0.10; 0.35%	0.044; 0.16%
13	12	0.12; 0.43%	0.053; 0.19%
14	14	0.0077; 0.027%	0.0040; 0.014%
15	3	0.29; 1.03%	0.14; 0.50%

Two important observations can be made by comparing the end-impact results from $1 \cdot 10^{-6}$ $1/yr$ (Tables 6.1.2-1 through 6.1.2-15) and $1 \cdot 10^{-7}$ $1/yr$ (Tables 6.2.2-1 through 6.2.2-15) annual frequencies of occurrence. First, the end impacts for the latter case are much more frequent and of higher intensity (as indicated by impact speed). Second, the damaged area that is not taken into account due to the damage overlap (as indicated by $\times 0.5$ and NC designators; see Section 6.1.2) is significantly larger.

6.2.3 Interaction between Waste Package and Drip Shield

The impact velocity between the WP and the DS is presented in this section. It is assumed in this calculation that these lateral impacts do not cause any damage to the WP (see Assumption 3.15).

Table 6.2.3-1 Lateral-Impact Parameters for Realization Number 1 at $1 \cdot 10^{-7}$ $1/yr$

Impact Location	Time (s)	Speed (m/s)	Angle (degree)
F 3	4.050	3.3	6.1
F 9	3.675	3.6	0.2
F 9	4.650	10.0	5.6
C 3	3.625	4.6	2.3
C 4	4.450	2.1	6.1
C 9	3.275	1.6	1.7
C 11	7.375	1.9	0.2
C 12	5.825	1.8	0.2

Table 6.2.3-2 Lateral-Impact Parameters for Realization Number 2 at $1 \cdot 10^{-7}$ $1/yr$

Impact Location	Time (s)	Speed (m/s)	Angle (degree)
F 1	4.700	3.3	0.1
F 1	5.350	1.9	6.3
F 9	3.800	2.1	0.1
C 1	3.675	2.6	1.3
C 3	4.075	1.2	0.3
C 4	2.900	2.4	1.7
C 5	5.225	4.8	2.5
C 6	5.500	1.9	6.3
C 9	2.150	2.7	0.3
C 10	4.725	2.5	0.6
C 10	4.775	4.7	0.2
C 12	3.550	3.0	1.1

Table 6.2.3-3 Lateral-Impact Parameters for Realization Number 3 at $1 \cdot 10^{-7}$ $1/yr$

Impact Location	Time (s)	Speed (m/s)	Angle (degree)
F 2	5.550	3.9	1.4
F 2	6.900	8.1	1.8
F 3	0.450	3.4	0.6
F 4	2.125	2.6	0.8
F 4	3.400	2.1	4.6
F 9	2.875	2.5	0.1
F 10	1.100	2.3	0.1
C 1	6.775	1.4	1.0
C 2	1.250	1.7	0.8
C 2	1.450	2.4	1.6
C 3	1.000	3.9	1.0
C 3	2.925	3.5	0.2
C 3	3.050	2.4	0.1

Impact Location	Time (s)	Speed (m/s)	Angle (degree)
C 3	3.150	2.9	0.9
C 9	5.625	1.6	0.2
C 11	6.950	4.7	0.1

Table 6.2.3-4 Lateral-Impact Parameters for Realization Number 4 at $1 \cdot 10^{-7}\ 1/yr$

Impact Location	Time (s)	Speed (m/s)	Angle (degree)
F 4	2.500	4.2	0.8
F 9	2.875	2.9	0.6
C 3	2.275	3.8	2.7
C 4	2.925	6.3	0.2
C 8	2.500	4.2	1.5
C 10	3.225	6.1	4.6

Table 6.2.3-5 Lateral-Impact Parameters for Realization Number 5 at $1 \cdot 10^{-7}\ 1/yr$

Impact Location	Time (s)	Speed (m/s)	Angle (degree)
F 9	0.475	1.0	0.2
C 3	0.425	2.1	1.6
C 10	0.675	1.0	2.7

Table 6.2.3-6 Lateral-Impact Parameters for Realization Number 6 at $1 \cdot 10^{-7}\ 1/yr$

Impact Location	Time (s)	Speed (m/s)	Angle (degree)
C 2	3.325	1.2	1.2

Table 6.2.3-7 Lateral-Impact Parameters for Realization Number 7 at $1 \cdot 10^{-7}\ 1/yr$

Impact Location	Time (s)	Speed (m/s)	Angle (degree)
F 2	2.800	7.8	1.0
F 3	3.500	5.2	2.4
F 4	4.275	8.0	1.7
F 9	2.550	6.1	0.1
F 9	4.025	5.9	0.8
F 10	4.95	3.3	0.6
C 1	2.325	4.0	9.2
C 1	2.475	1.5	10.2
C 2	4.550	6.3	4.9
C 3	1.450	1.8	1.5
C 8	4.250	7.1	1.5
C 8	4.300	1.7	0.6
C 9	1.900	3.0	1.2
C 10	2.875	1.8	2.5
C 10	3.600	1.8	2.5

Table 6.2.3-8 Lateral-Impact Parameters for Realization Number 8 at $1 \cdot 10^{-7}$ $1/yr$

Impact Location	Time (*s*)	Speed (*m/s*)	Angle (*degree*)
F 1	4.700	1.1	0.4
F 2	3.575	3.4	0.4
F 7	5.100	1.8	2.8
F 8	4.075	2.7	0.3
F 9	9.575	2.8	0.1
F 9	9.675	1.2	0.3
F 9	10.050	1.0	0.3
F 10	2.000	2.0	2.2
C 1	2.075	3.1	0.4
C 2	0.925	1.3	0.1
C 3	9.550	1.1	0.1
C 4	3.950	2.9	2.0
C 4	4.050	2.5	0.2
C 4	5.225	4.5	0.9
C 8	1.450	1.2	4.0
C 9	2.850	1.8	4.1
C 9	3.075	1.6	1.8
C 10	3.525	4.8	0.2
C 11	4.650	2.2	0.5
C 11	4.725	4.1	0.5

Table 6.2.3-9 Lateral-Impact Parameters for Realization Number 9 at $1 \cdot 10^{-7}$ $1/yr$

Impact Location	Time (*s*)	Speed (*m/s*)	Angle (*degree*)
F 1	2.150	2.4	2.8
F 2	1.550	4.0	0.9
F 8	2.550	3.9	0.3
C 3	1.125	2.4	1.8
C 4	2.475	3.9	1.3
C 11	2.225	5.5	1.0

Table 6.2.3-10 Lateral-Impact Parameters for Realization Number 10 at $1 \cdot 10^{-7}$ $1/yr$

Impact Location	Time (*s*)	Speed (*m/s*)	Angle (*degree*)
F 5	1.025	3.8	6.3
F 9	3.425	3.3	3.4
F 9	4.250	1.5	5.3
F 9	4.875	9.0	2.4
F 10	0.525	3.0	0.5
F 10	4.950	7.2	10.5
F 11	3.550	5.7	6.1
F 12	0.575	5.4	3.9
C 9	3.725	1.5	4.9
C 10	5.175	1.3	2.6
C 10	5.575	2.9	3.7
C 12	0.900	2.6	6.0
C 12	1.200	4.9	7.3

Table 6.2.3-11 Lateral-Impact Parameters for Realization Number 11 at $1 \cdot 10^{-7}\ 1/yr$

Impact Location	Time (s)	Speed (m/s)	Angle (degree)
F 2	3.075	1.8	0.2
F 2	3.100	1.1	0.6
F 9	3.825	4.5	2.0
F 9	5.325	3.4	2.1
F 9	5.400	1.8	3.3
C 4	2.550	5.2	2.4
C 10	2.750	5.9	3.5

Table 6.2.3-12 Lateral-Impact Parameters for Realization Number 12 at $1 \cdot 10^{-7}\ 1/yr$

Impact Location	Time (s)	Speed (m/s)	Angle (degree)
F 3	0.550	1.2	0
F 6	6.175	3.6	4.1
F 7	1.100	1.8	1.8
F 7	5.350	2.6	0.9
F 12	3.475	7.0	0.2
C 2	0.875	2.8	1.5
C 2	0.925	1.5	1.8
C 9	0.475	2.7	1.1
C 12	0.775	2.1	2.6
C 12	1.750	1.5	1.5
C 12	3.450	1.7	0.5

Table 6.2.3-13 Lateral-Impact Parameters for Realization Number 13 at $1 \cdot 10^{-7}\ 1/yr$

Impact Location	Time (s)	Speed (m/s)	Angle (degree)
F 1	6.675	2.8	2.3
F 2	9.150	2.4	0.6
F 7	8.775	1.1	0.1
F 8	5.025	1.8	1.8
F 9	1.475	2.3	1.8
F 9	3.125	2.0	4.6
C 10	2.750	1.6	1.1
C 10	3.700	2.0	2.3
C 10	10.625	1.3	0.2
C 11	6.800	2.2	1.9
C 11	10.000	3.1	0.2

Table 6.2.3-14 Lateral-Impact Parameters for Realization Number 14 at $1 \cdot 10^{-7}\ 1/yr$

Impact Location	Time (s)	Speed (m/s)	Angle (degree)
C 9 & F 3	6.150	5.9	0
F 2	5.975	1.8	0.1
F 2	6.425	1.5	0.5
F 3	6.050	5.0	0.2

Impact Location	Time (s)	Speed (m/s)	Angle (degree)
C 3	7.425	1.2	0.5
C 9	6.000	2.3	0.2
C 10	6.350	2.0	0.3

Table 6.2.3-15 Lateral-Impact Parameters for Realization Number 15 at $1 \cdot 10^{-7}$ $1/yr$

Impact Location	Time (s)	Speed (m/s)	Angle (degree)
F 2	0.400	14.3	4.6
F 2	0.650	4.5	3.0
C 8	0.450	3.2	0.3
C 10	0.800	11.4	2.3

Few important differences are indicated by the lateral-impact results presented in Tables 6.2.3-1 through 6.2.3-15 as compared with their $1 \cdot 10^{-6}$ $1/yr$ counterparts (Tables 6.1.3-1 through 6.1.3-5). First, while at $1 \cdot 10^{-6}$ $1/yr$ annual frequency of occurrence the WP-DS impacts are rare and low-intensity events, the same interaction at $1 \cdot 10^{-7}$ $1/yr$ annual frequency of occurrence is significantly more frequent and more intense. Not only there is no realization at $1 \cdot 10^{-7}$ $1/yr$ for which the WP-DS interaction is absent but also the impact speed is significantly larger. Second, the WP-DS interaction at $1 \cdot 10^{-6}$ $1/yr$ takes place exclusively between the trunnion collar sleeves and the "vertical" DS plates. On the other hand, at $1 \cdot 10^{-7}$ $1/yr$ the WP can impact any part of the DS. (Note that the impact between WP and invert takes place only once – in realization number 15; this WP-invert impact is, for convenience, included among the end-impacts in Table 6.2.2-15.)

6.2.4 Summary of Results for Events with Annual Frequency of Occurrence $1 \cdot 10^{-7}$ $1/yr$

Table 6.2.4-1 presents the maximum (peak) stress intensity in the WP OS in the course of the vibratory ground motion for 15 realizations. This stress measure can be used to estimate if the structure in question is safe from immediate breach (i.e., fracture, perforation).

The maximum stress intensities presented in Table 6.2.4-1 do not vary significantly, although the ground motion energy range is extremely wide. Also, there is no significant difference in the maximum peak stress intensity levels reached at $1 \cdot 10^{-6}$ $1/yr$ (Table 6.1.4-1) annual frequency of occurrence compared to $1 \cdot 10^{-7}$ $1/yr$ (Table 6.2.4-1). As suggested in Section 6.1.4, a possible explanation is that the pallet, as a thin-walled structure, can offer a limited resistance to the much heavier and stiffer WP. During the more intense WP-pallet interactions, the pallet bulges (see Fig. 9). This flexibility of the pallet provides a cushioning effect for the WP.

In analyzing the maximum stress intensity reached during the vibratory ground motion at $1 \cdot 10^{-7}$ $1/yr$ (Table 6.2.4-1) it is important to recall that the uniaxial tensile strength for Alloy 22 at 150 $°C$ is 1120 MPa (see Section 5.1.2). Thus, all maximum stress intensities presented in Table

6.2.4-1 are less than one-third of the uniaxial tensile strength implying that the immediate breach of the OS appears highly unlikely.

Table 6.2.4-1 Maximum Stress Intensity During Vibratory Ground Motion of Annual Frequency of Occurrence $1 \cdot 10^{-7}\ 1/yr$

Realization Number	Ground Motion Number	Maximum Stress Intensity (MPa)
1	7	365 *(Figure IV-31)*
2	16	359 *(Figure IV-32)*
3	4	362 *(Figure IV-33)*
4	8	353 *(Figure IV-34)*
5	11	350 *(Figure IV-36)*
6	1	360 *(Figure IV37)*
7	2	350 *(Figure IV39)*
8	13	363 *(Figure IV-40)*
9	10	357 *(Figure IV-42)*
10	9	365 *(Figure IV-43)*
11	5	358 *(Figure IV-44)*
12	6	358 *(Figure IV-45)*
13	12	355 *(Figure IV-47)*
14	14	356 *(Figure IV-48)*
15	3	349 *(Figure IV-50)*

The damaged areas characterizing 14 different realizations at annual frequency of occurrence $1 \cdot 10^{-7}\ 1/yr$ are summarized in Table 6.2.4-2. According to these results the cumulative damage area is dominated by the end-impact contribution. In most realizations the damaged area due to the WP-pallet interaction is much smaller than the one due to the WP-WP interaction. It should be kept in mind though that the damaged areas due to the WP-WP interaction are extremely conservatively estimated (see discussion in Section 6.1.2). More importantly, it is unclear to what extent the damaged area from WP-pallet interaction reflects the physics of the problem considering that the residual stress fields are significantly affected by FE representation (see Section 6.5 for detailed discussion). It is also noteworthy that the only two realizations conspicuous by the absence of the nonphysical damaged area at the boundary of the finely-meshed OS region – realization number 11 (see Figure IV-46) and realization number15 (see Figure IV-51) – are characterized by extremely small contribution from the damaged area from the end impacts to the cumulative damaged area.

Table 6.2.4-2 Damaged Area from Vibratory Ground Motion of Annual Frequency of Occurrence $1 \cdot 10^{-7}\ 1/yr$

Realization Number	Ground Motion Number	Damaged Area: WP-Pallet Interaction (m^2) 80% Yield Strength	WP-Pallet Interaction (m^2) 90% Yield Strength	WP-WP Interaction (m^2) 80% Yield Strength	WP-WP Interaction (m^2) 90% Yield Strength	Cumulative (m^2; % of total OS area) 80% Yield Strength	Cumulative (m^2; % of total OS area) 90% Yield Strength
1	7	0.20; 0.71%	0.17; 0.60%	0.16; 0.57%	0.086; 0.30%	0.36; 1.28%	0.26; 0.92%
3	4	0.096; 0.34%	0.083; 0.29%	0.42; 1.49%	0.17; 0.60%	0.52; 1.84%	0.25; 0.89%
4	8	0.12; 0.43%	0.096; 0.34%	0.11; 0.39%	0.050; 0.18%	0.23; 0.82%	0.15; 0.53%
5	11	0.093; 0.33%	0.071; 0.25%	0.18; 0.64%	0.080; 0.28%	0.27; 0.96%	0.15; 0.53%
6	1	0.046; 0.16%	0.024; 0.085%	0.42; 1.49%	0.15; 0.53%	0.47; 1.67%	0.17; 0.60%
7	2	0.038; 0.13%	0.028; 0.099%	0.32; 1.13%	0.12; 0.43%	0.36; 1.28%	0.15; 0.53%
8	13	0.095; 0.34%	0.068; 0.24%	0.32; 1.13%	0.14; 0.50%	0.42; 1.49%	0.21; 0.74%
9	10	0.0052; 0.018%	0.0035; 0.012%	0.034; 0.12%	0.017; 0.060%	0.039; 0.14%	0.021; 0.074%
10	9	0.16; 0.57%	0.14; 0.50%	0.33; 1.17%	0.15; 0.53%	0.49; 1.74%	0.29; 1.03%
11	5	0.0016; 0.0057%	0; 0	0.30; 1.06%	0.11; 0.39%	0.30; 1.06%	0.11; 0.39%
12	6	0.062; 0.22%	0.041; 0.15%	0.10; 0.35%	0.044; 0.16%	0.16; 0.57%	0.085; 0.30%
13	12	0.027; 0.096%	0.018; 0.064%	0.12; 0.43%	0.053; 0.19%	0.15; 0.53%	0.071; 0.25%
14	14	0.020; 0.071%	0.016; 0.057%	0.0077; 0.027%	0.0040; 0.014%	0.028; 0.099%	0.020; 0.071%
15	3	0.0045; 0.016%	0; 0	0.29; 1.03%	0.14; 0.50%	0.29; 1.03%	0.14; 0.50%

NOTE: Accuracy of the results (damaged area) due to the WP-pallet interaction is doubtful (see discussion in Section 6.5)

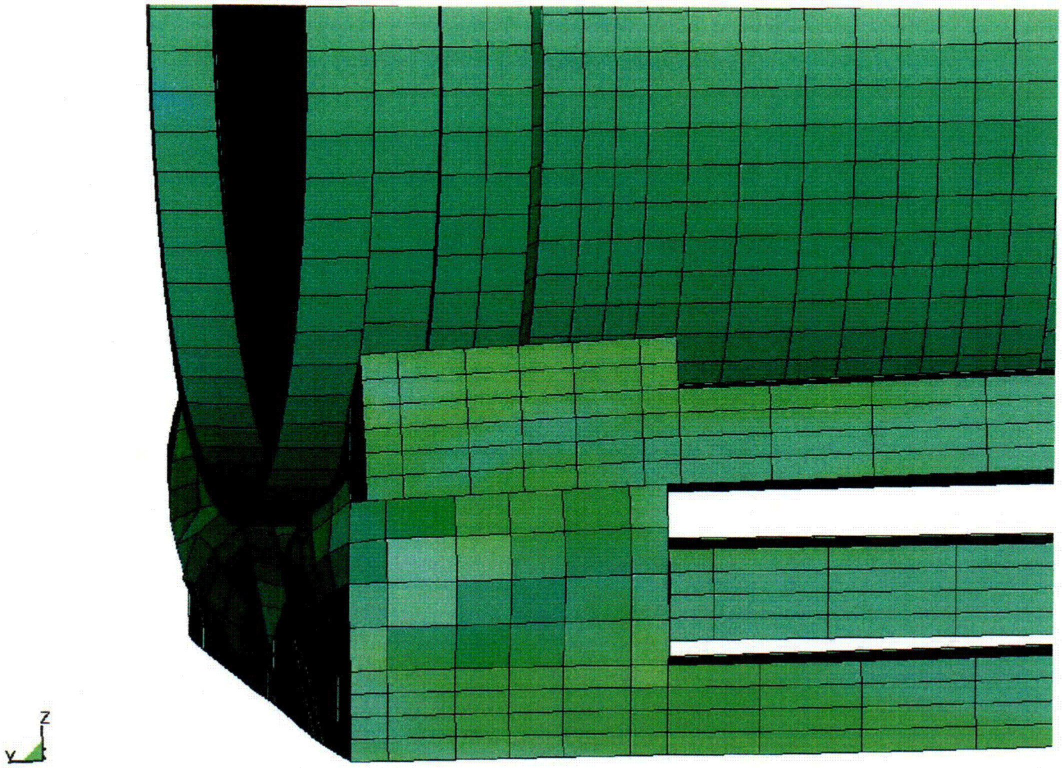

Figure 9. Bulging of the Pallet (Realization Number 10 at $1 \cdot 10^{-7}$ $1/yr$ Annual Frequency of Occurrence)

C07

6.3 EVENT WITH ANNUAL FREQUENCY OF OCCURRENCE $5 \cdot 10^{-4}$ 1/*yr*

The event with annual frequency of occurrence $5 \cdot 10^{-4}\ 1/yr$ is evaluated by using the same FE representation previously used for most of the $1 \cdot 10^{-6}\ 1/yr$ realizations (with the exception of the realization number 6). The simulation is performed at temperature of $150\ ^{o}C$. The simulation started at $3.0\ s$ of the ground motion time history (corresponding to 5 percent of energy of ground motion), and the ending time was $15\ s$ (corresponding to 65 percent of energy of ground motion) (see Ref. 31). This duration covered the most intense period of the ground motion time history. Further extension of the simulation is considered unnecessary based on the results presented in this section (see, as an example, Fig. 13).

The ground motion with annual frequency of occurrence $1 \cdot 10^{-4}\ 1/yr$ is much less intense then its $1 \cdot 10^{-6}\ 1/yr$ counterparts. Consequently, the rigid-body motion during the $1 \cdot 10^{-4}\ 1/yr$ vibratory simulation is extremely small. Specifically, the relative motion of the WP with respect to the pallet in longitudinal (Y) and vertical (Z) direction is practically nonexistent. Figure 10 indicates that – once the initial gap between WP and pallet is closed (see Section 6.3.1) – the relative displacement of two WP and pallet nodes (the locations of nodes number 20 and 18007 are depicted in Figure 17) is less than $\pm 0.01\ mm$ even for the raw (unfiltered) plot (i.e., it varies within the range $0.15 \pm 0.01\ mm$). The filtered plot is more meaningful since the noise – very pronounced due to the high-frequency excitation and the lack of damping – is eliminated. A Butterworth filter with cutoff frequency of $1000\ Hz$ is used for that purpose throughout this section.

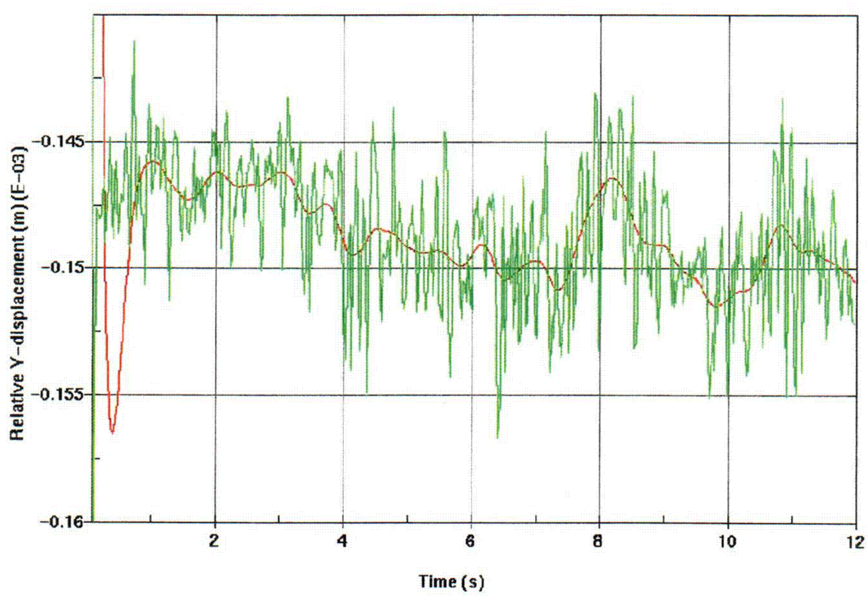

Figure 10. Relative Longitudinal (Y) Displacement (Raw and Filtered) of WP with respect to Pallet for Annual Frequency of Occurrence $5 \cdot 10^{-4}\ 1/yr$

The relative displacement in vertical (Z) direction of the WP with respect to the pallet is also small as indicated in Figure 11. Most of the time in varies within the range $0.44 \pm 0.03\ mm$. (Note the spikes in Figures 10 and 11 at the onset of simulations, which will be discussed at length in Section 6.3.1.)

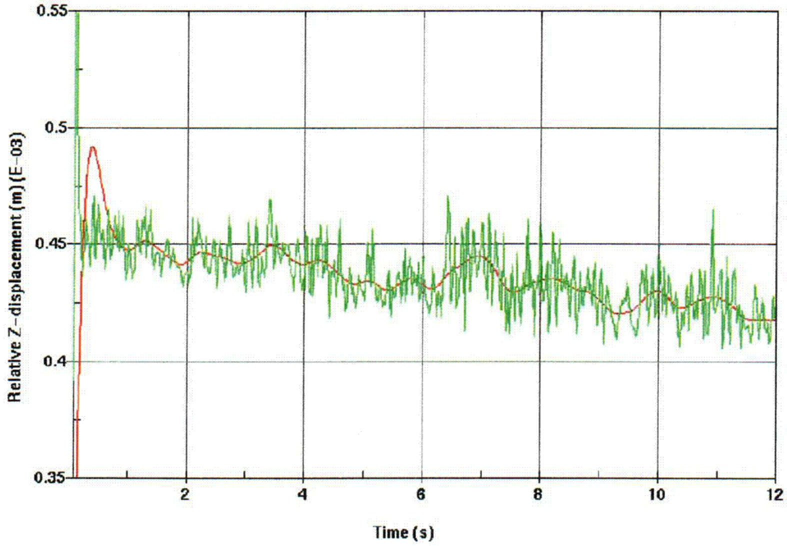

Figure 11. Relative Vertical (Z) Displacement (Raw and Filtered) of WP with respect to Pallet for Annual Frequency of Occurrence $5 \cdot 10^{-4}\ 1/yr$

As a consequence of the limited rigid-body motion, there is no contact between the WP and the longitudinal boundary in the course of $5 \cdot 10^{-4}\ 1/yr$ simulation. For the same reason, there is no contact between the WP and the drip shield either, at any time during the simulation. Thus, the only remaining interaction, relevant for the objective of this analysis, is the one between the WP and the pallet.

As far as the WP-pallet interaction is concerned, another important consequence of limited rigid-body motion (especially in the vertical direction) is the very small impact velocity characterizing that interaction. As Figure 12 indicates, the impact velocity between the WP and the pallet rarely exceeds $0.005\ m/s$ even for the raw (unfiltered) plot. (The apparent singularity at the onset of simulation will be discussed in Section 6.3.1.) The maximum impact velocity (between WP and the pallet) based on the filtered plot (Fig. 12) does not exceed $0.0015\ m/s$.

It seems appropriate to emphasize that the vibratory part of the simulation is performed without either the system damping or the contact damping (see Section 5.2). Keeping that in mind, the claim that the rigid-body motion is negligible at this annual frequency of occurrence seems well supported by the results presented in Figures 10 through 12.

C09

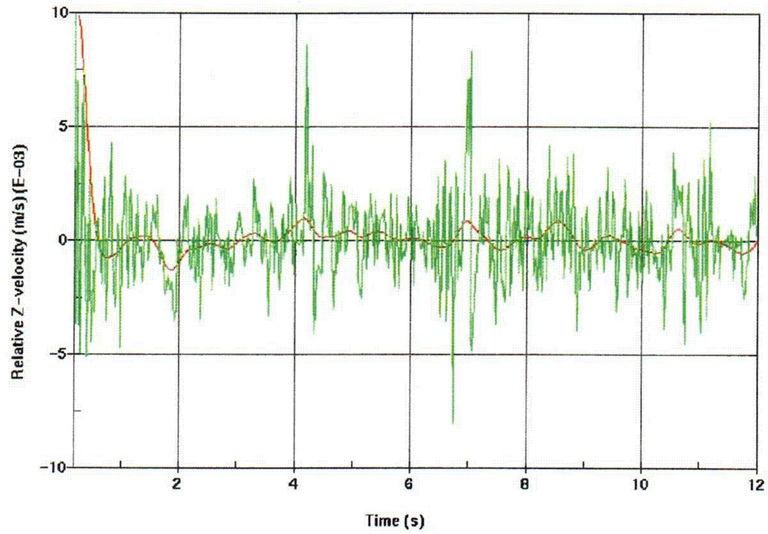

Figure 12. Relative Vertical (Z) Velocity (Raw and Filtered) of WP with respect to Pallet for Annual Frequency of Occurrence $5 \cdot 10^{-4}\ 1/yr$

Figure 13 presents the stress intensity plot for the vibratory part of the simulation. The maximum peak stress intensity remains comfortably below the yield strength ($310\,MPa$ at $150\ °C$, see Section 5.1.1) in the course of vibratory simulation. The peak value of the maximum stress intensity is $208\,MPa$ based on the filtered plot (Fig. 13). Thus, the WP deformation is elastic during the vibratory ground motion (see also Fig. 18). An apparent exception occurring only for the raw plot and a very brief period of time (less than $0.05\ s$) – is the beginning of the event, which will be demonstrated in Section 6.3.1 to be unrelated to the physics of the problem.

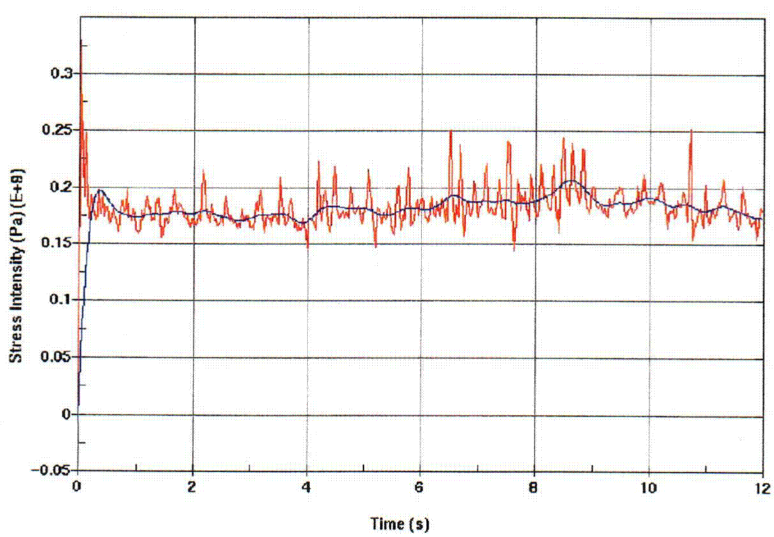

Figure 13. Stress Intensity (Raw and Filtered) for WP OS for Annual Frequency of Occurrence $5 \cdot 10^{-4}\ 1/yr$

C10

Finally, the maximum residual 1st principal stress (77 MPa, see Fig. 14) is below the stress limit (80%-90% of yield strength) by a large margin. It should be emphasized that since the deformation of the WP OS is elastic throughout the ground motion the residual stresses due to that motion should be theoretically zero, and the actual residual stresses approach the static emplacement solution.

In summary, it can be concluded that the WP OS remains undamaged throughout the $5 \cdot 10^{-4}\ 1/yr$ event (i.e., the OS area exceeding established stress limits is zero).

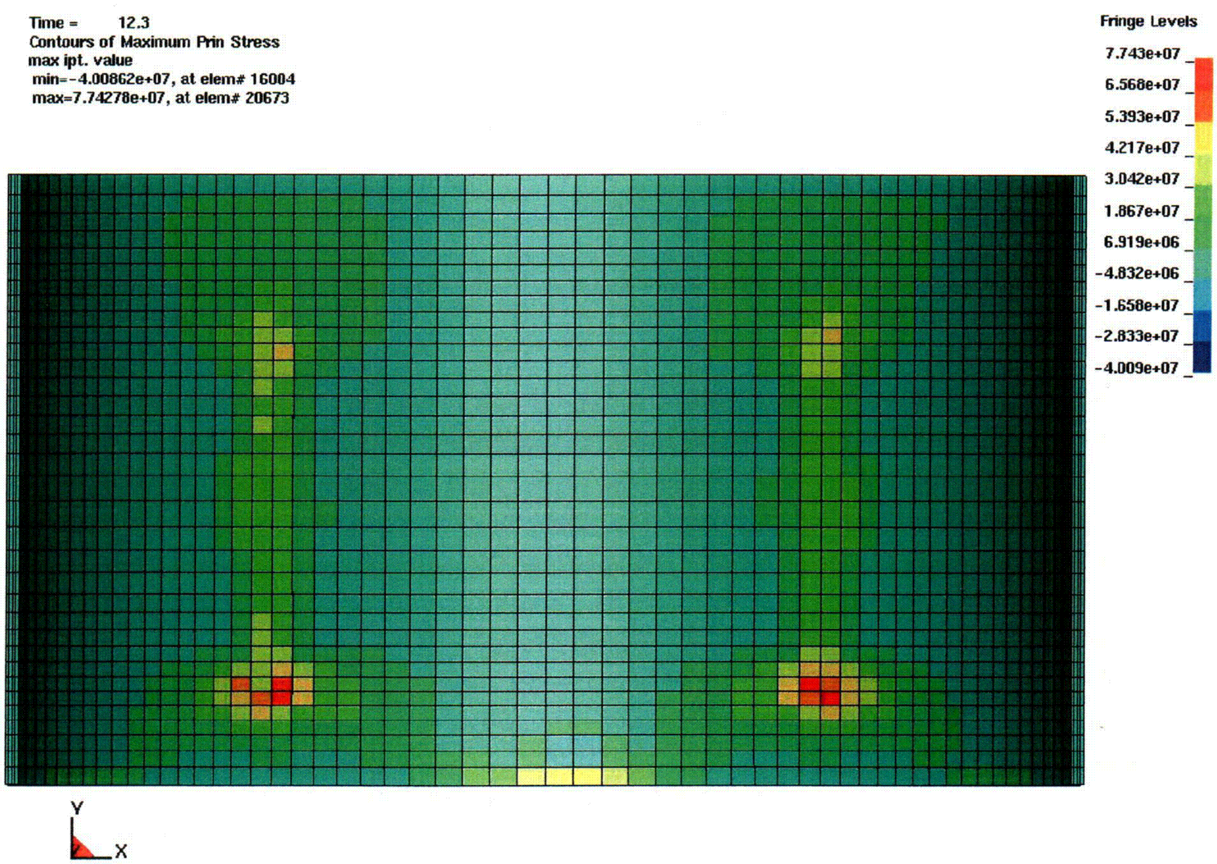

Figure 14. Residual 1st Principal Stress Plot in OS (Top View) for Annual Frequency of Occurrence $5 \cdot 10^{-4}\ 1/yr$

C11

6.3.1 Nonphysical Impact at Onset of Simulation Due to the Settling of WP on Pallet

The results presented in Section 6.3 repeatedly suggest two important conclusions regarding the simulation of the WP-pallet assembly exposed to the vibratory ground motion. First, the rigid-body motion of all freestanding components is negligible. Second, the deformation of the WP OS is elastic throughout the seismic event. An apparent exception is the onset of vibratory simulation (roughly first $0.1\ s$) that somewhat tarnishes otherwise consistent results. Fortunately, it can be convincingly demonstrated that the misleading singular behavior at the onset of simulation is nonphysical (unrelated to the nature of the problem), that it results from the small imperfections in the FE representation, and should be completely disregarded as such.

First, it is necessary to analyze Figures 15 and 16, which are – for the purpose at hand – more revealing versions of Figures 11 and 12, respectively (the latter were concerned with details difficult to observe in the former counterparts). A careful examination of Figures 15 and 16 indicates that the cause of the singular behavior at the onset of simulation is the existence of the initial gap between the WP OS and the pallet. Figure 15 suggest that the gap is approximately 0.42 mm, but the value is somewhat exaggerated due to the unavoidably limited resolution of the FE mesh. (The nodes are not perfectly positioned as seen in Fig. 17, but are the best available for the purpose; the actual gap is approximately 0.3 *mm*.) The gaps like this are side effects of the FE meshing; they are routinely introduced to avoid accidental merging of node of the parts in contact.

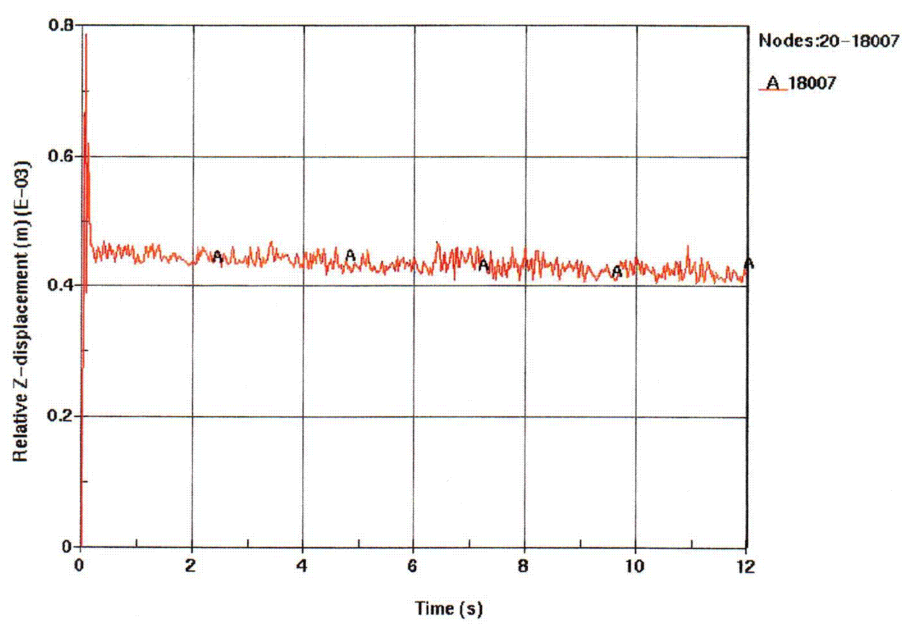

Figure 15. Relative Vertical (Z) Displacement of WP with respect to Pallet

C12

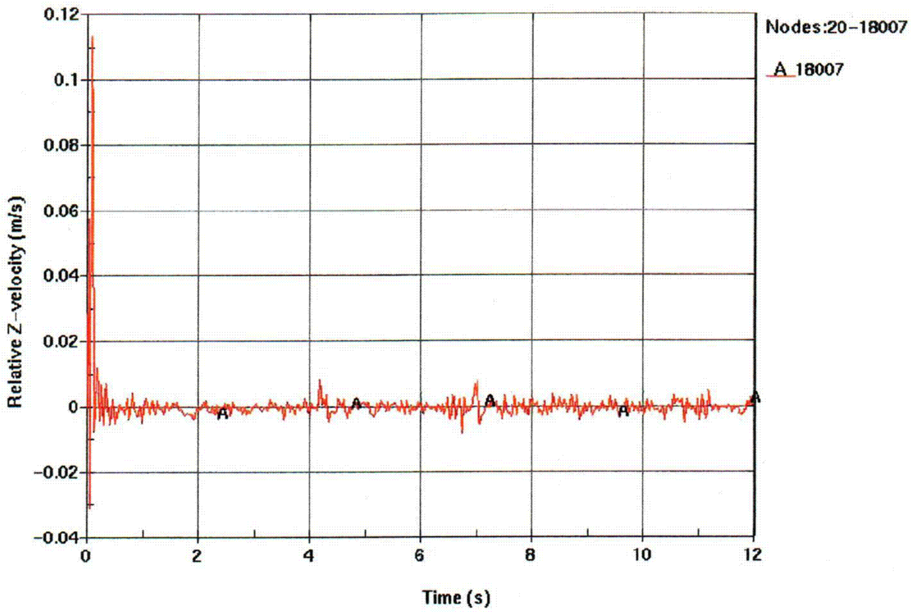

Figure 16. Relative Vertical (Z) Velocity of WP with respect to Pallet

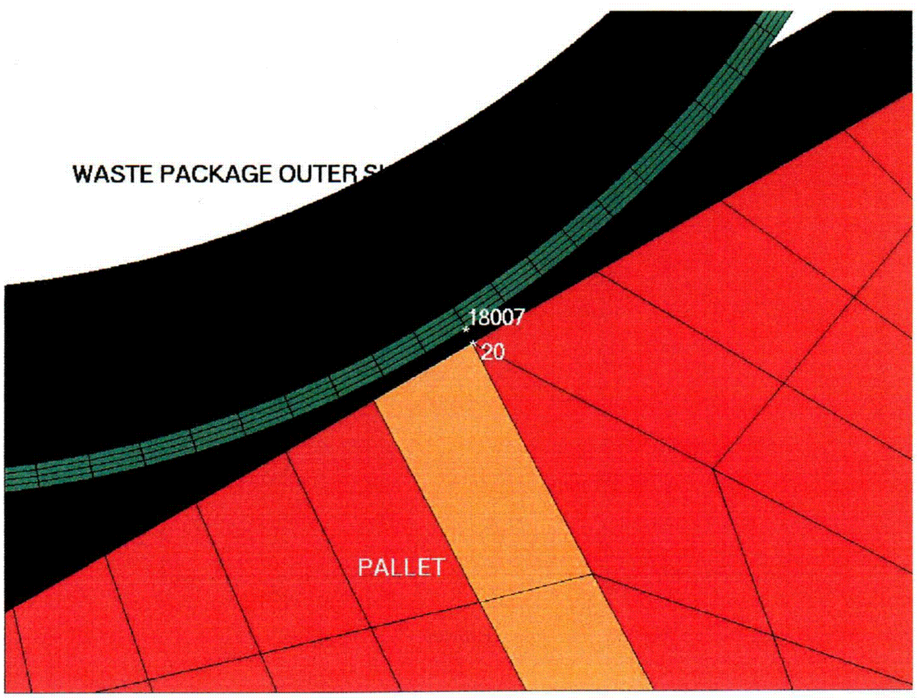

Figure 17. Detail of Contact Region between Pallet and WP OS (Depicting Nodes 20 and 18007)

The contact gaps could be minimized, even eliminated, but for the purpose of most of the vibratory simulations that was considered unnecessary. The rationale is twofold: first, the gap is negligible compared to the average rigid-body displacements (see Figs. 25 and 26, for example), and second, the WP is not likely to be ideally settled on the pallet at the onset of simulation, anyway, due to the time history cutoff. Needless to say, for the events with annual frequency of occurrence $1 \cdot 10^{-6}\ 1/yr$ or $1 \cdot 10^{-7}\ 1/yr$ the gaps are completely irrelevant for the calculation results. On the other hand, for the relatively low-intensity events (such as the $5 \cdot 10^{-4}\ 1/yr$) the initial gap of approximately 0.42 mm (Fig. 15) can result in the initial impact velocity of approximately $0.12\ m/s$ (Fig. 16). This small impact velocity is – in the absence of damping – sufficient to cause the stress intensity and effective stress exceeding the yield strength (see Figs. 13 and 18), and, thus, to cause the small plastic deformation (see Fig. 19).

Effective plastic strain, presented in Figure 19, is defined as

$$\varepsilon_{eff}^{p} = \int_{0}^{t} \left(2 \cdot \dot{\varepsilon}_{ij}^{p}\, \dot{\varepsilon}_{ij}^{p} / 3\right)^{1/2} dt$$

where $\dot{\varepsilon}_{ij}^{p}$ is plastic strain rate tensor (Ref. 17, p. 16.11), t is time, and repeated indices imply summation.

The effective plastic strain is a hardening parameter that, similar to plastic work, provides a cumulative measure of plastic distortion. If a specimen of an isotropic material, characterized by plastic incompressibility, is subjected to a uniaxial test, the effective plastic strain reduces to the true strain (Ref. 20, Chapter II, Section 3). The effective plastic strain is non-decreasing strain invariant; in other words, it is increasing during plastic deformation, and is constant during elastic deformation.

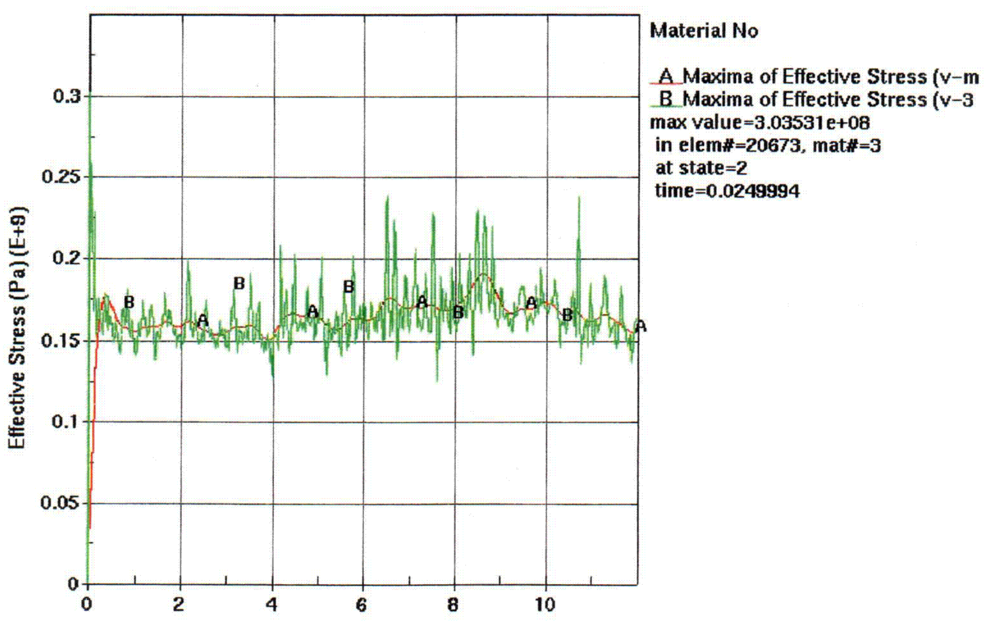

Figure 18. Raw and Filtered Effective Stress for WP OS

C14

It is important to recognize that the entire plastic deformation results from an isolated spike barely exceeding the yield strength for an extremely small period of time (Fig. 19) in the absence of any kind of damping. The entire deformation following the initial singularity (essentially at $t = 0^+$) is elastic as indicated by Figure 19.

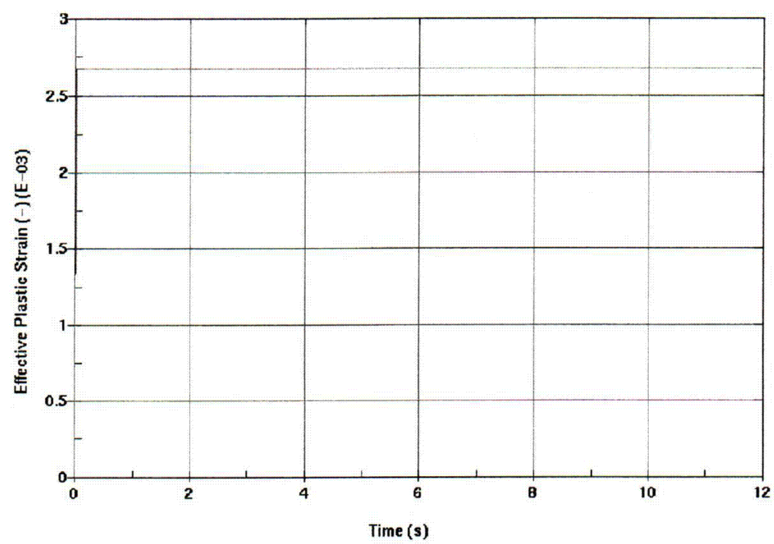

Figure 19. Effective Plastic Strain in WP OS

It can be easily verified that once the initial gap is closed and the WP is settled on the pallet:

(1) relative (rigid-body) motion of WP with respect to pallet becomes negligible (Figs. 10 and 11),
(2) WP-pallet impact velocity becomes extremely small (Fig. 12),
(3) stress intensity (Fig. 13) and effective (von Mises) stress (Fig. 18) are significantly below the yield strength,
(4) effective plastic strain remains constant (Fig. 19), implying the elastic deformation.

In summary, the singularity at the onset of the simulation is due to the impact caused by the settling of the WP on the pallet (i.e., closing of the initial gap). Thus, the results at the onset of simulation (roughly first $0.1\ s$) are not representative of the physics of the problem, and should be disregarded as misleading, although they do not affect the final results (i.e., the damaged area) and conclusions.

6.4 EVENT WITH ANNUAL FREQUENCY OF OCCURRENCE $1\cdot10^{-4}$ $1/yr$

The event with annual frequency of occurrence $1\cdot10^{-4}\ 1/yr$ is evaluated by using the same FE representation previously used for the $5\cdot10^{-4}\ 1/yr$ realization and most of the $1\cdot10^{-6}\ 1/yr$ realizations (with the exception of realization number 6). The simulation is performed at a temperature of 150 ^oC. The simulation started at $9.7\ s$ of the ground motion time history (corresponding to 5 percent of energy of ground motion), and the ending time was $34.9\ s$ (corresponding to 65 percent of energy of ground motion) (see Ref. 38). This duration covered the most intense period of this ground motion time history. Further extension of the simulation is considered unnecessary based on the results presented in this section (see, as an example, Figs. 21 and 22).

The rigid-body motion during the $1\cdot10^{-4}\ 1/yr$ vibratory simulation is very small due to the small intensity of the ground motion. Figure 20 indicates that—once the initial gap between WP and pallet is closed (see Section 6.3.1)—the relative displacement of two typical WP and pallet nodes (the locations of nodes number 20 and 18007 are depicted in Figure 17) is less than $\pm0.07\ mm$ even for the raw plot. The filtered plot is more meaningful since the high-frequency noise—very pronounced due to the high-frequency excitation and the absence of damping—is eliminated. A Butterworth filter with cutoff frequency of 1000 Hz is used for that purpose throughout this section.

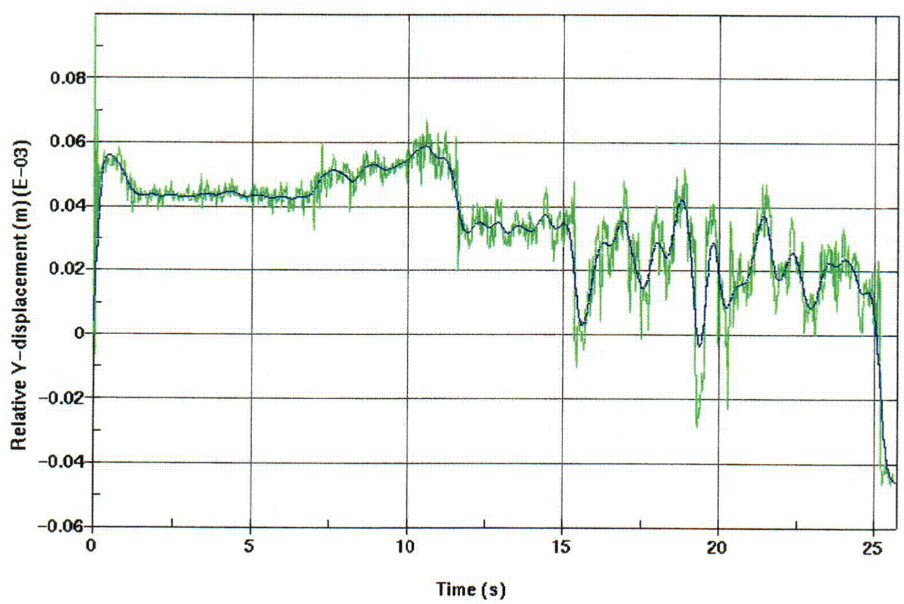

Figure 20. Relative Longitudinal (Y) Displacement (Raw and Filtered) of WP with respect to Pallet for Annual Frequency of Occurrence $1\cdot10^{-4}\ 1/yr$

C15

The relative displacement in vertical (Z) direction of the WP with respect to the pallet is also small as indicated in Figure 21. Most of the time it varies within the range from 0 to 0.3 *mm*. (Note the spikes in Figures 20 and 21 at the onset of simulations, which are discussed at length in Section 6.3.1.)

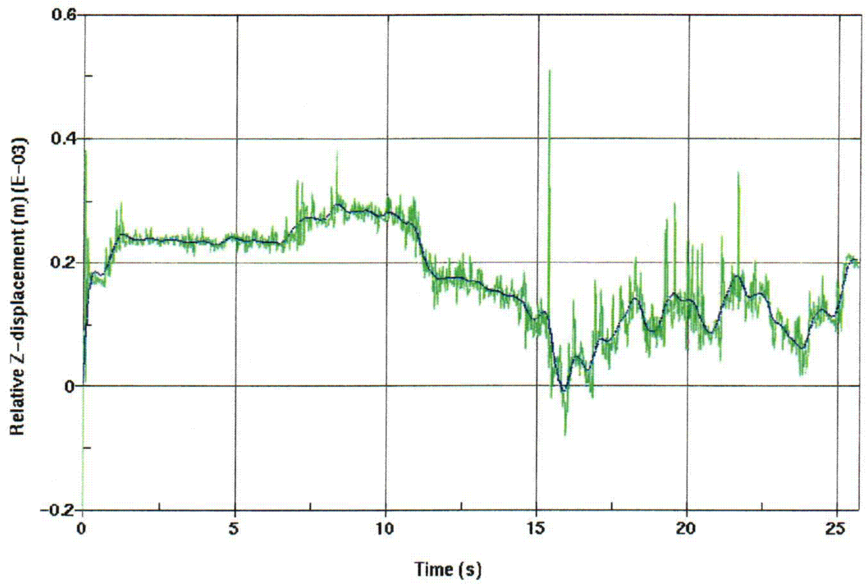

Figure 21. Relative Vertical (Z) Displacement (Raw and Filtered) of WP with respect to Pallet for Annual Frequency of Occurrence $1 \cdot 10^{-4}\ 1/yr$

As a consequence of the limited rigid-body motion, there is no contact between the WP and the longitudinal boundary in the course of the $1 \cdot 10^{-4}\ 1/yr$ simulation. For the same reason, there is no contact between the WP and the drip shield either. Thus, the only remaining interaction, relevant for the objective of this analysis, is the one between the WP and the pallet.

As far as the WP-pallet interaction is concerned, another important consequence of limited rigid-body motion (especially in the vertical direction) is the very small impact velocity characterizing that interaction. As Figure 22 indicates, the impact velocity between the WP and the pallet rarely exceeds $0.005\ m/s$ (for the filtered plot). (The apparent singularity at the onset of the simulation is discussed in Section 6.3.1.) The maximum impact velocity (between the WP and the pallet) based on the filtered plot (blue curve in Fig. 22) does not exceed $0.006\ m/s$.

It seems appropriate to emphasize that the vibratory part of the simulation is performed without either the system damping or the contact damping (see Section 5.2). Keeping that in mind, the claim that the rigid-body motion is negligible at this annual frequency of occurrence is well supported by the results presented in Figures 20 through 22.

C16

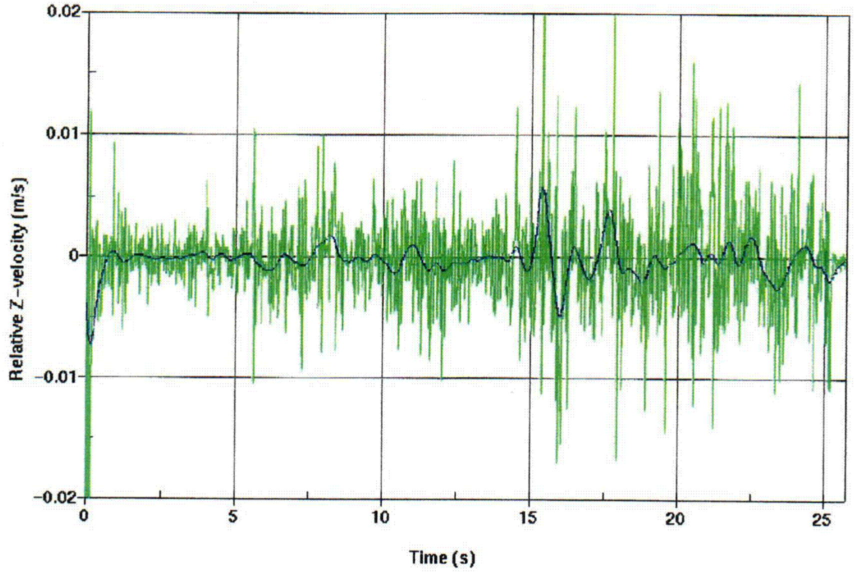

Figure 22. Relative Vertical (Z) Velocity (Raw and Filtered) of WP with respect to Pallet for Annual Frequency of Occurrence $1 \cdot 10^{-4}\ 1/yr$

Finally, according to Figure 23, the maximum residual 1st principal stress (87 MPa) is below the stress limit (80%-90% of yield strength) by a large margin. (Note that the stress unit in Figure 23 is Pascal.) It should be emphasized that since the deformation of the WP OS is elastic throughout the ground motion the residual stresses due to that motion should be theoretically zero, and the actual residual stresses approach the static emplacement solution.

In summary, it can be concluded that the WP OS remains undamaged throughout the $1 \cdot 10^{-4}\ 1/yr$ event (i.e., the OS area exceeding established stress limits is zero).

C17

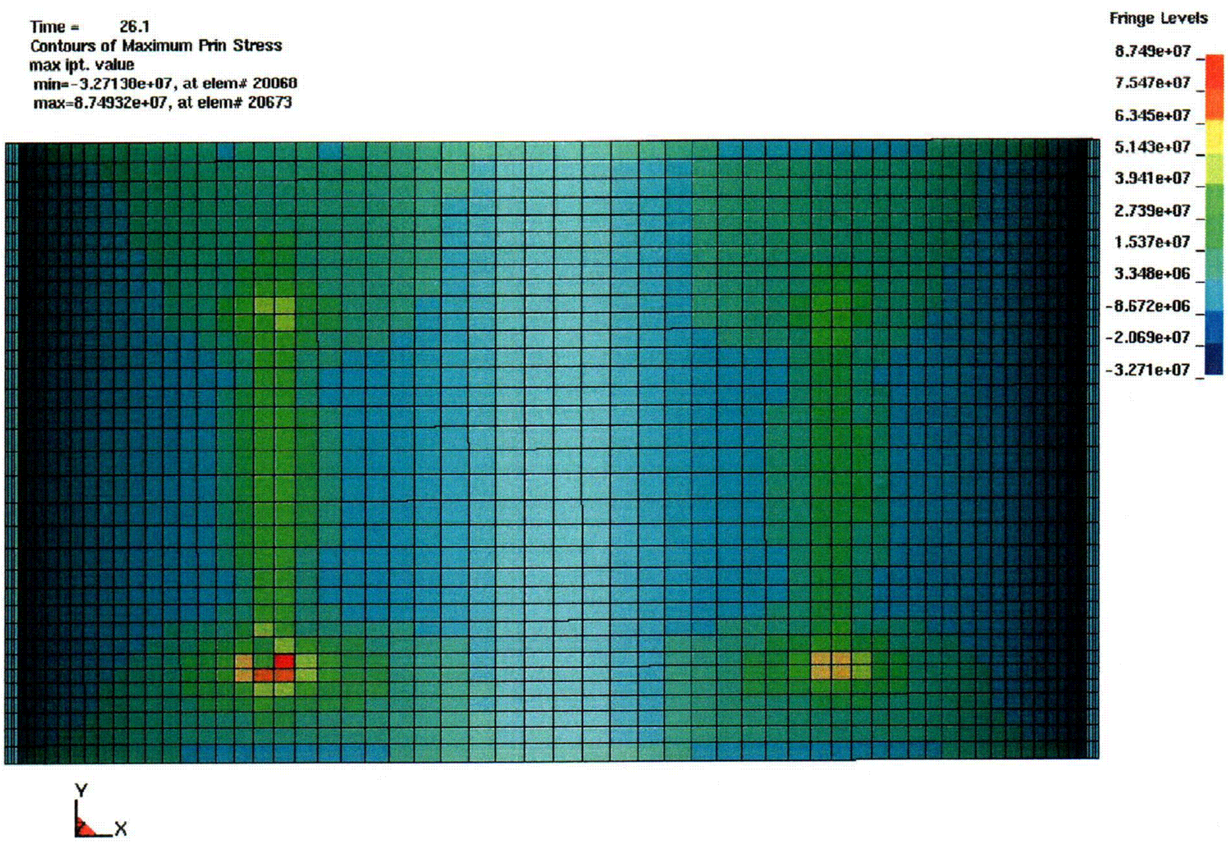

Figure 23. Residual 1st Principal Stress Plot in OS (Top View) for Annual Frequency of Occurrence $1 \cdot 10^{-4}\ 1/yr$

C18

6.5 SOME COMMENTS ON THE VIBRATORY SIMULATIONS

The purpose of this section is to emphasize complexities of the simulation of the unanchored structures exposed to the vibratory ground motion and to highlight some problems encountered during this effort. The additional goal is also to estimate the effects of the discussed issues on the cumulative damaged area presented in this document.

It is important to recognize that the issues discussed herein affect significantly only the damaged area from WP-pallet interaction. This part of the damaged area accounts (on average) for less than 10 percent of the cumulative damaged area at the annual frequency of occurrence of $1 \cdot 10^{-6}$ $1/yr$ (presented in Table 6.1.4-2). For the simulations at annual frequency of occurrence of $1 \cdot 10^{-7}$ $1/yr$ it is not appropriate to make similar estimate of the relative contribution of the two interactions since in most realizations the validity of the results from the WP-pallet interaction is clouded by the nonphysical residual stress distributions. Since the damaged area from WP-pallet interaction is obtained directly from the residual 1st principal stress plots this adversely affects the accuracy of the damaged area from WP-pallet interaction (see detailed discussion in Section 6.5.1). Nonetheless, as already mentioned (see Section 6.2.4), realizations number 11 and 15 are conspicuous (among $1 \cdot 10^{-7}$ $1/yr$ realizations) by absence of the damaged area at the boundary of the finely-meshed OS region. Thus, the damaged area from WP-pallet interaction for these two realizations is not affected by the presence of the boundary. Hence, it is noteworthy that for these two realizations the damaged area from WP-pallet interaction accounts (on average) for less than 1 percent of the cumulative damaged area (see Table 6.2.4-2).

6.5.1 Overview

The complexities inherent to the nature of the problem (enumerated at the beginning of Section 6.5.2) render a comprehensive FE simulation (that would result in direct estimate of the cumulative damaged area) prohibitively time-consuming. Consequently, the contributions to the cumulative damaged area are separated into two groups: i) the damaged area from WP-pallet interaction, and ii) the damaged area from WP-WP interaction. The former results directly from this calculation (i.e., it is evaluated based on the residual 1st principal stress plots [see Attachment IV]). The latter is evaluated indirectly based on the end-impact parameters obtained in this simulation and the damaged area resulting from the WP end impacts on the unyielding surface (Ref. 27, Tables 4 through 8). Common to both of these calculations is the conservatism of the criterion used to define the damaged area (independently of the conservatism related to the choice of the residual stress-threshold distribution, which is beyond the scope of this work). Specifically, the method used to evaluate the damaged area conservatively neglects the residual stress distribution across the thickness of the OS since it is entirely based on the residual stress distributions at the OS surfaces (see Section 2 for discussion). Additional conservatism in estimating the damaged area from the end impacts is inherent to the FE representation (see Section 6.1.2 for details). The entire kinetic energy associated with the impact of two WPs is transferred into deformation energy of one WP. This approximately doubles the deformation energy imparted to the WP. Moreover, this deformation energy is overestimated to begin with since the unanchored neighboring WP is represented by the rigid wall anchored to the invert. Finally, the damage accumulation technique is inherently unable to capture the "damage relaxation", which results in further significant overestimate of the damaged area (discussed in Section 6.1.2). All this conservatism is necessitated by the reasons of the computational economy.

Some features of the FE representation and the kinematics of unanchored structures (resulting from the extremely intense ground motions) impair – to a certain extent – the accuracy of the damaged area resulting from the WP-pallet interaction, which is discussed in detail in Sections 6.5.2 and 6.5.7 and in Attachments VI through IX. It should be emphasized though that the nonphysical residual stress plots, which is the most troublesome adverse effect: 1) are not observed in any $1 \cdot 10^{-6}$ $1/yr$ realization, and 2) have no influence on the damaged area from the end impacts that is dominant contributor to the cumulative damaged area (more than 90 percent, on average, for $1 \cdot 10^{-6}$ $1/yr$ realizations). Therefore it can be concluded that discussed problems have low consequence on the cumulative damaged area (presented in Tables 6.1.4-2 and 6.2.4-2) and that the cumulative damage area is conservatively estimated.

6.5.2 Limitations of WP-Pallet Interactions

The structural calculations of the WP-pallet assembly exposed to the vibratory ground motion are beset with complexities inherent in the nature of the problem.

First, the externally applied loads (i.e., the ground motion time histories) are extremely intense. This causes variety of problems even at $1 \cdot 10^{-6}$ $1/yr$ level but is especially troublesome at $1 \cdot 10^{-7}$ $1/yr$. The extremely large ground velocities and accelerations are either directly causing or further aggravating almost all difficulties discussed henceforth.

Second, the phenomena are highly nonlinear. Momentum is transferred among the repository emplacement drift and unanchored repository components (WP, pallet, and DS) solely by the way of friction and impact. Geometrical nonlinearity (large deformations) is coupled with nonlinear constitutive behavior of materials (elastoplastic behavior with kinematic hardening).

Third, the FE simulation must directly capture the physical phenomena on two different scales (both in space and time). The appropriate simulation of the large-scale kinematics is essential for appropriate definition of the boundary value problem, that is, boundary conditions and contact forces. The contact forces, on the other hand, act locally causing small-scale deformations at individual time instances. Capturing of these small-scale deformations (in the WP OS) is crucial for obtaining sufficiently detailed residual stress plots, but this small-scale (at particular instant of time) deformation can cover – in the course of vibratory ground motion – a relatively large portion of the OS. Needless to say, this imposes difficult meshing requirements.

Fourth, the extraordinary meshing requirements are, together with the intensity of ground motion, mainly responsible for the very small time step (approximately a fraction of microsecond, depending of annual frequency of occurrence and particular ground-motion time history). The very small time step is, in turn, necessary for simulation of a long-duration event ($\approx 30 - 40\,s$).

Fifth, the modes of deformation of the WP OS defy readily available and commonly used simplifications. The most important example is the use of time-efficient shell elements. The shell elements are used in this study for structural representation of the pallet where the dominant deformation mode is local bending. The deformation modes of the OS are, on the other hand, more complex; involving relatively significant local denting (very localized thinning of the OS) and, possibly, in-plane loading. This makes it necessary to use more computationally costly 8-node brick elements over a relatively large portion of the OS. (In order to properly represent stiffness of the OS represented by brick elements, the minimum requirements regarding the number of brick layers need to be met, which, in turn, significantly contributes to the size of the FE representation.)

All discussed complexities impose extreme computational requirements. (The feasibility study was, therefore, by no means a routine exercise in this case.) Consequently, it is requisite to sacrifice some details while retaining all pertinent features of the problem. The most important simplification – already discussed in detail in Section 5.2 – was to define a part of the OS (on one side of the WP only) that can come in contact with the pallet. This part of the OS (designated by F in Fig. 4) is finely meshed, and all results are evaluated for this part of the structure exclusively (see also Assumption 3.18). The remaining part of the OS, and the rest of the mesh for that matter, serve only to ensure that the contact forces and boundary conditions are appropriately captured.

It is important to emphasize that the capability of the FE representation to capture accurately the damaged area from WP-pallet interaction is limited by the intensity of the applied loads. The contact between WP OS and pallet has to remain within the finely meshed region, preferably as far as possible from the region boundaries. The increase of the intensity of the ground motion has twofold effect on the reliability of the results derived from the WP-pallet interaction. Directly, the more intense ground motion causes larger contact forces (see Fig. 24), which in itself may lead to excessive deformation of the elements at the boundary of the finely meshed region due to its limited size (in longitudinal direction). Indirectly, the more intense ground motion results in increased rigid-body motion of all freestanding components (see Figs. 25 and 26), which can again lead to the WP-pallet contacts very close to the boundary of the finely meshed region. The cumulative result of these two adverse effects is that the boundaries of finely-meshed region may be overstrained if the size of that region is insufficient or if density of the trunnion-collar-sleeve mesh is insufficient for the applied load. (The term "overstrained", as used herein and henceforth, implies that the elements at the boundary of the finely-meshed region are nonphysically and excessively deformed due to the presence of the tied-interface boundary.) This is the problem with the simulations performed at $1 \cdot 10^{-7}\ 1/yr$ annual frequency of occurrence, as indicated by the residual stress plots (see, for example, Figs. IV-35 and IV-38). This is further supported by Figures IV-46, IV-49, and IV-51 presenting the residual 1st principal stress plot for realizations number 11, 13, and 15, respectively. These three realizations are characterized among the $1 \cdot 10^{-7}\ 1/yr$ ground motions by relatively small intensity. Consequently, in Figures IV-46 and IV-51 there is very little damage on the bottom side of the region (similar to many $1 \cdot 10^{-6}\ 1/yr$ realizations) but, more importantly, there is no damage due to the overstrain of the boundary elements. In Figure IV-49 there is a little damage on the outer side of the region (bottom view) but significant damage appears on the boundary (top view). The trend continues in Figure IV-41. Finally, at sufficiently intense ground motions all damage is concentrated around the region boundaries as indicated in Figure IV-38 (note the location of the trunnion collar sleeve). Most $1 \cdot 10^{-7}$ $1/yr$ realizations for which stress plots are not presented in Attachment IV qualitatively resemble Figure IV-38. This clearly indicates that with the increased intensity of the ground motion the elements at the boundary of the finely-meshed region are increasingly overstrained.

Finally, it should be reiterated that: first, there is no damaged area at the boundary of the finely meshed OS region at $1 \cdot 10^{-6}$ $1/yr$, and second, the residual stress field has no effect on the damaged area from the end impacts (WP-WP interaction).

6.5.3 Effect of Time-History Cutoff

The cutoff of ground-motion time history is discussed in detail in Section 5.2 and Attachments VII. The effect of the cutoff on the calculation results is negligible according to the detailed study presented in Attachment VII. Energy plots in Figure 27 support this claim. Figure 27a presents energies (total, kinetic, internal, sliding, and hourglass) for realization number 1 at $1 \cdot 10^{-6}$ $1/yr$ annual frequency of occurrence. The kinetic energy plot indicates that there is no motion by the end of simulation. Also, the total energy does not increase substantially anymore. Both of these observations support the claim that the further ground motion cannot substantially change the overall results. The energy plots for realization number 1 at $1 \cdot 10^{-7}$ $1/yr$ annual frequency of occurrence presented in Figure 27b are similar although the simulations are performed up to the 90%-time.

6.5.4 Hourglass Control

Energy plots presented in Figure 27 indicate that the hourglass energy is negligible compared to the total energy. Thus, it can be concluded that the hourglassing is properly controlled and does not constitute a problem, even at the very intense ground motions. This conclusion applies to all simulations performed in this study. This is important since undesirable hourglass modes are the biggest disadvantage of the one-point integration in the 8-node hexahedron elements (see Ref. 17, page 3.4). Use of the one-point integration elements is, on the other hand, a necessity in the vibratory simulations in order to reduce the computer execution time.

6.5.5 Effect of Rigid Elements

The use of rigid elements in OS representation is a more complex issue discussed at length in Attachment VI. There was no indication initially (i.e., based on the stress time histories) that use of rigid elements in OS representation can have any effect on the calculation results, since the relatively pronounced differences are limited almost exclusively to the damaged area (and even then only to the cases where cumulative damage is rather small). Nonetheless, as indicated in Attachment VI, the introduction of the rigid parts has only minor effect on the calculation results for the annual frequency of occurrence of $1 \cdot 10^{-6}$ $1/yr$. Since the differences in the damaged area, if any, amount to only very small portion of the total OS area (less than 0.04 percent), the effect of different FE representations is not pronounced for most realizations. On the other hand, both attempts to perform the simulation without rigid OS parts for the annual frequency of occurrence of $1 \cdot 10^{-7}$ $1/yr$ failed due to inability to achieve numerical convergence (see Attachment X: 1E-7/Deformable OS/RN15/d3hsp and 1E-7/Deformable OS/RN4/d3hsp). The extremely intense ground motion time histories at this annual frequency of occurrence, cause an extremely high deformation (and deformation rate), perpetual reduction of the computational time step (down to $\approx 1 \cdot 10^{-8}\ s$), and finally failure to converge. It is, consequently, impossible to make any estimate of the effect of the difference in FE representations (with and without the rigid OS parts) for $1 \cdot 10^{-7}\ 1/yr$ annual frequency of occurrence. Nonetheless, the effect of the use of rigid elements should not be more pronounced for the $1 \cdot 10^{-7}\ 1/yr$ simulations than for the $1 \cdot 10^{-6}\ 1/yr$ simulations judging by the locations of the rigid parts (compare Fig. 5 with Fig. 7b).

6.5.6 Mesh Sensitivity

Finally, the mesh-sensitivity study presented in Attachment IX indicates that the mesh size (i.e., relatively small variation [from 70 percent to 100 percent] of the average element size) does not have notable effect on the calculation results from the viewpoint of the cumulative damaged area.

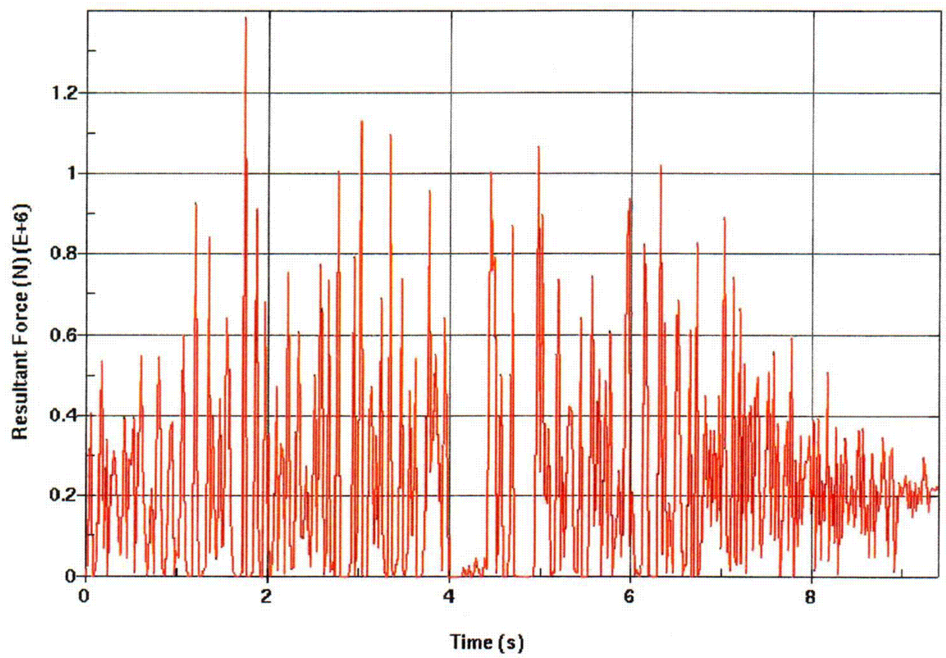

(a)

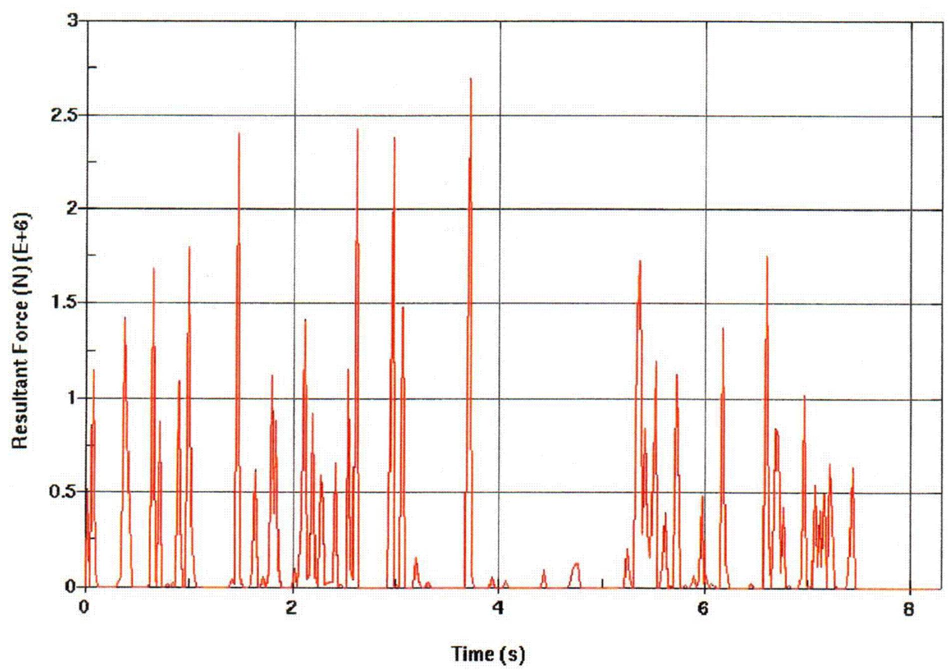

(b)

Figure 24. Resultant Contact Force Between Finely-Meshed OS Region and Pallet for Realization Number 1 at Annual Frequency of Occurrence: (a) $1 \cdot 10^{-6}\ 1/yr$, and (b) $1 \cdot 10^{-7}\ 1/yr$

C19

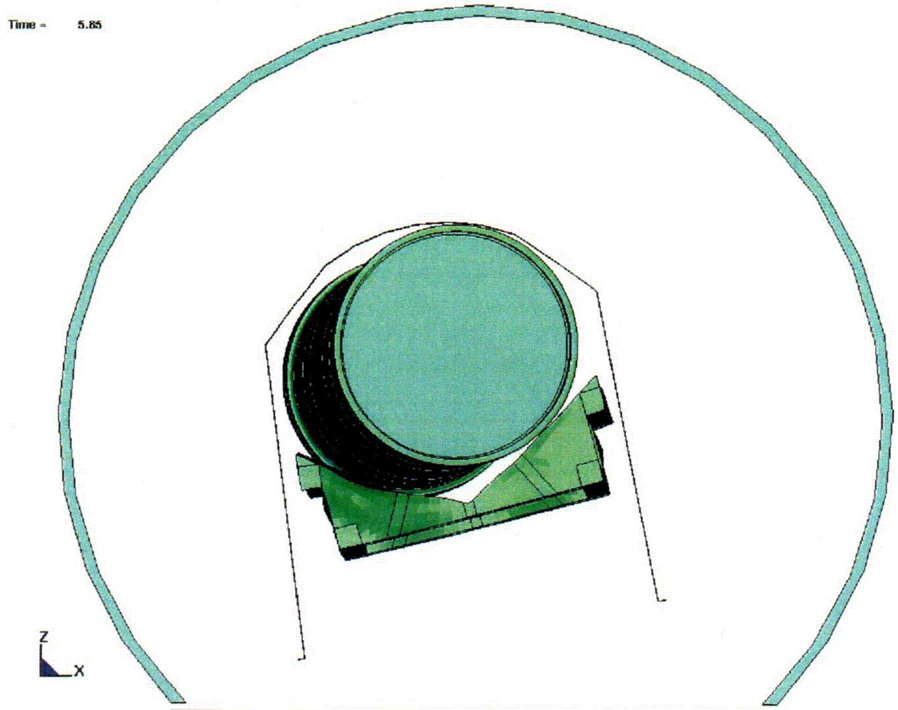

Figure 25. Snapshot at Component Locations in Realization Number 3 at $1 \cdot 10^{-7}$ $1/yr$ Annual Frequency of Occurrence (t = 5.85 *s*)

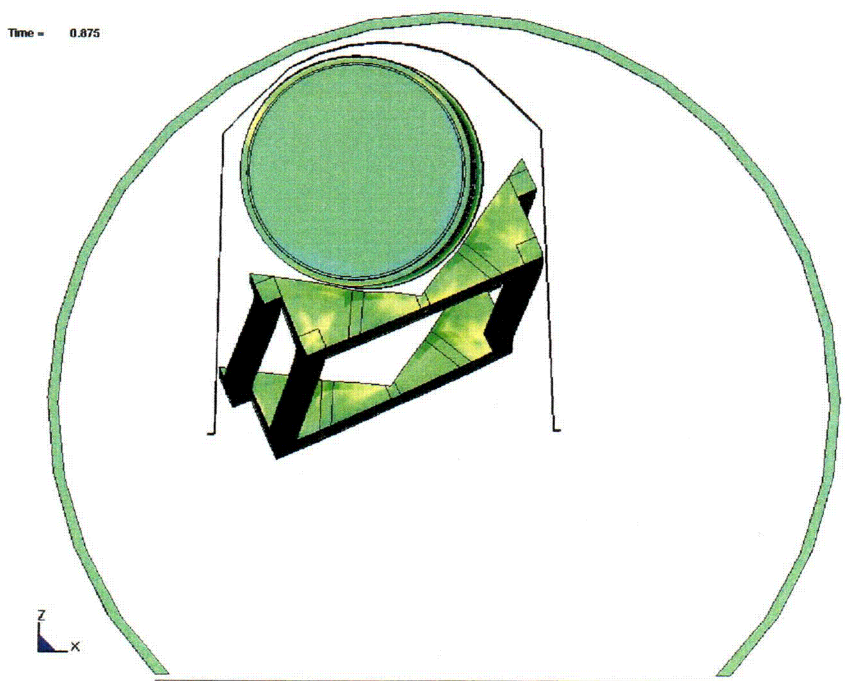

Figure 26. Snapshot at Component Locations in Realization Number 15 at $1 \cdot 10^{-7}$ $1/yr$ Annual Frequency of Occurrence (t = 0.875 *s*)

C20

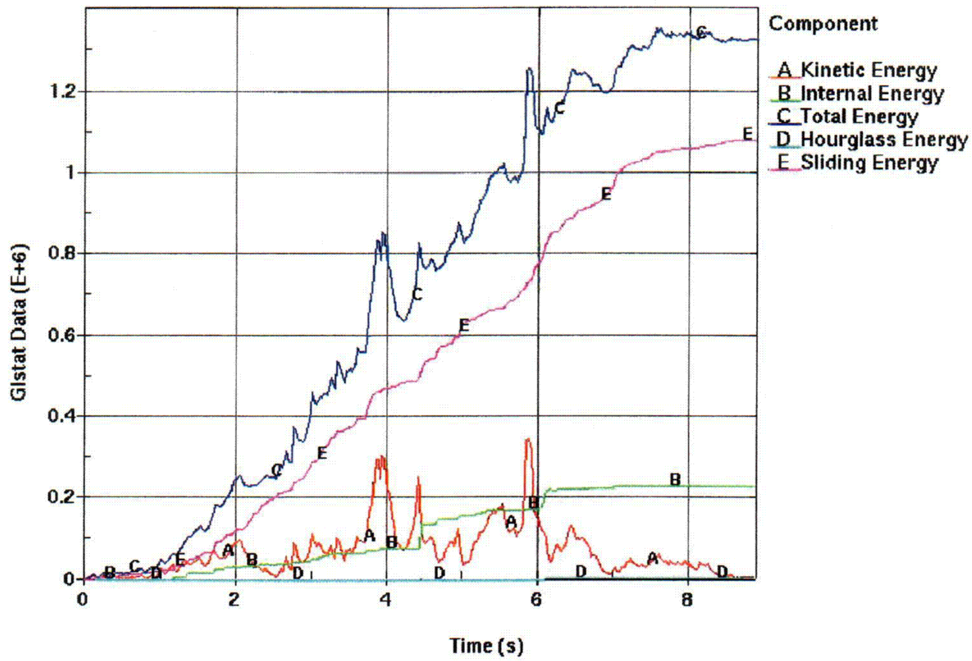

(a)

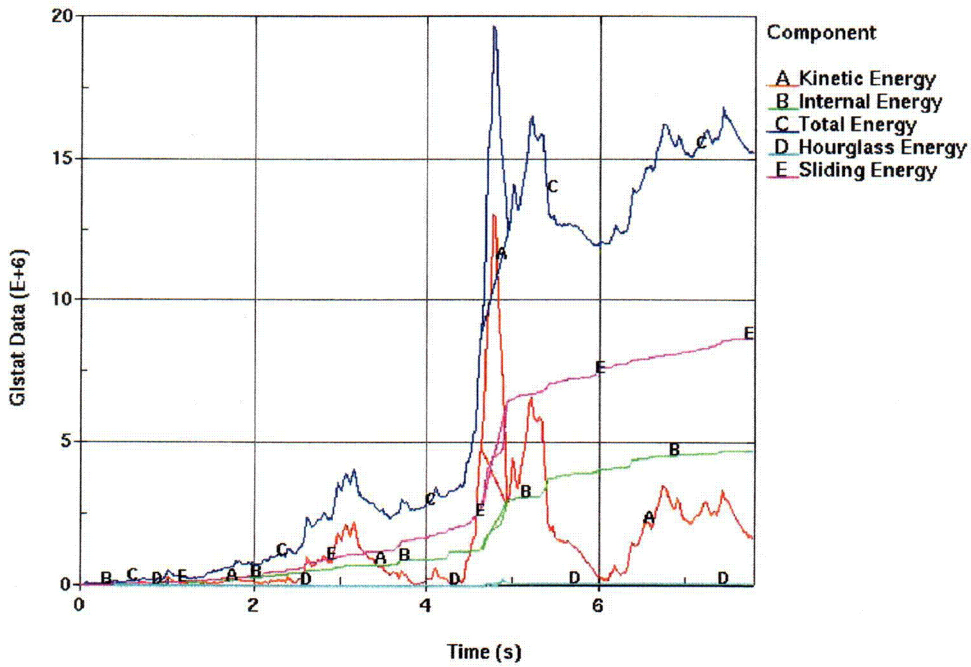

(b)

Figure 27. Energy Plots for Realization Number 1 at Annual Frequency of Occurrence: (a) $1 \cdot 10^{-6}\ 1/yr$, and (b) $1 \cdot 10^{-7}\ 1/yr$

C21

6.5.7 Some Issues of Kinematics at $1 \cdot 10^{-7}$ $1/yr$

As already discussed the capability of FE representation to capture accurately the damaged area from the WP-pallet interaction depends to a large extent on the kinematics of the WP and the pallet. It must be acknowledged that it is imperative for the validity of this portion of results to contain the WP-pallet interaction to the finely-meshed OS region (designated F in Fig. 4), preferably as far as possible from the region boundaries.

This requirement was satisfied for realizations at the $1 \cdot 10^{-6}$ $1/yr$ annual frequency of occurrence. (The only exception being realization number 6, which was for that reason redone with the $1 \cdot 10^{-7}$ $1/yr$ FE representation.)

On the other hand, kinematics of the unanchored repository components is qualitatively different for the $1 \cdot 10^{-7}$ $1/yr$ ground motions. The qualitative difference between ground motions at these two annual frequencies of occurrence is nicely illustrated in Figure 24. The WP-pallet interaction at $1 \cdot 10^{-6}$ $1/yr$ (Fig. 24a) is characterized by frequent low-to-moderate-intensity contacts. The WP-pallet interaction at $1 \cdot 10^{-7}$ $1/yr$ (Fig. 24b) is, on the other hand, characterized by less frequent high-intensity contacts. In other words, the WP and pallet are not in contact for a large portion of the duration of vibratory ground motion. This absence of contact is then followed by strong impacts. This description, based on the contact-force time history (Fig. 24), is directly supported by Figures 25 and 26. (As a further illustration, see the note below Table 6.2.2-15 that indicated an 8.6 m/s -impact between WP and invert.)

Two realization at the $1 \cdot 10^{-7}$ $1/yr$ annual frequency of occurrence were conspicuous for their kinematics characterized by excessive rigid-body motion and excessive contact forces. Realization number 10 is, at the $1 \cdot 10^{-7}$ $1/yr$ annual frequency of occurrence, characterized by the extremely intense ground motion (number 9, see Reference 30). The ground motion number 9 is noticeable for the peak ground acceleration exceeding $34 \cdot g$ in vertical direction (g being gravity acceleration). As a consequence of this high-intensity motion in vertical direction, the WP is at one moment (by the end of simulation) thrown in the air with an extreme velocity and at a high angle of inclination, and it is jammed in between the rigid longitudinal walls (see Fig. 28). The impact is followed by a significant plastic deformation of the trunnion collar sleeves. The WP remained wedged from that moment on.

Finally, in realization number 14, a strong lateral motion of the DS resulted in a localized contact penetration (with the lateral [i.e., drift] wall). As a result, the motion of the DS was "arrested", i.e., it could not break from the contact with the drift wall (see Fig. 29). The motion of the WP and DS continued, but it was naturally affected by – essentially – the new boundary condition.

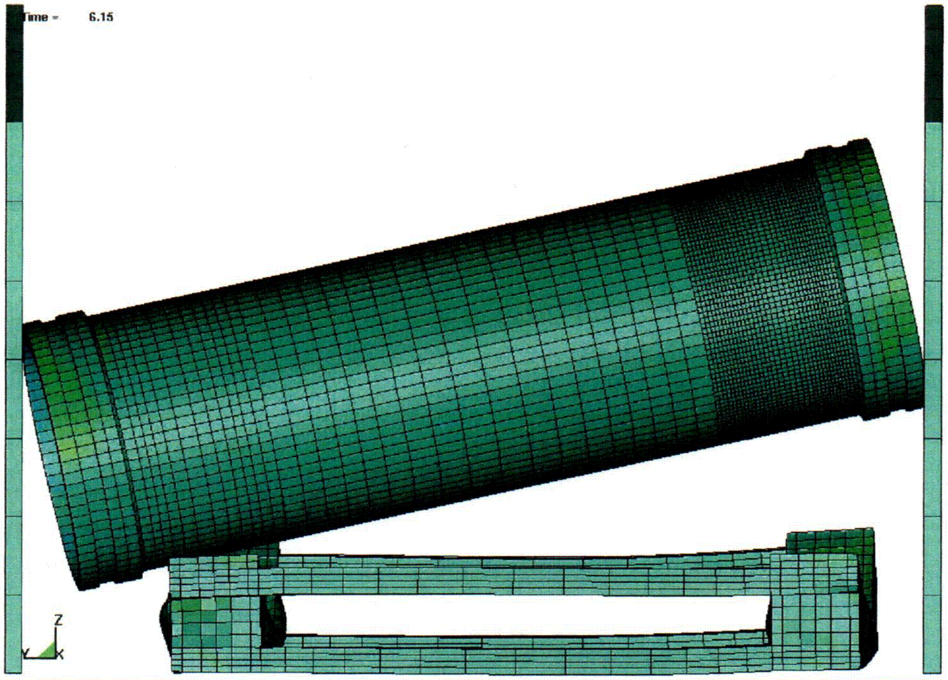

Figure 28. Final Configuration for Realization Number 10 ($1 \cdot 10^{-7}$ $1/yr$)

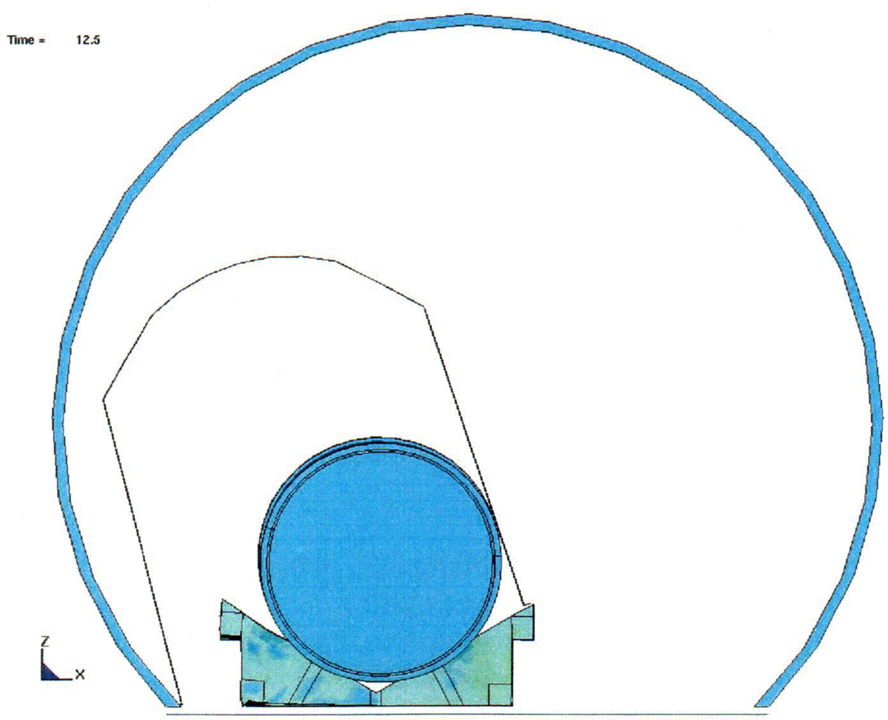

Figure 29. Final Configuration for Realization Number 14 ($1 \cdot 10^{-7}$ $1/yr$)

C21A

7. REFERENCES

1. AP-3.12Q, Rev. 2, ICN 1. *Design Calculations and Analyses*. Washington, D.C.: U.S. Department of Energy, Office of Civilian Radioactive Waste Management. ACC: DOC.20030827.0013.

2. AP-SI.1Q, Rev. 5, ICN 2. *Software Management*. Washington, D.C.: U.S. Department of Energy, Office of Civilian Radioactive Waste Management. ACC: DOC.20030902.0003.

3. BSC (Bechtel SAIC Company) 2004. *D&E / PA/C IED Typical Waste Package Components Assembly*. 800-IED-WIS0-00201-000-00D. Las Vegas, Nevada: Bechtel SAIC Company. ACC: ENG.20040202.0009.

4. DOE (U.S. Department of Energy) 2003. *Quality Assurance Requirements and Description*. DOE/RW-0333P, Rev. 13. Washington, D.C.: U.S. Department of Energy, Office of Civilian Radioactive Waste Management. ACC: DOC.20030422.0003.

5. BSC (Bechtel SAIC Company) 2003. *Q-List*. TDR-MGR-RL-000005 REV 00. Las Vegas, Nevada: Bechtel SAIC Company. ACC: DOC.20030930.0002.

6. BSC (Bechtel SAIC Company) 2002. *Software Code: ANSYS*. V5.6.2. HP-UX 11.00. 10364-5.6.2-01.

7. BSC (Bechtel SAIC Company) 2002. *Software Code: LS-DYNA*. V960.1106. HP9000. 10300-960.1106-00.

8. Mecham, D.C. 2004. *Waste Package Component Design Methodology Report*. 000-30R-WIS0-00100-000-000. Las Vegas, Nevada: Bechtel SAIC Company. ACC: ENG.20040113.0001.

9. MO0003RIB00071.000. Physical and Chemical Characteristics of Alloy 22. Submittal date: 03/13/2000.

10. ASM (American Society for Metals) 1980. *Properties and Selection: Stainless Steels, Tool Materials and Special-Purpose Metals*. Volume 3 of *Metals Handbook*. 9th Edition. Benjamin, D., ed. Metals Park, Ohio: American Society for Metals. TIC: 209801.

11. ASTM G 1-90 (Reapproved 1999). 1999. *Standard Practice for Preparing, Cleaning, and Evaluating Corrosion Test Specimens*. West Conshohocken, Pennsylvania: American Society for Testing and Materials. TIC: 238771.

12. ASME (American Society of Mechanical Engineers) 2001. *2001 ASME Boiler and Pressure Vessel Code (includes 2002 addenda)*. New York, New York: American Society of Mechanical Engineers. TIC: 251425.

13. Dieter, G.E. 1976. *Mechanical Metallurgy.* 2nd Edition. Materials Science and Engineering Series. New York, New York: McGraw-Hill Book Company. TIC: 247879.

14. Allegheny Ludlum. 1999. "Technical Data Blue Sheet, Stainless Steels, Chromium-Nickel-Molybdenum, Types 316 (S31600), 316L (S31603), 317 (S31700), 317L (S31703)." Pittsburgh, Pennsylvania: Allegheny Ludlum Corporation. Accessed July 31, 2000. TIC: 248631. http://www.alleghenytechnologies.com/ludlum/ pages/products/t316_317.pdf

15. LL020603612251.015. Slow Strain Rate Test Generated Stress Corrosion Cracking Data. Submittal date: 08/27/2002.

16. Boyer, H.E., ed. 2000. *Atlas of Stress-Strain Curves.* Metals Park, Ohio: ASM International. TIC: 248901.

17. Hallquist, J.O. 1998. *LS-DYNA, Theoretical Manual.* Livermore, California: Livermore Software Technology Corporation. TIC: 238997.

18. Livermore Software Technology Corporation. 2001. *LS-DYNA Keyword User's Manual.* Version 960. Two volumes. Livermore, California: Livermore Software Technology Corporation. TIC: 252119.

19. MO0003RIB00073.000. Physical and Chemical Characteristics of TI Grades 7 and 16. Submittal date: 03/13/2000.

20. Hill, R. 1998. *The Mathematical Theory of Plasticity.* New York, New York: Oxford University Press. TIC: 240262.

21. BSC (Bechtel SAIC Company) 2001. *Repository Multiple Waste Package Thermal Calculation.* CAL-WIS-TH-000010 REV 00. Las Vegas, Nevada: Bechtel SAIC Company. ACC: MOL.20010814.0330.

22. BSC (Bechtel SAIC Company) 2003. *Emplacement Pallet.* 000-MW0-TEP0-00101-000-00A, and -00102-000-00A. 2 Sheets. Las Vegas, Nevada: Bechtel SAIC Company. ACC: ENG.20030205.0007; ENG.20030205.0008.

23. MO9808RIB00041.000. Reference Information Base Data Item: Rock Geomechanical Properties. Submittal date: 08/05/1998.

24. BSC (Bechtel SAIC Company) 2001. *Repository Design, Waste Package, Project 21-PWR Waste Package with Absorber Plates, Sheet 1 of 3, Sheet 2 of 3, and Sheet 3 of 3.* DWG-UDC-ME-000001 REV A. Las Vegas, Nevada: Bechtel SAIC Company. ACC: MOL.20020102.0174.

25. Plinski, M.J. 2001. *Waste Package Operations Fabrication Process Report.* TDR-EBS-ND-000003 REV 02. Las Vegas, Nevada: Bechtel SAIC Company. ACC: MOL.20011003.0025.

26. Avallone, E.A. and Baumeister, T., III, eds. 1987. *Marks' Standard Handbook for Mechanical Engineers.* 9th Edition. New York, New York: McGraw-Hill. TIC: 206891.

27. BSC (Bechtel SAIC Company) 2003. *21-PWR Waste Package Side and End Impacts.* 000-00C-DSU0-01000-000-00B. Las Vegas, Nevada: Bechtel SAIC Company. ACC: ENG.20030227.0067.

28. MO0003RIB00079.000. Rock Mechanical Properties. Submittal date: 03/30/2000.

29. MO0301TMHIS106.001. Acceleration, Velocity, and Displacement Time Histories for the Repository Level at 10-6 Annual Exceedance Frequency.. Submittal date: 01/28/2003.

30. MO0211AVTMH107.001. Acceleration, Velocity, and Displacement Spectrally Conditioned Time Histories for the Repository Level at 10-7 Annual Exceedance Frequency. Submittal date: 11/12/2002.

31. MO0211TMHIS104.002. Acceleration, Velocity, and Displacement Time Histories for the Repository Level at 5X10-4 Annual Exceedance Frequency. Submittal date: 11/14/2002.

32. DeGrassi, G. 1992. *Review of the Technical Basis and Verification of Current Analysis Methods Used to Predict Seismic Response of Spent Nuclear Fuel Racks.* NUREG/CR-5912. Washington, DC: U.S. Nuclear Regulatory Commission. TIC: 253724.

33. Williams, N.H. 2002. "Thermal Inputs for Evaluations Supporting TSPA-LA." Interoffice memorandum from N.H. Williams (BSC) to Distribution, September 16, 2002, 0911024159, with enclosures. ACC: MOL.20021008.0141.

34. CRWMS M&O 1997. *Waste Container Cavity Size Determination.* BBAA00000-01717-0200-00026 REV 00. Las Vegas, Nevada: CRWMS M&O. ACC: MOL.19980106.0061.

35. MO0301SPASIP27.004. Sampling of Stochastic Input Parameters for Rockfall Calculations and for Structural Response Calculations Under Vibratory Ground Motions.. Submittal date: 01/15/2003.

36. MO0303SPARESST.000. Residual Stress Failure Criteria for Seismic Damage Models of the Drip Shield and Waste Package. Submittal date: 03/04/2003.

37. MO0305SPASFEGM.000. Scaling Factor for Estimating the 10-5 Per Year Ground Motions at the Emplacement Drifts. Submittal date: 05/07/2003.

38. MO0306SDSAVDTH.000. Seismic Design Spectra and Acceleration, Velocity, and Displacement Time Histories for the Emplacement Level at 10-4 Annual Exceedance Frequency. Submittal date: 06/26/2003.

39. BSC (Bechtel SAIC Company) 2003. *Software Code: LS-DYNA.* V970.3858 D SMP. HP Itanium2 (IA64), HP-UX 11.22. 10300-970.3858 D SMP-00.

40. BSC (Bechtel SAIC Company) 2003. *WAPDEG Analysis of Waste Package and Drip Shield Degradation.* ANL-EBS-PA-000001 REV 01. Las Vegas, Nevada: Bechtel SAIC Company. ACC: DOC.20031208.0004.

8. ATTACHMENTS

Attachment I (2 pages):	Design sketch (*21-PWR Waste Package Configuration for Site Recommendation* [SK-0175 REV 02, 2 sheets]) (Includes Reference 34)
Attachment II (13 pages):	Design sketch (*Emplacement Pallet Long* [SK-0232 REV 00, 13 sheets])
Attachment III (24 pages):	Design sketch (*Interlocking Drip Shield* [SK-0230 REV 00, 24 sheets])
Attachment IV (28 pages):	Stress Plots
Attachment V (4 pages):	Effect of Ambient Temperature on Results
Attachment VI (8 pages):	Effect of Rigid Elements in Representation of Outer Shell on Results
Attachment VII (5 pages):	Effect of Acceleration Time History Cutoff on Results
Attachment VIII (4 pages):	Effect of Constrained Drip Shield on Results
Attachment IX (15 pages):	Mesh Objectivity
Attachment X (3 Compact Discs):	ANSYS V5.6.2, LS-DYNA V960.1106 and LS-DYNA V970.3858 electronic files
Attachment XI (4 pages):	Events at Annual Frequency of Occurrence of $1 \cdot 10^{-5}$ $1/yr$

Table 8-1 provides a list of files submitted on compact discs as Attachment X.

Table 8-1. List of Electronic Files in Attachment X

CONTENT OF CD1

File name	Size (kB)	Date	Time
1E-6\Constrained DS			
acc10h1.dat	25	2/10/2003	10:59am
acc10h2.dat	24	2/10/2003	10:59am
acc10v.dat	24	2/10/2003	10:59am
constraint.dat	4	2/10/2003	10:59am
d3hsp	8833	2/10/2003	10:59am
d3hsp1	41	2/10/2003	10:59am
d3hsp2	120	2/10/2003	10:59am
d3hsp3	69	2/10/2003	10:59am
d3plot	14450	3/13/2003	08:36am

d3plot177	6009	3/13/2003	08:36am
element.inc	1563	2/10/2003	10:59am
messag	16	2/11/2003	08:42am
nodes.inc	1662	2/10/2003	11:00am
nodese10.inc	21	2/10/2003	11:00am
nodese11.inc	4	2/10/2003	11:00am
nodese12.inc	21	2/10/2003	11:00am
nodese13.inc	4	2/10/2003	11:00am
nodeset.inc	5	2/10/2003	11:00am
nodeset3.inc	15	2/10/2003	11:00am
nodeset4.inc	3	2/10/2003	11:00am
nodeset5.inc	1	2/10/2003	11:00am
relaxWPP.k	1	2/10/2003	11:00am
segmen20.inc	4	2/10/2003	11:00am
segmen21.inc	2	2/10/2003	11:00am
segmen25.inc	7	2/10/2003	11:00am
segmen26.inc	6	2/10/2003	11:00am
segmen27.inc	30	2/10/2003	11:00am
segmen28.inc	6	2/10/2003	11:00am
seisWPPcDS.k	12	2/10/2003	11:00am
seisWPPcDS1.k	12	2/10/2003	11:00am
1E-6\Constrained DS\FER			
wpp6CDS.inp	36	2/10/2003	11:49am
wpp6CDS.out	369	2/10/2003	11:49am
1E-6\Deformable OS\RN15			
acc3h1.dat	69	2/10/2003	09:50am
acc3h2.dat	71	2/10/2003	09:50am
acc3v.dat	70	2/10/2003	09:50am
constraint.dat	7	2/10/2003	09:50am
d3hsp	9662	2/10/2003	09:50am
d3hsp1	83	2/10/2003	09:50am
d3hsp2	81	2/10/2003	09:50am
d3plot	8667	3/13/2003	09:31am
d3plot81	6214	3/13/2003	09:31am
element.inc	1577	2/10/2003	09:50am
messag	11	2/11/2003	08:48am
nodes.inc	1677	2/10/2003	09:51am
nodese10.inc	21	2/10/2003	09:51am
nodese11.inc	4	2/10/2003	09:51am
nodese12.inc	21	2/10/2003	09:51am
nodese13.inc	4	2/10/2003	09:51am
nodeset.inc	8	2/10/2003	09:51am
nodeset3.inc	15	2/10/2003	09:51am
nodeset4.inc	3	2/10/2003	09:51am
nodeset5.inc	1	2/10/2003	09:51am
relaxWPP.k	1	2/10/2003	11:11am
segmen20.inc	4	2/10/2003	09:51am
segmen21.inc	2	2/10/2003	09:50am
segmen25.inc	7	2/10/2003	09:50am
segmen26.inc	6	2/10/2003	09:50am

segmen27.inc	30	2/10/2003	09:50am
segmen28.inc	6	2/10/2003	09:50am
seisWPcE.k	12	2/10/2003	11:11am
1E-6\Deformable OS\RN4			
acc8h1.dat	106	2/10/2003	09:27am
acc8h2.dat	107	2/10/2003	09:27am
acc8v.dat	105	2/10/2003	09:27am
constraint.dat	7	2/10/2003	09:27am
d3hsp	9857	2/10/2003	09:27am
d3hsp1	51	2/10/2003	09:27am
d3hsp2	51	2/10/2003	09:27am
d3hsp3	88	2/10/2003	09:27am
d3plot	8667	3/13/2003	08:34am
d3plot126	6214	3/13/2003	08:34am
element.inc	1577	2/10/2003	11:12am
messag	17	2/11/2003	08:41am
nodes.inc	1677	2/10/2003	09:26am
nodese10.inc	21	2/10/2003	09:26am
nodese11.inc	4	2/10/2003	09:26am
nodese12.inc	21	2/10/2003	09:26am
nodese13.inc	4	2/10/2003	09:26am
nodeset.inc	8	2/10/2003	09:26am
nodeset3.inc	15	2/10/2003	09:26am
nodeset4.inc	3	2/10/2003	09:26am
nodeset5.inc	1	2/10/2003	09:26am
relaxWPP.k	1	2/10/2003	09:26am
segmen20.inc	4	2/10/2003	09:26am
segmen21.inc	2	2/10/2003	09:26am
segmen25.inc	7	2/10/2003	09:26am
segmen26.inc	6	2/10/2003	09:26am
segmen27.inc	30	2/10/2003	09:26am
segmen28.inc	6	2/10/2003	09:26am
seisWPcE.k	12	2/10/2003	09:26am
1E-6\Deformable OS\RN5			
acc11h1.dat	140	2/10/2003	10:04am
acc11h2.dat	139	2/10/2003	10:04am
acc11v.dat	139	2/10/2003	10:04am
constraint.dat	7	2/10/2003	10:04am
d3hsp	9980	2/10/2003	10:04am
d3hsp1	129	2/10/2003	10:04am
d3hsp2	87	2/10/2003	10:04am
d3plot	8667	3/13/2003	09:35am
d3plot175	6214	3/13/2003	09:35am
element.inc	1577	2/10/2003	10:04am
messag	17	2/11/2003	08:51am
nodes.inc	1677	2/10/2003	10:05am
nodese10.inc	21	2/10/2003	10:05am
nodese11.inc	4	2/10/2003	10:05am
nodese12.inc	21	2/10/2003	10:05am
nodese13.inc	4	2/10/2003	10:05am

nodeset.inc	8	2/10/2003	10:05am
nodeset3.inc	15	2/10/2003	10:05am
nodeset4.inc	3	2/10/2003	10:05am
nodeset5.inc	1	2/10/2003	10:05am
relaxWPP.k	1	2/10/2003	10:05am
segmen20.inc	4	2/10/2003	10:05am
segmen21.inc	2	2/10/2003	10:05am
segmen25.inc	7	2/10/2003	10:05am
segmen26.inc	6	2/10/2003	10:05am
segmen27.inc	30	2/10/2003	10:05am
segmen28.inc	6	2/10/2003	10:05am
seisWPPc.k	12	2/10/2003	10:05am
1E-6\Elevated Temp			
acc10h1.dat	25	2/10/2003	10:46am
acc10h2.dat	24	2/10/2003	10:46am
acc10v.dat	24	2/10/2003	10:46am
constraint.dat	7	2/10/2003	10:46am
d3hsp	9437	2/10/2003	10:46am
d3hsp1	135	2/10/2003	10:46am
d3hsp2	88	2/10/2003	10:46am
d3plot	8667	3/13/2003	10:05am
d3plot178	6214	3/13/2003	10:05am
element.inc	1577	2/10/2003	10:47am
messag	17	2/11/2003	09:00am
nodes.inc	1677	2/10/2003	10:47am
nodese10.inc	21	2/10/2003	10:47am
nodese11.inc	4	2/10/2003	10:47am
nodese12.inc	21	2/10/2003	10:47am
nodese13.inc	4	2/10/2003	10:47am
nodeset.inc	8	2/10/2003	10:47am
nodeset3.inc	15	2/10/2003	10:47am
nodeset4.inc	3	2/10/2003	10:47am
nodeset5.inc	1	2/10/2003	10:47am
relaxWPP.k	1	2/10/2003	10:47am
segmen20.inc	4	2/10/2003	10:47am
segmen21.inc	2	2/10/2003	10:47am
segmen25.inc	7	2/10/2003	10:47am
segmen26.inc	6	2/10/2003	10:47am
segmen27.inc	30	2/10/2003	10:47am
segmen28.inc	6	2/10/2003	10:47am
seisWPPc.k	12	2/10/2003	10:47am
1E-6\RN1			
acc7h1.dat	43	2/10/2003	10:39am
acc7h2.dat	43	2/10/2003	10:39am
acc7v.dat	42	2/10/2003	10:39am
constraint.dat	7	2/10/2003	10:39am
d3hsp	9573	2/10/2003	10:39am
d3hsp1	48	2/10/2003	10:39am
d3hsp2	85	2/10/2003	10:39am
d3hsp3	88	2/10/2003	10:39am

d3plot	8667	3/13/2003	09:57am
d3plot190	6214	3/13/2003	09:57am
element.inc	1577	2/10/2003	10:40am
glstat	353	2/11/2003	08:59am
messag	17	2/11/2003	08:58am
messag_1	21	2/11/2003	08:58am
nodes.inc	1677	2/10/2003	10:40am
nodese10.inc	21	2/10/2003	10:40am
nodese11.inc	4	2/10/2003	10:40am
nodese12.inc	21	2/10/2003	10:40am
nodese13.inc	4	2/10/2003	10:40am
nodeset.inc	8	2/10/2003	10:40am
nodeset3.inc	15	2/10/2003	10:40am
nodeset4.inc	3	2/10/2003	10:40am
nodeset5.inc	1	2/10/2003	10:40am
rcforc	1568	2/11/2003	08:58am
relaxWPP.k	1	2/10/2003	10:40am
segmen20.inc	4	2/10/2003	10:40am
segmen21.inc	2	2/10/2003	10:40am
segmen25.inc	7	2/10/2003	10:40am
segmen26.inc	6	2/10/2003	10:40am
segmen27.inc	30	2/10/2003	10:40am
segmen28.inc	6	2/10/2003	10:40am
seisWPPc.k	12	2/10/2003	10:40am
1E-6\RN10			
acc9h1A.dat	97	2/10/2003	09:58am
acc9h2A.dat	98	2/10/2003	09:58am
acc9vA.dat	108	2/10/2003	09:58am
constraint.dat	7	2/10/2003	09:58am
d3hsp	9885	2/10/2003	09:58am
d3hsp1	74	2/10/2003	09:58am
d3hsp2	87	2/10/2003	09:58am
d3plot	8667	3/13/2003	09:34am
d3plot157	6214	3/13/2003	09:34am
element.inc	1577	2/10/2003	09:59am
messag	17	2/11/2003	08:50am
nodes.inc	1677	2/10/2003	09:59am
nodese10.inc	21	2/10/2003	09:59am
nodese11.inc	4	2/10/2003	09:59am
nodese12.inc	21	2/10/2003	09:59am
nodese13.inc	4	2/10/2003	09:59am
nodeset.inc	8	2/10/2003	09:59am
nodeset3.inc	15	2/10/2003	09:59am
nodeset4.inc	3	2/10/2003	09:59am
nodeset5.inc	1	2/10/2003	09:59am
relaxWPP.k	1	2/10/2003	09:59am
segmen20.inc	4	2/10/2003	09:59am
segmen21.inc	2	2/10/2003	09:59am
segmen25.inc	7	2/10/2003	09:59am
segmen26.inc	6	2/10/2003	09:59am

segmen27.inc	30	2/10/2003	09:59am
segmen28.inc	6	2/10/2003	09:59am
seisWPPc.k	12	2/10/2003	09:59am
1E-6\RN11			
acc5h1.dat	50	2/10/2003	09:37am
acc5h2.dat	50	2/10/2003	09:37am
acc5v.dat	49	2/10/2003	09:37am
constraint.dat	7	2/10/2003	09:37am
d3hsp	9666	2/10/2003	09:37am
d3hsp1	88	2/10/2003	09:37am
d3plot	8667	3/13/2003	09:30am
d3plot177	6214	3/13/2003	09:30am
element.inc	1577	2/10/2003	09:48am
messag	17	2/11/2003	08:45am
nodes.inc	1677	2/10/2003	09:48am
nodese10.inc	21	2/10/2003	09:48am
nodese11.inc	4	2/10/2003	09:48am
nodese12.inc	21	2/10/2003	09:48am
nodese13.inc	4	2/10/2003	09:48am
nodeset.inc	8	2/10/2003	09:48am
nodeset3.inc	15	2/10/2003	09:48am
nodeset4.inc	3	2/10/2003	09:48am
nodeset5.inc	1	2/10/2003	09:48am
relaxWPP.k	1	2/10/2003	09:37am
segmen20.inc	4	2/10/2003	09:48am
segmen21.inc	2	2/10/2003	09:48am
segmen25.inc	7	2/10/2003	09:48am
segmen26.inc	6	2/10/2003	09:48am
segmen27.inc	30	2/10/2003	09:48am
segmen28.inc	6	2/10/2003	09:48am
seisWPPc.k	12	2/10/2003	09:37am
1E-6\RN12\Long Run			
acc6h1.dat	71	2/10/2003	10:38am
acc6h2.dat	70	2/10/2003	10:38am
acc6v.dat	71	2/10/2003	10:38am
constraint.dat	7	2/10/2003	10:38am
d3hsp	9733	2/10/2003	10:38am
d3hsp1	74	2/10/2003	10:38am
d3hsp2	87	2/10/2003	10:38am
d3plot	8667	3/13/2003	09:56am
d3plot189	6214	3/13/2003	09:56am
element.inc	1577	2/10/2003	10:39am
messag	16	2/11/2003	08:58am
messag_1	141	2/11/2003	08:58am
nodes.inc	1677	2/10/2003	10:39am
nodese10.inc	21	2/10/2003	10:39am
nodese11.inc	4	2/10/2003	10:39am
nodese12.inc	21	2/10/2003	10:39am
nodese13.inc	4	2/10/2003	10:39am
nodeset.inc	8	2/10/2003	10:39am

nodeset3.inc	15	2/10/2003	10:39am
nodeset4.inc	3	2/10/2003	10:39am
nodeset5.inc	1	2/10/2003	10:39am
relaxWPP.k	1	2/10/2003	10:39am
segmen20.inc	4	2/10/2003	10:39am
segmen21.inc	2	2/10/2003	10:39am
segmen25.inc	7	2/10/2003	10:39am
segmen26.inc	6	2/10/2003	10:39am
segmen27.inc	30	2/10/2003	10:39am
segmen28.inc	6	2/10/2003	10:39am
seisWPPc.k	12	2/10/2003	10:39am
1E-6\RN12\Short Run			
acc6h1.dat	71	2/10/2003	10:37am
acc6h2.dat	70	2/10/2003	10:37am
acc6v.dat	71	2/10/2003	10:37am
constraint.dat	7	2/10/2003	10:37am
d3hsp	9733	2/10/2003	10:37am
d3hsp1	87	2/10/2003	10:37am
d3plot	8667	3/13/2003	09:56am
d3plot149	6214	3/13/2003	09:56am
element.inc	1577	2/10/2003	10:37am
messag	16	2/11/2003	08:58am
messag_1	141	2/11/2003	08:58am
nodes.inc	1677	2/10/2003	10:38am
nodese10.inc	21	2/10/2003	10:38am
nodese11.inc	4	2/10/2003	10:38am
nodese12.inc	21	2/10/2003	10:38am
nodese13.inc	4	2/10/2003	10:38am
nodeset.inc	8	2/10/2003	10:38am
nodeset3.inc	15	2/10/2003	10:38am
nodeset4.inc	3	2/10/2003	10:38am
nodeset5.inc	1	2/10/2003	10:38am
relaxWPP.k	1	2/10/2003	10:38am
segmen20.inc	4	2/10/2003	10:38am
segmen21.inc	2	2/10/2003	10:38am
segmen25.inc	7	2/10/2003	10:38am
segmen26.inc	6	2/10/2003	10:38am
segmen27.inc	30	2/10/2003	10:38am
segmen28.inc	6	2/10/2003	10:38am
seisWPPc.k	12	2/10/2003	10:38am
1E-6\RN13			
acc12h1.dat	34	2/10/2003	10:23am
acc12h2.dat	34	2/10/2003	10:23am
acc12v.dat	34	2/10/2003	10:23am
constraint.dat	7	2/10/2003	10:23am
d3hsp	9649	2/10/2003	10:23am
d3hsp1	88	2/10/2003	10:23am
d3plot	8667	3/13/2003	09:46am
d3plot241	6214	3/13/2003	09:46am
element.inc	1577	2/10/2003	10:24am

messag	17	2/11/2003	08:55am
nodes.inc	1677	2/10/2003	10:24am
nodese10.inc	21	2/10/2003	10:24am
nodese11.inc	4	2/10/2003	10:24am
nodese12.inc	21	2/10/2003	10:24am
nodese13.inc	4	2/10/2003	10:24am
nodeset.inc	8	2/10/2003	10:24am
nodeset3.inc	15	2/10/2003	10:24am
nodeset4.inc	3	2/10/2003	10:24am
nodeset5.inc	1	2/10/2003	10:24am
relaxWPP.k	1	2/10/2003	10:24am
segmen20.inc	4	2/10/2003	10:24am
segmen21.inc	2	2/10/2003	10:24am
segmen25.inc	7	2/10/2003	10:24am
segmen26.inc	6	2/10/2003	10:24am
segmen27.inc	30	2/10/2003	10:24am
segmen28.inc	6	2/10/2003	10:24am
seisWPPc.k	12	2/10/2003	10:24am
1E-6\RN14			
acc14h1.dat	150	2/10/2003	10:24am
acc14h2.dat	147	2/10/2003	10:24am
acc14v.dat	148	2/10/2003	10:24am
constraint.dat	7	2/10/2003	10:24am
d3hsp	10209	2/10/2003	10:24am
d3hsp1	88	2/10/2003	10:24am
d3plot	8667	3/13/2003	09:46am
d3plot229	6214	3/13/2003	09:46am
element.inc	1577	2/10/2003	10:25am
messag	17	2/11/2003	08:55am
messag_1	222	2/11/2003	08:55am
nodes.inc	1677	2/10/2003	10:25am
nodese10.inc	21	2/10/2003	10:25am
nodese11.inc	4	2/10/2003	10:25am
nodese12.inc	21	2/10/2003	10:25am
nodese13.inc	4	2/10/2003	10:25am
nodeset.inc	8	2/10/2003	10:25am
nodeset3.inc	15	2/10/2003	10:25am
nodeset4.inc	3	2/10/2003	10:25am
nodeset5.inc	1	2/10/2003	10:25am
relaxWPP.k	1	2/10/2003	10:25am
segmen20.inc	4	2/10/2003	10:25am
segmen21.inc	2	2/10/2003	10:25am
segmen25.inc	7	2/10/2003	10:25am
segmen26.inc	6	2/10/2003	10:25am
segmen27.inc	30	2/10/2003	10:25am
segmen28.inc	6	2/10/2003	10:25am
seisWPPc.k	12	2/10/2003	10:25am
1E-6\RN15			
acc3h1.dat	69	2/10/2003	09:52am
acc3h2.dat	71	2/10/2003	09:52am

acc3v.dat	70	2/10/2003	09:52am
constraint.dat	7	2/10/2003	09:52am
d3hsp	9660	2/10/2003	09:52am
d3hsp1	83	2/10/2003	09:52am
d3hsp2	81	2/10/2003	09:52am
d3plot	8667	3/13/2003	09:30am
d3plot81	6214	3/13/2003	09:30am
element.inc	1577	2/10/2003	09:52am
messag	11	2/11/2003	08:45am
nodes.inc	1677	2/10/2003	09:52am
nodese10.inc	21	2/10/2003	09:52am
nodese11.inc	4	2/10/2003	09:52am
nodese12.inc	21	2/10/2003	09:52am
nodese13.inc	4	2/10/2003	09:52am
nodeset.inc	8	2/10/2003	09:52am
nodeset3.inc	15	2/10/2003	09:52am
nodeset4.inc	3	2/10/2003	09:52am
nodeset5.inc	1	2/10/2003	09:52am
relaxWPP.k	1	2/10/2003	09:52am
segmen20.inc	4	2/10/2003	09:52am
segmen21.inc	2	2/10/2003	09:52am
segmen25.inc	7	2/10/2003	09:52am
segmen26.inc	6	2/10/2003	09:52am
segmen27.inc	30	2/10/2003	09:52am
segmen28.inc	6	2/10/2003	09:52am
seisWPPc.k	12	2/10/2003	09:52am
1E-6\RN2\Long Run			
acc16h1.dat	50	2/10/2003	10:42am
acc16h2.dat	50	2/10/2003	10:42am
acc16v.dat	50	2/10/2003	10:42am
constraint.dat	7	2/10/2003	10:42am
d3hsp	9590	2/10/2003	10:42am
d3hsp1	42	2/10/2003	10:42am
d3hsp2	60	2/10/2003	10:42am
d3hsp3	54	2/10/2003	10:42am
d3hsp4	54	2/10/2003	10:42am
d3hsp5	87	2/10/2003	10:42am
d3plot	8667	3/13/2003	09:58am
d3plot192	6214	3/13/2003	09:58am
element.inc	1577	2/10/2003	10:42am
messag	16	2/11/2003	08:59am
messag_1	101	2/11/2003	08:59am
nodes.inc	1677	2/10/2003	10:43am
nodese10.inc	21	2/10/2003	10:43am
nodese11.inc	4	2/10/2003	10:43am
nodese12.inc	21	2/10/2003	10:43am
nodese13.inc	4	2/10/2003	10:43am
nodeset.inc	8	2/10/2003	10:43am
nodeset3.inc	15	2/10/2003	10:43am
nodeset4.inc	3	2/10/2003	10:43am

nodeset5.inc	1	2/10/2003	10:43am
relaxWPP.k	1	2/10/2003	10:43am
segmen20.inc	4	2/10/2003	10:43am
segmen21.inc	2	2/10/2003	10:43am
segmen25.inc	7	2/10/2003	10:43am
segmen26.inc	6	2/10/2003	10:43am
segmen27.inc	30	2/10/2003	10:43am
segmen28.inc	6	2/10/2003	10:43am
seisWPPc.k	12	2/10/2003	10:43am
1E-6\RN2\Short Run			
acc16h1.dat	50	2/10/2003	10:41am
acc16h2.dat	50	2/10/2003	10:41am
acc16v.dat	50	2/10/2003	10:41am
constraint.dat	7	2/10/2003	10:41am
d3hsp	9590	2/10/2003	10:41am
d3hsp1	42	2/10/2003	10:41am
d3hsp2	60	2/10/2003	10:41am
d3hsp3	54	2/10/2003	10:41am
d3hsp4	87	2/10/2003	10:41am
d3plot	8667	3/13/2003	09:58am
d3plot172	6214	3/13/2003	09:58am
element.inc	1577	2/10/2003	10:41am
messag	16	2/11/2003	08:59am
messag_1	101	2/11/2003	08:59am
nodes.inc	1677	2/10/2003	10:42am
nodese10.inc	21	2/10/2003	10:42am
nodese11.inc	4	2/10/2003	10:42am
nodese12.inc	21	2/10/2003	10:42am
nodese13.inc	4	2/10/2003	10:42am
nodeset.inc	8	2/10/2003	10:42am
nodeset3.inc	15	2/10/2003	10:42am
nodeset4.inc	3	2/10/2003	10:42am
nodeset5.inc	1	2/10/2003	10:42am
relaxWPP.k	1	2/10/2003	10:42am
segmen20.inc	4	2/10/2003	10:42am
segmen21.inc	2	2/10/2003	10:42am
segmen25.inc	7	2/10/2003	10:42am
segmen26.inc	6	2/10/2003	10:42am
segmen27.inc	30	2/10/2003	10:42am
segmen28.inc	6	2/10/2003	10:42am
seisWPPc.k	12	2/10/2003	10:42am
1E-6\RN3			
acc4h1.dat	40	2/10/2003	09:59am
acc4h2.dat	40	2/10/2003	09:59am
acc4v.dat	40	2/10/2003	09:59am
constraint.dat	7	2/10/2003	09:59am
d3hsp	9727	2/10/2003	09:59am
d3hsp1	88	2/10/2003	09:59am
d3plot	8667	3/13/2003	09:34am
d3plot267	6214	3/13/2003	09:34am

element.inc	1577	2/10/2003	10:00am
messag	17	2/11/2003	08:51am
nodes.inc	1677	2/10/2003	10:00am
nodese10.inc	21	2/10/2003	10:00am
nodese11.inc	4	2/10/2003	10:00am
nodese12.inc	21	2/10/2003	10:00am
nodese13.inc	4	2/10/2003	10:00am
nodeset.inc	8	2/10/2003	10:00am
nodeset3.inc	15	2/10/2003	10:00am
nodeset4.inc	3	2/10/2003	10:00am
nodeset5.inc	1	2/10/2003	10:00am
relaxWPP.k	1	2/10/2003	10:00am
segmen20.inc	4	2/10/2003	10:00am
segmen21.inc	2	2/10/2003	10:00am
segmen25.inc	7	2/10/2003	10:00am
segmen26.inc	6	2/10/2003	10:00am
segmen27.inc	30	2/10/2003	10:00am
segmen28.inc	6	2/10/2003	10:00am
seisWPPc.k	12	2/10/2003	10:00am
1E-6\RN4			
acc8h1.dat	106	2/10/2003	09:23am
acc8h2.dat	107	2/10/2003	09:23am
acc8v.dat	105	2/10/2003	09:23am
constraint.dat	7	2/10/2003	09:23am
d3hsp	9853	2/10/2003	09:23am
d3hsp1	51	2/10/2003	09:23am
d3hsp2	51	2/10/2003	09:23am
d3hsp3	87	2/10/2003	09:23am
d3plot	8667	3/13/2003	08:35am
d3plot125	6214	3/13/2003	08:35am
element.inc	1577	2/10/2003	09:23am
messag	17	2/11/2003	08:42am
nodese10.inc	21	2/10/2003	09:23am
nodese11.inc	4	2/10/2003	09:23am
nodese12.inc	21	2/10/2003	09:23am
nodese13.inc	4	2/10/2003	09:23am
nodeset.inc	8	2/10/2003	09:23am
nodeset3.inc	15	2/10/2003	09:23am
nodeset4.inc	3	2/10/2003	09:23am
nodeset5.inc	1	2/10/2003	09:23am
relaxWPP.k	1	2/10/2003	09:23am
segmen20.inc	4	2/10/2003	09:23am
segmen21.inc	2	2/10/2003	09:23am
segmen25.inc	7	2/10/2003	09:23am
segmen26.inc	6	2/10/2003	09:23am
segmen27.inc	30	2/10/2003	09:23am
segmen28.inc	6	2/10/2003	09:23am
seisWPPc.k	12	2/10/2003	09:23am
1E-6\RN5			
acc11h1.dat	140	2/10/2003	10:45am

acc11h2.dat	139	2/10/2003	10:45am
acc11v.dat	139	2/10/2003	10:45am
constraint.dat	7	2/10/2003	10:45am
d3hsp	10095	2/10/2003	10:45am
d3hsp1	41	2/10/2003	10:45am
d3hsp2	41	2/10/2003	10:45am
d3hsp3	88	2/10/2003	10:45am
d3plot	8667	3/13/2003	10:04am
d3plot175	6214	3/13/2003	10:04am
element.inc	1577	2/10/2003	10:45am
messag	17	2/11/2003	09:00am
nodes.inc	1677	2/10/2003	10:46am
nodese10.inc	21	2/10/2003	10:46am
nodese11.inc	4	2/10/2003	10:46am
nodese12.inc	21	2/10/2003	10:46am
nodese13.inc	4	2/10/2003	10:46am
nodeset.inc	8	2/10/2003	10:46am
nodeset3.inc	15	2/10/2003	10:46am
nodeset4.inc	3	2/10/2003	10:46am
nodeset5.inc	1	2/10/2003	10:46am
relaxWPP.k	1	2/10/2003	10:46am
segmen20.inc	4	2/10/2003	10:46am
segmen21.inc	2	2/10/2003	10:46am
segmen25.inc	7	2/10/2003	10:46am
segmen26.inc	6	2/10/2003	10:46am
segmen27.inc	30	2/10/2003	10:46am
segmen28.inc	6	2/10/2003	10:46am
seisWPPc.k	12	2/10/2003	10:46am
1E-6\RN6			
acc1h1.dat	70	2/10/2003	10:28am
acc1h2.dat	70	2/10/2003	10:28am
acc1v.dat	65	2/10/2003	10:28am
constraint.dat	7	2/10/2003	10:28am
d3hsp	15092	2/10/2003	10:28am
d3hsp1	75	2/10/2003	10:28am
d3hsp2	89	2/10/2003	10:28am
d3plot	13464	3/13/2003	09:48am
d3plot269	9019	3/13/2003	09:48am
element.inc	2906	2/10/2003	10:29am
messag	18	2/11/2003	08:56am
messag_1	99	2/11/2003	08:56am
nodes.inc	2932	2/10/2003	10:29am
nodese10.inc	55	2/10/2003	10:29am
nodese11.inc	10	2/10/2003	10:29am
nodese12.inc	55	2/10/2003	10:29am
nodese13.inc	10	2/10/2003	10:29am
nodeset.inc	8	2/10/2003	10:29am
nodeset3.inc	20	2/10/2003	10:29am
nodeset4.inc	4	2/10/2003	10:29am
nodeset5.inc	1	2/10/2003	10:29am

relaxWPP.k	1	2/10/2003	10:29am
segmen20.inc	4	2/10/2003	10:29am
segmen21.inc	2	2/10/2003	10:29am
segmen25.inc	26	2/10/2003	10:29am
segmen26.inc	6	2/10/2003	10:29am
segmen27.inc	26	2/10/2003	10:29am
segmen28.inc	6	2/10/2003	10:29am
segmen35.inc	7	2/10/2003	10:29am
segmen36.inc	6	2/10/2003	10:29am
segmen37.inc	7	2/10/2003	10:29am
segmen38.inc	6	2/10/2003	10:29am
seisWPPc.k	13	2/10/2003	10:29am
wpp7C.inp	38	2/11/2003	08:56am
1E-6\RN7			
acc2h1.dat	91	2/10/2003	10:05am
acc2h2.dat	92	2/10/2003	10:05am
acc2v.dat	91	2/10/2003	10:05am
constraint.dat	7	2/10/2003	10:05am
d3hsp	9822	2/10/2003	10:05am
d3hsp1	35	2/10/2003	10:05am
d3hsp2	54	2/10/2003	10:05am
d3hsp3	79	2/10/2003	10:05am
d3hsp4	88	2/10/2003	10:05am
d3plot	8667	3/13/2003	09:36am
d3plot173	6214	3/13/2003	09:36am
element.inc	1577	2/10/2003	10:06am
messag	18	2/11/2003	08:51am
nodes.inc	1677	2/10/2003	10:06am
nodese10.inc	21	2/10/2003	10:06am
nodese11.inc	4	2/10/2003	10:06am
nodese12.inc	21	2/10/2003	10:06am
nodese13.inc	4	2/10/2003	10:06am
nodeset.inc	8	2/10/2003	10:06am
nodeset3.inc	15	2/10/2003	10:06am
nodeset4.inc	3	2/10/2003	10:06am
nodeset5.inc	1	2/10/2003	10:06am
relaxWPP.k	1	2/10/2003	10:06am
segmen20.inc	4	2/10/2003	10:06am
segmen21.inc	2	2/10/2003	10:06am
segmen25.inc	7	2/10/2003	10:06am
segmen26.inc	6	2/10/2003	10:06am
segmen27.inc	30	2/10/2003	10:06am
segmen28.inc	6	2/10/2003	10:06am
seisWPPc.k	12	2/10/2003	10:06am
1E-6\RN8			
acc13h1.dat	139	2/10/2003	10:06am
acc13h2.dat	138	2/10/2003	10:06am
acc13v.dat	139	2/10/2003	10:06am
constraint.dat	7	2/10/2003	10:06am
d3hsp	10136	2/10/2003	10:06am

d3hsp1	117	2/10/2003	10:06am
d3hsp2	88	2/10/2003	10:06am
d3plot	8667	3/13/2003	09:36am
d3plot281	6214	3/13/2003	09:36am
element.inc	1577	2/10/2003	10:07am
messag	17	2/11/2003	08:51am
nodes.inc	1677	2/10/2003	10:07am
nodese10.inc	21	2/10/2003	10:07am
nodese11.inc	4	2/10/2003	10:07am
nodese12.inc	21	2/10/2003	10:07am
nodese13.inc	4	2/10/2003	10:07am
nodeset.inc	8	2/10/2003	10:07am
nodeset3.inc	15	2/10/2003	10:07am
nodeset4.inc	3	2/10/2003	10:07am
nodeset5.inc	1	2/10/2003	10:07am
relaxWPP.k	1	2/10/2003	10:07am
segmen20.inc	4	2/10/2003	10:07am
segmen21.inc	2	2/10/2003	10:07am
segmen25.inc	7	2/10/2003	10:07am
segmen26.inc	6	2/10/2003	10:07am
segmen27.inc	30	2/10/2003	10:07am
segmen28.inc	6	2/10/2003	10:07am
seisWPPc.k	12	2/10/2003	10:07am
1E-6\RN9\Long Run			
acc10h1.dat	25	2/10/2003	10:10am
acc10h2.dat	24	2/10/2003	10:10am
acc10v.dat	24	2/10/2003	10:10am
constraint.dat	7	2/10/2003	10:10am
d3hsp	9479	2/10/2003	10:10am
d3hsp1	43	2/10/2003	10:10am
d3hsp2	76	2/10/2003	10:10am
d3hsp3	76	2/10/2003	10:10am
d3hsp4	88	2/10/2003	10:10am
d3plot	8667	3/13/2003	09:38am
d3plot217	6214	3/13/2003	09:38am
element.inc	1577	2/10/2003	10:16am
messag	17	2/11/2003	08:52am
messag_1	16	2/11/2003	08:52am
messag_2	49	2/11/2003	08:52am
nodes.inc	1677	2/10/2003	10:16am
nodese10.inc	21	2/10/2003	10:16am
nodese11.inc	4	2/10/2003	10:16am
nodese12.inc	21	2/10/2003	10:16am
nodese13.inc	4	2/10/2003	10:16am
nodeset.inc	8	2/10/2003	10:16am
nodeset3.inc	15	2/10/2003	10:16am
nodeset4.inc	3	2/10/2003	10:16am
nodeset5.inc	1	2/10/2003	10:16am
relaxWPP.k	1	2/10/2003	10:16am
segmen20.inc	4	2/10/2003	10:16am

segmen21.inc	2	2/10/2003	10:16am
segmen25.inc	7	2/10/2003	10:16am
segmen26.inc	6	2/10/2003	10:16am
segmen27.inc	30	2/10/2003	10:16am
segmen28.inc	6	2/10/2003	10:16am
seisWPPc.k	12	2/10/2003	10:16am
1E-6\RN9\Short Run			
acc10h1.dat	25	2/10/2003	10:09am
acc10h2.dat	24	2/10/2003	10:09am
acc10v.dat	24	2/10/2003	10:09am
constraint.dat	7	2/10/2003	10:09am
d3hsp	9479	2/10/2003	10:09am
d3hsp1	43	2/10/2003	10:08am
d3hsp2	76	2/10/2003	10:08am
d3hsp3	88	2/10/2003	10:08am
d3plot	8667	3/13/2003	09:37am
d3plot177	6214	3/13/2003	09:37am
element.inc	1577	2/10/2003	10:09am
messag	17	2/11/2003	08:52am
messag_1	16	2/11/2003	08:52am
messag_2	49	2/11/2003	08:52am
nodes.inc	1677	2/10/2003	10:09am
nodese10.inc	21	2/10/2003	10:09am
nodese11.inc	4	2/10/2003	10:09am
nodese12.inc	21	2/10/2003	10:09am
nodese13.inc	4	2/10/2003	10:09am
nodeset.inc	8	2/10/2003	10:09am
nodeset3.inc	15	2/10/2003	10:09am
nodeset4.inc	3	2/10/2003	10:09am
nodeset5.inc	1	2/10/2003	10:09am
relaxWPP.k	1	2/10/2003	10:09am
segmen20.inc	4	2/10/2003	10:09am
segmen21.inc	2	2/10/2003	10:09am
segmen25.inc	7	2/10/2003	10:09am
segmen26.inc	6	2/10/2003	10:09am
segmen27.inc	30	2/10/2003	10:09am
segmen28.inc	6	2/10/2003	10:09am
seisWPPc.k	12	2/10/2003	10:09am

CONTENT OF CD2

1E-6\FER			
wpp6C.inp	37	2/10/2003	11:46am
wpp6C.out	370	2/10/2003	11:46am
1E-6\Refined Mesh\FER			
wpp6Crm.inp	37	2/10/2003	11:47am
wpp6Crm.out	371	2/10/2003	11:47am
1E-6\Refined Mesh\RN2			
acc16h1.dat	50	2/10/2003	10:44am
acc16h2.dat	50	2/10/2003	10:44am

acc16v.dat	50	2/10/2003	10:44am
constraint.dat	7	2/10/2003	10:44am
d3hsp	11900	2/10/2003	10:44am
d3hsp1	50	2/10/2003	10:43am
d3hsp2	65	2/10/2003	10:43am
d3hsp3	60	2/10/2003	10:43am
d3hsp4	60	2/10/2003	10:43am
d3hsp5	90	2/10/2003	10:43am
d3plot	11162	3/13/2003	10:02am
d3plot381	7905	3/13/2003	10:02am
element.inc	2123	2/10/2003	10:44am
messag	19	2/11/2003	08:59am
nodes.inc	2174	2/10/2003	10:45am
nodese10.inc	27	2/10/2003	10:45am
nodese11.inc	5	2/10/2003	10:45am
nodese12.inc	27	2/10/2003	10:45am
nodese13.inc	5	2/10/2003	10:45am
nodeset.inc	8	2/10/2003	10:45am
nodeset3.inc	15	2/10/2003	10:45am
nodeset4.inc	3	2/10/2003	10:45am
nodeset5.inc	1	2/10/2003	10:45am
relaxWPP.k	1	2/10/2003	10:45am
segmen20.inc	4	2/10/2003	10:45am
segmen21.inc	2	2/10/2003	10:45am
segmen25.inc	8	2/10/2003	10:45am
segmen26.inc	6	2/10/2003	10:44am
segmen27.inc	43	2/10/2003	10:44am
segmen28.inc	6	2/10/2003	10:44am
seisWPPc.k	12	2/10/2003	10:44am
1E-6\Refined Mesh\RN4			
acc8h1.dat	106	2/10/2003	10:26am
acc8h2.dat	107	2/10/2003	10:26am
acc8v.dat	105	2/10/2003	10:26am
constraint.dat	7	2/10/2003	10:26am
d3hsp	12162	2/10/2003	10:26am
d3hsp1	55	2/10/2003	10:26am
d3hsp2	55	2/10/2003	10:26am
d3hsp3	90	2/10/2003	10:26am
d3plot	11162	3/13/2003	09:47am
d3plot249	7905	3/13/2003	09:47am
element.inc	2123	2/10/2003	10:27am
messag	19	2/11/2003	08:55am
nodes.inc	2174	2/10/2003	10:27am
nodese10.inc	27	2/10/2003	10:27am
nodese11.inc	5	2/10/2003	10:27am
nodese12.inc	27	2/10/2003	10:27am
nodese13.inc	5	2/10/2003	10:27am
nodeset.inc	8	2/10/2003	10:27am
nodeset3.inc	15	2/10/2003	10:27am
nodeset4.inc	3	2/10/2003	10:27am

nodeset5.inc	1	2/10/2003	10:27am
relaxWPP.k	1	2/10/2003	10:27am
segmen20.inc	4	2/10/2003	10:27am
segmen21.inc	2	2/10/2003	10:27am
segmen25.inc	8	2/10/2003	10:27am
segmen26.inc	6	2/10/2003	10:27am
segmen27.inc	43	2/10/2003	10:27am
segmen28.inc	6	2/10/2003	10:27am
seisWPPc.k	12	2/10/2003	10:27am
1E-7\RN1			
acc7h1.dat	41	2/10/2003	10:17am
acc7h2.dat	41	2/10/2003	10:17am
acc7v.dat	41	2/10/2003	10:17am
constraint.dat	7	2/10/2003	10:17am
d3hsp	15173	2/10/2003	10:17am
d3hsp1	62	2/10/2003	10:17am
d3hsp2	39	2/10/2003	10:17am
d3hsp3	99	2/10/2003	10:17am
d3hsp4	89	2/10/2003	10:17am
d3plot	13779	3/13/2003	09:39am
d3plot334	9277	3/13/2003	09:39am
element.inc	2944	2/10/2003	10:17am
glstat	324	2/11/2003	08:54am
messag	18	2/11/2003	08:54am
nodes.inc	2973	2/10/2003	10:18am
nodese10.inc	55	2/10/2003	10:18am
nodese11.inc	10	2/10/2003	10:18am
nodese12.inc	55	2/10/2003	10:18am
nodese13.inc	10	2/10/2003	10:18am
nodeset.inc	8	2/10/2003	10:18am
nodeset2.inc	2	2/10/2003	10:18am
nodeset3.inc	20	2/10/2003	10:18am
nodeset4.inc	5	2/10/2003	10:18am
nodeset5.inc	2	2/10/2003	10:18am
rcforc	1440	2/11/2003	08:54am
relaxWPP.k	1	2/10/2003	10:18am
segmen20.inc	4	2/10/2003	10:18am
segmen21.inc	2	2/10/2003	10:18am
segmen25.inc	26	2/10/2003	10:18am
segmen26.inc	6	2/10/2003	10:18am
segmen27.inc	26	2/10/2003	10:18am
segmen28.inc	6	2/10/2003	10:18am
segmen35.inc	7	2/10/2003	10:18am
segmen36.inc	6	2/10/2003	10:18am
segmen37.inc	7	2/10/2003	10:18am
segmen38.inc	6	2/10/2003	10:18am
seisWPPc.k	13	2/10/2003	10:18am
1E-7\RN10			
acc9h1.dat	97	2/10/2003	09:33am
acc9h2.dat	97	2/10/2003	09:33am

acc9v.dat	97	2/10/2003	09:33am
constraint.dat	7	2/10/2003	09:33am
d3hsp	15519	2/10/2003	09:33am
d3hsp1	35	2/10/2003	09:33am
d3hsp2	39	2/10/2003	09:33am
d3hsp3	35	2/10/2003	09:33am
d3hsp4	88	2/10/2003	09:33am
d3plot	13779	3/13/2003	08:37am
d3plot247	9277	3/13/2003	08:37am
element.inc	2944	2/10/2003	09:54am
messag	18	2/11/2003	08:43am
nodes.inc	2973	2/10/2003	09:54am
nodese10.inc	55	2/10/2003	09:54am
nodese11.inc	10	2/10/2003	09:54am
nodese12.inc	55	2/10/2003	09:54am
nodese13.inc	10	2/10/2003	09:54am
nodeset.inc	8	2/10/2003	09:54am
nodeset3.inc	20	2/10/2003	09:54am
nodeset4.inc	5	2/10/2003	09:54am
nodeset5.inc	2	2/10/2003	09:54am
relaxWPP.k	1	2/10/2003	09:34am
segmen20.inc	4	2/10/2003	09:54am
segmen21.inc	2	2/10/2003	09:54am
segmen25.inc	26	2/10/2003	09:54am
segmen26.inc	6	2/10/2003	09:54am
segmen27.inc	26	2/10/2003	09:54am
segmen28.inc	6	2/10/2003	09:54am
segmen35.inc	7	2/10/2003	09:54am
segmen36.inc	6	2/10/2003	09:54am
segmen37.inc	7	2/10/2003	09:54am
segmen38.inc	6	2/10/2003	09:54am
seisWPPc.k	13	2/10/2003	09:34am
1E-7\RN11			
acc5h1.dat	29	2/10/2003	10:29am
acc5h2.dat	29	2/10/2003	10:29am
acc5v.dat	29	2/10/2003	10:29am
constraint.dat	7	2/10/2003	10:29am
d3hsp	15186	2/10/2003	10:29am
d3hsp1	88	2/10/2003	10:29am
d3plot	13779	3/13/2003	09:49am
d3plot325	9277	3/13/2003	09:49am
element.inc	2944	2/10/2003	10:30am
messag	17	2/11/2003	08:56am
nodes.inc	2973	2/10/2003	10:30am
nodese10.inc	55	2/10/2003	10:30am
nodese11.inc	10	2/10/2003	10:30am
nodese12.inc	55	2/10/2003	10:30am
nodese13.inc	10	2/10/2003	10:30am
nodeset.inc	8	2/10/2003	10:30am
nodeset3.inc	20	2/10/2003	10:30am

nodeset4.inc	5	2/10/2003	10:30am
nodeset5.inc	2	2/10/2003	10:30am
relaxWPP.k	1	2/10/2003	10:30am
segmen20.inc	4	2/10/2003	10:30am
segmen21.inc	2	2/10/2003	10:30am
segmen25.inc	26	2/10/2003	10:30am
segmen26.inc	6	2/10/2003	10:30am
segmen27.inc	26	2/10/2003	10:30am
segmen28.inc	6	2/10/2003	10:30am
segmen35.inc	7	2/10/2003	10:30am
segmen36.inc	6	2/10/2003	10:30am
segmen37.inc	7	2/10/2003	10:30am
segmen38.inc	6	2/10/2003	10:30am
seisWPPc.k	13	2/10/2003	10:30am
1E-7\RN12			
acc6h1.dat	28	2/10/2003	10:31am
acc6h2.dat	28	2/10/2003	10:31am
acc6v.dat	28	2/10/2003	10:31am
constraint.dat	7	2/10/2003	10:31am
d3hsp	15078	2/10/2003	10:31am
d3hsp1	118	2/10/2003	10:31am
d3hsp2	88	2/10/2003	10:31am
d3plot	13779	3/13/2003	09:44am
d3plot293	9277	3/13/2003	09:44am
element.inc	2944	2/10/2003	10:32am
messag	17	2/11/2003	08:57am
nodes.inc	2973	2/10/2003	10:32am
nodese10.inc	55	2/10/2003	10:32am
nodese11.inc	10	2/10/2003	10:32am
nodese12.inc	55	2/10/2003	10:32am
nodese13.inc	10	2/10/2003	10:32am
nodeset.inc	8	2/10/2003	10:32am
nodeset3.inc	20	2/10/2003	10:32am
nodeset4.inc	5	2/10/2003	10:32am
nodeset5.inc	2	2/10/2003	10:32am
relaxWPP.k	1	2/10/2003	10:32am
segmen20.inc	4	2/10/2003	10:32am
segmen21.inc	2	2/10/2003	10:32am
segmen25.inc	26	2/10/2003	10:32am
segmen26.inc	6	2/10/2003	10:32am
segmen27.inc	26	2/10/2003	10:32am
segmen28.inc	6	2/10/2003	10:32am
segmen35.inc	7	2/10/2003	10:32am
segmen36.inc	6	2/10/2003	10:32am
segmen37.inc	7	2/10/2003	10:32am
segmen38.inc	6	2/10/2003	10:32am
seisWPPc.k	13	2/10/2003	10:32am
1E-7\RN13			
acc12h1.dat	30	2/10/2003	10:48am
acc12h2.dat	33	2/10/2003	10:47am

acc12v.dat	33	2/10/2003	10:47am
constraint.dat	7	2/10/2003	10:47am
d3hsp	10080	2/10/2003	10:47am
d3hsp1	88	2/10/2003	10:47am
d3plot	9232	3/13/2003	10:07am
d3plot225	6664	3/13/2003	10:07am
element.inc	1649	2/10/2003	10:48am
messag	18	2/11/2003	09:00am
nodes.inc	1757	2/10/2003	10:48am
nodese10.inc	21	2/10/2003	10:48am
nodese11.inc	4	2/10/2003	10:48am
nodese12.inc	21	2/10/2003	10:48am
nodese13.inc	4	2/10/2003	10:48am
nodeset.inc	8	2/10/2003	10:48am
nodeset3.inc	15	2/10/2003	10:48am
nodeset4.inc	5	2/10/2003	10:48am
nodeset5.inc	2	2/10/2003	10:48am
relaxWPP.k	1	2/10/2003	10:48am
segmen20.inc	4	2/10/2003	10:48am
segmen21.inc	2	2/10/2003	10:48am
segmen25.inc	7	2/10/2003	10:48am
segmen26.inc	6	2/10/2003	10:48am
segmen27.inc	30	2/10/2003	10:48am
segmen28.inc	6	2/10/2003	10:48am
seisWPPc.k	13	2/10/2003	10:48am
1E-7\RN14			
acc14h1.dat	116	2/10/2003	10:48am
acc14h2.dat	116	2/10/2003	10:48am
acc14v.dat	116	2/10/2003	10:48am
constraint.dat	7	2/10/2003	10:48am
d3hsp	10539	2/10/2003	10:48am
d3hsp1	35	2/10/2003	10:48am
d3hsp2	87	2/10/2003	10:48am
d3plot	9232	3/13/2003	10:07am
d3plot253	6664	3/13/2003	10:07am
element.inc	1649	2/10/2003	10:49am
messag	17	2/11/2003	09:00am
nodes.inc	1757	2/10/2003	10:49am
nodese10.inc	21	2/10/2003	10:49am
nodese11.inc	4	2/10/2003	10:49am
nodese12.inc	21	2/10/2003	10:49am
nodese13.inc	4	2/10/2003	10:49am
nodeset.inc	8	2/10/2003	10:49am
nodeset3.inc	15	2/10/2003	10:49am
nodeset4.inc	5	2/10/2003	10:49am
nodeset5.inc	2	2/10/2003	10:49am
relaxWPP.k	1	2/10/2003	10:49am
segmen20.inc	4	2/10/2003	10:49am
segmen21.inc	2	2/10/2003	10:49am
segmen25.inc	7	2/10/2003	10:49am

segmen26.inc	6	2/10/2003	10:49am
segmen27.inc	30	2/10/2003	10:49am
segmen28.inc	6	2/10/2003	10:49am
seisWPPc.k	12	2/10/2003	10:49am
1E-7\RN15			
acc3h1.dat	31	3/13/2003	08:23am
acc3h2.dat	31	3/13/2003	08:23am
acc3v.dat	31	3/13/2003	08:23am
constraint.dat	7	3/13/2003	08:23am
d3hsp	15088	3/13/2003	08:23am
d3hsp1	88	3/13/2003	08:23am
d3plot	13779	3/13/2003	09:27am
d3plot90	9277	3/13/2003	09:27am
element.inc	2944	3/13/2003	08:23am
messag	17	3/13/2003	08:23am
nodes.inc	2973	3/13/2003	08:23am
nodese10.inc	55	3/13/2003	08:23am
nodese11.inc	10	3/13/2003	08:23am
nodese12.inc	55	3/13/2003	08:23am
nodese13.inc	10	3/13/2003	08:23am
nodeset.inc	8	3/13/2003	08:23am
nodeset2.inc	2	3/13/2003	08:23am
nodeset3.inc	20	3/13/2003	08:23am
nodeset4.inc	5	3/13/2003	08:23am
nodeset5.inc	2	3/13/2003	08:23am
relaxWPP.k	1	3/13/2003	08:23am
segmen20.inc	4	3/13/2003	08:23am
segmen21.inc	2	3/13/2003	08:23am
segmen25.inc	26	3/13/2003	08:23am
segmen26.inc	6	3/13/2003	08:23am
segmen27.inc	26	3/13/2003	08:23am
segmen28.inc	6	3/13/2003	08:23am
segmen35.inc	7	3/13/2003	08:23am
segmen36.inc	6	3/13/2003	08:23am
segmen37.inc	7	3/13/2003	08:23am
segmen38.inc	6	3/13/2003	08:23am
seisWPPc.k	13	3/13/2003	08:23am
1E-7\RN2			
acc16h1.dat	50	2/10/2003	10:32am
acc16h2.dat	50	2/10/2003	10:32am
acc16v.dat	50	2/10/2003	10:32am
constraint.dat	7	2/10/2003	10:32am
d3hsp	9990	2/10/2003	10:32am
d3hsp1	119	2/10/2003	10:32am
d3hsp2	88	2/10/2003	10:32am
d3plot	9232	3/13/2003	09:44am
d3plot124	6664	3/13/2003	09:44am
element.inc	1649	2/10/2003	10:33am
messag	17	2/11/2003	08:57am
nodes.inc	1757	2/10/2003	10:33am

nodese10.inc	21	2/10/2003	10:33am
nodese11.inc	4	2/10/2003	10:33am
nodese12.inc	21	2/10/2003	10:33am
nodese13.inc	4	2/10/2003	10:33am
nodeset.inc	8	2/10/2003	10:33am
nodeset2.inc	2	2/10/2003	10:33am
nodeset3.inc	15	2/10/2003	10:33am
nodeset4.inc	5	2/10/2003	10:33am
nodeset5.inc	2	2/10/2003	10:33am
relaxWPP.k	1	2/10/2003	10:33am
segmen20.inc	4	2/10/2003	10:33am
segmen21.inc	2	2/10/2003	10:33am
segmen25.inc	7	2/10/2003	10:33am
segmen26.inc	6	2/10/2003	10:33am
segmen27.inc	30	2/10/2003	10:33am
segmen28.inc	6	2/10/2003	10:33am
seisWPPc.k	13	2/10/2003	10:33am
1E-7\RN3			
acc4h1.dat	39	2/10/2003	09:31am
acc4h2.dat	39	2/10/2003	09:31am
acc4v.dat	39	2/10/2003	09:31am
constraint.dat	7	2/10/2003	09:31am
d3hsp	15208	2/10/2003	09:31am
d3hsp1	134	2/10/2003	09:31am
d3hsp2	89	2/10/2003	09:31am
d3plot	13779	3/13/2003	08:38am
d3plot434	9277	3/13/2003	08:38am
element.inc	2944	2/10/2003	09:54am
messag	18	2/11/2003	08:43am
nodes.inc	2973	2/10/2003	09:54am
nodese10.inc	55	2/10/2003	09:54am
nodese11.inc	10	2/10/2003	09:54am
nodese12.inc	55	2/10/2003	09:54am
nodese13.inc	10	2/10/2003	09:54am
nodeset.inc	8	2/10/2003	09:54am
nodeset3.inc	20	2/10/2003	09:54am
nodeset4.inc	5	2/10/2003	09:54am
nodeset5.inc	2	2/10/2003	09:54am
relaxWPP.k	1	2/10/2003	09:31am
segmen20.inc	4	2/10/2003	09:54am
segmen21.inc	2	2/10/2003	09:54am
segmen25.inc	26	2/10/2003	09:54am
segmen26.inc	6	2/10/2003	09:54am
segmen27.inc	26	2/10/2003	09:54am
segmen28.inc	6	2/10/2003	09:54am
segmen35.inc	7	2/10/2003	09:54am
segmen36.inc	6	2/10/2003	09:54am
segmen37.inc	7	2/10/2003	09:54am
segmen38.inc	6	2/10/2003	09:54am
seisWPPc.k	13	2/10/2003	09:31am

1E-7\RN4			
acc8h1.dat	69	2/10/2003	10:49am
acc8h2.dat	68	2/10/2003	10:49am
acc8v.dat	68	2/10/2003	10:49am
constraint.dat	7	2/10/2003	10:49am
d3hsp	15322	2/10/2003	10:49am
d3hsp1	88	2/10/2003	10:49am
d3plot	13779	3/13/2003	10:08am
d3plot177	9277	3/13/2003	10:08am
element.inc	2944	2/10/2003	10:50am
messag	17	2/11/2003	09:01am
nodes.inc	2973	2/10/2003	10:50am
nodese10.inc	55	2/10/2003	10:50am
nodese11.inc	10	2/10/2003	10:50am
nodese12.inc	55	2/10/2003	10:50am
nodese13.inc	10	2/10/2003	10:50am
nodeset.inc	8	2/10/2003	10:50am
nodeset2.inc	2	2/10/2003	10:50am
nodeset3.inc	20	2/10/2003	10:50am
nodeset4.inc	5	2/10/2003	10:50am
nodeset5.inc	2	2/10/2003	10:50am
relaxWPP.k	1	2/10/2003	10:50am
segmen20.inc	4	2/10/2003	10:50am
segmen21.inc	2	2/10/2003	10:50am
segmen25.inc	26	2/10/2003	10:50am
segmen26.inc	6	2/10/2003	10:50am
segmen27.inc	26	2/10/2003	10:50am
segmen28.inc	6	2/10/2003	10:50am
segmen35.inc	7	2/10/2003	10:50am
segmen36.inc	6	2/10/2003	10:50am
segmen37.inc	7	2/10/2003	10:50am
segmen38.inc	6	2/10/2003	10:50am
seisWPPc.k	13	2/10/2003	10:50am
1E-7\RN5			
acc11h1.dat	61	2/10/2003	09:44am
acc11h2.dat	61	2/10/2003	09:44am
acc11v.dat	61	2/10/2003	09:44am
constraint.dat	7	2/10/2003	09:44am
d3hsp	15310	2/10/2003	09:44am
d3hsp1	63	2/10/2003	09:44am
d3hsp2	89	2/10/2003	09:44am
d3plot	13779	3/13/2003	09:28am
d3plot277	9277	3/13/2003	09:28am
element.inc	2944	2/10/2003	09:45am
messag	18	2/11/2003	08:50am
nodes.inc	2973	2/10/2003	09:45am
nodese10.inc	55	2/10/2003	09:45am
nodese11.inc	10	2/10/2003	09:45am
nodese12.inc	55	2/10/2003	09:45am
nodese13.inc	10	2/10/2003	09:45am

nodeset.inc	8	2/10/2003	09:45am
nodeset3.inc	20	2/10/2003	09:45am
nodeset4.inc	5	2/10/2003	09:45am
nodeset5.inc	2	2/10/2003	09:45am
relaxWPP.k	1	2/10/2003	09:45am
segmen20.inc	4	2/10/2003	09:45am
segmen21.inc	2	2/10/2003	09:45am
segmen25.inc	26	2/10/2003	09:45am
segmen26.inc	6	2/10/2003	09:45am
segmen27.inc	26	2/10/2003	09:45am
segmen28.inc	6	2/10/2003	09:45am
segmen35.inc	7	2/10/2003	09:45am
segmen36.inc	6	2/10/2003	09:45am
segmen37.inc	7	2/10/2003	09:45am
segmen38.inc	6	2/10/2003	09:45am
seisWPPc.k	13	2/10/2003	09:45am
1E-7\RN6			
acc1h1.dat	67	2/10/2003	09:46am
acc1h2.dat	67	2/10/2003	09:46am
acc1v.dat	63	2/10/2003	09:46am
constraint.dat	7	2/10/2003	09:46am
d3hsp	15326	2/10/2003	09:46am
d3hsp1	88	2/10/2003	09:46am
d3plot	13779	3/13/2003	09:29am
d3plot229	9277	3/13/2003	09:29am
element.inc	2944	2/10/2003	09:46am
messag	17	2/11/2003	08:50am
nodes.inc	2973	2/10/2003	09:47am
nodese10.inc	55	2/10/2003	09:47am
nodese11.inc	10	2/10/2003	09:47am
nodese12.inc	55	2/10/2003	09:47am
nodese13.inc	10	2/10/2003	09:47am
nodeset.inc	8	2/10/2003	09:47am
nodeset3.inc	20	2/10/2003	09:47am
nodeset4.inc	5	2/10/2003	09:47am
nodeset5.inc	2	2/10/2003	09:47am
relaxWPP.k	1	2/10/2003	09:47am
segmen20.inc	4	2/10/2003	09:47am
segmen21.inc	2	2/10/2003	09:47am
segmen25.inc	26	2/10/2003	09:47am
segmen26.inc	6	2/10/2003	09:47am
segmen27.inc	26	2/10/2003	09:47am
segmen28.inc	6	2/10/2003	09:47am
segmen35.inc	7	2/10/2003	09:47am
segmen36.inc	6	2/10/2003	09:47am
segmen37.inc	7	2/10/2003	09:47am
segmen38.inc	6	2/10/2003	09:47am
seisWPPc.k	13	2/10/2003	09:47am
1E-7\RN7			
acc2h1.dat	69	2/10/2003	09:35am

acc2h2.dat	68	2/10/2003	09:35am
acc2v.dat	68	2/10/2003	09:35am
constraint.dat	7	2/10/2003	09:35am
d3hsp	15353	2/10/2003	09:35am
d3hsp1	88	2/10/2003	09:35am
d3plot	13779	3/13/2003	08:39am
d3plot221	9277	3/13/2003	08:39am
element.inc	2944	2/10/2003	09:56am
messag	17	2/11/2003	08:43am
nodes.inc	2973	2/10/2003	09:56am
nodese10.inc	55	2/10/2003	09:55am
nodese11.inc	10	2/10/2003	09:55am
nodese12.inc	55	2/10/2003	09:55am
nodese13.inc	10	2/10/2003	09:55am
nodeset.inc	8	2/10/2003	09:55am
nodeset2.inc	2	2/10/2003	09:55am
nodeset3.inc	20	2/10/2003	09:55am
nodeset4.inc	5	2/10/2003	09:55am
nodeset5.inc	2	2/10/2003	09:55am
relaxWPP.k	1	2/10/2003	09:36am
segmen20.inc	4	2/10/2003	09:55am
segmen21.inc	2	2/10/2003	09:55am
segmen25.inc	26	2/10/2003	09:55am
segmen26.inc	6	2/10/2003	09:55am
segmen27.inc	26	2/10/2003	09:55am
segmen28.inc	6	2/10/2003	09:55am
segmen35.inc	7	2/10/2003	09:55am
segmen36.inc	6	2/10/2003	09:55am
segmen37.inc	7	2/10/2003	09:55am
segmen38.inc	6	2/10/2003	09:55am
seisWPPc.k	13	2/10/2003	09:36am
1E-7\RN8			
acc13h1.dat	127	2/10/2003	10:21am
acc13h2.dat	127	2/10/2003	10:21am
acc13v.dat	127	2/10/2003	10:21am
constraint.dat	7	2/10/2003	10:21am
d3hsp	10641	2/10/2003	10:21am
d3hsp1	89	2/10/2003	10:21am
d3plot	9232	3/13/2003	09:41am
d3plot277	6664	3/13/2003	09:41am
element.inc	1649	2/10/2003	10:22am
messag	18	2/11/2003	08:54am
nodes.inc	1757	2/10/2003	10:22am
nodese10.inc	21	2/10/2003	10:22am
nodese11.inc	4	2/10/2003	10:22am
nodese12.inc	21	2/10/2003	10:22am
nodese13.inc	4	2/10/2003	10:22am
nodeset.inc	8	2/10/2003	10:22am
nodeset3.inc	15	2/10/2003	10:22am
nodeset4.inc	5	2/10/2003	10:22am

nodeset5.inc	2	2/10/2003	10:22am
relaxWPP.k	1	2/10/2003	10:22am
segmen20.inc	4	2/10/2003	10:22am
segmen21.inc	2	2/10/2003	10:22am
segmen25.inc	7	2/10/2003	10:22am
segmen26.inc	6	2/10/2003	10:22am
segmen27.inc	30	2/10/2003	10:22am
segmen28.inc	6	2/10/2003	10:22am
seisWPPc.k	12	2/10/2003	10:22am
1E-7\RN9			
acc10h1.dat	14	2/10/2003	10:34am
acc10h2.dat	14	2/10/2003	10:34am
acc10v.dat	14	2/10/2003	10:34am
constraint.dat	7	2/10/2003	10:34am
d3hsp	9899	2/10/2003	10:34am
d3hsp1	88	2/10/2003	10:34am
d3plot	9232	3/13/2003	09:45am
d3plot123	6664	3/13/2003	09:45am
element.inc	1649	2/10/2003	10:34am
messag	18	2/11/2003	08:57am
nodes.inc	1757	2/10/2003	10:34am
nodese10.inc	21	2/10/2003	10:34am
nodese11.inc	4	2/10/2003	10:34am
nodese12.inc	21	2/10/2003	10:34am
nodese13.inc	4	2/10/2003	10:34am
nodeset.inc	8	2/10/2003	10:34am
nodeset2.inc	2	2/10/2003	10:34am
nodeset3.inc	15	2/10/2003	10:34am
nodeset4.inc	5	2/10/2003	10:34am
nodeset5.inc	2	2/10/2003	10:34am
relaxWPP.k	1	2/10/2003	10:34am
segmen20.inc	4	2/10/2003	10:34am
segmen21.inc	2	2/10/2003	10:34am
segmen25.inc	7	2/10/2003	10:34am
segmen26.inc	6	2/10/2003	10:34am
segmen27.inc	30	2/10/2003	10:34am
segmen28.inc	6	2/10/2003	10:34am
seisWPPc.k	13	2/10/2003	10:34am

CONTENT OF CD3

1E-7\Deformable OS\RN15			
acc3h1.dat	31	2/10/2003	10:19am
acc3h2.dat	31	2/10/2003	10:19am
acc3v.dat	31	2/10/2003	10:19am
d3hsp	15075	2/10/2003	10:19am
d3plot	13779	3/13/2003	09:40am
d3plot46	9277	3/13/2003	09:40am
d3plot47	9277	3/13/2003	09:40am
element.inc	2944	2/10/2003	10:20am

messag	32	2/11/2003	08:54am
nodes.inc	2973	2/10/2003	10:20am
nodese10.inc	55	2/10/2003	10:20am
nodese11.inc	10	2/10/2003	10:20am
nodese12.inc	55	2/10/2003	10:20am
nodese13.inc	10	2/10/2003	10:20am
nodeset.inc	8	2/10/2003	10:20am
nodeset2.inc	2	2/10/2003	10:20am
nodeset3.inc	20	2/10/2003	10:20am
nodeset4.inc	5	2/10/2003	10:20am
nodeset5.inc	2	2/10/2003	10:20am
segmen20.inc	4	2/10/2003	10:20am
segmen21.inc	2	2/10/2003	10:20am
segmen25.inc	26	2/10/2003	10:20am
segmen26.inc	6	2/10/2003	10:20am
segmen27.inc	26	2/10/2003	10:20am
segmen28.inc	6	2/10/2003	10:20am
segmen35.inc	7	2/10/2003	10:20am
segmen36.inc	6	2/10/2003	10:20am
segmen37.inc	7	2/10/2003	10:20am
segmen38.inc	6	2/10/2003	10:20am
seisWPcE.k	13	2/10/2003	10:20am
1E-7\Deformable OS\RN4			
acc8h1.dat	69	2/10/2003	10:20am
acc8h2.dat	68	2/10/2003	10:20am
acc8v.dat	68	2/10/2003	10:20am
d3hsp	15242	2/10/2003	10:20am
d3hsp1	67	2/10/2003	10:20am
d3plot	13779	3/13/2003	09:41am
d3plot131	9277	3/13/2003	09:41am
d3plot132	9277	3/13/2003	09:41am
element.inc	2944	2/10/2003	10:20am
messag	63	2/11/2003	08:54am
nodes.inc	2973	2/10/2003	10:21am
nodese10.inc	55	2/10/2003	10:21am
nodese11.inc	10	2/10/2003	10:21am
nodese12.inc	55	2/10/2003	10:21am
nodese13.inc	10	2/10/2003	10:21am
nodeset.inc	8	2/10/2003	10:21am
nodeset2.inc	2	2/10/2003	10:21am
nodeset3.inc	20	2/10/2003	10:21am
nodeset4.inc	5	2/10/2003	10:21am
nodeset5.inc	2	2/10/2003	10:21am
segmen20.inc	4	2/10/2003	10:21am
segmen21.inc	2	2/10/2003	10:21am
segmen25.inc	26	2/10/2003	10:21am
segmen26.inc	6	2/10/2003	10:21am
segmen27.inc	26	2/10/2003	10:21am
segmen28.inc	6	2/10/2003	10:21am
segmen35.inc	7	2/10/2003	10:21am

segmen36.inc	6	2/10/2003	10:21am
segmen37.inc	7	2/10/2003	10:21am
segmen38.inc	6	2/10/2003	10:21am
seisWPcE.k	13	2/10/2003	10:21am
1E-7\FER			
wpp7C.inp	38	2/10/2003	11:50am
wpp7C.out	400	2/10/2003	11:50am
1E-7\Mesh Study\Mesh1			
acc3h1.dat	31	3/17/2003	08:32am
acc3h2.dat	31	3/17/2003	08:32am
acc3v.dat	31	3/17/2003	08:32am
constraint.dat	7	3/17/2003	08:32am
d3hsp	15087	3/17/2003	08:32am
d3hsp1	87	3/17/2003	08:32am
d3plot	13779	3/17/2003	08:34am
d3plot89	9227	3/17/2003	08:34am
element.inc	2944	3/17/2003	08:32am
messag0	43	3/17/2003	08:32am
messag	17	3/17/2003	08:32am
nodes.inc	2973	3/17/2003	08:32am
nodese10.inc	55	3/17/2003	08:32am
nodese11.inc	10	3/17/2003	08:32am
nodese12.inc	55	3/17/2003	08:32am
nodese13.inc	10	3/17/2003	08:32am
nodeset.inc	8	3/17/2003	08:32am
nodeset2.inc	2	3/17/2003	08:32am
nodeset3.inc	20	3/17/2003	08:32am
nodeset4.inc	5	3/17/2003	08:32am
nodeset5.inc	2	3/17/2003	08:32am
relaxWPP.k	1	3/17/2003	08:32am
segmen20.inc	4	3/17/2003	08:32am
segmen21.inc	2	3/17/2003	08:32am
segmen25.inc	26	3/17/2003	08:32am
segmen26.inc	6	3/17/2003	08:32am
segmen27.inc	26	3/17/2003	08:32am
segmen28.inc	6	3/17/2003	08:32am
segmen35.inc	7	3/17/2003	08:32am
segmen36.inc	6	3/17/2003	08:32am
segmen37.inc	7	3/17/2003	08:32am
segmen38.inc	6	3/17/2003	08:32am
seisWPPc.k	13	3/17/2003	08:32am
1E-7\ Mesh Study\Mesh2			
acc3h1.dat	31	2/13/2003	07:53am
acc3h2.dat	31	2/13/2003	07:53am
acc3v.dat	31	2/13/2003	07:53am
constraint.dat	7	2/13/2003	07:53am
d3hsp	19840	2/13/2003	07:53am
d3hsp1	90	2/13/2003	07:53am
d3plot	18080	3/13/2003	08:43am
d3plot89	11674	3/13/2003	08:42am

element.inc	4279	2/13/2003	07:54am
messag	20	2/13/2003	07:54am
nodes.inc	4064	2/13/2003	07:54am
nodese10.inc	78	2/13/2003	07:54am
nodese11.inc	10	2/13/2003	07:54am
nodese12.inc	78	2/13/2003	07:54am
nodese13.inc	10	2/13/2003	07:54am
nodeset.inc	8	2/13/2003	07:54am
nodeset3.inc	20	2/13/2003	07:54am
nodeset4.inc	5	2/13/2003	07:54am
nodeset5.inc	3	2/13/2003	07:54am
relaxWPP.k	1	2/13/2003	07:54am
segmen20.inc	4	2/13/2003	07:54am
segmen21.inc	2	2/13/2003	07:54am
segmen25.inc	37	2/13/2003	07:54am
segmen26.inc	6	2/13/2003	07:53am
segmen27.inc	37	2/13/2003	07:53am
segmen28.inc	6	2/13/2003	07:53am
segmen35.inc	7	2/13/2003	07:53am
segmen36.inc	6	2/13/2003	07:53am
segmen37.inc	7	2/13/2003	07:53am
segmen38.inc	6	2/13/2003	07:53am
seisWPPc.k	13	2/13/2003	07:53am
1E-7\ Mesh Study\Mesh2\FER			
wpp7Crm.inp	38	2/10/2003	11:51am
wpp7Crm.out	400	2/10/2003	11:51am
5E-4			
acc_h1.dat	144	2/10/2003	09:57am
acc_h2.dat	143	2/10/2003	09:57am
acc_v.dat	144	2/10/2003	09:57am
constraint.dat	7	2/10/2003	09:57am
d3hsp	10070	2/10/2003	09:57am
d3hsp1	126	2/10/2003	09:56am
d3hsp2	83	2/10/2003	09:56am
d3plot	8674	3/13/2003	09:33am
d3plot247	6224	3/13/2003	09:33am
element.inc	1577	2/10/2003	09:57am
messag	12	2/11/2003	08:53am
messag_1	137	2/11/2003	08:53am
nodes.inc	1677	2/10/2003	09:58am
nodese10.inc	21	2/10/2003	09:58am
nodese11.inc	4	2/10/2003	09:58am
nodese12.inc	21	2/10/2003	09:58am
nodese13.inc	4	2/10/2003	09:58am
nodeset.inc	8	2/10/2003	09:58am
nodeset3.inc	15	2/10/2003	09:58am
nodeset4.inc	3	2/10/2003	09:58am
nodeset5.inc	1	2/10/2003	09:58am
relaxWPP.k	1	2/10/2003	09:58am
segmen20.inc	4	2/10/2003	09:58am

segmen21.inc	2	2/10/2003	09:58am
segmen25.inc	7	2/10/2003	09:58am
segmen26.inc	6	2/10/2003	09:58am
segmen27.inc	30	2/10/2003	09:58am
segmen28.inc	6	2/10/2003	09:58am
seisWPPc.k	12	2/10/2003	09:58am
Modal Analysis			
wpp6Bmod.inp	29	2/10/2003	11:48am
wpp6Bmod.out	239	2/10/2003	11:48am
1E-5\RN6			
a1h1.dat	23	4/28/2003	08:56am
a1h2.dat	23	4/28/2003	08:56am
a1v.dat	23	4/28/2003	08:56am
constraint.dat	7	4/28/2003	08:56am
d3hsp	6672	4/28/2003	08:56am
d3hsp1	89	4/28/2003	08:56am
d3plot	8667	4/28/2003	08:57am
d3plot287	6214	4/28/2003	08:57am
element.inc	1577	4/28/2003	08:56am
messag	18	4/28/2003	08:56am
messag0	125	4/28/2003	08:56am
nodes.inc	1677	4/28/2003	08:56am
nodese10.inc	21	4/28/2003	08:56am
nodese11.inc	4	4/28/2003	08:56am
nodese12.inc	21	4/28/2003	08:56am
nodese13.inc	4	4/28/2003	08:56am
nodeset.inc	8	4/28/2003	08:56am
nodeset3.inc	15	4/28/2003	08:56am
nodeset4.inc	3	4/28/2003	08:56am
nodeset5.inc	1	4/28/2003	08:56am
relaxWPP.k	1	4/28/2003	08:56am
segmen20.inc	4	4/28/2003	08:56am
segmen21.inc	2	4/28/2003	08:56am
segmen25.inc	7	4/28/2003	08:56am
segmen26.inc	6	4/28/2003	08:56am
segmen27.inc	30	4/28/2003	08:56am
segmen28.inc	6	4/28/2003	08:56am
seisWPPc.k	12	4/28/2003	08:56am
1E-5\RN7			
a2h1.dat	26	4/28/2003	08:59am
a2h2.dat	28	4/28/2003	08:59am
a2v.dat	26	4/28/2003	08:59am
constraint.dat	7	4/28/2003	08:59am
d3hsp	6718	4/28/2003	08:59am
d3hsp1	90	4/28/2003	08:59am
d3plot	8667	4/28/2003	08:58am
d3plot329	6214	4/28/2003	08:58am
element.inc	1577	4/28/2003	08:59am
messag	19	4/28/2003	08:59am
messag0	150	4/28/2003	08:59am
nodes.inc	1677	4/28/2003	08:59am
nodese10.inc	21	4/28/2003	08:59am
nodese11.inc	4	4/28/2003	08:59am

nodese12.inc	21	4/28/2003	08:59am
nodese13.inc	4	4/28/2003	08:59am
nodeset.inc	8	4/28/2003	08:59am
nodeset3.inc	15	4/28/2003	08:59am
nodeset4.inc	3	4/28/2003	08:59am
nodeset5.inc	1	4/28/2003	08:59am
relaxWPP.k	1	4/28/2003	08:59am
segmen20.inc	4	4/28/2003	08:59am
segmen21.inc	2	4/28/2003	08:59am
segmen25.inc	7	4/28/2003	08:59am
segmen26.inc	6	4/28/2003	08:59am
segmen27.inc	30	4/28/2003	08:59am
segmen28.inc	6	4/28/2003	08:59am
seisWPPc.k	12	4/28/2003	08:59am
1E-5\RN9			
a10h1.dat	8	4/28/2003	09:26am
a10h2.dat	8	4/28/2003	09:26am
a10v.dat	9	4/28/2003	09:26am
constraint.dat	7	4/28/2003	09:26am
d3hsp	6642	4/28/2003	09:26am
d3hsp1	88	4/28/2003	09:26am
d3plot	8667	4/28/2003	09:27am
d3plot409	6214	4/28/2003	09:27am
element.inc	1577	4/28/2003	09:26am
messag	18	4/28/2003	09:26am
nodes.inc	1677	4/28/2003	09:26am
nodese10.inc	21	4/28/2003	09:26am
nodese11.inc	4	4/28/2003	09:26am
nodese12.inc	21	4/28/2003	09:26am
nodese13.inc	4	4/28/2003	09:26am
nodeset.inc	8	4/28/2003	09:26am
nodeset3.inc	15	4/28/2003	09:26am
nodeset4.inc	3	4/28/2003	09:26am
nodeset5.inc	1	4/28/2003	09:26am
relaxWPP.k	1	4/28/2003	09:26am
segmen20.inc	4	4/28/2003	09:26am
segmen21.inc	2	4/28/2003	09:26am
segmen25.inc	7	4/28/2003	09:26am
segmen26.inc	6	4/28/2003	09:26am
segmen27.inc	30	4/28/2003	09:26am
segmen28.inc	6	4/28/2003	09:26am
seisWPPc.k	12	4/28/2003	09:26am
1E-4			
acc_h1.dat	240	1/30/2004	12:26pm
acc_h2.dat	240	1/30/2004	12:26pm
acc_v.dat	238	1/30/2004	12:26pm
constraint.dat	7	1/30/2004	12:26pm
d3hsp0	10540	1/30/2004	12:26pm
d3hsp01	231	1/30/2004	12:26pm
d3hsp02	86	1/30/2004	12:26pm
d3plot	8464	1/30/2004	12:27pm
d3plot523	12132	1/30/2004	12:27pm
d3plot524	6068	1/30/2004	12:26pm
element.inc	1540	1/30/2004	12:26pm

messag0	259	1/30/2004	12:26pm
messag1	205	1/30/2004	12:26pm
messag2	16	1/30/2004	12:26pm
nodes.inc	1638	1/30/2004	12:26pm
nodese10.inc	21	1/30/2004	12:26pm
nodese11.inc	4	1/30/2004	12:26pm
nodese12.inc	21	1/30/2004	12:26pm
nodese13.inc	4	1/30/2004	12:26pm
nodeset.inc	8	1/30/2004	12:26pm
nodeset3.inc	15	1/30/2004	12:26pm
nodeset4.inc	3	1/30/2004	12:26pm
nodeset5.inc	1	1/30/2004	12:26pm
relaxWPP.k	1	1/30/2004	12:26pm
segmen20.inc	4	1/30/2004	12:26pm
segmen21.inc	2	1/30/2004	12:26pm
segmen25.inc	7	1/30/2004	12:26pm
segmen26.inc	7	1/30/2004	12:26pm
segmen27.inc	30	1/30/2004	12:26pm
segmen28.inc	7	1/30/2004	12:26pm
seisWPPc.k	13	1/30/2004	12:26pm

NOTE 1: The file sizes and times may vary with operating system.
NOTE 2: The only change in Attachment X of this revision of the document, compared to the previous revision, is addition of the 1E-4 files to CD3. (The contents of CD1 and CD2 are identical to those in the previous revision and the initial issue of the document.) Nonetheless, depending on the dates the CDs were recorded, the times in Table 8-1 may be shifted for one hour from one revision to the other.

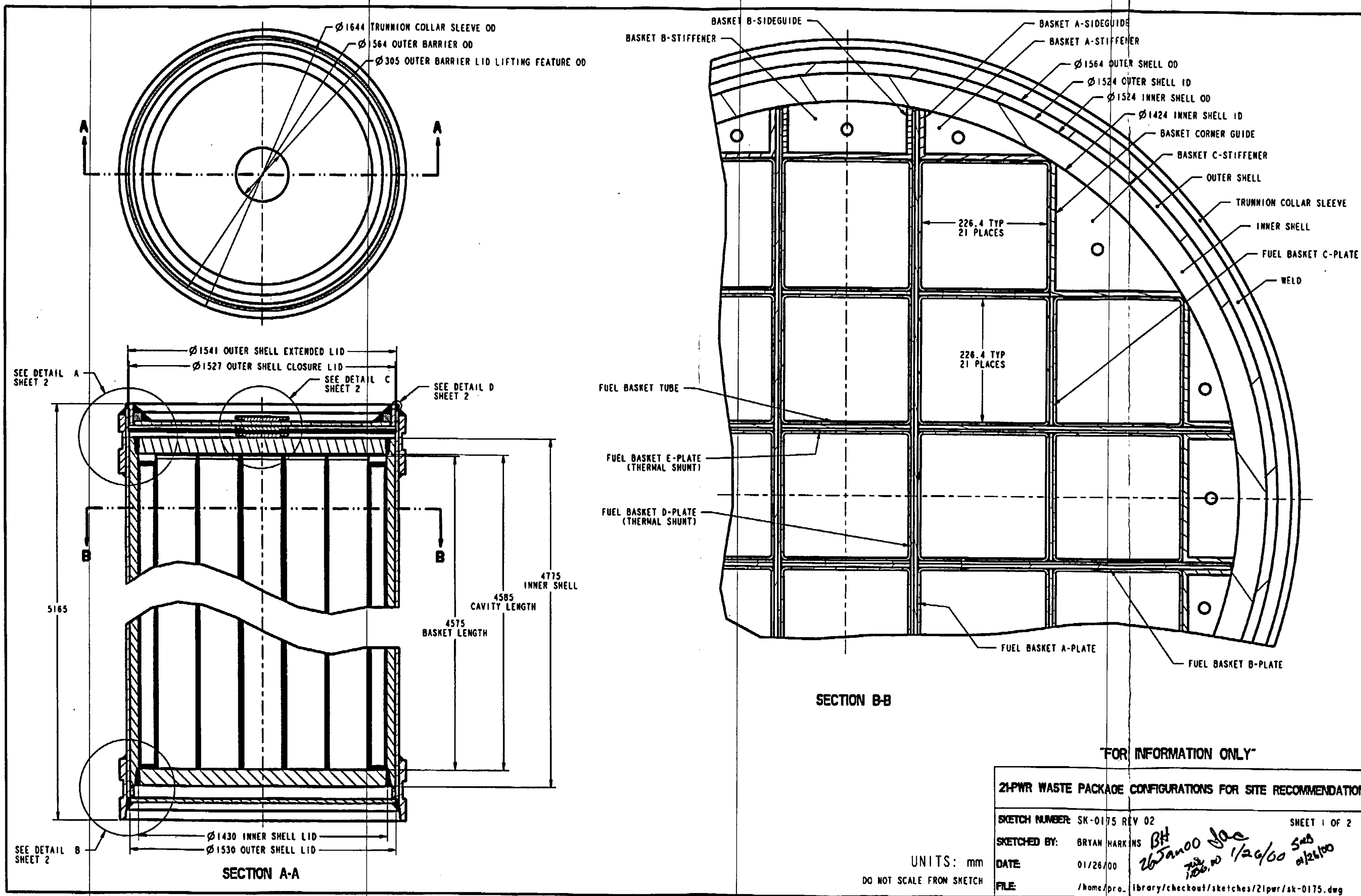
Ø1644 TRUNNION COLLAR SLEEVE OD
Ø1564 OUTER BARRIER OD
Ø305 OUTER BARRIER LID LIFTING FEATURE OD
A
A
Ø1541 OUTER SHELL EXTENDED LID
Ø1527 OUTER SHELL CLOSURE LID
SEE DETAIL A SHEET 2
SEE DETAIL C SHEET 2
SEE DETAIL D SHEET 2
B
B
5165
4775 INNER SHELL
4585 CAVITY LENGTH
4575 BASKET LENGTH
SEE DETAIL B SHEET 2
Ø1430 INNER SHELL LID
Ø1530 OUTER SHELL LID
SECTION A-A
BASKET B-SIDEGUIDE
BASKET B-STIFFENER
BASKET A-SIDEGUIDE
BASKET A-STIFFENER
Ø1564 OUTER SHELL OD
Ø1524 OUTER SHELL ID
Ø1524 INNER SHELL OD
Ø1424 INNER SHELL ID
BASKET CORNER GUIDE
BASKET C-STIFFENER
OUTER SHELL
TRUNNION COLLAR SLEEVE
INNER SHELL
FUEL BASKET C-PLATE
WELD
226.4 TYP 21 PLACES
226.4 TYP 21 PLACES
FUEL BASKET TUBE
FUEL BASKET E-PLATE (THERMAL SHUNT)
FUEL BASKET D-PLATE (THERMAL SHUNT)
FUEL BASKET A-PLATE
FUEL BASKET B-PLATE
SECTION B-B
"FOR INFORMATION ONLY"
21-PWR WASTE PACKAGE CONFIGURATIONS FOR SITE RECOMMENDATION
SKETCH NUMBER: SK-0175 REV 02
SHEET 1 OF 2
SKETCHED BY: BRYAN HARKINS
DATE: 01/26/00
FILE: /home/pro_library/checkout/sketches/21pwr/sk-0175.dwg
UNITS: mm
DO NOT SCALE FROM SKETCH

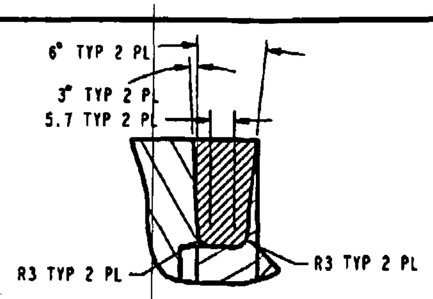

DETAIL D

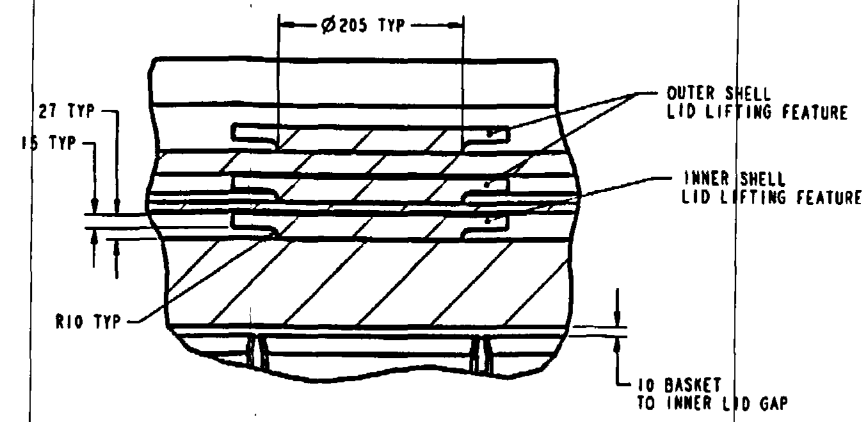

DETAIL C

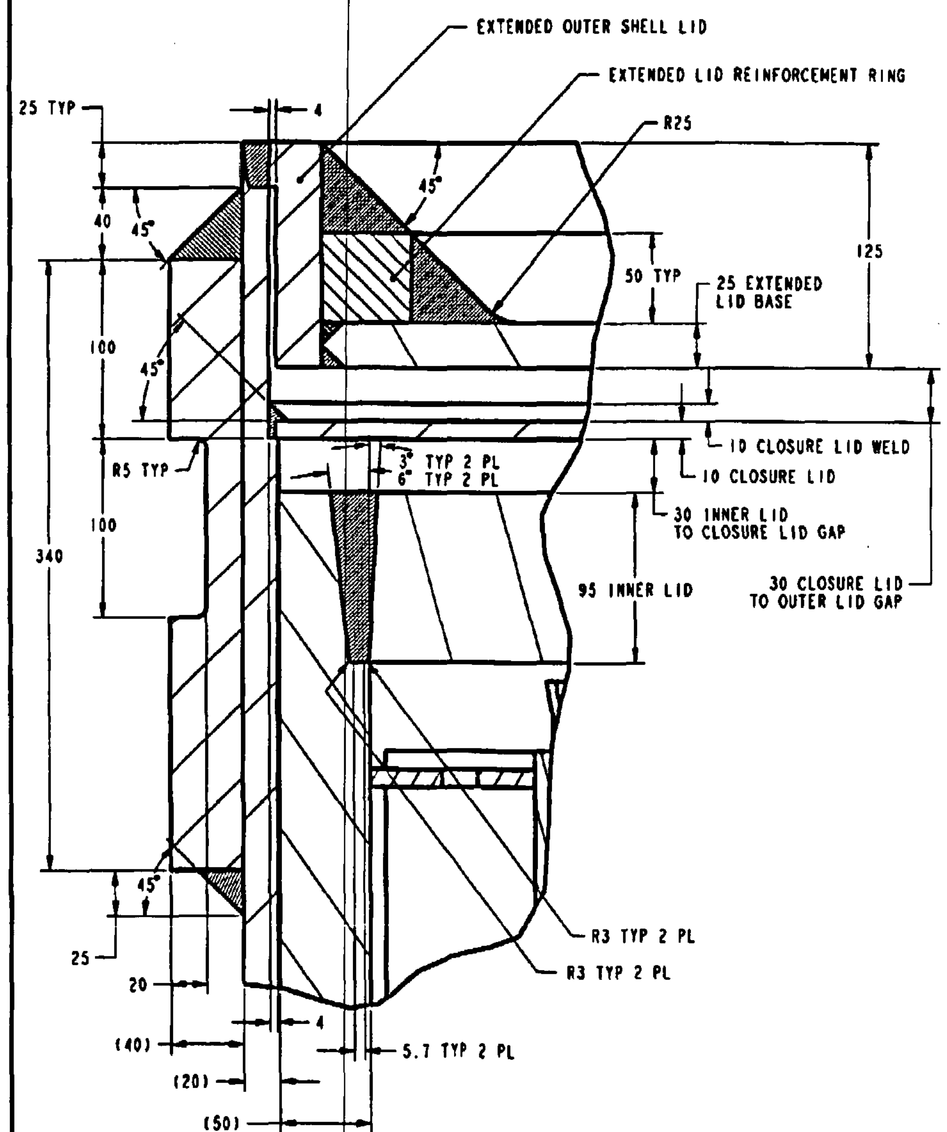

DETAIL A

21-PWR WASTE PACKAGE ASSEMBLY WITH STAINLESS STEEL/BORON PLATES

21-PWR CONTROL ROD WASTE PACKAGE ASSEMBLY WITH CARBON STEEL PLATES

COMPONENT NAME	MATERIAL	THICKNESS	MASS (KG)	QTY ROD
BASKET A-SIDEGUIDE	SA-516 K02700	10	27	32
BASKET A-STIFFENER	SA-516 K02700	10	0.72	64
BASKET B-SIDEGUIDE	SA-516 K02700	10	36	16
BASKET B-STIFFENER	SA-516 K02700	10	1.5	32
BASKET C-STIFFENER	SA-516 K02700	10	2.3	32
BASKET CORNERGUIDE	SA-516 K02700	10	42	16
FUEL BASKET A-PLATE	NEUTRONIT A 978	7	85	8
	#SA-516 K02700	#7	#86	#8
FUEL BASKET B-PLATE	NEUTRONIT A 978	7	85	8
	#SA-516 K02700	#7	#86	#8
FUEL BASKET C-PLATE	NEUTRONIT A 978	7	44	16
	#SA-516 K02700	#7	#45	#16
FUEL BASKET D-PLATE	SB-209 A96061 T4	5	21	8
FUEL BASKET E-PLATE	SB-209 A96061 T4	5	21	8
FUEL BASKET TUBE	SA-516 K02700	5	164	21
INNER SHELL	SA-240 S31600	50	8709	1
INNER SHELL LID	SA-240 S31600	95	1200	2
INNER LID LIFTING FEATURE	SA-240 S31600	27	12	1
OUTER SHELL	SB-575 N06022	20	4193	1
EXTENDED OUTER SHELL LID	SB-575 N06022	25	132	1
EXTENDED OUTER SHELL LID BASE	SB-575 N06022	25	366	1
OUTER LID LIFTING FEATURE	SB-575 N06022	27	13	2
EXTENDED LID REINFORCEMENT RING	SB-575 N06022	50	97	1
OUTER SHELL FLAT CLOSURE LID	SB-575 N06022	10	159	1
OUTER SHELL FLAT BOTTOM LID	SB-575 N0-6022	25	396	1
UPPER TRUNNION COLLAR SLEEVE	SB-575 N06022	40	507	1
LOWER TRUNNION COLLAR SLEEVE	SB-575 N06022	40	497	1
INNER SHELL SUPPORT RING	SB-575 N06022	20	41	1
TOTAL ALLOY 22 WELDS	SFA-5.14 N06022	-	249	**
TOTAL 316 WELDS	SFA-5.9 S31680	-	128	**
WASTE PACKAGE ASSEMBLY	-	-	26035	1
	-	-	#26059	#1
PWR FUEL ASSEMBLY	-	-	773.4*	21
WP ASSEMBLY WITH SNF	-	-	42277	1
	-	-	#42301	#1

* CRWMS M&O 1997. WASTE CONTAINER CAVITY SIZE DETERMINATION. BBAA00000-01717-0200-00026 REV 00. LAS VEGAS, NV: CRWMS M&O. ACC: MOL.19980106.0061

** REFER TO SK-0191 REV 00 "21-PWR WASTE PACKAGE WELD CONFIGURATION"

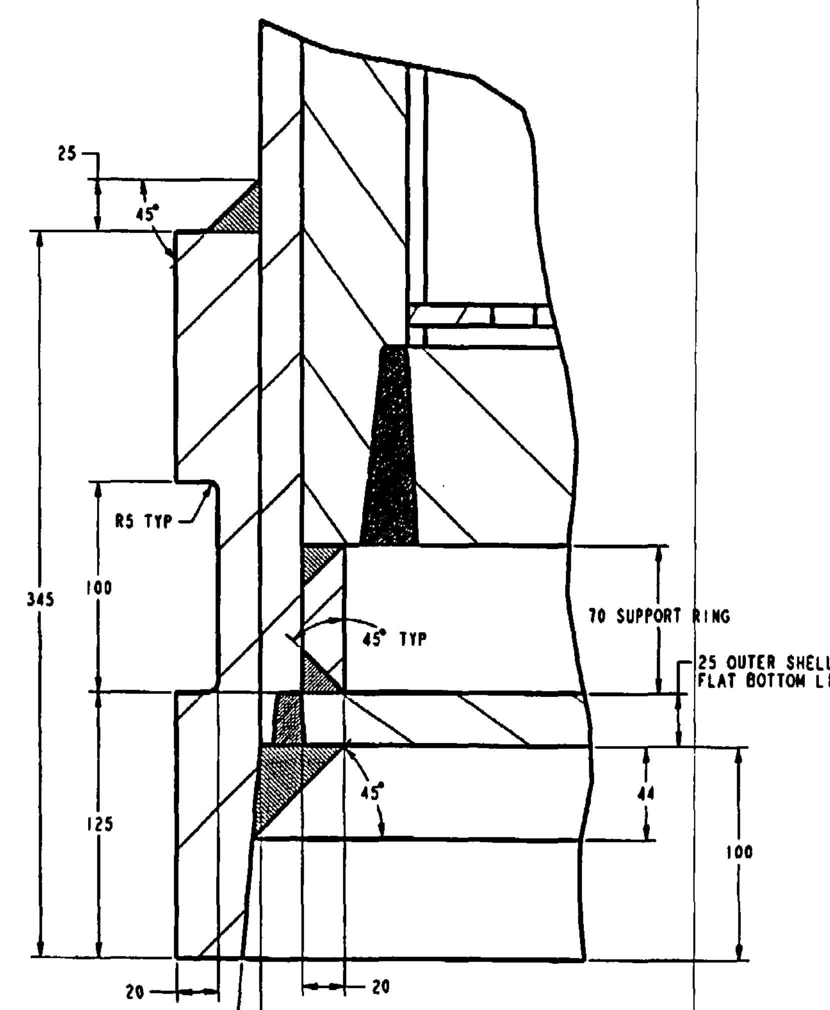

DETAIL B

02 SMB 01/27/00

SK-0175 REV ~~01~~	SHEET 2 OF 2

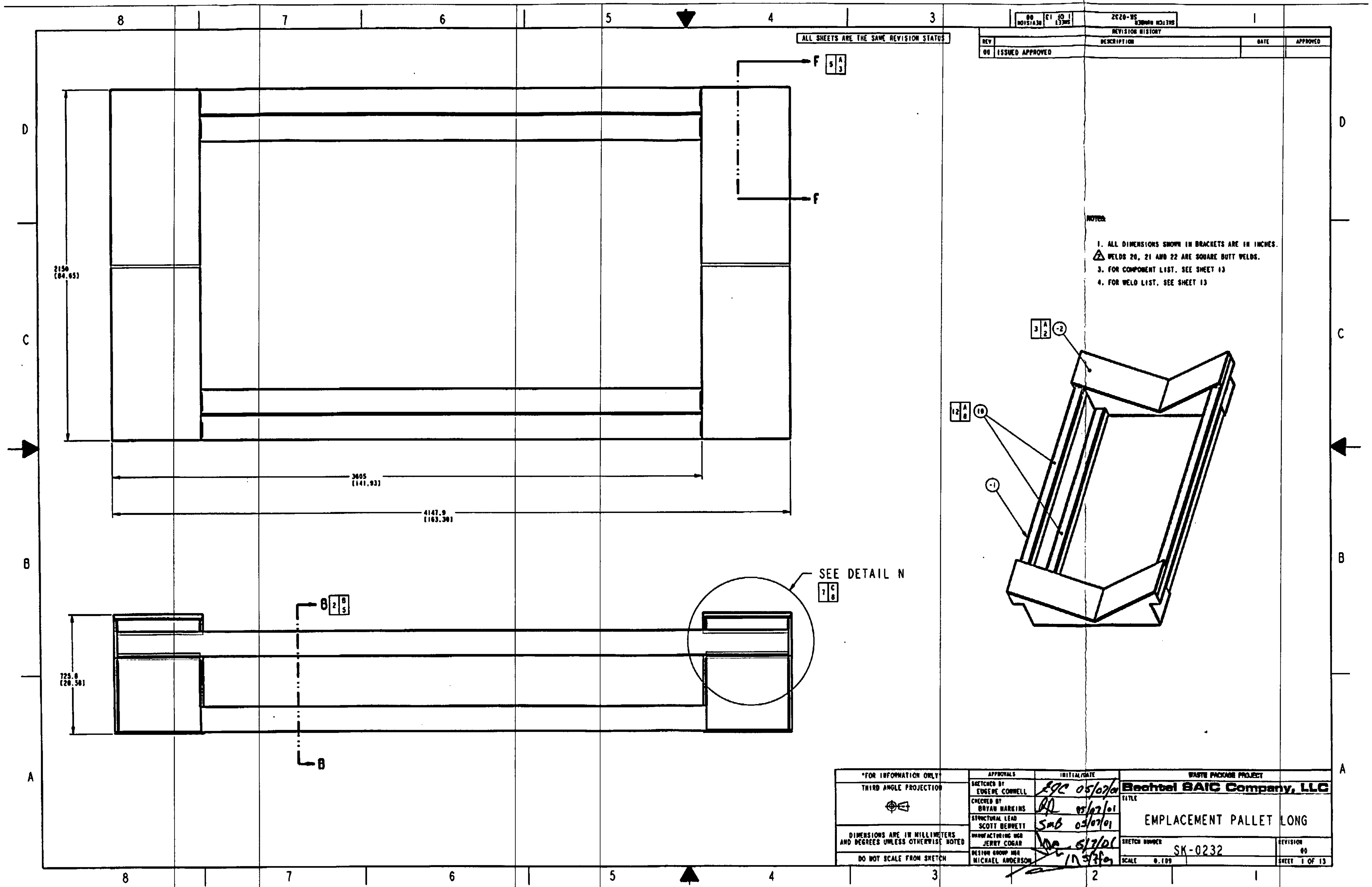
ALL SHEETS ARE THE SAME REVISION STATUS
REVISION HISTORY
REV | DESCRIPTION | DATE | APPROVED
00 ISSUED APPROVED
NOTES:
1. ALL DIMENSIONS SHOWN IN BRACKETS ARE IN INCHES.
2. WELDS 20, 21 AND 22 ARE SQUARE BUTT WELDS.
3. FOR COMPONENT LIST, SEE SHEET 13
4. FOR WELD LIST, SEE SHEET 13
2150 [84.65]
3605 [141.93]
4147.9 [163.30]
725.8 [28.58]
SEE DETAIL N
"FOR INFORMATION ONLY"
THIRD ANGLE PROJECTION
DIMENSIONS ARE IN MILLIMETERS AND DEGREES UNLESS OTHERWISE NOTED
DO NOT SCALE FROM SKETCH
APPROVALS
INITIAL/DATE
SKETCHED BY EUGENE CONNELL 05/07/01
CHECKED BY BRYAN HARKINS 05/07/01
STRUCTURAL LEAD SCOTT BENNETT 05/07/01
MANUFACTURING MGR JERRY COGAR 5/7/01
DESIGN GROUP MGR MICHAEL ANDERSON
WASTE PACKAGE PROJECT
Bechtel SAIC Company, LLC
TITLE
EMPLACEMENT PALLET LONG
SKETCH NUMBER SK-0232
REVISION 00
SCALE 0.109
SHEET 1 OF 13

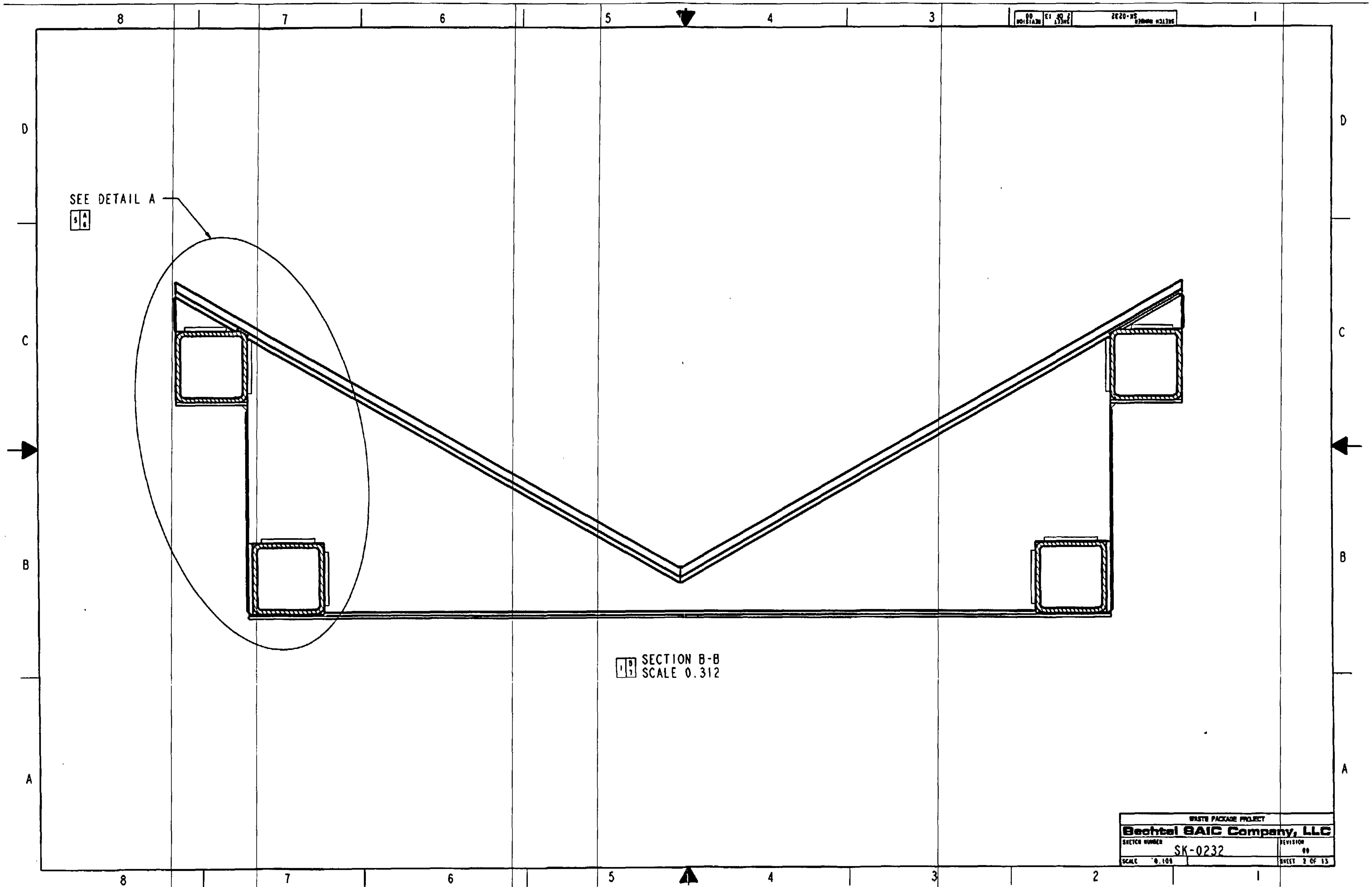
SEE DETAIL A
SECTION B-B
SCALE 0.312
WASTE PACKAGE PROJECT
Bechtel SAIC Company, LLC
SK-0232

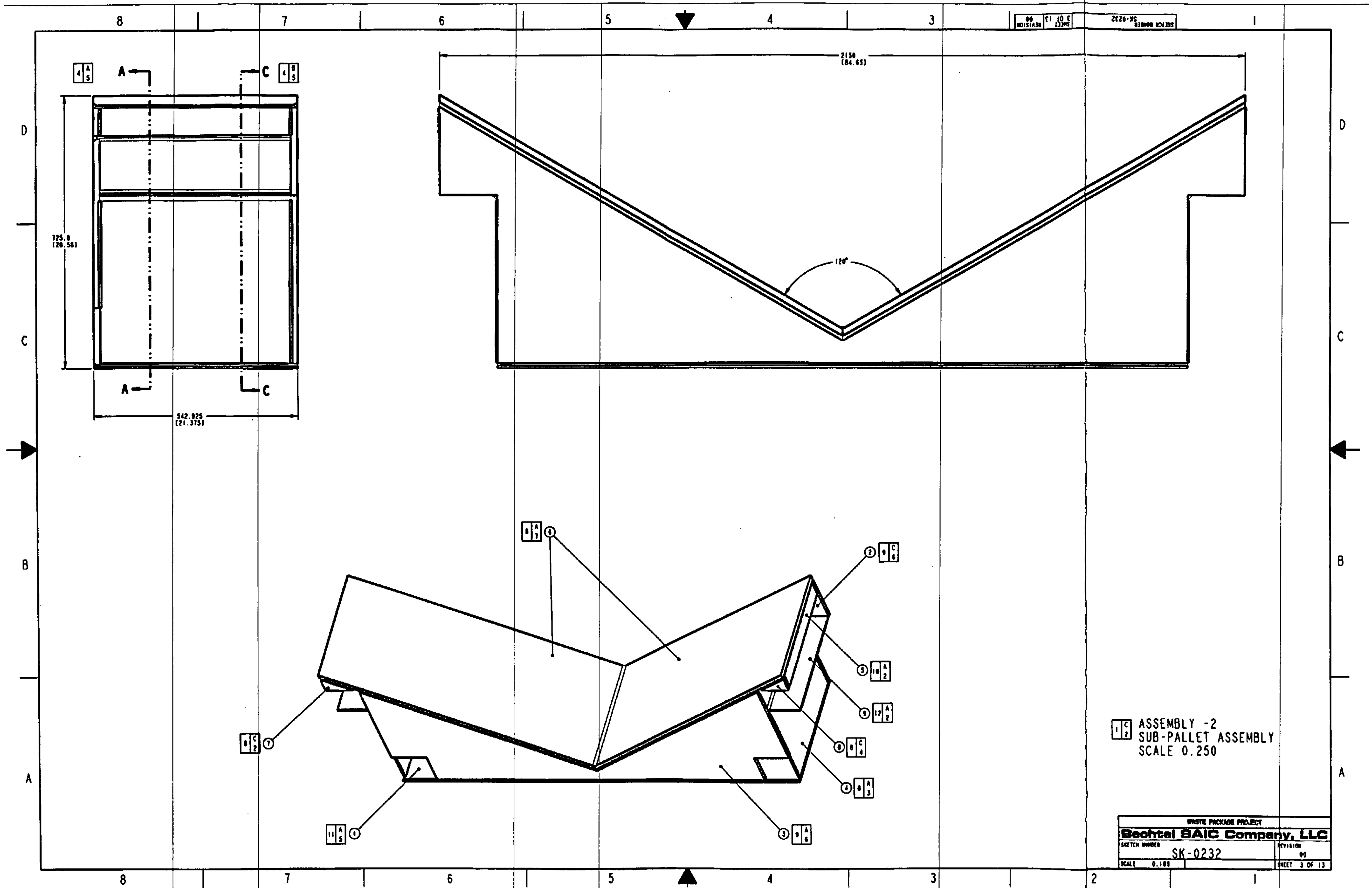
A
C
2150
[84.65]
120°
725.8
[28.58]
542.925
[21.375]
ASSEMBLY -2
SUB-PALLET ASSEMBLY
SCALE 0.250
WASTE PACKAGE PROJECT
Bechtel SAIC Company, LLC
SKETCH NUMBER
SK-0232
REVISION
00
SCALE 0.100
SHEET 3 OF 13

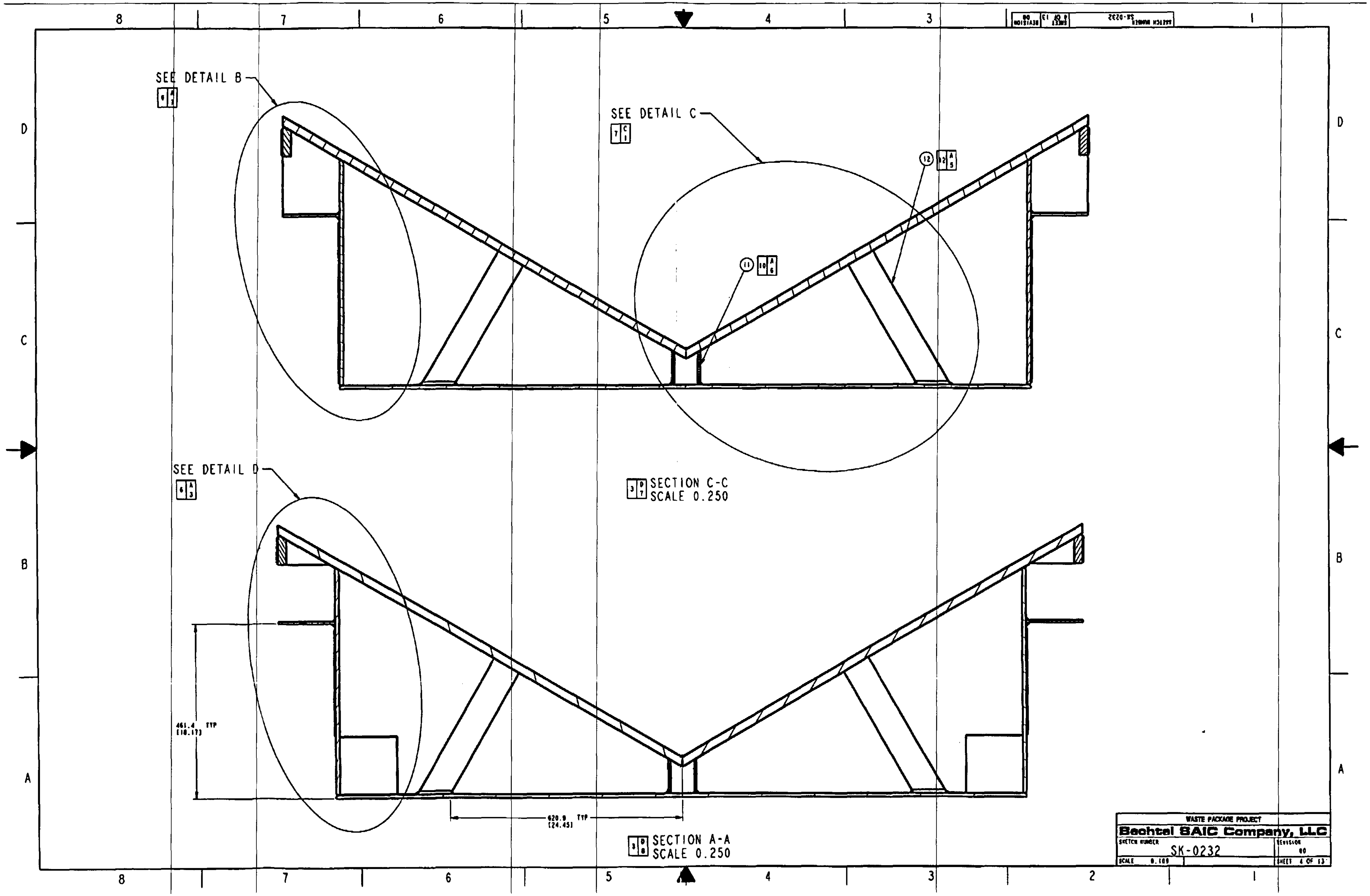
SEE DETAIL B
SEE DETAIL C
SEE DETAIL D
SECTION C-C
SCALE 0.250
SECTION A-A
SCALE 0.250
461.4 TYP
[18.17]
620.9 TYP
[24.45]
WASTE PACKAGE PROJECT
Bechtel SAIC Company, LLC
SK-0232
D
C
B
A
8
7
6
5
4
3
2
1

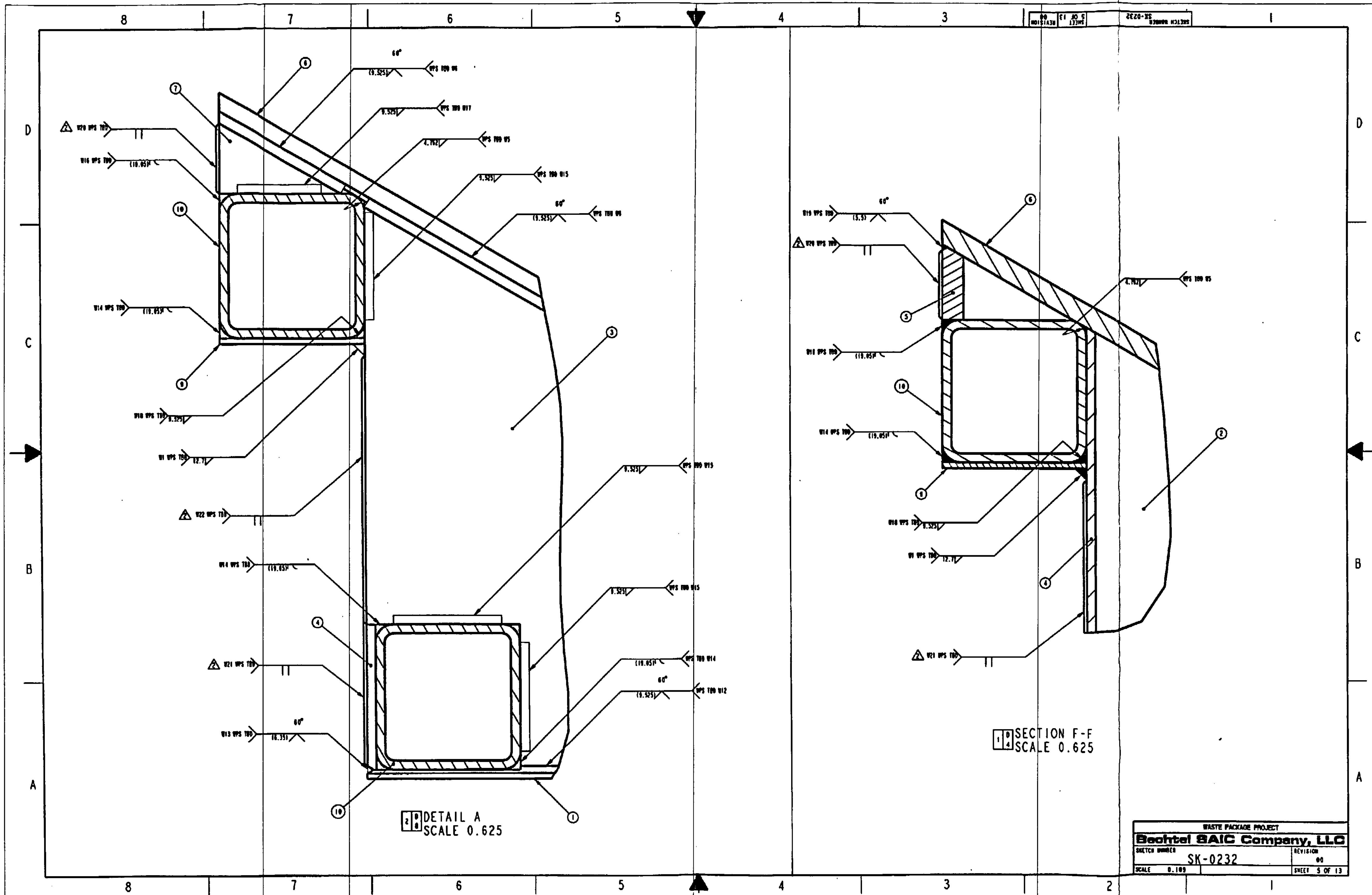
DETAIL A
SCALE 0.625
SECTION F-F
SCALE 0.625
WASTE PACKAGE PROJECT
Bechtel SAIC Company, LLC
SK-0232
SHEET 5 OF 13

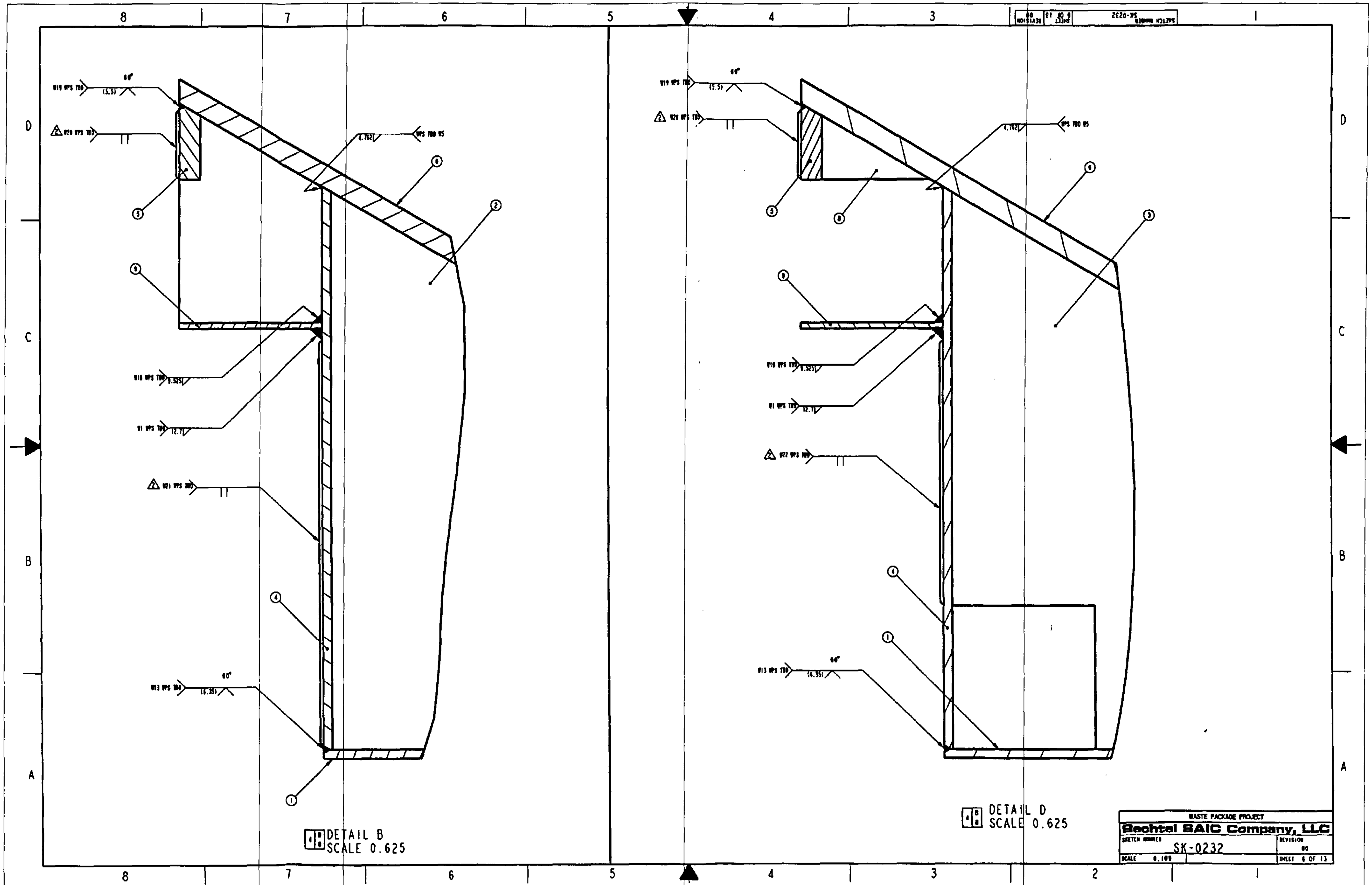
DETAIL B
SCALE 0.625
DETAIL D
SCALE 0.625
WASTE PACKAGE PROJECT
Bechtel SAIC Company, LLC
SK-0232
SHEET 6 OF 13

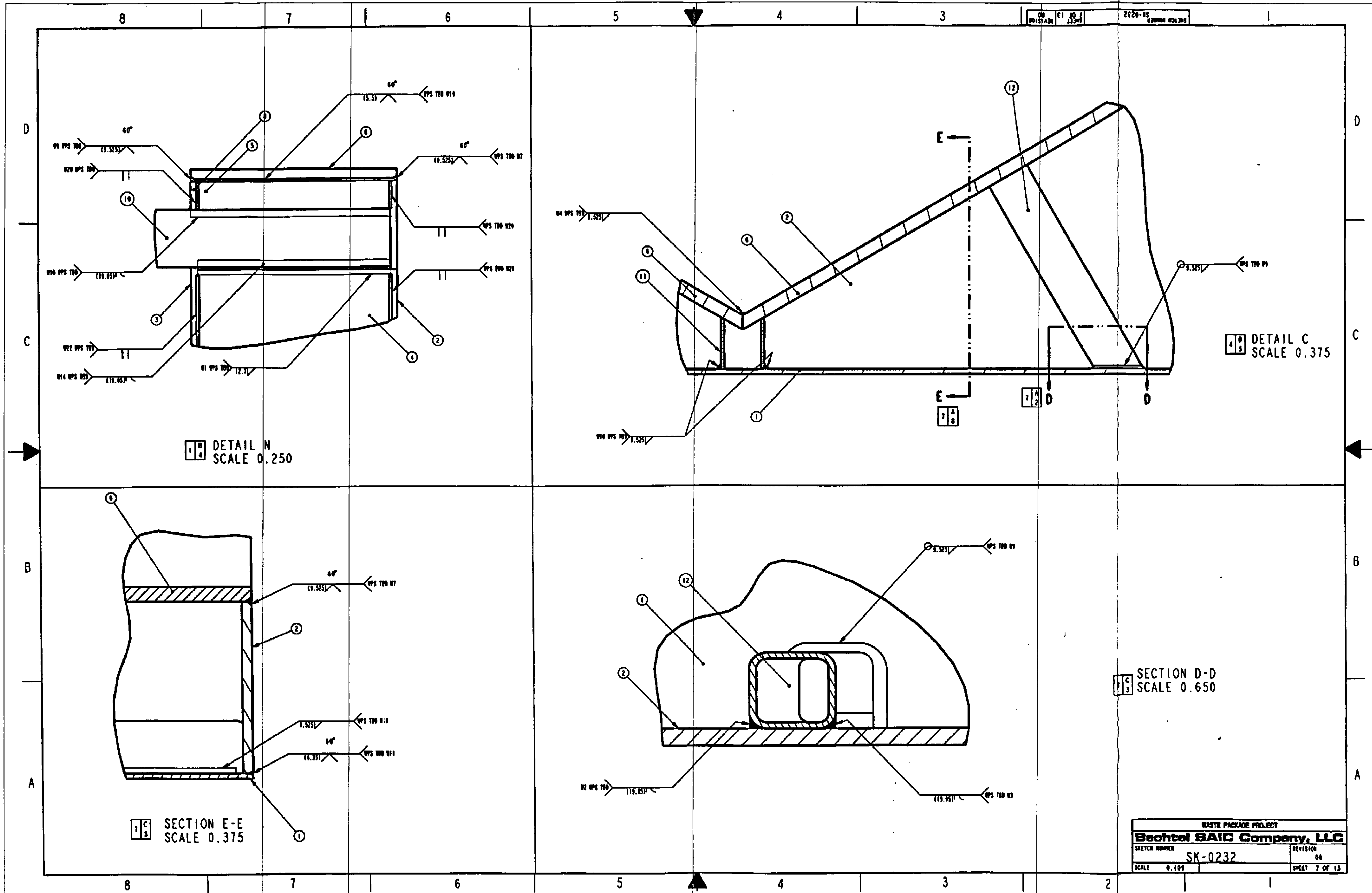
DETAIL N
SCALE 0.250
DETAIL C
SCALE 0.375
SECTION E-E
SCALE 0.375
SECTION D-D
SCALE 0.650
WASTE PACKAGE PROJECT
Bechtel SAIC Company, LLC
SK-0232
00
7 OF 13

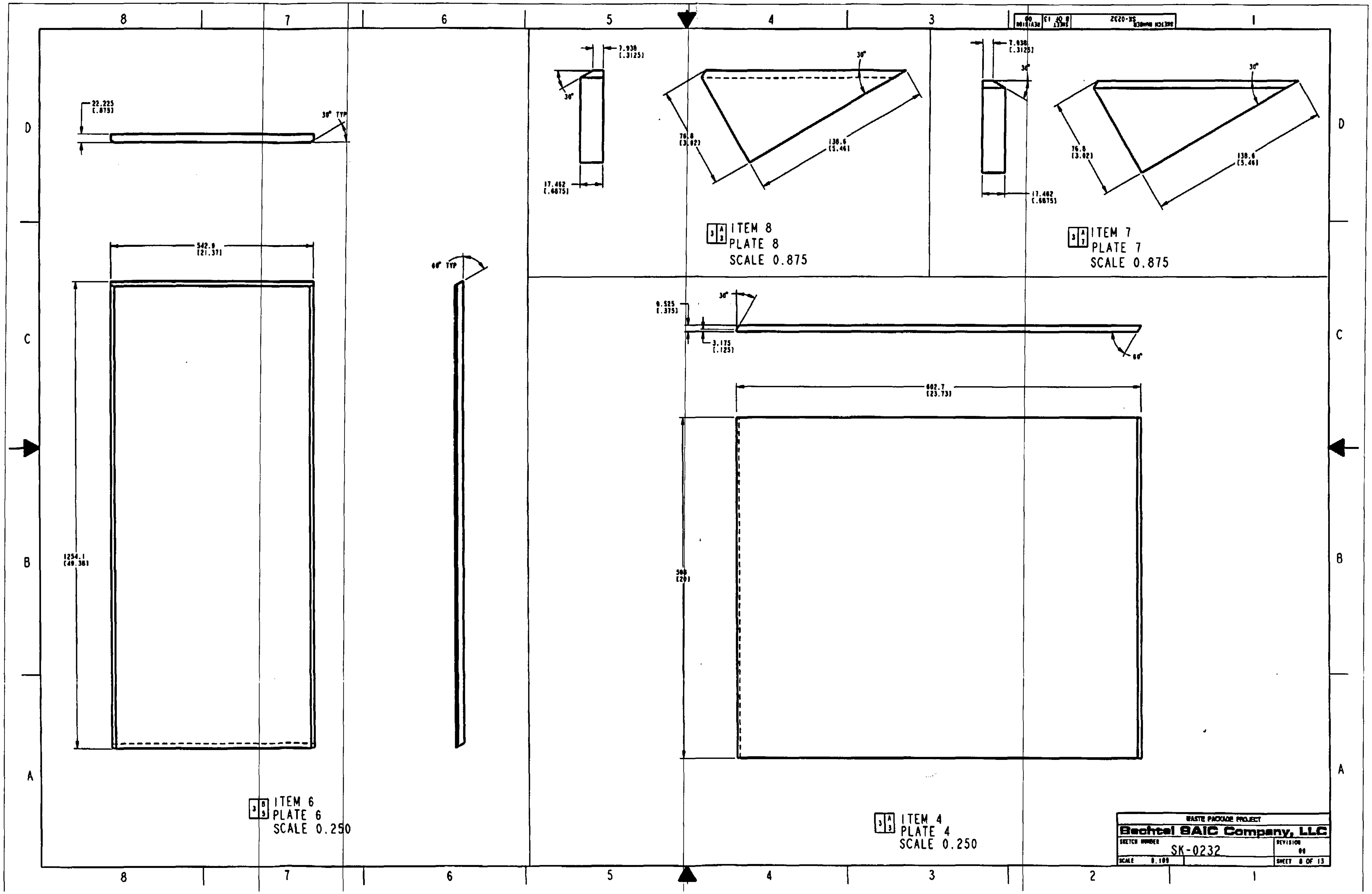
ITEM 6
PLATE 6
SCALE 0.250
ITEM 8
PLATE 8
SCALE 0.875
ITEM 7
PLATE 7
SCALE 0.875
ITEM 4
PLATE 4
SCALE 0.250
WASTE PACKAGE PROJECT
Bechtel SAIC Company, LLC
SK-0232

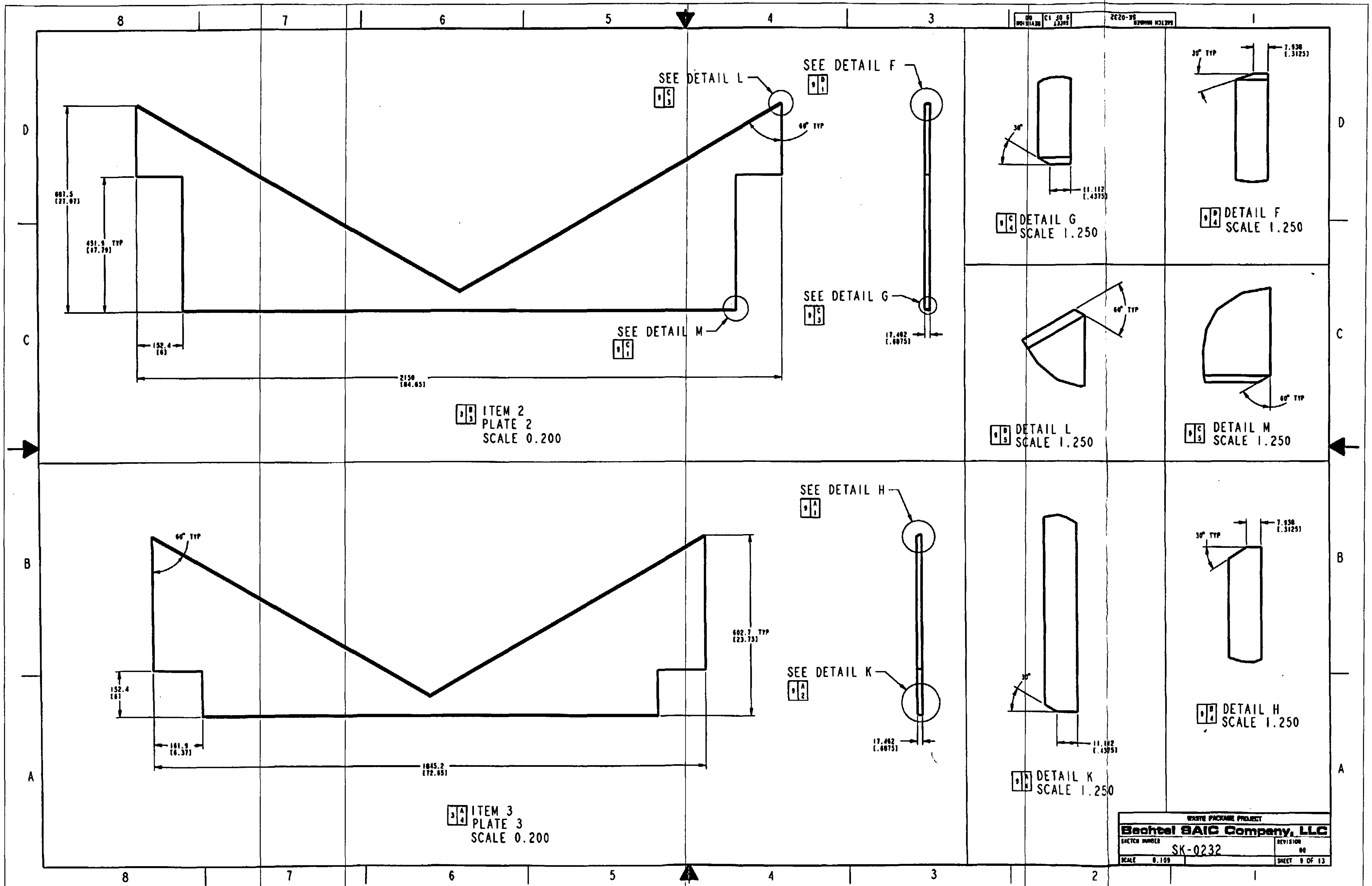
SEE DETAIL L
SEE DETAIL F
SEE DETAIL G
SEE DETAIL M
60° TYP
2150
[84.65]
152.4
[6]
ITEM 2
PLATE 2
SCALE 0.200
DETAIL G
SCALE 1.250
DETAIL F
SCALE 1.250
DETAIL L
SCALE 1.250
DETAIL M
SCALE 1.250
SEE DETAIL H
SEE DETAIL K
1845.2
[72.65]
152.4
[6]
ITEM 3
PLATE 3
SCALE 0.200
DETAIL K
SCALE 1.250
DETAIL H
SCALE 1.250
WASTE PACKAGE PROJECT
Bechtel SAIC Company, LLC
SK-0232
00

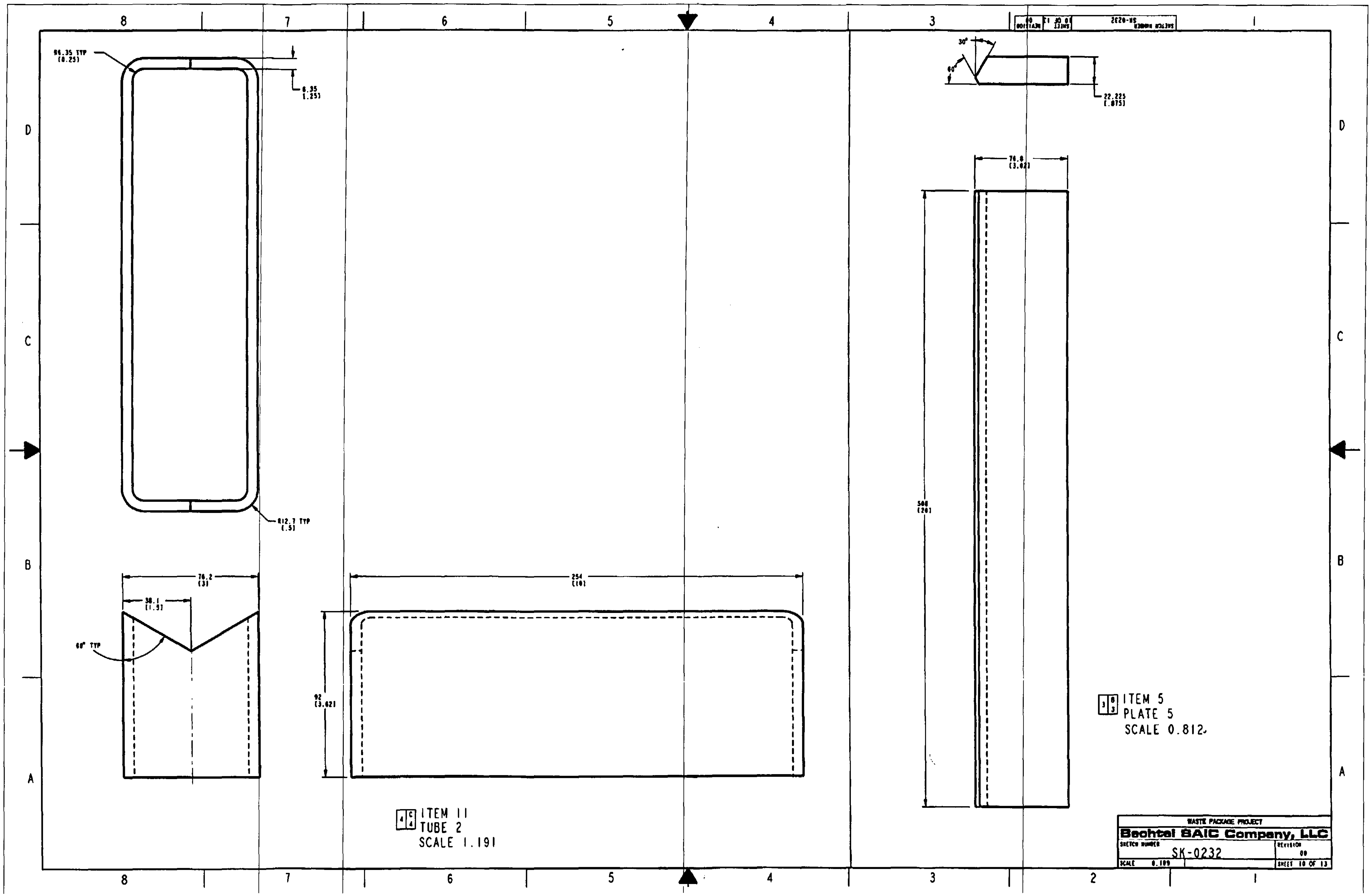
ITEM 11
TUBE 2
SCALE 1.191
ITEM 5
PLATE 5
SCALE 0.812
WASTE PACKAGE PROJECT
Bechtel SAIC Company, LLC
SK-0232

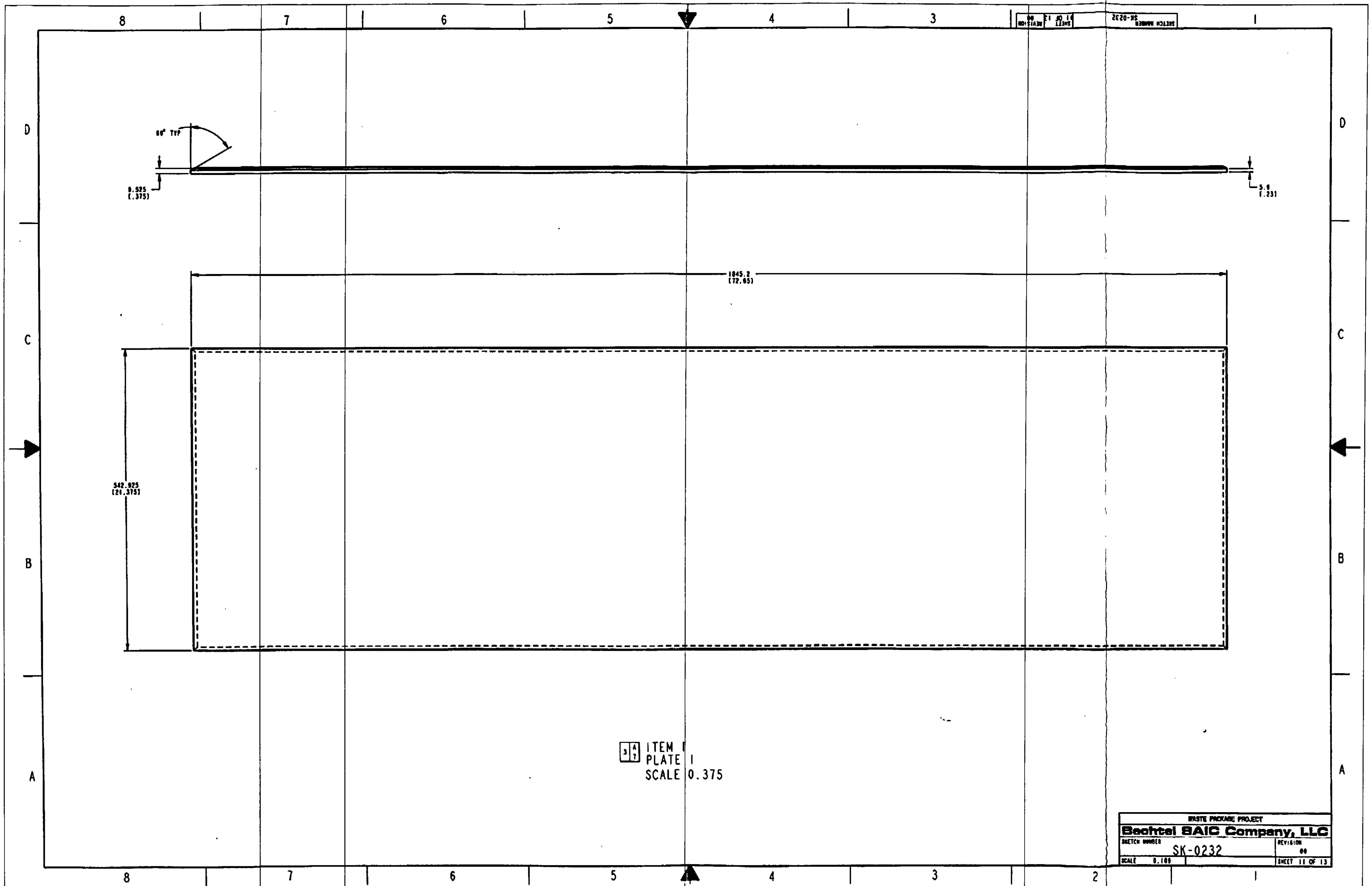
60° TYP
9.525
(.375)
5.9
(.23)
1845.2
(72.65)
542.925
(21.375)
ITEM 1
PLATE 1
SCALE 0.375
WASTE PACKAGE PROJECT
Bechtel SAIC Company, LLC
SKETCH NUMBER
SK-0232
REVISION
00
SCALE 0.109
SHEET 11 OF 13

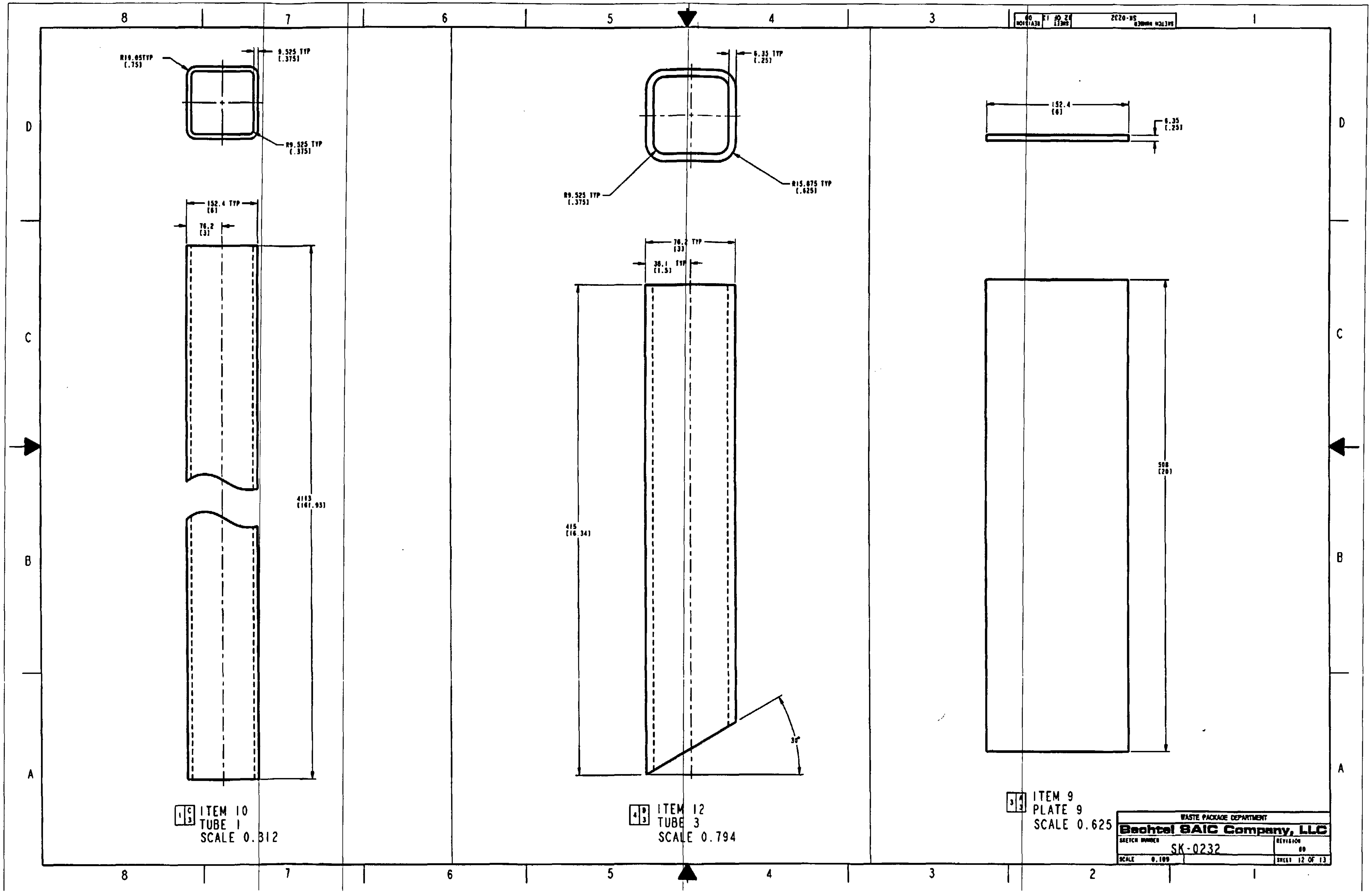
R19.05TYP
[.75]
9.525 TYP
[.375]
R9.525 TYP
[.375]
152.4 TYP
[6]
76.2
[3]
4113
[161.93]
ITEM 10
TUBE 1
SCALE 0.312
6.35 TYP
[.25]
R9.525 TYP
[.375]
R15.875 TYP
[.625]
76.2 TYP
[3]
38.1 TYP
[1.5]
415
[16.34]
30°
ITEM 12
TUBE 3
SCALE 0.794
152.4
[6]
6.35
[.25]
508
[20]
ITEM 9
PLATE 9
SCALE 0.625
WASTE PACKAGE DEPARTMENT
Bechtel SAIC Company, LLC
SKETCH NUMBER
SK-0232
REVISION
00
SCALE 0.109
SHEET 12 OF 13

COMPONENT LIST							
ITEM NUMBER	ASSEMBLY	SUBASSEMBLY	COMPONENT NAME	MATERIAL	THICKNESS	MASS (KG)	QTY REQ
-1	EMPLACEMENT PALLET LONG	-	-	-	-	1971	1
10	-	-	TUBE 1	SA-240 S31600	9.525	171	4
-2	-	SUB-PALLET ASSEMBLY	-	-	-	640	2
1	-	-	PLATE 1	SB-575 N06022	9.525	82	2
2	-	-	PLATE 2	SB-575 N06022	17.462	102	2
3	-	-	PLATE 3	SB-575 N06022	17.462	86	2
4	-	-	PLATE 4	SB-575 N06022	9.525	25	4
5	-	-	PLATE 5	SB-575 N06022	22.225	7.1	4
6	-	-	PLATE 6	SB-575 N06022	22.225	130	4
7	-	-	PLATE 7	SB-575 N06022	17.462	0.80	2
8	-	-	PLATE 8	SB-575 N06022	17.462	0.80	2
9	-	-	PLATE 9	SB-575 N06022	6.35	4.3	4
11	-	-	TUBE 2	SB-575 N06022	6.35	3.0	4
12	-	-	TUBE 3	SB-575 N06022	6.35	5.5	8
-	-	-	TOTAL ALLOY 22 WELDS	SFA-5.14 N06022	-	21	-

WELD LIST				
WELD NUMBER	WELD	MATERIAL	MASS (KG)	QTY REQ
1	FILLET	SFA-5.14 N06022	0.36	4
2	GROOVE	SFA-5.14 N06022	0.17	8
3	GROOVE	SFA-5.14 N06022	0.20	8
4	FILLET	SFA-5.14 N06022	0.19	2
5	FILLET	SFA-5.14 N06022	0.23	4
6	GROOVE	SFA-5.14 N06022	0.07	4
7	GROOVE	SFA-5.14 N06022	0.57	4
8	GROOVE	SFA-5.14 N06022	0.48	4
9	FILLET	SFA-5.14 N06022	0.08	8
10	FILLET	SFA-5.14 N06022	0.09	8
11	GROOVE	SFA-5.14 N06022	0.37	2
12	GROOVE	SFA-5.14 N06022	0.31	2
13	GROOVE	SFA-5.14 N06022	0.11	4
14	GROOVE	SFA-5.14 N06022	0.34	12
15	FILLET	SFA-5.14 N06022	0.05	12
16	GROOVE	SFA-5.14 N06022	0.35	4
17	FILLET	SFA-5.14 N06022	0.03	4
18	FILLET	SFA-5.14 N06022	0.20	4
19	GROOVE	SFA-5.14 N06022	0.08	4
20	SQUARE	SFA-5.14 N06022	0.01	8
21	SQUARE	SFA-5.14 N06022	0.04	4
22	SQUARE	SFA-5.14 N06022	0.06	4
TOTAL ALLOY 22 WELDS	-	-	21	-

WASTE PACKAGE DEPARTMENT
Bechtel SAIC Company, LLC
SKETCH NUMBER SK-0232
REVISION 00
SCALE 0.109
SHEET 13 OF 13

NAME: MCKENZIED2 OBJECT: SK-0230_REV00.1 DATE: 06-Nov-02 12:38:33

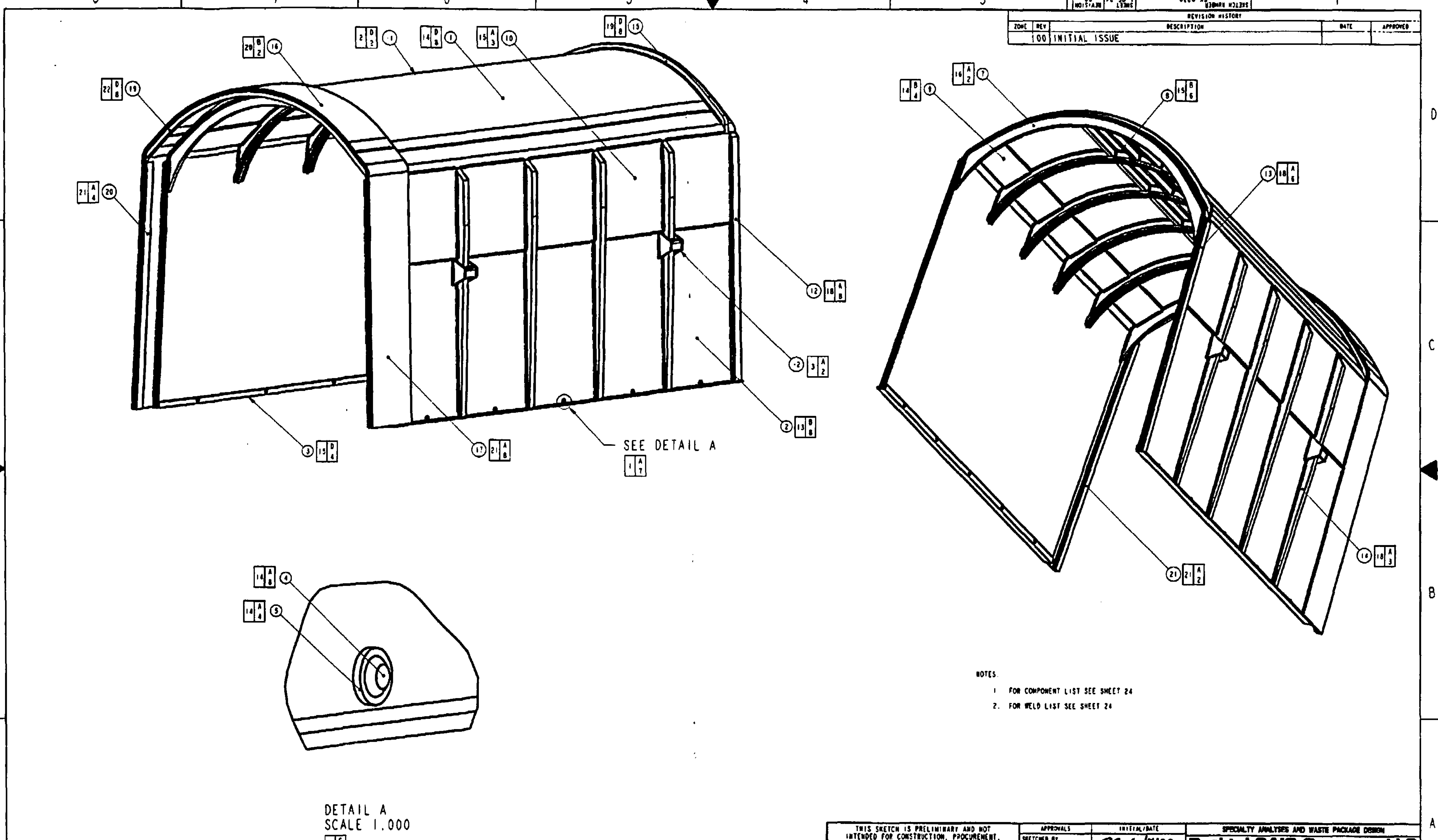

NOTES.

1. FOR COMPONENT LIST SEE SHEET 24
2. FOR WELD LIST SEE SHEET 24

THIS SKETCH IS PRELIMINARY AND NOT INTENDED FOR CONSTRUCTION, PROCUREMENT, OR FABRICATION.	APPROVALS	INITIAL/DATE	SPECIALTY ANALYSES AND WASTE PACKAGE DESIGN
ALL DIMENSIONS SHOWN ARE BASIC DIMENSIONS. THICKNESS CALCULATED FROM THE DIMENSIONS SHOWN IN THIS SKETCH ARE MINIMUMS. FOR CALCULATIONS AND ANALYSES IT IS UP TO THE ORIGINATOR TO DETERMINE APPROPRIATE TOLERANCES.	SKETCHED BY DAN McKENZIE	6NOV02	Bechtel BAIC Company, LLC
DIMENSIONS ARE IN MILLIMETERS AND DEGREES UNLESS OTHERWISE NOTED. INCH DIMENSIONS IN BRACKETS.	CHECKED BY ZEKAI CEYLAN	Z.C. 11/6/02	TITLE: INTERLOCKING DRIP SHIELD
DO NOT SCALE FROM SKETCH	APPROVED BY ADAM SCHEIDER	AKS/NOV6,2002	SKETCH NUMBER SK-0230 REVISION 00
	MANUFACTURING MGR JERRY COGAR	11/6/02	SCALE NONE SHEET 1 OF 24
	SA & WPD MGR MICHAEL ANDERSON	11/6/02	

NAME:MCKENZIED2 OBJECT:SK-0230_REV00_2 DATE:06-Nov-02 12:38:35

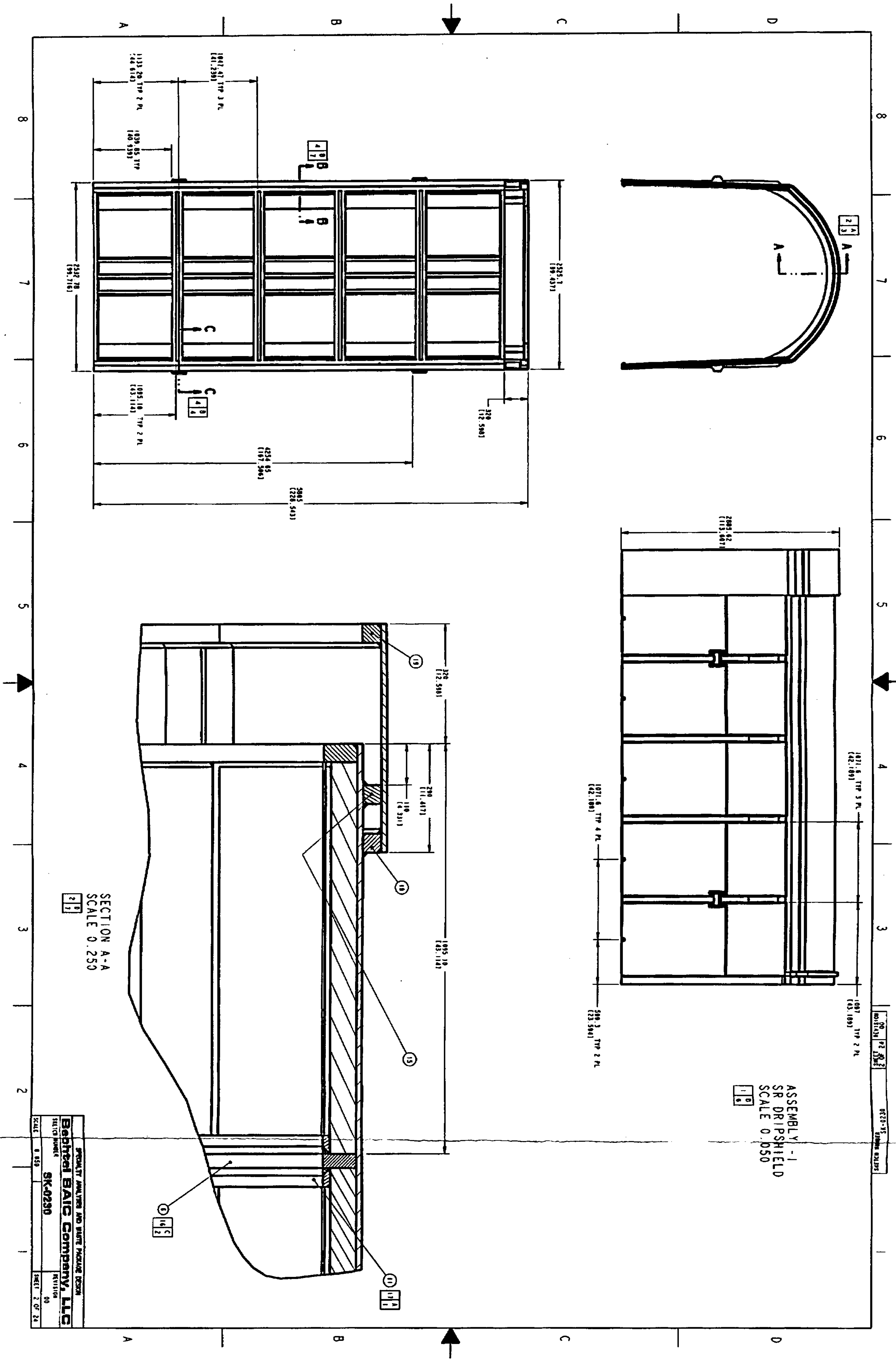

NAME:MCKENZIED2 OBJECT:SK-0230_REV00.3 DATE:06-Nov-02 12:38:38

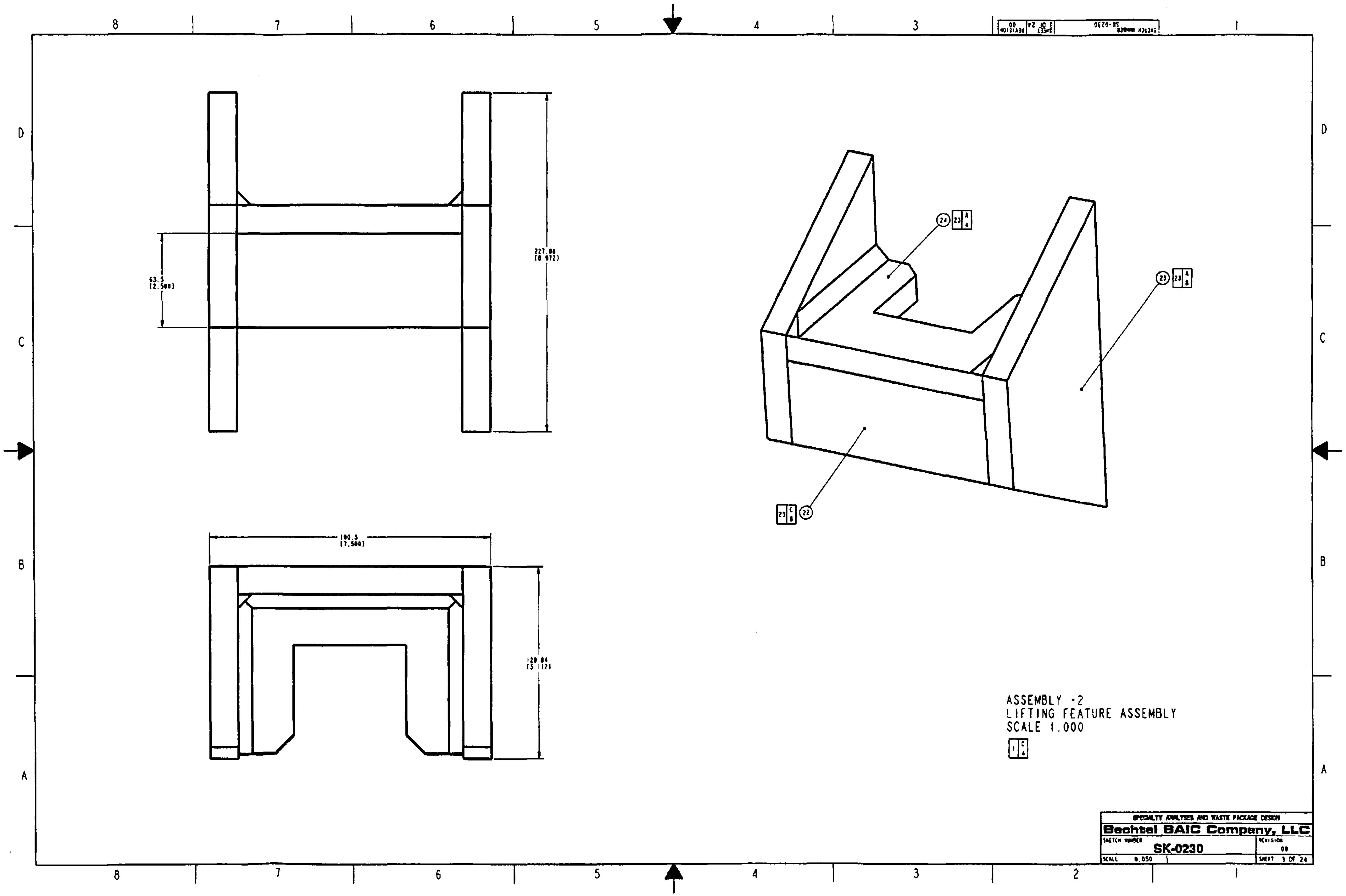

NAME:MCKENZIED2 OBJECT:SK-0230.REV00.4 DATE:06-Nov-02 12:38:38

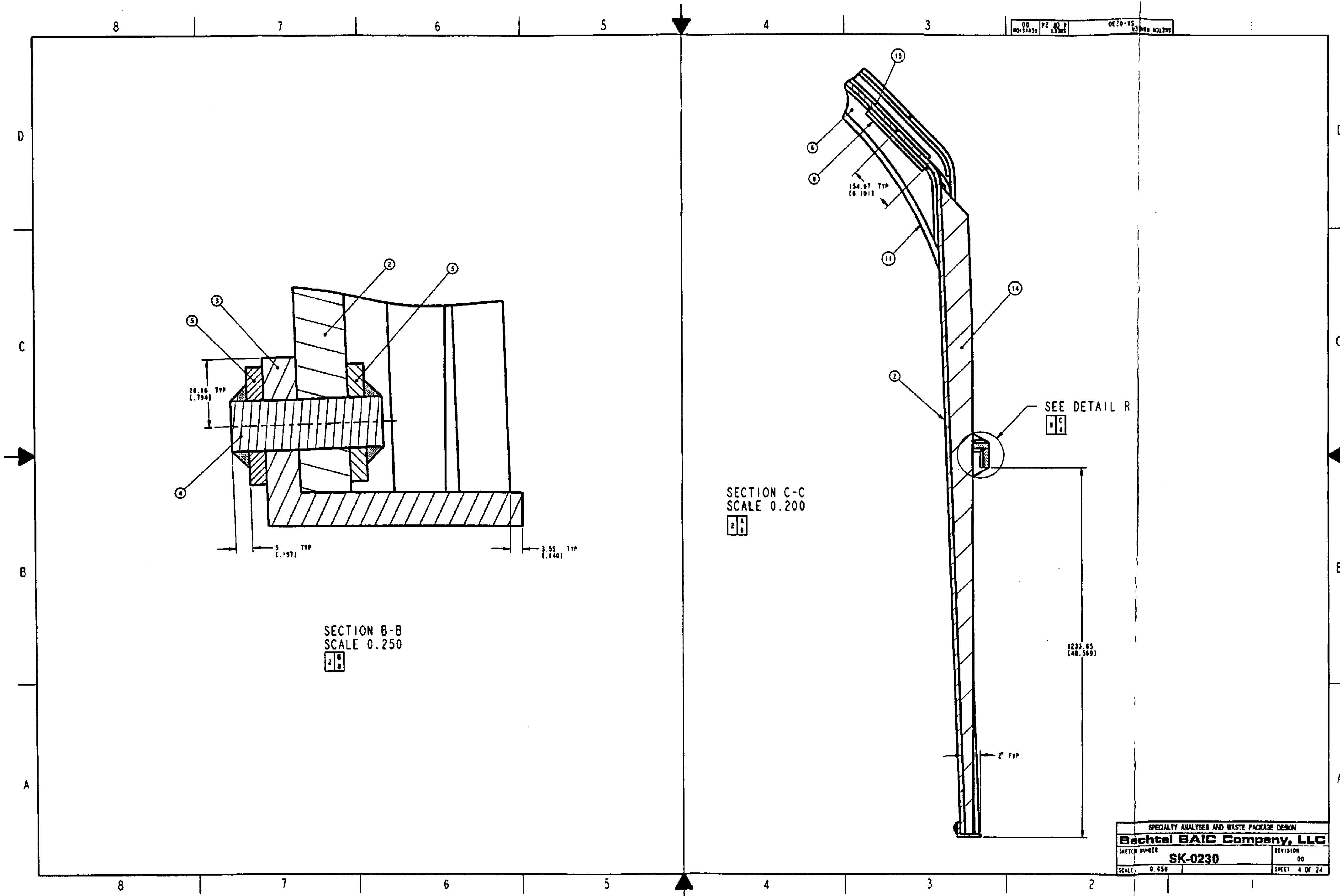

NAME:MCKENZIED2 OBJECT:SK-0230.REV00.5 DATE:06-Nov-02 12:38:40

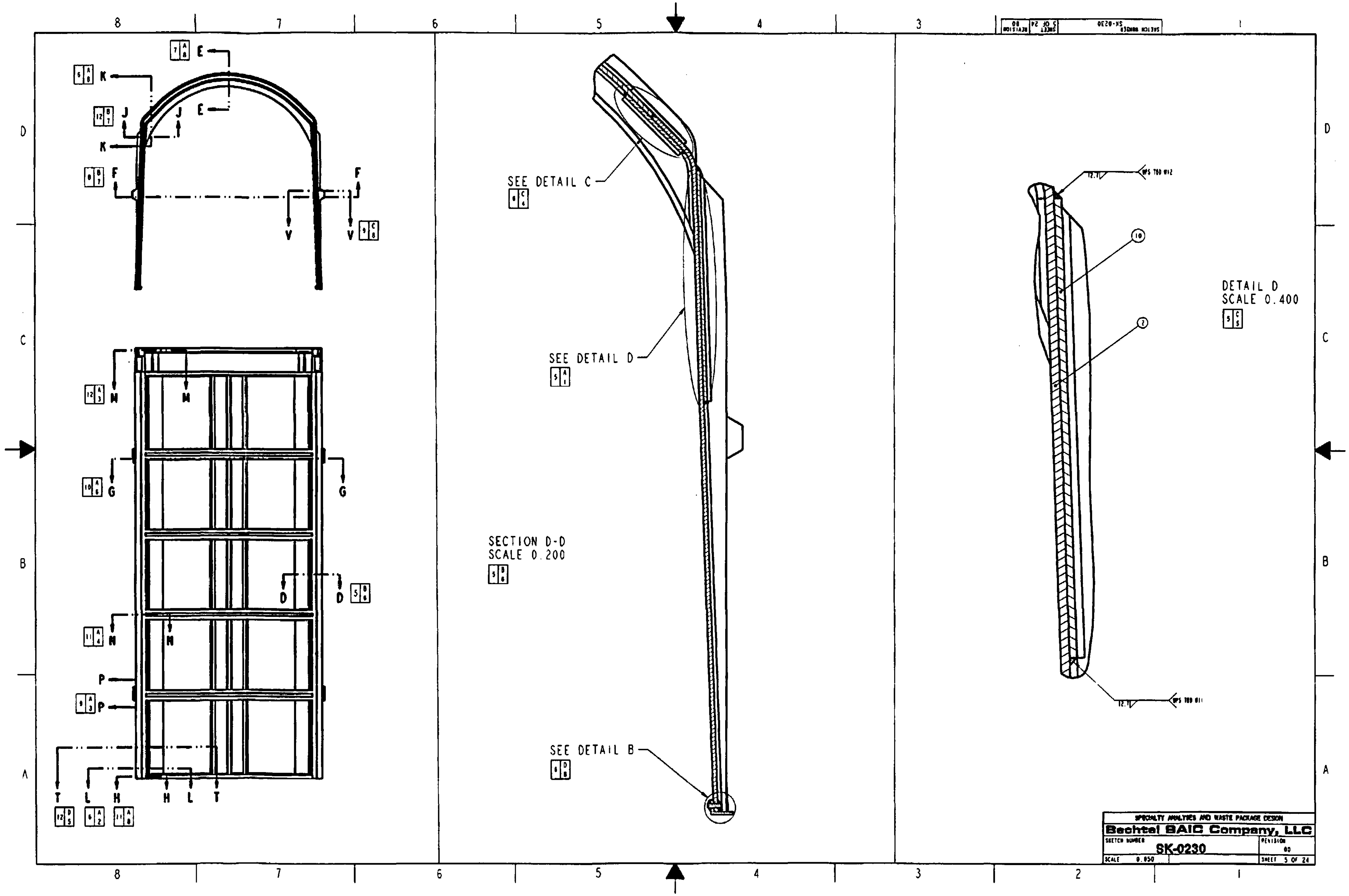

NAME:MCKENZIED2 OBJECT:SK-0230_REV00_6 DATE:06-Nov-02 12:38:42

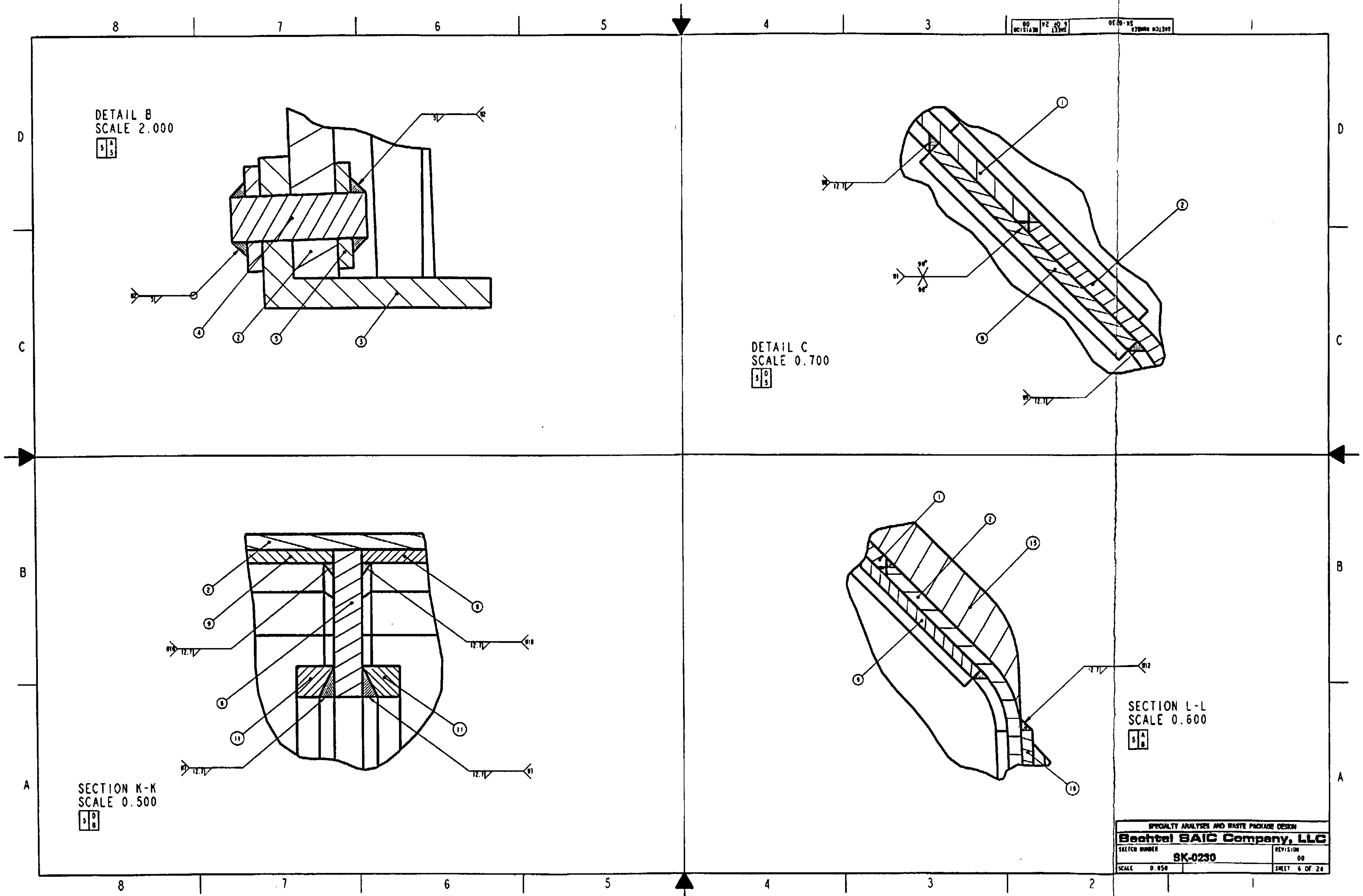

NAME:MCKENZIED2 OBJECT:SK-0230_REV00.7 DATE:06-Nov-02 12:38:43

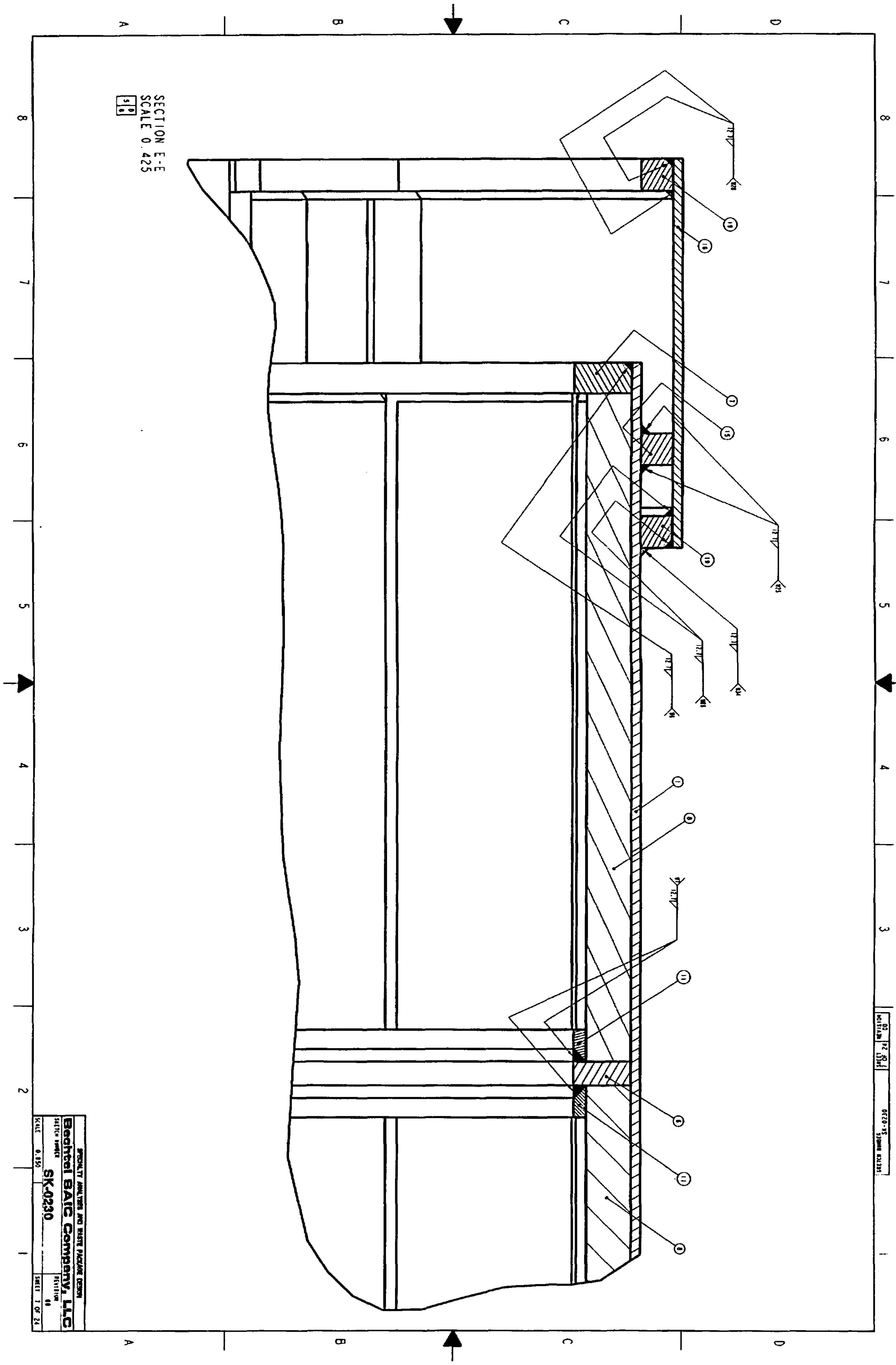

NAME:MCKENZIED2 OBJECT:SK-0230.REV00.8 DATE:06-Nov-02 12:38:44

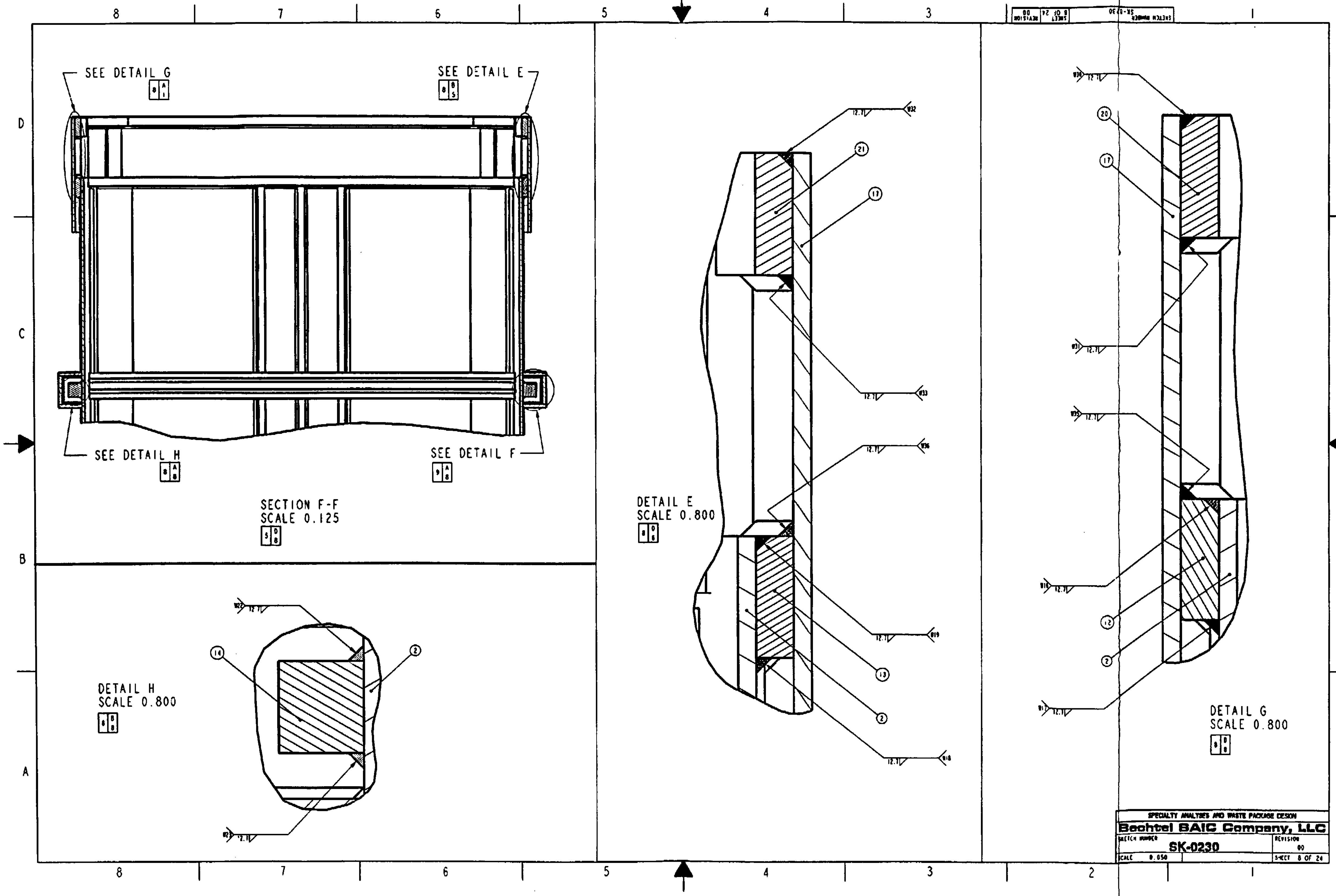

NAME:MCKENZIED2 OBJECT:SK-0230_REV00_9 DATE:06-Nov-02 12:38:46

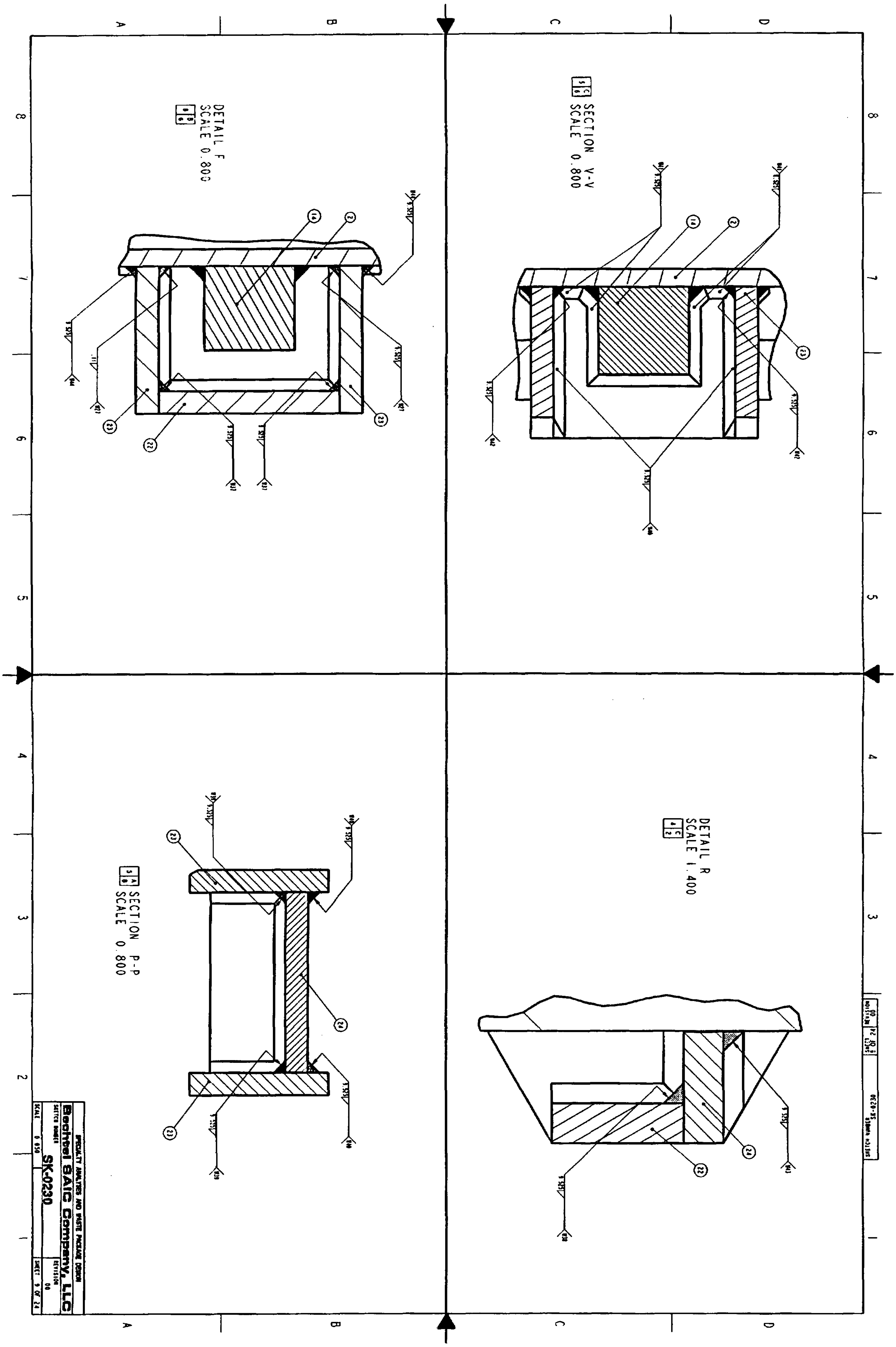

NAME:MCKENZIED2 OBJECT:SK-0230_REV00_10 DATE:06-Nov-02 12:38:48

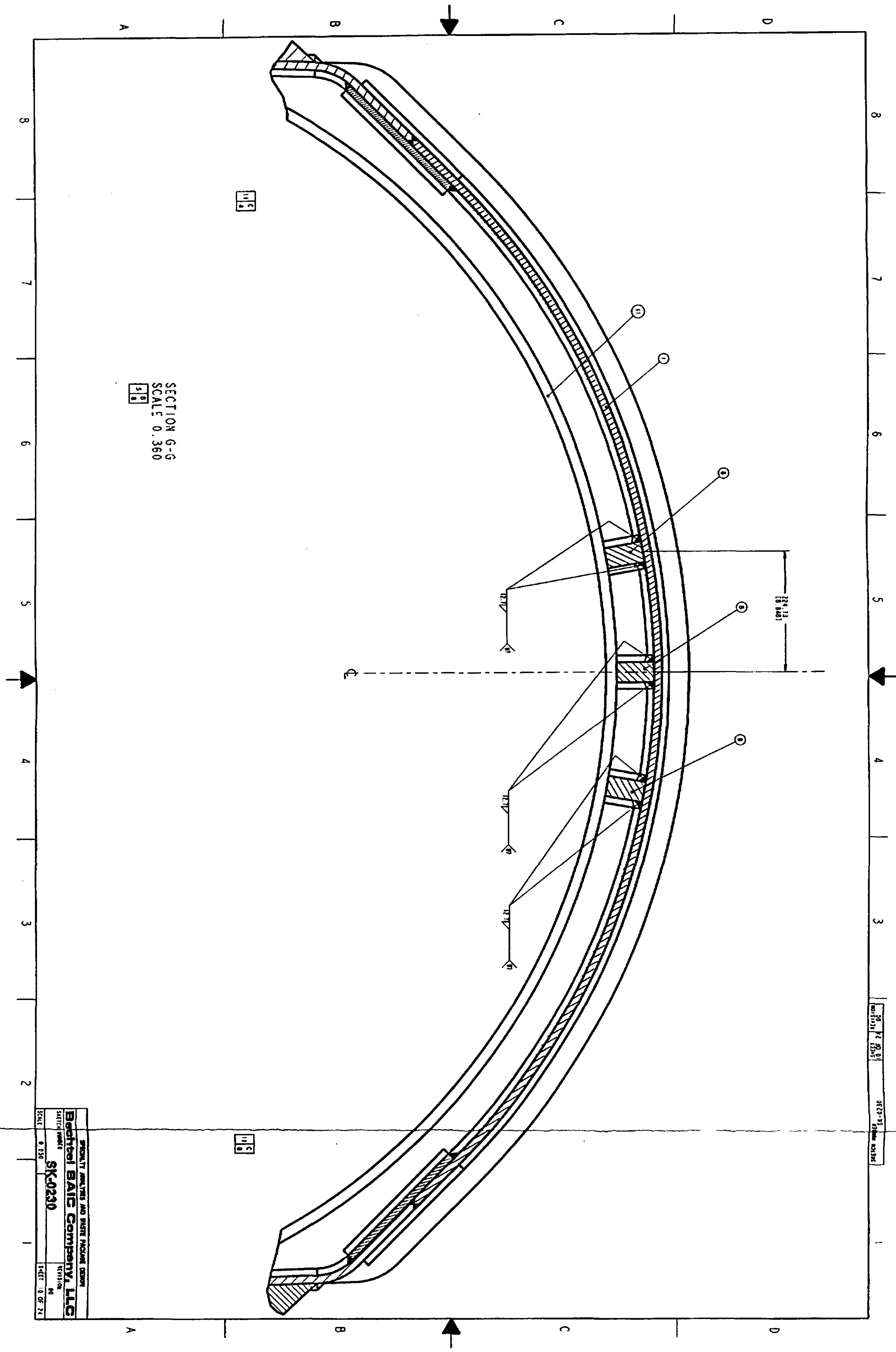

NAME:MCKENZIED2 OBJECT:SK-0230_REV00.11 DATE:06-Nov-02 12:38:49

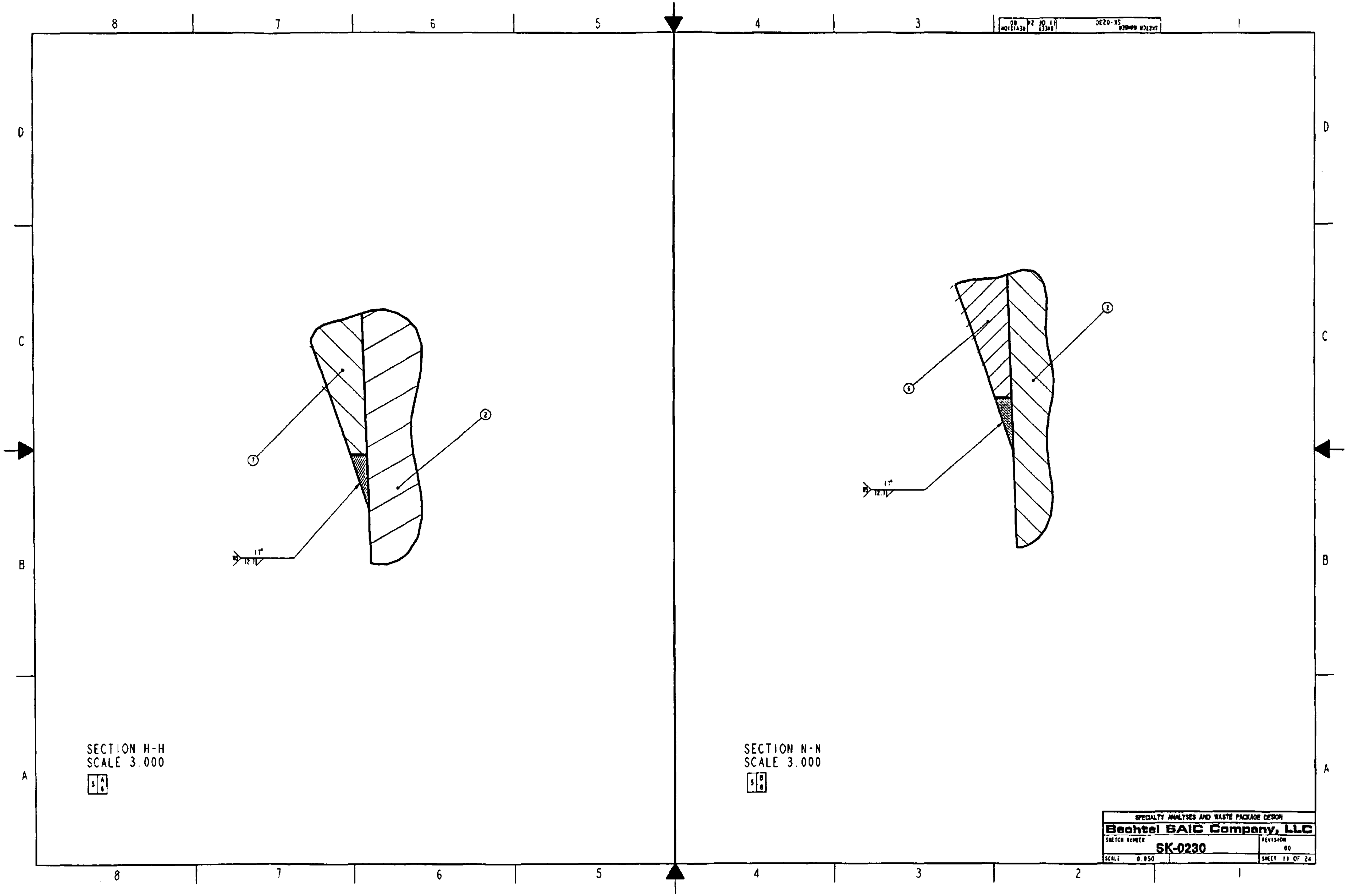

NAME:MCKENZIED2 OBJECT:SK-0230_REV00_12 DATE:06-Nov-02 12:38:50

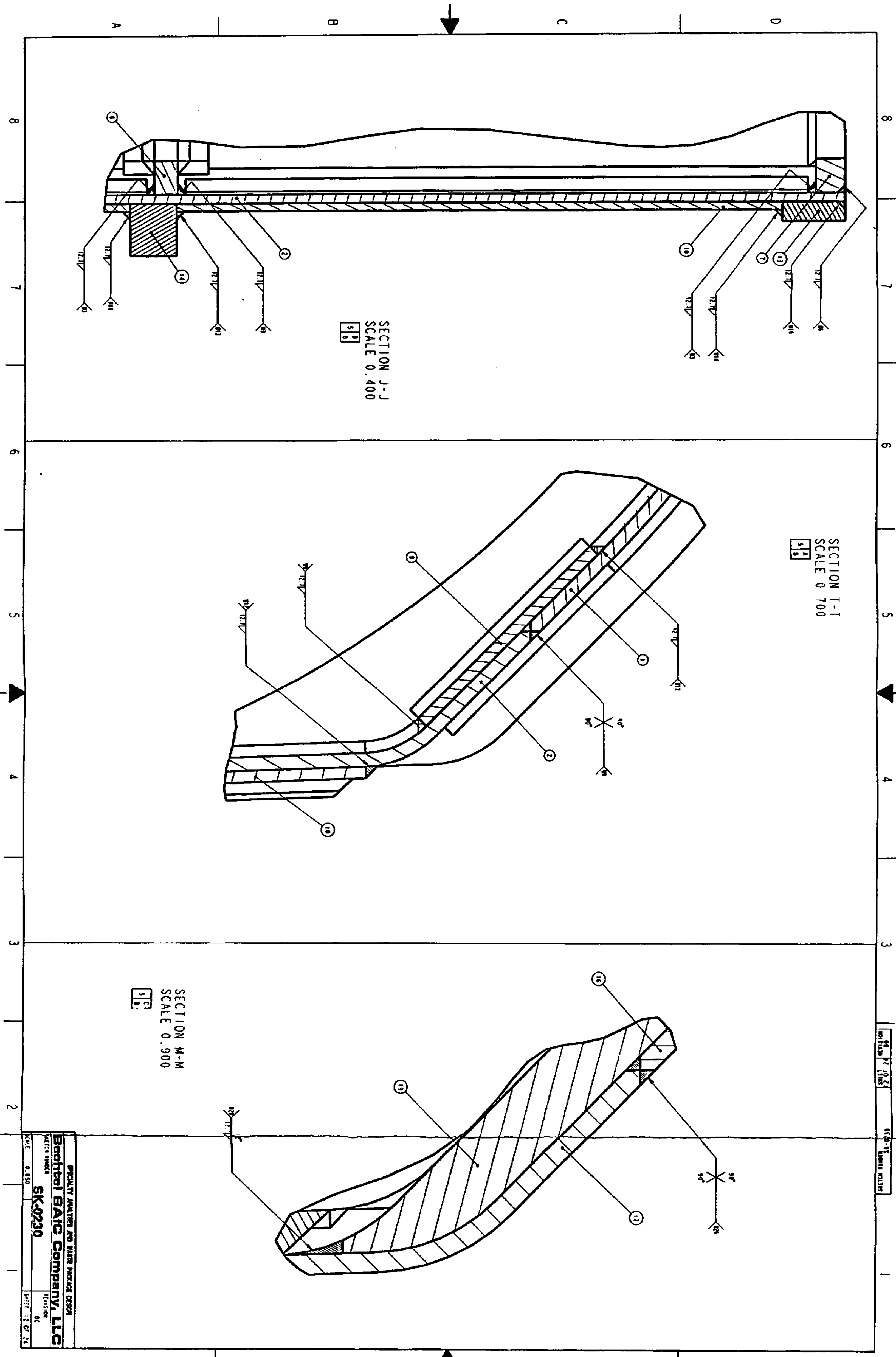

NAME:MCKENZIED2 OBJECT:SK-0230_REV00_13 DATE:06-Nov-02 12:38:52

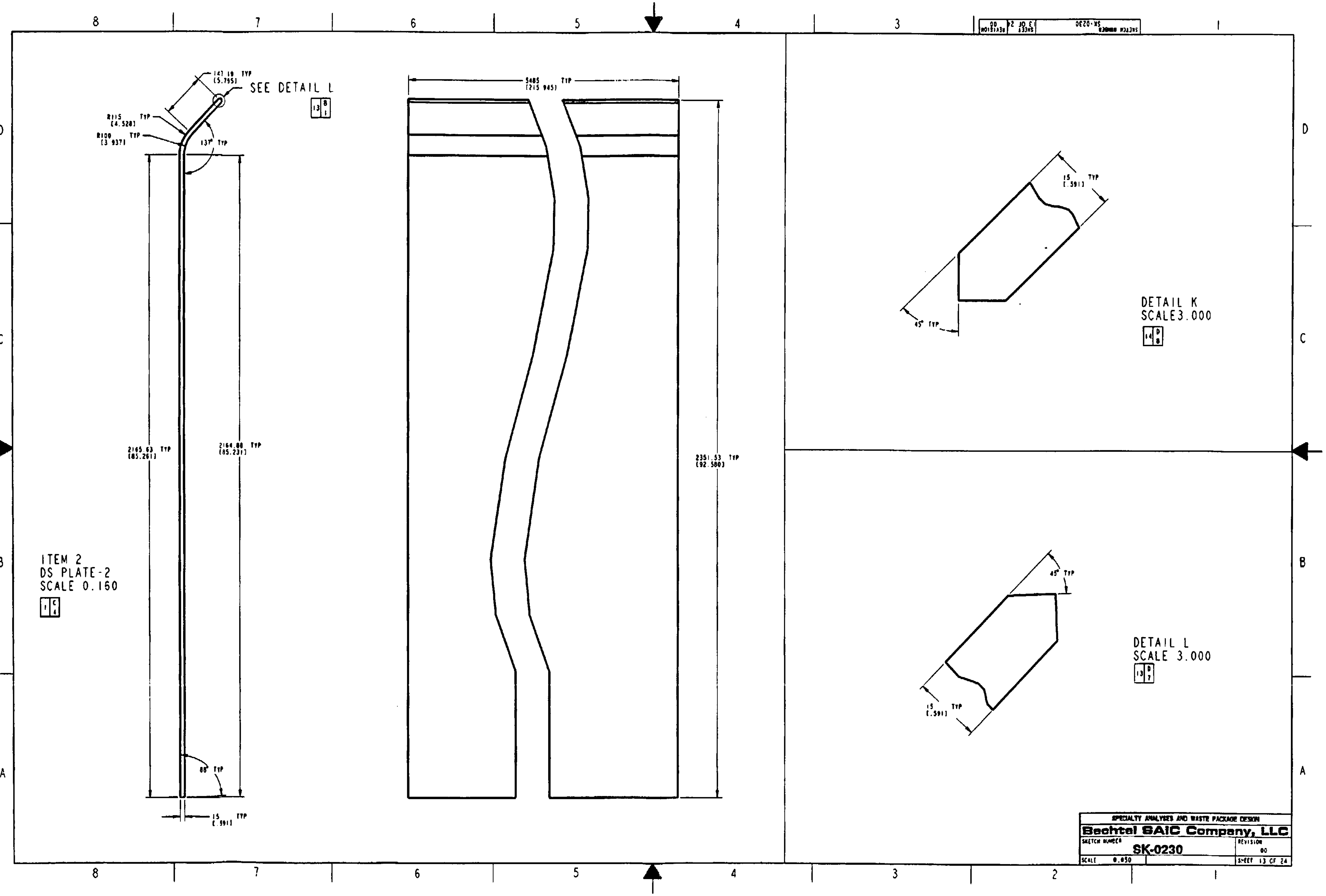

NAME:MCKENZIED2 OBJECT:SK-0230_REV00.14 DATE:06-Nov-02 12:38:53

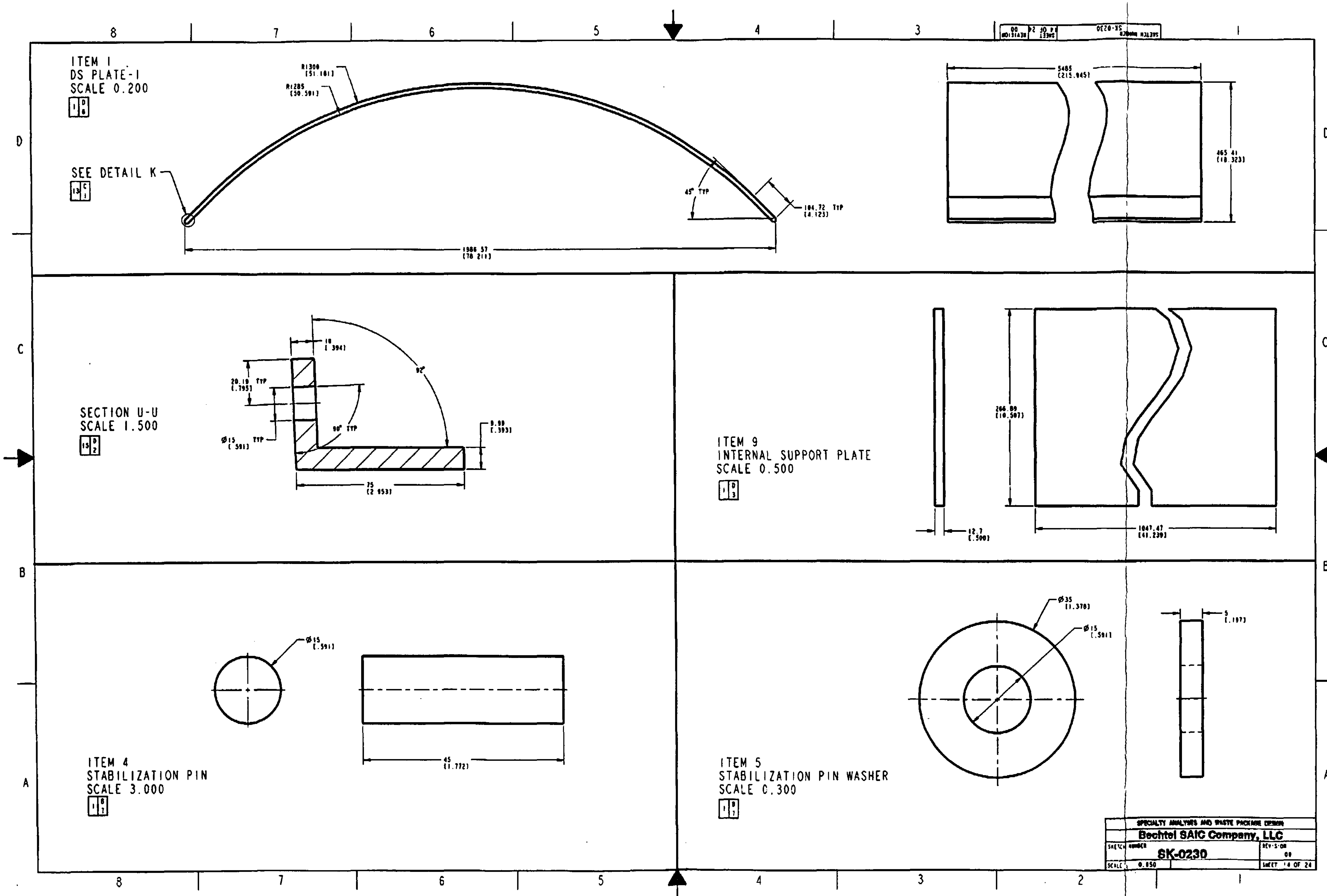

NAME: MCKENZIED2 OBJECT: SK-0230_REV00_15 DATE: 06-Nov-02 12:38:53

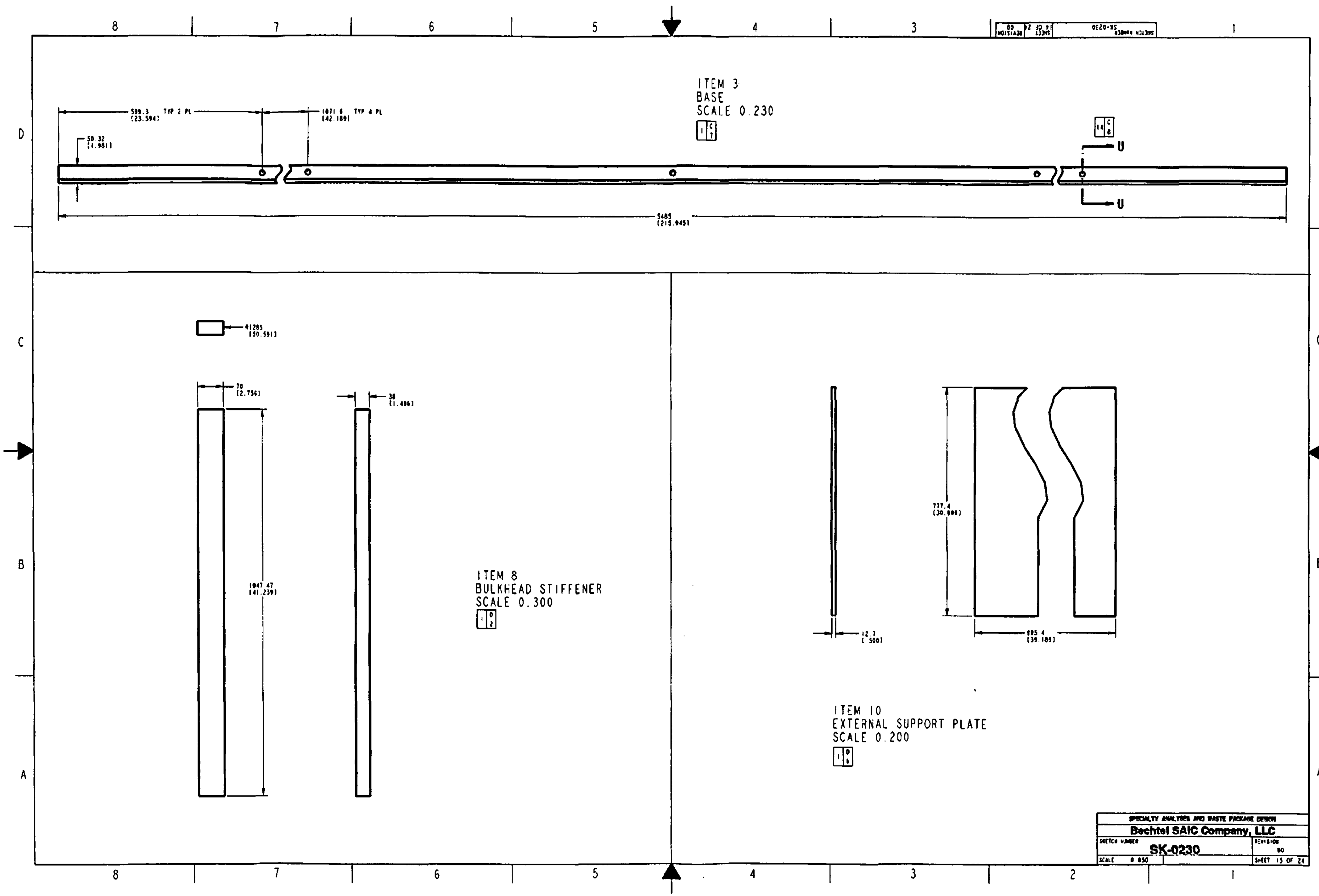

NAME:MCKENZIED2 OBJECT:SK-0230_REV00_16 DATE:06-Nov-02 12:38:54

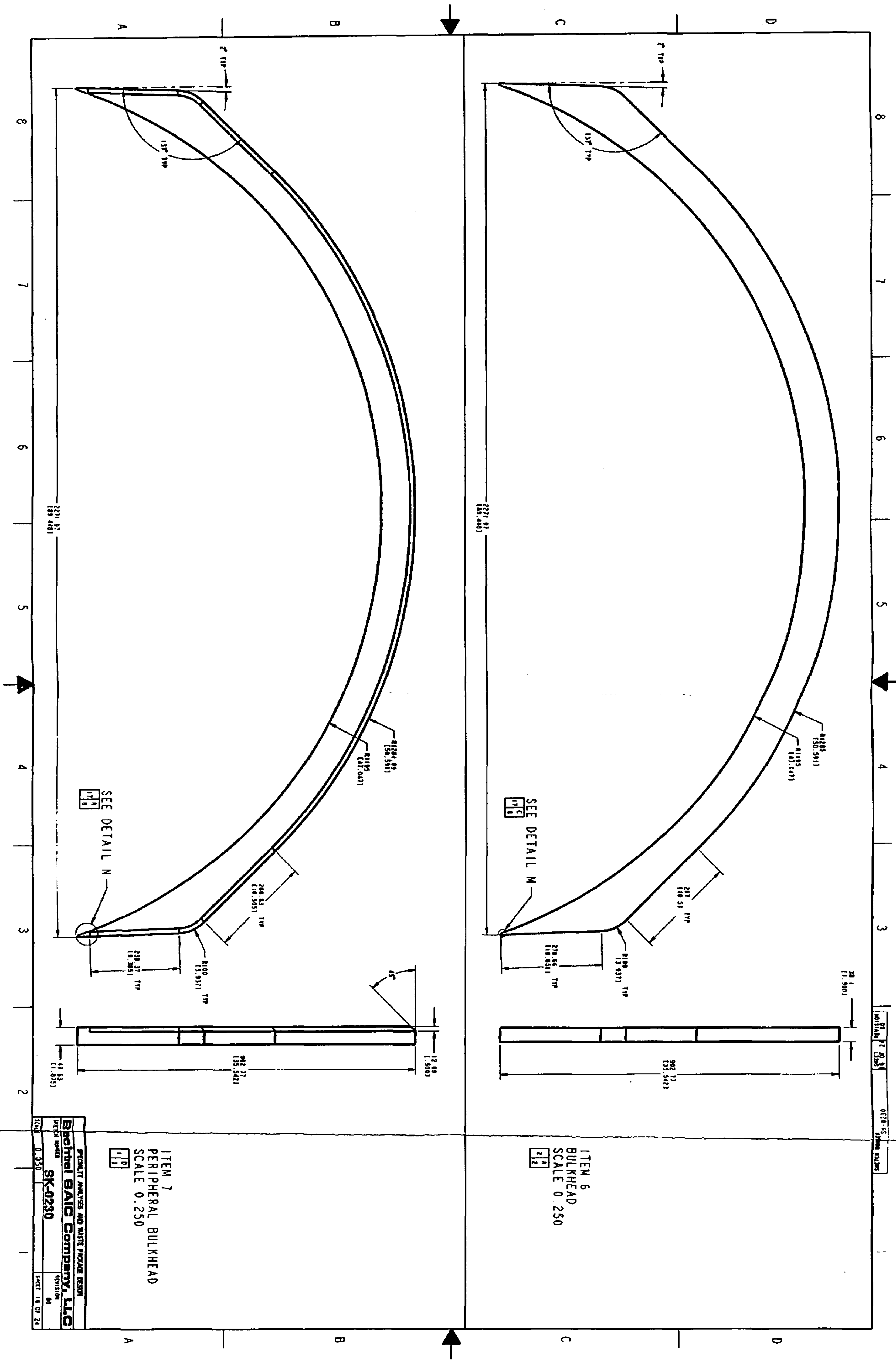

NAME: MCKENZIED2 OBJECT: SK-0230.REV00.17 DATE: 06-Nov-02 12:38:54

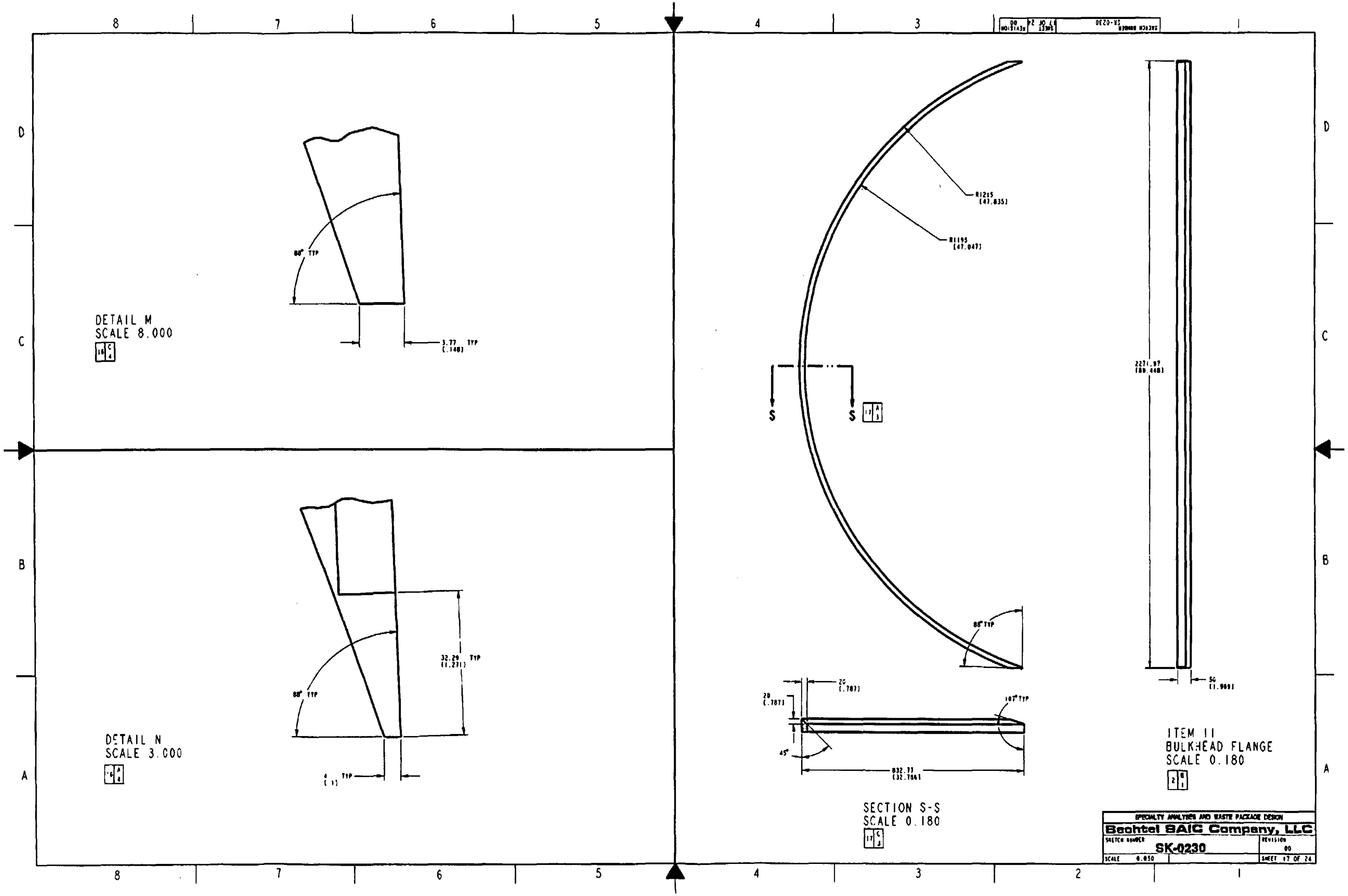

NAME:MCKENZIED2 OBJECT:SK-0230_REV00_18 DATE:06-Nov-02 12:38:55

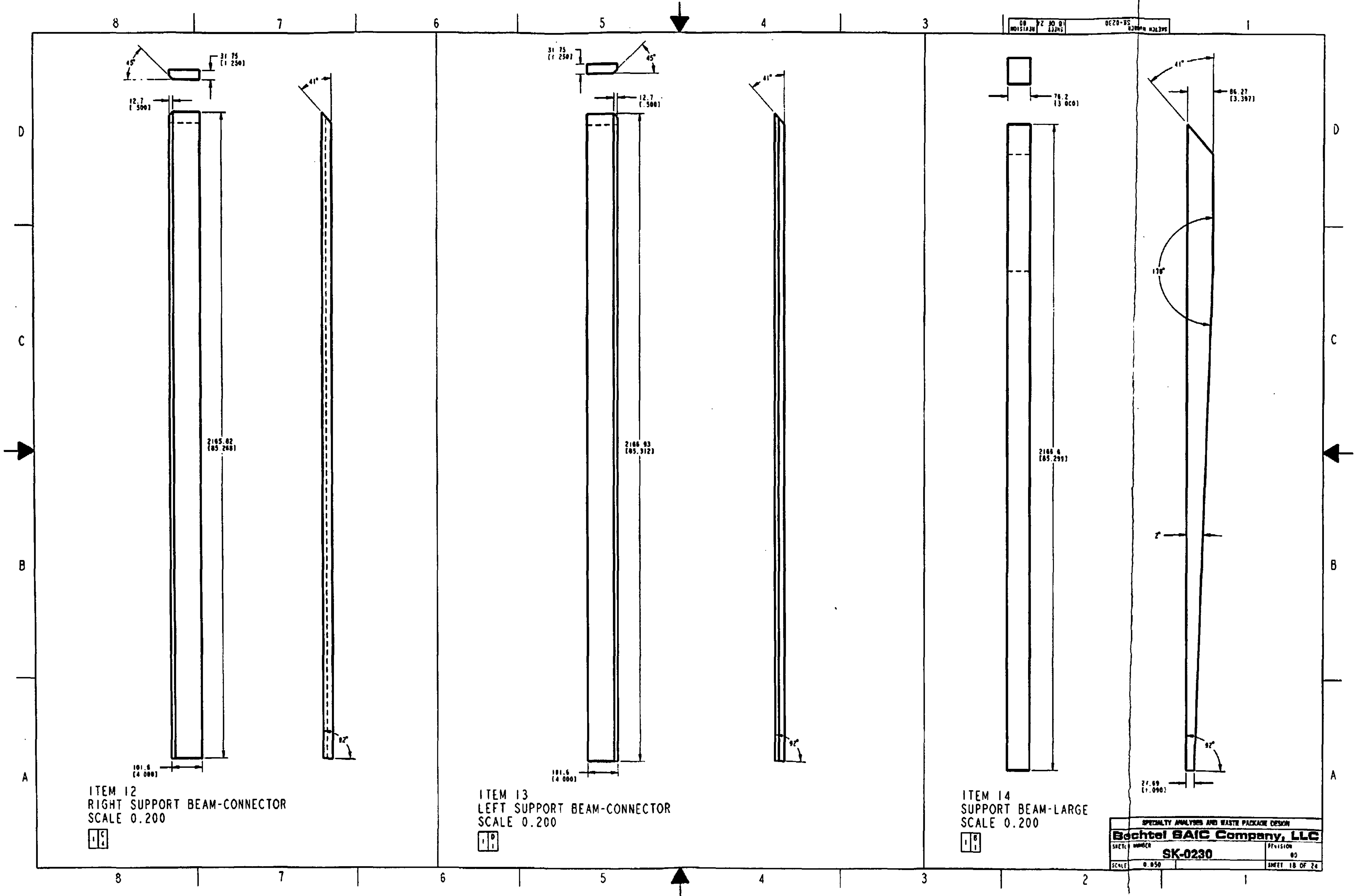

NAME:MCKENZIED2 OBJECT:SK-0230_REV00.19 DATE:06-Nov-02 12:38:55

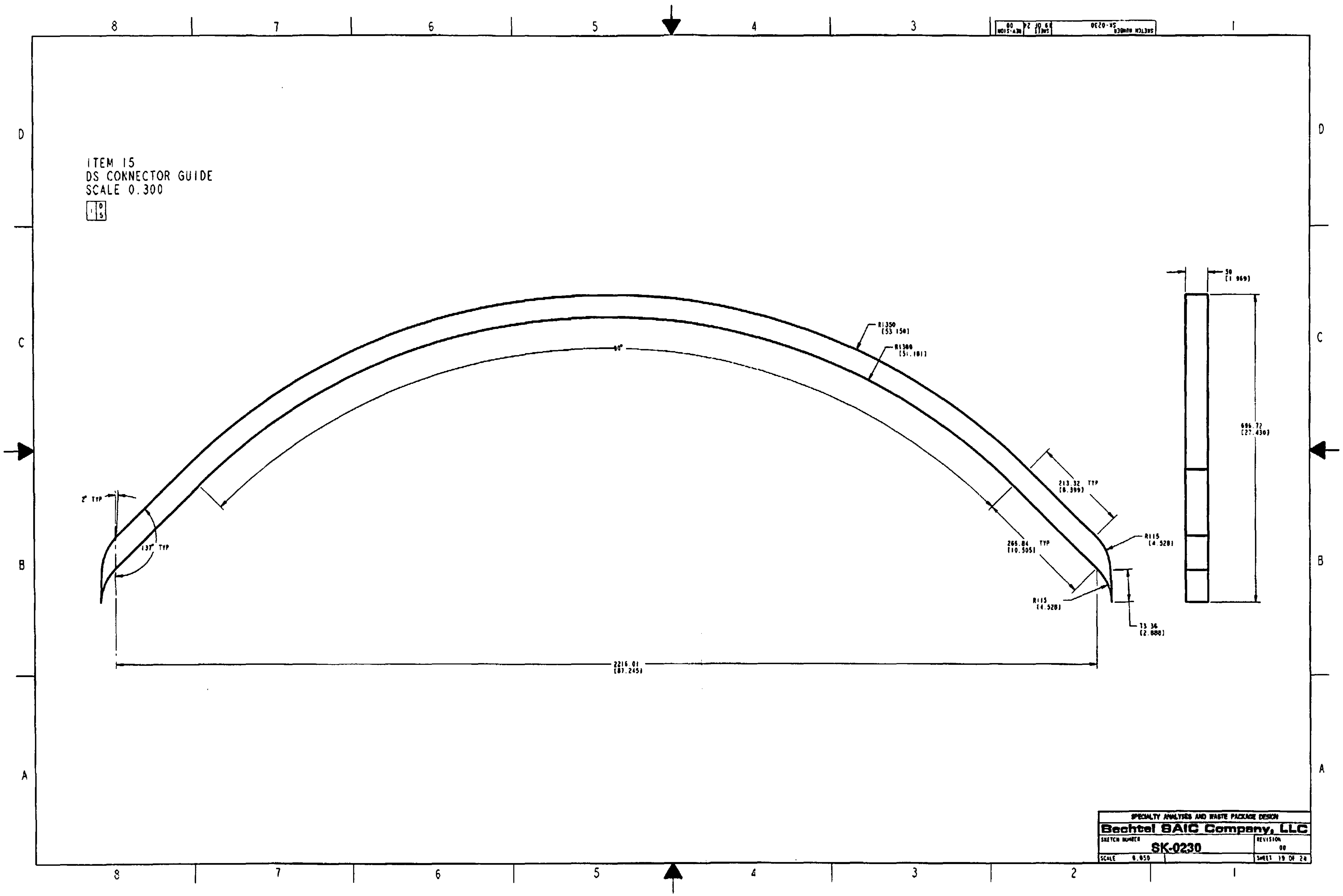

NAME: MCKENZIE02 OBJECT: SK-0230_REV00.20 DATE: 06-Nov-02 12:38:56

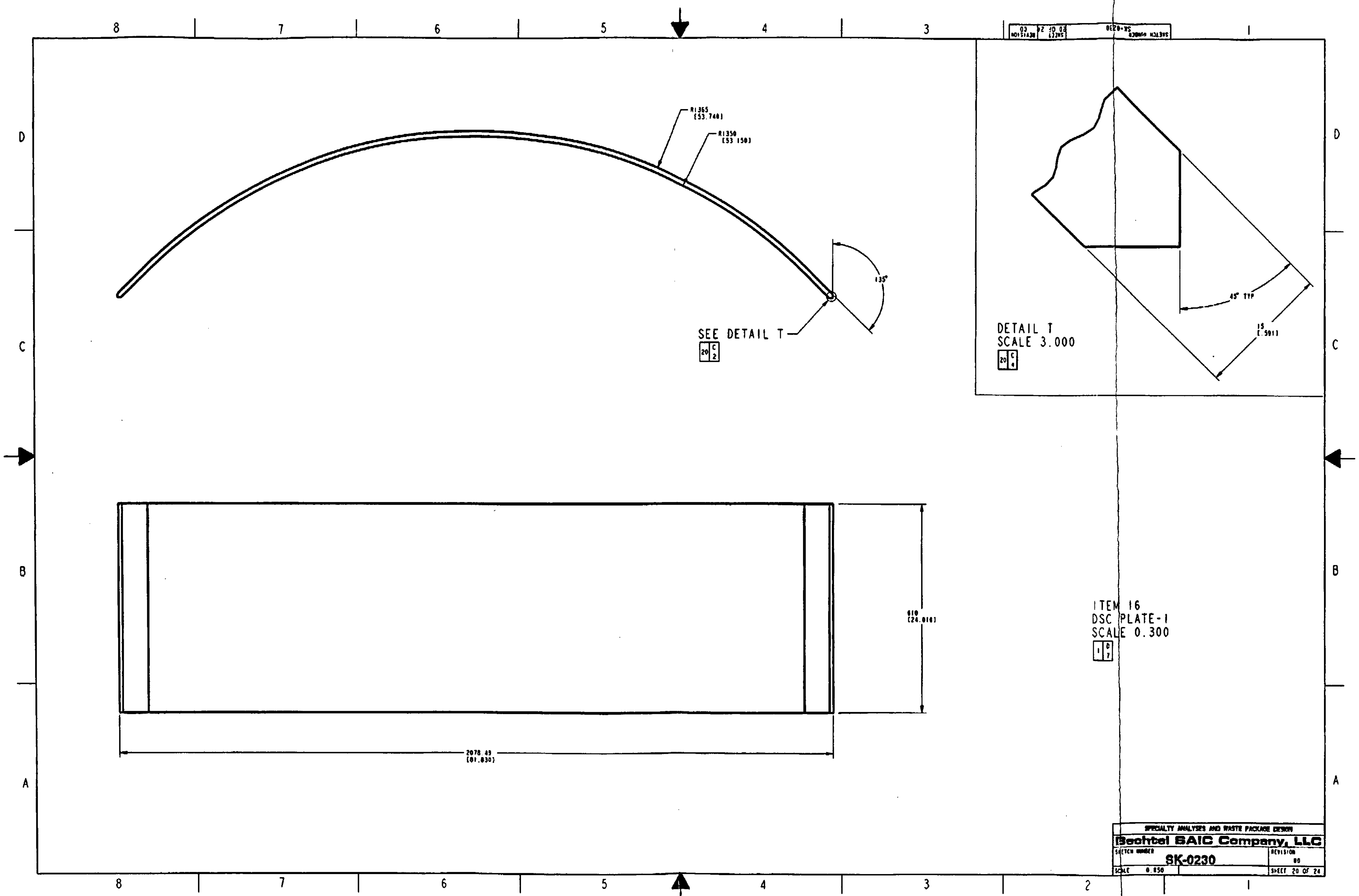

NAME:MCKENZIED2 OBJECT:SK-0230_REV00_21 DATE:06-Nov-02 12:38:56

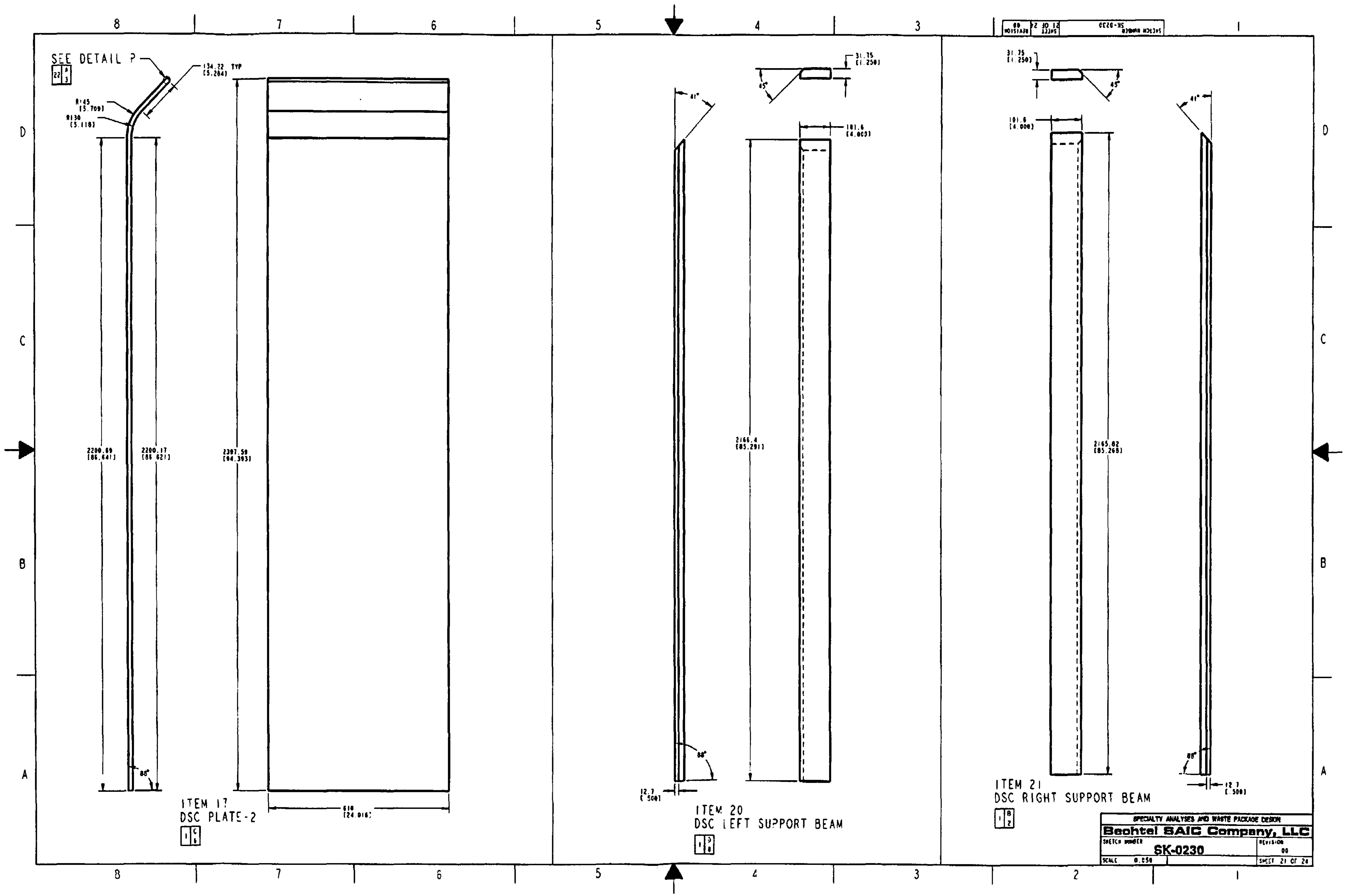

NAME:MCKENZIED2 OBJECT:SK-0230.REV00.22 DATE:06-Nov-02 12:38:56

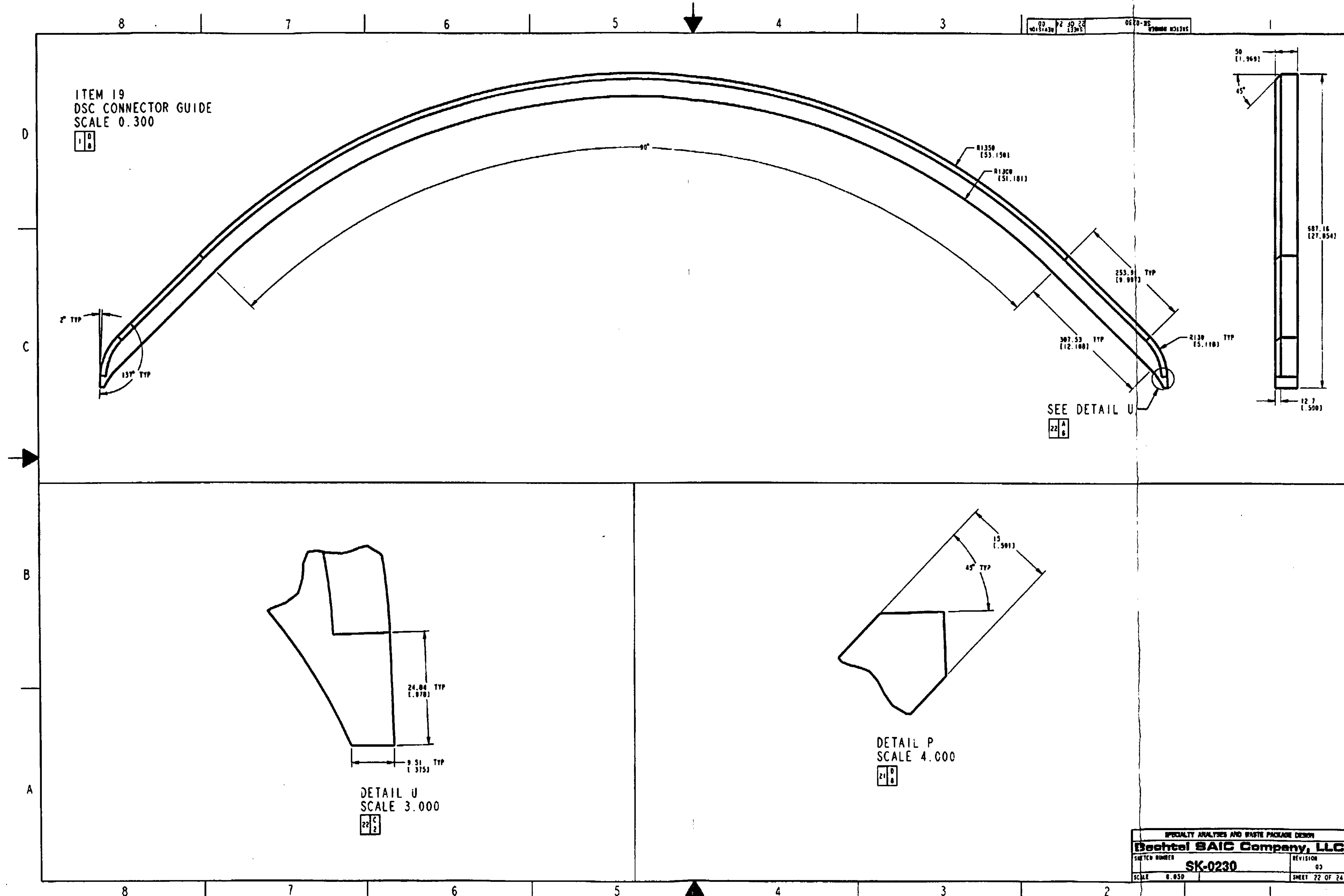

NAME:MCKENZIED2 OBJECT:SK-0230_REV00.23 DATE:06-Nov-02 12:38:57

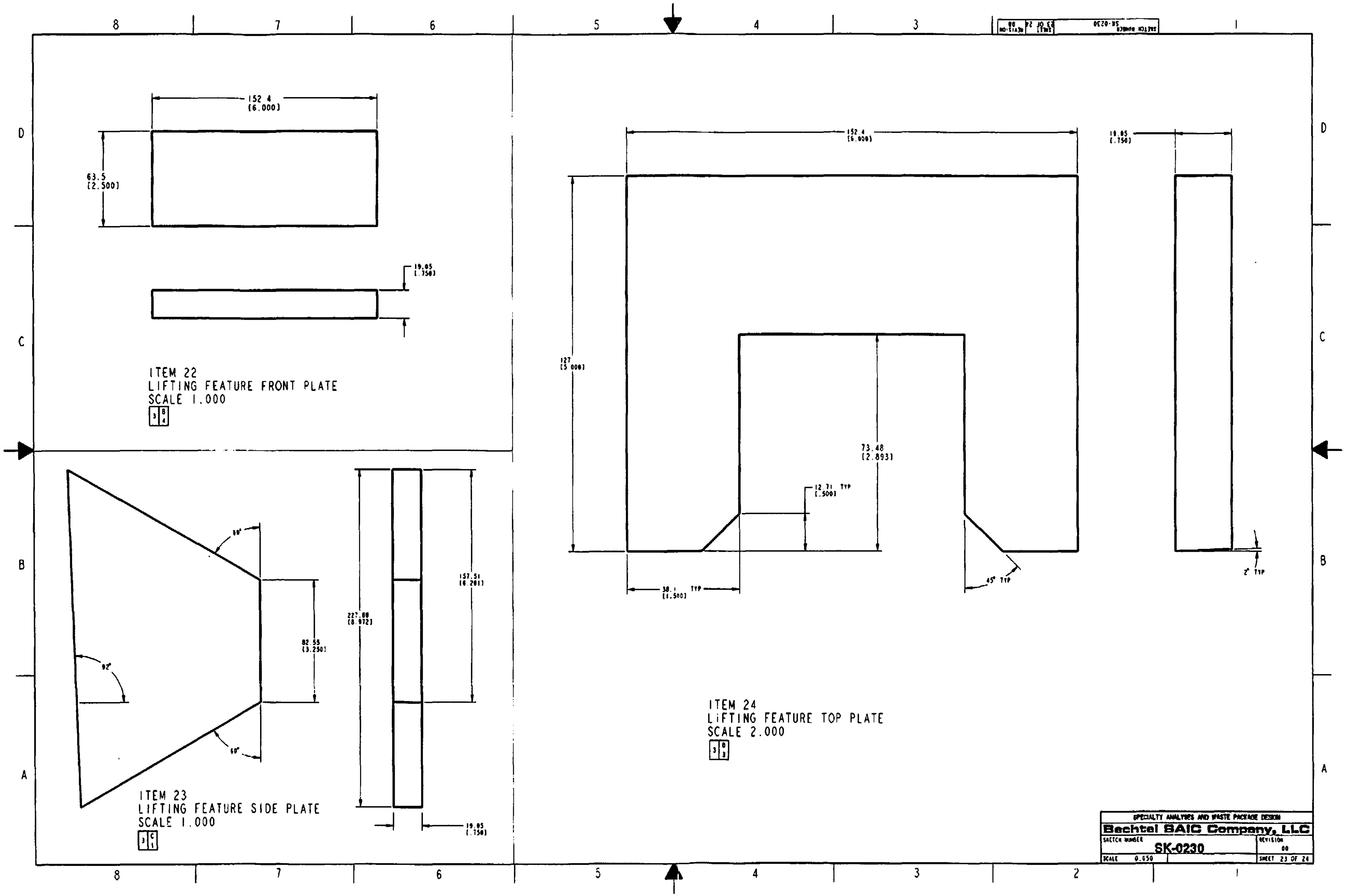

NAME: MCKENZIED2 OBJECT: SK-0230_REV00_24 DATE: 06-Nov-02 12:38:57

COMPONENT LIST							
ITEM NUMBER	ASSEMBLY	SUBASSEMBLY	COMPONENT NAME	MATERIAL	THICKNESS	MASS (KG)	QTY FOR
-1	SR DRIPSHIELD	-	SR DRIPSHIELD	-	-	5000	1
1	-	-	DS PLATE-1	SB-265 R52400	15	834	1
2	-	-	DS PLATE-2	SB-265 R52400	15	890	2
3	-	-	BASE	SB-575 N06022	10	55	2
4	-	-	STABILIZATION PIN	SB-575 N06022	15	.07	10
5	-	-	STABILIZATION PIN WASHER	SB-575 N06022	5	.03	20
6	-	-	BULKHEAD	SB-265 R56405	38	45	4
7	-	-	PERIPHERAL BULKHEAD	SB-265 R56405	48	55	2
8	-	-	BULKHEAD LONGITUDINAL STIFFENER	SB-265 R56405	38	12	15
9	-	-	INTERNAL SUPPORT PLATE	SB-265 R52400	12.7	16	10
10	-	-	EXTERNAL SUPPORT PLATE	SB-265 R52400	12.7	44	10
11	-	-	BULKHEAD FLANGE	SB-265 R56405	20	10	8
12	-	-	RIGHT SUPPORT BEAM-CONNECTOR	SB-265 R56405	102	30	2
13	-	-	LEFT SUPPORT BEAM-CONNECTOR	SB-265 R56405	102	30	2
14	-	-	SUPPORT BEAM-LARGE	SB-265 R56405	76	45	8
15	-	-	DS CONNECTOR GUIDE	SB-265 R52400	50	29	2
16	-	-	DSC PLATE-1	SB-265 R52400	15	100	1
17	-	-	DSC PLATE-2	SB-265 R52400	15	101	2
18	-	-	NOT USED	-	-	-	-
19	-	-	DSC CONNECTOR GUIDE	SB-265 R52400	50	30	2
20	-	-	DSC LEFT SUPPORT BEAM	SB-265 R56405	102	30	1
21	-	-	DSC RIGHT SUPPORT BEAM	SB-265 R56405	102	30	1
-2	-	LIFTING FEATURE ASSEMBLY	-	-	-		4
22	-	-	LIFTING FEATURE FRONT PLATE	SB-265 R56405	19.1	.82	4
23	-	-	LIFTING FEATURE SIDE PLATE	SB-265 R56405	19.1	1.7	8
24	-	-	LIFTING FEATURE TOP PLATE	SB-265 R56405	19.1	1.1	4
-	-	-	TOTAL TITANIUM GRADE 7 WELDS	SFA-5.16 R52401	-	110	-

WELD LIST			
WELD NUMBER	MATERIAL	MASS (KG)	QTY FOR
1	SFA-5.16 R52401	1.4	4
2	SFA-5.16 R52401	.006	20
3	SFA-5.16 R52401	.892	10
4	SFA-5.16 R52401	.004	8
5	SFA-5.16 R52401	.005	4
6	SFA-5.16 R52401	1.2	2
7	SFA-5.16 R52401	2.6	8
8	SFA-5.16 R52401	.380	10
9	SFA-5.16 R52401	.366	10
10	SFA-5.16 R52401	097	20
11	SFA-5.16 R52401	.362	10
12	SFA-5.16 R52401	.377	10
13	SFA-5.16 R52401	.276	10
14	SFA-5.16 R52401	.276	10
15	SFA-5.16 R52401	.420	30
16	SFA-5.16 R52401	.786	2
17	SFA-5.16 R52401	.614	2
18	SFA-5.16 R52401	.614	2
19	SFA-5.16 R52401	786	2
20	NOT USED	-	-
21	NOT USED	-	-
22	SFA-5.16 R52401	.614	8
23	SFA-5.16 R52401	.614	8
24	NOT USED	-	-
25	SFA-5.16 R52401	.930	4
26	SFA-5.16 R52401	.155	4
27	SFA-5.16 R52401	.168	2
28	SFA-5.16 R52401	1.0	4
29	SFA-5.16 R52401	034	4
30	SFA-5.16 R52401	.777	1
31	SFA-5.16 R52401	.777	1
32	SFA-5.16 R52401	.777	1
33	SFA-5.16 R52401	.777	1
34	SFA-5.16 R52401	1.0	1
35	SFA-5.16 R52401	.777	1
36	SFA-5.16 R52401	.777	1
37	SFA-5.16 R52401	013	8
38	SFA-5.16 R52401	.030	4
39	SFA-5.16 R52401	.020	8
40	SFA-5.16 R52401	.025	8
41	SFA-5.16 R52401	.007	8
42	SFA-5.16 R52401	.014	8
43	SFA-5.16 R52401	.043	4
44	SFA-5.16 R52401	.046	8
TOTAL TITANIUM GRADE 7 WELDS	SFA-5.16 R52401	110	-

SPECIALTY ANALYSES AND WASTE PACKAGE DESIGN
Bechtel SAIC Company, LLC
SKETCH NUMBER SK-0230
REVISION 00
SCALE 0.050
SHEET 24 OF 24